UNIVERSITÀ DEGLI STUDI DI UDINE

Dottorato di Ricerca in Scienze e Biotecnologie Agrarie
Ciclo XXVIII
Coordinatore: prof. Mauro Spanghero

TESI DI DOTTORATO DI RICERCA

Phosphorus and iron acquisition strategies in crops: common and unique features

DOTTORANDO
Dott. Silvia Venuti

SUPERVISORE
Prof. Roberto Pinton

CO-SUPERVISORE
Dott. Nicola Tomasi

ANNO ACCADEMICO 2015/2016

SUMMARY

The ever-increasing request of food necessitates developing more sustainable agricultural practices in order to improve productivity while decreasing the environmental and economic costs. It is therefore necessary to increase the nutrient use efficiency (NUE) of crops; however to achieve this goal a deeper comprehension of soil-plant relationships and of plant mechanisms involved in nutrient acquisition is needed. It is known that phosphorus (P) and iron (Fe) are among the main nutrients responsible for determining the quality and quantity of the yield. In fact, both P and Fe are poorly available in well-aerated soils, including acid (for P) and alkaline (P and Fe) soils. To cope with these nutritional problems, some plants have evolved the capacity to release in the soil a wide range of molecules, called root exudates, which can modify the chemical, biological and physical characteristics of the rhizosphere, allowing the mobilization of the two nutrients. The aim of the present PhD thesis was to deepen the knowledge about plant mechanisms involved in the acquisition of these two nutrients and to unravel possible links between the two responses in different plant species.

Maize (*Zea mays*, L.) is one of the most widespread cultivated cereals, both for human and animal consumption. For this reasons, this plant has been used in this PhD thesis to study the capacity to take up Fe, supplied as a sparingly soluble form (Ferrihydrite) or as soluble complexes made up between Fe and natural chelating agents normally occurring in the rhizosphere (Fe-phytosiderophores (Fe-PS) or Fe-citrate). Moreover, the effects of Fe deficiency on the mechanisms involved in P acquisition have been studied. Transcriptomic data showed that Fe deficiency induced the expression of genes coding for proteins involved in the so-called *Strategy II*, which enhance extra-radical availability of Fe and its acquisition. Moreover, genes encoding proteins involved in the methionine cycle and in the synthesis and release of MAs were positively modulated. The treatments of Fe-deficient plants with three natural sources (Fe-citrate, Fe-PS and Ferrihydrite) determined a downregulation of *Strategy II* mechanisms, indicating that the sources were used by plants with different efficiency. At the physiological level, the nutritional status influenced the acquisition and allocation of the micronutrient. Indeed, roots of Fe-deficient maize plants accumulated more Fe than the sufficient ones. An opposite behavior was detected in shoots, suggesting that the translocation system might be readily active in Fe-sufficient plants. The capability of Fe-deficient plants to acquire P from readily- or scarcely-available forms was also investigated. In –Fe plants a higher P content in roots and shoots was detected in comparison with the Fe-sufficient plants. In addition, it emerged from transcriptional data that genes encoding P transporters were

upregulated in –Fe plants. In particular, ZmPHT1;7, which is putatively involved in the high affinity transport and translocation of P, seems to take part in the Fe starvation response. Indeed, when Fe-deficient plants were treated (re-supplied) with natural Fe-sources, its transcription level was repressed down to that recorded in Fe-sufficient plants.

A fundamental step of the plant response to P and Fe deficiency is the release of root exudates, which are able to mobilize these poorly available nutrients in soils. White lupin (*Lupinus albus* L.) is considered a model plant for root exudation studies, especially when related to P deficiency. Using molecular, physiological and metabolic approaches the response to Fe-deficiency and P-deficiency was characterized with the aim to highlight possible links between the two responses. Analyzing the root transcriptoma in the two different growth conditions (-Fe or –P), a reciprocal interaction was observed between the plant adaptation to each of the two nutritional stresses. Indeed, low Fe availability triggered the positive modulation of P-deficiency-responsive genes and *vice versa*. Furthermore, the study of the root exudation patterns showed that compounds such as isoflavonoids (genistein and its derivatives) and coumarins (scopoletin and its derivatives) were released in response to either Fe or P deficiency. The chemical characterization of the root content showed that the same compounds were present in any growth condition but in glycosylated or malonate-glycoside forms.

From previous studies, a gene called *LaMATE2*, putatively involved in the genistein release was identified and functionally characterized. This gene was overexpressed in roots of P-deficient lupin plants and, in particular, in cluster root tissues. Silencing of *LaMATE2* transcript severely affected the genistein release from roots. The LaMATE2 protein was localized in the plasmalemma, as shown by the expression of a *GFP-LaMATE2* construct in *Arabidopsis* protoplast. Finally, the transport of different compounds in *LaMATE2*-transformed yeast microsomes was studied, demonstrating that LaMATE2 protein catalyzed the transmembrane transport of genistein, and potentially also of other flavonoids, via a co-transport with H^+.

Finally, a study of plant response to Fe and P deficiency was also extended to a tree plant species, *Malus x domestica* Borkh. RNA sequencing was carried out on apple tree roots and highlighted that the deficiency of Fe and P affected different metabolic pathways, thus suggesting that apple tree plants adopt different strategies to cope with these two nutritional disorders.

TABLE OF CONTENTS

1. INTRODUCTION

1.1 Iron nutrition in plants

Iron (Fe) is an essential micronutrient for plant growth and development (Vigani et al., 2013) and its imbalance influence the whole cell metabolism, affecting crop yield. Fe is a transition metal, which changes easily its oxidation state (Fe^{2+}/Fe^{3+}) and is able to form octahedral complexes with different ligands. Depending on the ligand, the redox potential of Fe (II/III) varies largely. This variability clarifies the importance of Fe in biological redox systems (Marschner, 2011) and determine its versatile functions. Iron acts as co-factor of several heme and non-heme (Fe-S) enzymes and thus many life-sustaining processes depend on the presence of this metal. Indeed it is a metal component of a wide range of proteins involved in both the respiratory (RET) and the photosynthetic electron transport (PET) chains in mitochondria and in chloroplasts, respectively (Vigani et al., 2013). Under Fe-deficiency conditions, chloroplasts development and chlorophyll biosynthesis are impaired, resulting in the typical symptom of leaf chlorosis. Moreover, a general reduction of plant growth, a reprogramming of metabolism and induction of Fe-acquisition mechanisms are also observed (Marschner, 2011).

1.1.1 Iron in soil: dynamics and availability

Fe is the fourth most abundant element in the earth's crust and it contribues from 2 to 5% of the soil weight. This element is present in the crystal structure of many minerals, such as insoluble oxides and hydroxides (hematite, magnetite, siderite), ferromagnesian silicates (olivine, augite, biotite) and amorphous oxides. However, it also occurs in available forms for plants absorption: complexed with organic substances, adsorbed on solid surfaces and in limited quantities, in solution (Cornell et al., 1996). Fe solubility is extremely low, in particular in well-aerated alkaline soils. Plants need to maintain Fe in the concentration of 10^{-9}–10^{-4} M inside the plants to achieve optimal growth. It has been observed that in an aerated system at physiological pH, the concentration of free Fe in soil solution is below 10^{-15} M (Marschner, 2011), that is at least six orders of magnitude lower than the concentration required for normal plant growth. In the soil soluble fraction the ion forms are the followings: Fe^{3+}, Fe^{2+}, $Fe(OH)^{2+}$, $Fe(OH)^{+}$, $Fe(OH)_2^{+}$. The solubility of Fe is dependent on the dissociation of $Fe(OH)_3$ hydroxide, whose formation is given by the following reaction

$$Fe^{3+} + 3\,H_2O \longrightarrow Fe(OH)_3\,(solid) + 3\,H^{+}$$

In this reaction the equilibrium position lies to the right side $Fe(OH)_3$ and it is strictly dependent on pH (Fig. 1.1).

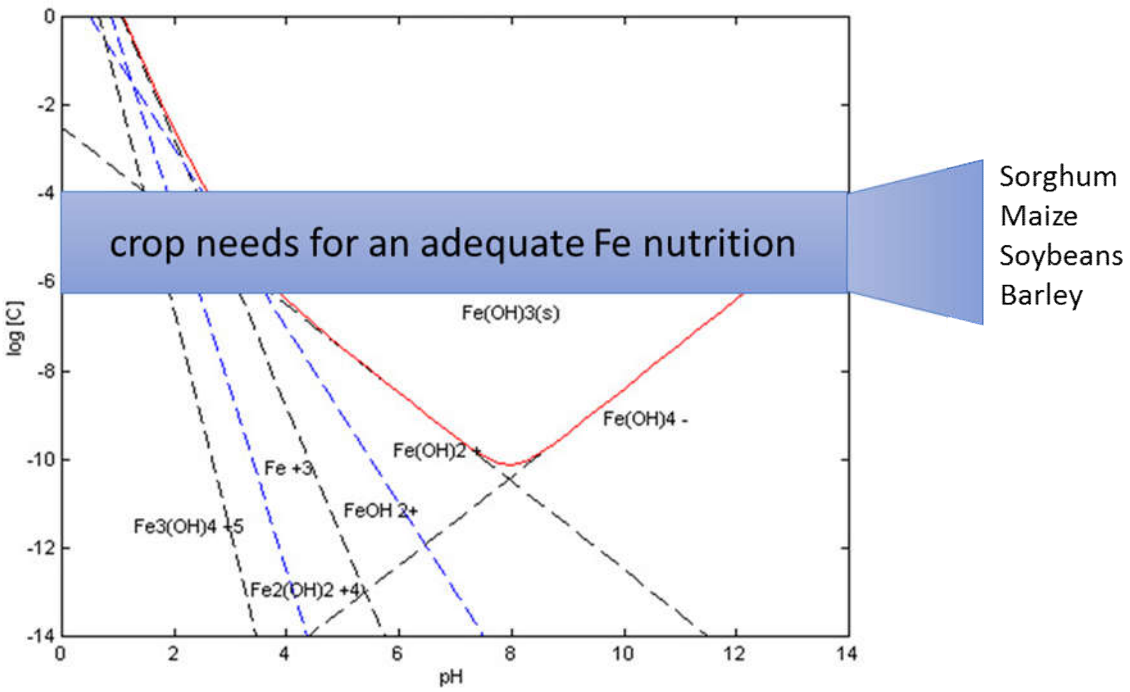

Figure 1.1 - Fe solubility changes depending on soil pH

The iron solubility decreases by three orders of magnitude for each pH unit increased (Lindsay and Schwab, 1982). For this reason, in acid soils the concentration of free iron is higher than in the alkaline and calcareous ones. Soil redox potential (Eh) is another important factor influencing mineral stability and therefore Fe solubility; as described by Colombo et al. (2014), Fe (II) is more soluble than Fe (III). Unfortunately, in well-aerated soils with pH ranging 6-8, the most prevalent form is Fe (III). Nevertheless, in many soils the total iron concentration reaches values around 10^{-8} or 10^{-6} M thanks to organic and soluble ligands which form complexes with iron. In the rhizosphere, several different classes of organic compounds of microbial (siderophores) and plant (phytosiderophores, carboxylic acids and phenolic molecules) origin are able to modify Fe availability. In addition, water-extractable humic substances (fulvic acids) can complex Fe increasing its solubility (Pinton et al., 2001). The Fe-deficiency is a yield-limiting factor and affects alkalin and an in particular the calcareous soils (Lucena, 2000), which covered more than 30% of the Earth's crust. Fe deficiency is the most important nutritional disorder that occurs in

calcareous soils (Mortvedt, 1991). The pH in these soils is highly buffered due to the high amount of $CaCO_3$, thus limiting Fe solubility (Lindsay, 1979).

1.1.2 Fe acquisition and response to Fe deficiency

Plants have developed two different strategies in order to cope with the Fe limitation in soil: *Strategy I* (reduction –based strategy) which occurs in dicots and non-graminaceous monocots and *Strategy II* that is found in grasses (Marschner et al., 1986; Römheld, 1987; Schmidt, 1999; White and Broadley, 2009; Guerinot, 2010). In both strategies, plants induce a coordinate set of responses in order to increase and maximize Fe mobilization and its uptake from the rhizosphere.

1.1.2.1 Strategy I

Strategy I (Römheld 1987) is a three-step mechainism, characterized by: (i) the acidification of the rhizosphere, (ii) an increased capability of Fe (III)-chelate reduction at the root surface and (iii) the release of chelating molecules in the rhizosphere. Fe solubility is enhanced by the acidification of the rhizosphere which follows the activation of the plasma membrane H^+-ATPase belonging to the HA family (Santi et al., 2005; Santi and Schmidt, 2009). The Fe(III) reduction step is carried out by a plasma membrane-bound enzyme called FRO2 (ferric reductase oxidate) (Guerinot, 2010, Brüggemann et al., 1990; Holden et al., 1991). Moreover, in order to increase the bioavailability of the poorly soluble Fe, plants release compounds such as phenolic acids, organic acids and flavins (Lucena et al., 2007; Gerke et al., 1994; Jones, Darrah et al., 1996) that have either reduction or complexing properties. In the last step the Fe reduced ionic form (Fe^{2+}) is taken up into the root cells through a specific iron-regulated transporter (IRT1) (Eide et al., 1996; Varotto et al.,2002). *FRO* and *IRT* genes have been isolated and cloned from several species as *Arabidopsis thaliana* and *Oryza sativa*, and their up-regulation is considered as plant response to Fe deficiency stress (Hindt and Guerinot, 2012). The plants defective in IRT1 expression, showed a strong chlorotic phenotype, suggesting that this gene encodes an high affinity Fe-transporter, which is the main system of Fe uptake into roots (Vert et al., 2002). The IRT1 functional characterization was performed restoring the growth of the Fe deficiency-sensitive *Saccharomyces cerevisiae* yeast strain *fet3fet4* (Eide et al., 1996). Different studies proposed that the rate-limiting step in Fe-uptake is Fe(III)-reduction; for this reason, Conolly et al. (2003) produced transgenic plants with *FRO2* gene overexpressed. Even if new plants showed

an enhanced tolerance to low Fe availability the *FRO2* overexpression led only to an increase of the ferric-reductase activity in Fe deficiency suggesting a post-transcriptional regulation of FRO2 by Fe or by the Fe nutritional status. Other genes belonging to HA family are induced under Fe starvation, like *CsHA1* and *AtAHA2* (Santi et al., 2005; Santi and Schmidt, 2009).

Until recently, few specific information on genes encoding for transporters involved in phenolic secretion by non-graminaceous plants was available. Fourcroy et al. (2014) have isolated and identifies an ABC transporter ABCG37 involved in the release of coumarins in particular of scopoletin, through the analysis of mutants defective in this transporter. In addition, to *IRT* other high affinity iron transporter genes (*Nramp*) identified in *A. thaliana* as *NRAMP 1, 3, 4,* are induced under iron deficiency and they could contribute to iron homeostasis (Curie et al., 2001; Thomine et al., 2000). In the *Strategy I* mechanism other genes played a key role in the transcriptional regulation of the Fe deficiency response, like the basic helix-loop-helix (bHlH) transcription factor *FIT/FER, bHlH38* and *bHlH39* (Colangelo and Guerinot, 2004.). FIT is involved in induction of *FRO2* and *IRT1* transcription and it may also act indirectly to prevent turnover of IRT1 protein. It is constitutively expressed but it is overexpressed in outer root cells under Fe starvation condition. Thus, in order to perform its function FIT needs to interact with a binding partner that is expressed only in response to Fe limitation. BHLH38 and BHLH39 are the two proteins, which physically interact with FIT: together they control the expression of the *Strategy I* Fe-uptake machinery (Yuan, 2008).

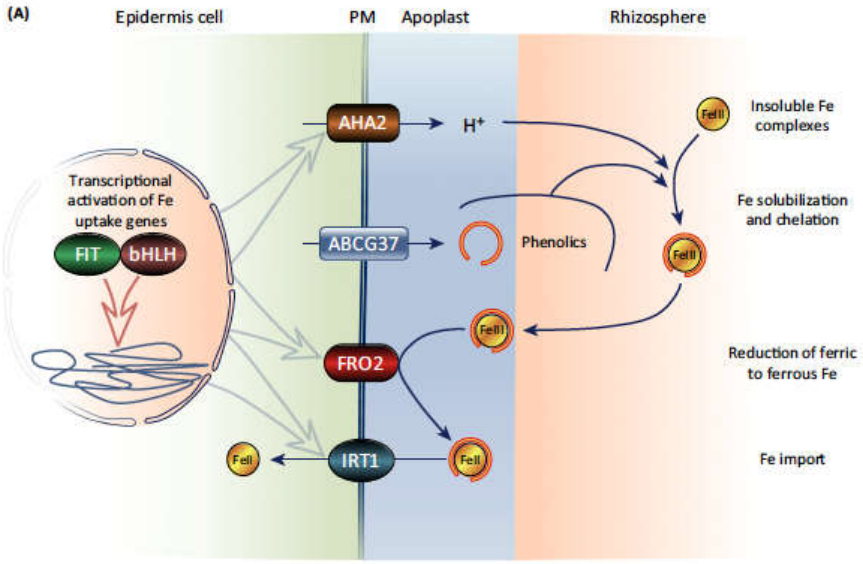

Figure 1.2 – Fe-uptake strategy I (Brumbarova, 2015)

Besides these physiological and transcriptional mechanisms, plants respond to Fe deficiency also through morphological changes in order to increase the root area available for Fe solubilisation and uptake; this behaviour results into an increase in root hairs production, thickening of the root tips and formation of rhizodermal transfer cells (Landsberg ,1982; Römheld and Kramer, 1983).

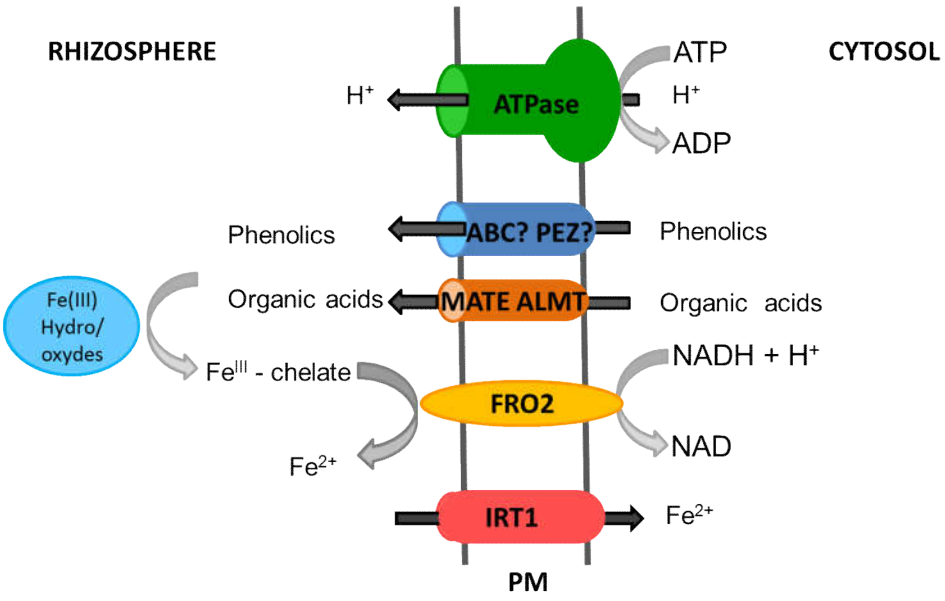

Figure 1.3 - Model for root responses to iron deficiency in dicots and non-graminaceous monocots (*Strategy I*)

1.1.2.2 Strategy II

As compared to the other plants, grasses have evolved a different mechanism, known as *Strategy II*, in order to mobilize and transport Fe into the roots cell. Under iron deficiency, graminaceous plants produce and secrete non-proteinogenic amino acids, called phytosiderophores (PSs), which contains six functional groups that coordinate Fe (Ma and Nomoto, 1996). These molecules chelate Fe(III), and the Fe(III)-PS complexes are then taken up into roots (Römheld and Marschner, 1986). PSs, belong to the mugineic acid (MA) family and several types of MAs have been identified in different plant species. Their biosynthesis starts from three S-adenosyl-L-methionine molecules (SAM). This pathway includes three main enzymes: nicotianamine synthase (NAS), nicotianamine aminotransferase (NAAT) and deoxymugineic acid synthase (DMAS), producing in the final step the 2' deoximugineic acid (DMA) which is the precursor for

all the MAs. Genes, encoding for these enzyme, are strongly induced under Fe deficiency. Recently, Nozoye et al. (2011) have identified and isolated from rice and barley the transporter belonging to the major facilitator superfamily (MFS) involved in PSs secretion, which has been named TOM1 (transporter of mugineic acid 1). The released PSs follows the circadian rhythm, with a maximum after the onset of the light period and it is influenced the temperature (Ma et al., 2003). The Fe(III)-PSs complex is taken into the root cells through a specific plasma membrane-bound transporter, called YELLOW STRIPE 1 (YS1) (Fig. 1.4). *YS1* gene was isolated from a maize mutant, *yellow stripe 1*, which shows leaf interveinal chlorosis due to its inability to take up the Fe(III)-PS complex (Curie et al., 2009).

In rice, it has been studied that the *Stategy II* is regulated by the bHlH transcription factor OsIRO2 (Hindt and Guerinot, 2012). Indeed, under Fe deficiency *OsIRO2* is up-regulated and in expriments in which this transcription factor is overexpressed an induction of the genes involved in PS synthesis and transport was detected (Ogo et al 2006; Hindt and Guerinot, 2012). Furthermore, other genes like *OsIDEF1* and *2* (*iron deficiency-responsive element 1 and 2*) code for positive regulators of Fe starvation (Kobayashi and Nishizawa, 2012).

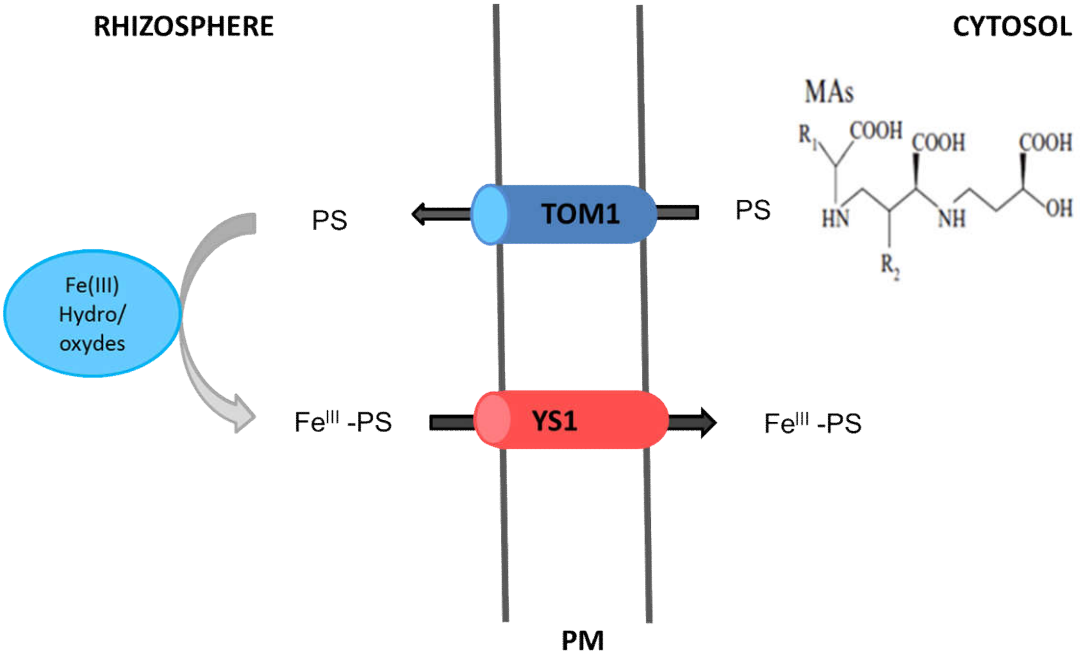

Figure 1.4 - Model for root responses to iron deficiency in graminaceous species (*Strategy II*)

1.1.3 Allocation and transport

After its uptake into the roots, Fe follows different fates moving through the plant via the xylematic or phloematic system to be distributed to the different tissues. Since Fe is poorly soluble and highly reactive, it requires to be complexed with a suitable compound in order to be translocated inside the plants. Recently, Rellan-Alvarez et al. (2010) have confirmed that in the xylem sap, Fe is associated to organic acids and more specifically to citrate. Moreover, a MATE (multidrug and toxin efflux family) protein called FRD3 (ferric reductase defective 3) was characterized in the *fdr3* mutant in Arabidopsis as a citrate efflux transporter involved in the citrate loading into the xylem (Yi and Guerinot, 1996; Rogers and Guerinot, 2002). PEZ1 has been identified as a further effluxer, which is thought to be responsible for xylem loading of phenolics as protocatechuic acid and caffeic acid (Ishimaru et al., 2011), putatively involved in the remobilization of precipitated apoplastic Fe.

FRD3 and PEZ1 are only involved in the release of these chelating molecules in their Fe-free form. It has been proposed that AtFPN1/AtREG1 (Arabidopsis ferroportin 1/ iron regulated 1) (Morrisey et al., 2009) could be to a certain extent implicated in the loading of Fe into the xylem for root-to-shoot delivery. Members of YSL family are largely involved in Fe translocation. ZmYS1, responsible for Fe (III)-Deoxy Mugineic Acid (DMA) uptake from soil is upregulated both in roots and shoots under Fe starvation (Curie et al., 2001). This suggests that in addition to be involved in the influx of molecule inside the roots they are also responsible for translocation mechanisms. Furthermore, YLS genes are also present in non-graminaceous species, which do not produce MAs. Curie et al. (2009) proposed that these YLS transporters are implicated in translocation of the NA chelated with metals. In fact, NA is a precursor of MAs and it is synthesized by all the plants. AtYSL1 and AtYSL2 are involved respectively in translocation and the lateral movement of Fe and other metals. In rice, a strategy II plant, YLS2 transporter is involved in the long-distance transport of Fe (II)-NA and not of Fe (III)-MAs into leaves and grains (Koike et al., 2004).

1.2 Phosphorus nutrition in plants

All living organisms need to acquire phosphorus (P) for surviving; phosphorus is one of 17 essential elements required for plant growth (Raghothama 1999; Bieleski 1973; Vance et al. 2003). In fact, the concentration of P in plants ranges from 0.05 to 0.50% dry weight, where it

plays a key role in all major metabolism processes, such as photosynthesis and respiration. Phosphorus is also a fundamental constituent of macromolecular structures like nucleic acids, and it is involved in energy transfer. In fact, many metabolites are Pi monoesters, whereas the phosphoanhydride bonds of compounds such as ATP have a role in energy (Plaxton and Tran, 2011). Glycolysis, membrane synthesis and stability, carbohydrate metabolism are other processes in which P carries out a fundamental function (Vance et al. 2003; H Lambers et al. 2006). Moreover, phosphorylation reactions and dephosphorylation of proteins are crucial for signal transduction in plants (Maathuis, 2009). Phosphorus is considered to be one of the most limiting factor in plant nutrition; due to its important role in growth and metabolism of plants, phosphorus nutritional disorder results in crop yield reductions (Grabau et al. 1986).

1.2.1 Phosphorus in soil: dynamics and availability

In soil, P is mainly present in organic (Po) and inorganic (Pi) forms not readily available for plant acquisition. The amount of the organic and inorganic fractions occurring in the rhizosphere and their behaviour depend on chemical, physical and microbiological soil conditions (Hansen et al. 2004.) Pi usually accounts for 35% to 70% of total P in soil (Harrison 1987). The inorganic phosphorus is predominantly present as adsorbed to soil particles or as mineral precipitates (Sims and Pierzynski, 2005). Pi is present in minerals as apatites, strengite, and variscite, which are very stable. For this reason, the release of bioavailable P from these minerals by weathering is generally too slow to cope with the plant nutritional requirements. Secondary P minerals, including calcium (Ca), iron (Fe), and aluminum (Al) phosphates, differ in their dissolution rates, depending on size of mineral particles and soil pH (Pierzynski et al. 2005). The adsorption and precipitation of P in soil is strictly dependent on pH and its maximum availability occures in the range between 5.5 and 7 (Fig. 1.5). For this reason, the solubility of Fe and Al phosphates increases with increasing soil pH, whereas the solubility of Ca phosphate decreases, except for pH above 8 (Hinsinger 2001).

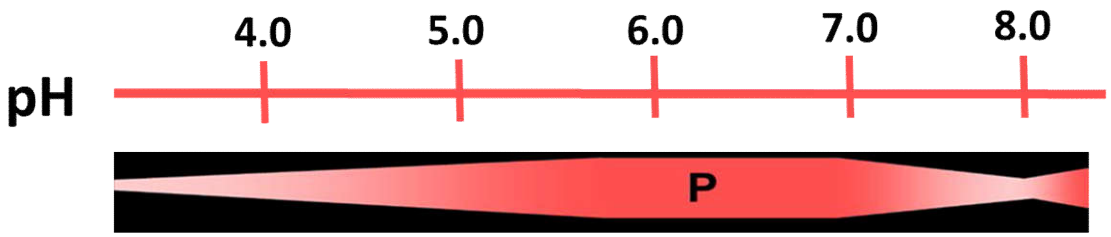

Figure 1.5 - Availability of P in relation to pH

Organic P (Po) is about 30% to 65% of the total P in soils (Harrison 1987). In the organic form the major component is represented by phytic acid (inositol hexaphosphate) (Richardson, 1994) in addition to the labile orthophosphate monoesters and the organic polyphosphates (Condron et al.2005). The Po is released through mineralization processes mediated by both soil microorganisms and plant roots. However, the average content of phosphorus in the earth crust is 1 g kg^{-1}, while plants for an appropriate growth require a P level approximately of 2 g kg^{-1} (Taiz and Zeiger, 1998); so P application is essential to support the crop productivity (Richardson et al., 2009). Nevertheless, only 10-20% of P given through fertilizers is taken up by plants, while the remaining fraction is adsorbed by soil with the formation of poorly soluble compounds.

1.2.2 Phosphorus acquisition and response to deficiency

The orthophosphate forms $H_2PO_4^-$ HPO_4^{2-} (Pi) are the two anion forms absorbed by the roots. They are generally present in the soil solution at very low concentrations comprised between 0.1 and 10 µM and they diffused in soil with very low rate in comparison to their uptake (Shachtman et al., 1998). Plants adaptation to P poor soils is mediated through the exploitation of many several mechanisms as: (i) modification of root morphology and architecture (Linkohr et al., 2002), (ii) release of low molecular weight ligands (Neumann and Romheld, 1999), (iii) secretion of enzymes (Wasaki et al., 2003), (iv) increase in the expression of Pi high affinity transporters (Chen et al., 2008) and (v) formation of mycorrhizal symbiosis (Olsson et al., 2002) (Fig. 1.6).

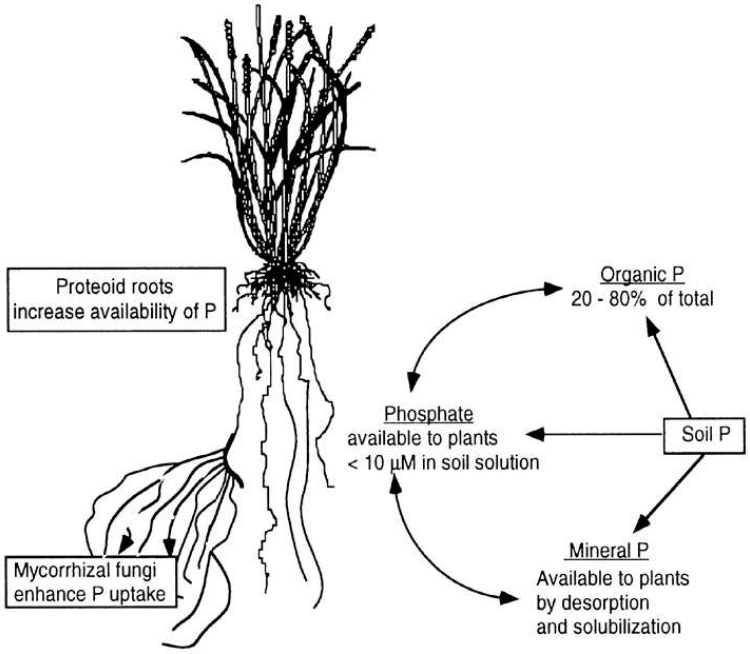

Figure 1.6 - P acquisition in soil (Schatchman, 1998)

In order to optimize the exploration of the soil in P limited conditions, the plant shoot/root ration is altered to promote the development of lateral roots (Williamson et al., 2001). In addition, a proliferation of root hairs occurs (Linkhor et al., 2002); for instance in *Arabidopsis thaliana* it has been shown that root hairs of P-deficient plants have a density 5 times greater compared to plants grown in P-sufficiency (Ma et al., 2001). In the *Proteaceae* plants changes in the root system induced by P limitation are more dramatic leading to the formation of proteoid roots or cluster roots (Vance et al., 2003). All these modifications result in a greater root surface in contact with the soil and a higher phosphate absorption capacity. Biochemical changes induced in the rhizosphere by root activities play a crucial role in improving the bioavailability of soil P (Hinsinger 2001). These root-induced changes mainly involve proton release for the acidification of the rhizosphere, carboxylate exudation for the mobilization of sparingly available P by chelation and ligand exchange mechanisms (Fig. 1.7). Root-induced acidification can decrease rhizosphere pH by 2 to 3 units with respect to that of bulk soil, resulting in substantial dissolution of sparingly available soil P (Marschner 2011). Moreover, organic phosphorus could be a substrate for phytase and acid phosphatases (Miller et al., 2001, Zhang et al. 2010), which hydrolyse P present in organic form in the rhizosphere, thus increasing the availability of Pi for absorption. It has been shown that under conditions of P deficiency there is an upregulation both

of the activity and the transcription levels of these enzymes (Li DP et al., 2002). The concentration of phosphate concentration within the cells is much higher (2-20 mM) than that of soil solution (Schatchmann et al., 1998). For this reason, the anion has to be taken up against a steep concentration gradient through specific high-affinity transporters (Km between 3 and 10 µM) (Furihata et al., 1992). The genes coding for high affinity transporters (PHT1) have been cloned in different species. Pi deficiency is known to increase the Pi import capacity of cells, in part, through an increase in the level of expression of Pi transporters.

Symbiotic association with mycorrhizal fungi allow plants to increase the portion of explored soil. This symbiosis is based on a mutualistic exchange of nutrients between fungi and plants. These latter give carbon in exchange of nutrients such as phosphorus.

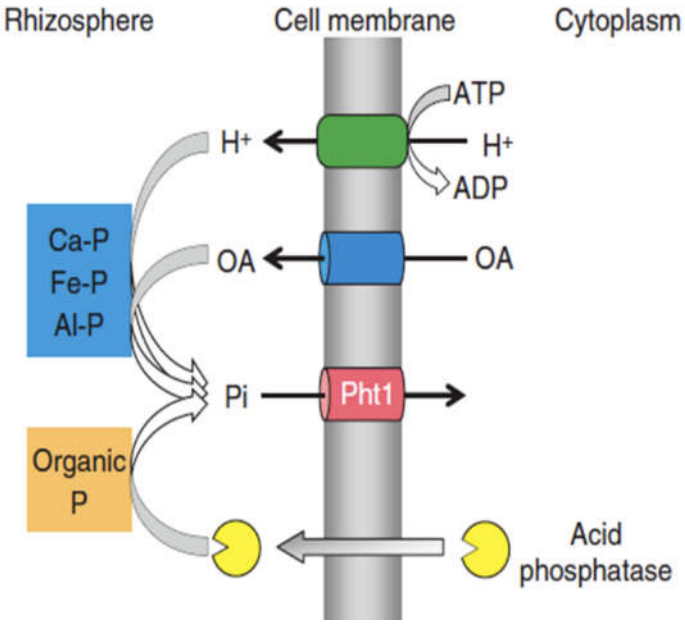

Figure 1.7 – Schematic representation of the mechanisms for P acquisition in plants (Hiradate et al., 2007)

1.2.3 Phosphorus translocation

Once Pi is taken up by the roots, it is loaded into the xylem vessels and *via* transpiration stream and root pressure subsequently translocated into shoots, where it is imported again into leaf cells. In rice (*Oryza sativa*) two genes encoding for phosphate transporters OsPht1;2 and OsPht1;6 with different kinetic properties are implicated in Pi translocation from roots to shoots (Ai et al., 2009). The putative regulators PHO1 and PHO1;H1 containing the SPX (for

SYG/PHO81/XPR1) tripartite domain also contribute to Pi translocation by loading Pi into the xylem (Hamburger et al., 2002; Stefanovic et al., 2007). Under Pi deficiency, Pi is re-distributed from the old fully expanded source leaves towards young sink leaves, a process requiring Pi transfer to the phloem vessel (Mimura, 1999). Moreover, in plants grown in Pi-sufficient conditions, a major portion of Pi is transported into the vacuole, whereas under Pi-deficient conditions, the anion is exported out of the vacuole in order to maintain a relatively stable cytoplasmic concentration of Pi (Mimura, 1999).

1.3 Functions of Root exudates

The main function of plant roots is the anchorage to the soil and the absorption of water and nutrients. However, roots are also able to release a large variety of inorganic and organic compounds (exudates) as well as root debris and even living cells (border cells) in the rhizosphere, generally defined as rhizodepositions (Uren, 2007). Collectively, rhizodeposition are responsible for inducing substantial changes in the chemical, physical and biological characteristics of the rhizosphere (Bais et al., 2004; Broeckling et al., 2008; Neumann and Römheld, 2007).

Root exudates carry out several functions relevant to plant-soil interactions, such as: (i) modulation of nutrient availability (Fe, P, Zn; Dakora and Phillips, 2002); (ii) root protection against toxic metals (e.g. Al, Zn, Cd; Jones, 1998) or pathogens (Bais et al., 2006); (iii) attraction and/or repulsion of microorganisms (Bais et al. 2006) and (iv) allelopathy, which is the chemical interactions that occur among plants in the rhizosphere. Root exudates include ions (H^+), inorganic acids, oxygen and water, but mainly carbon-based compounds (Uren 2007; Bais et al., 2006). These latter are further subdivided into two classes: (a) low-molecular weight (LMW) and (b) high-molecular weight (HMW) compounds.

The LMW exudates comprise amino acids, organic acids, carboxylic acids, phenolics, phytosiderophores, sugars and vitamins. Phenolics, phytosiderophores and carboxylates possess reducing/chelating properties towards the metal cations present in the rhizosphere; this action is important for modifying nutrient availability or to avoid metal toxicity. For example, in nutrient deficiency conditions these compounds are released to mobilize sparingly soluble compounds such as Fe and P. In particular, carboxylates released by dicotyledonous species (Neumann & Römheld 1999; Jones 1998) can mobilize poorly soluble calcium phosphates in alkaline and calcareous soils and iron/aluminium phosphates in acidic soils by ligand exchange, dissolution or

occupation of phosphorus sorption sites. In grasses, phytosiderophores are released under iron deficiency to increase iron availability and uptake; interestingly, these molecules are also able to mobilize useful amounts of zinc, manganese and copper in the rhizozpshere (Treeby et al. 1989; Römheld and Awad 2000).

The HMW exudates include mucilages and proteins, which are released via exocytosis in the rhizosphere. The role of mucigel is associated with lubrication of root allowing the movement through the soil, maintenance of proper root hydration and protection against toxic elements (*e.g.* Al); these actions would create a suitable environment for the growth and development of roots and rhizosphere microorganisms.

Table 1.1 - Possible functional roles of rhizodeposition and root exudates present in the rhizosphere (modified from Jones et al., 2004).

Compound	Rhizosphere Function
Phenolics	Nutrient source Chemoattractant signals to microbes Microbial growth promoters Nod inducers/inhibitors in rhizobia Resistance inducers against phytoalexins Chelators of poorly soluble mineral nutrients (e.g. Fe) Detoxifiers of Al Phytoalexins against soil pathogens
Organic acids	Nutrient source Chemoattractant signals to microbes Chelators of poorly soluble mineral nutrients Acidifiers of soil Detoxifiers of Al Nod gene inducers
Amino acids and phytosiderophores	Nutrient source Chelators of poorly soluble mineral nutrients Chemoattractant signals to microbes
Vitamins	Promoters of plant and microbial growth Nutrient source
Purines	Nutrient source
Enzymes	Catalysts for P release from organic molecules Biocatalysts for organic matter transformation in soil
Root border cells	Produce signals that control mitosis Produce signals controlling gene expression Stimulate microbial growth Release chemoattractants Synthesize defence molecules for the rhizosphere Act as decoys that keep root cap infection free Release mucilage and proteins
Sugars	Nutrient source Promoters of microbial growth

1.4 Root exudates: the role of phenylpropanoids

Root exudates included a wide range of compounds called secondary metabolites and synthetized through the phenylpropanoid pathway (Walker S.T et al., 2003).These are involved in overcoming biotic and abiotic stress conditions. Indeed, several studies demonstrated an increase of phenylpropanoid concentration in both roots and roots exudates under nutritional stresses as iron and phosphorus deficiency (Marschener, 1991; Ramakrishna A and Ravishankar GA, 2011; Vogt, 2010). The phenylpropanoid metabolism is a source of an enormous array of molecules deriving from efficient modification and amplification of a very restricted number of core structures. These compounds are produced from the shikimate pathway (Vogt, 2010), which is responsible of the aromatic aminoacids biosynthesis. Phenyalanine is a final product of this pathway. The first step in phenylpropanoid metabolism is catalysed by phenylalanine ammonia-lyase (PAL) which converts the phenyalanine in *trans*-cinnamic acid and ammonia. Several isoforms of PAL have been found in all plants species; for example four genes *PAL1-4* have been identified in Arabidopsis (Raes et al., 2003). The next enzyme involved in the synthesis, is a cytochrome P450, cinnamate 4-hydroxylase (C4H), which catalysed the hydroxylation of cinnamate to 4-coumarate. This compound is the substrate for the 4-coumarate:CoA ligase (4CL) responsible to the production of the CoA thioester 4-coumroyl CoA, better known as p-coumaroyl CoA. These are the early steps of the phenylpropanoid biosynthesis which lead to the common precursor for the breaching point to the pathway. Some of phenylpropanoid groups are lignings and lignans, phenolics and coumarins. Lignins are polymeric molecules involved in the reinforcement of cell walls meanwhile the correlated lignans play an important role in the plant defence against pathogens. The monolignol synthesis from the hydroxycinammic acids (HCAs) required aromatic hydroxilations, CoA ligations and O-methylations catalysed by p-coumaroyl shikimate 3’ hydroxylase (C3’H) and caffeoyl CoA 3-O-methyl transfarase (CCoAMT), leading to the ferloyl CoA production (Davies, 2004). Other three enzymes fundamental in the lignis and lignans production are Cynnamoyl-CoA reductase (CCR), caffeic acid/5’-hydroxyferulic acid O-methyltransferase (COMT) and Cinnamyl alchol dehydrogenase (CAD).

Phenylpropanoids are the largest class of phenolic plant metabolites, which includes more than 10.000 compounds and the number of new discovered molecules is continually increasing. These members perform several physiological functions in plants and their accumulation is a characteristic response of plant stresses. Furthermore, many evidences indicate that they could

manipulate the biological and chemical interactions between microorganisms and root system (Cheynier et al., 2013). One relevant subclass of phenolic compounds is represented by (iso) flavonoids. The first step in flavonoid biosynthesis is determined by the formation of chalcones, catalysed by chalcone synthase (CHS). The metabolic pathway continues with different enzymatic modifications to yield anthocyanins, flavones and flavonols. Other important enzymes are the chalcone reductase (CHR), flavone synthase (FNS) forming flavones, flavanone reductase (FNR) producing the 3-deoxyanthocyanin precursor, flavonol and isoflavone synthase (FLS and IFS) which catalyse the production of flavonols and isoflavonoids respectively.

The coumarins is another group of secondary metabolites expressed in all plant organs. They are characterized by a core structure, *i.e.* feruloyl CoA. Many studies reported that these molecules carry out several activities in plants. For example, in tobacco scopoletin is accumulated during a hypersensitive response (Gachon et al., 2004) and is correlated with virus resistance (Chong et al., 2002). Furthermore, in *Arabidopsis thaliana*, coumarins act as Fe chelators of in soils (Fourcroy et al., 2013; Schmid et al., 2013; Schmidt et al., 2014).

In plants coumarins can be divided in simple coumarins, furanocoumarins, and pyranocoumarins (Keating and O'kennedy, 1997). Simple coumarins present the hydroxy (-OH), alkoxy (-OR), and/or alkyl (-R) group(s) in their benzene ring. Moreover, their hydroxy group can be involved in conjugation to produce glycosides (Bayoumi et al., 2008b; Wu et al., 2009).

For the synthesis of simple coumarins, the *ortho*-hydroxylation is a fundamental step which is branch from the lignin biosynthetic pathway. This enzymatic reaction is catalysed by 2-Oxoglutarate-dependent dioxygenases (F6’h1), which convert cinnamate derivatives into simple coumarins (Shimizu BI, 2014).

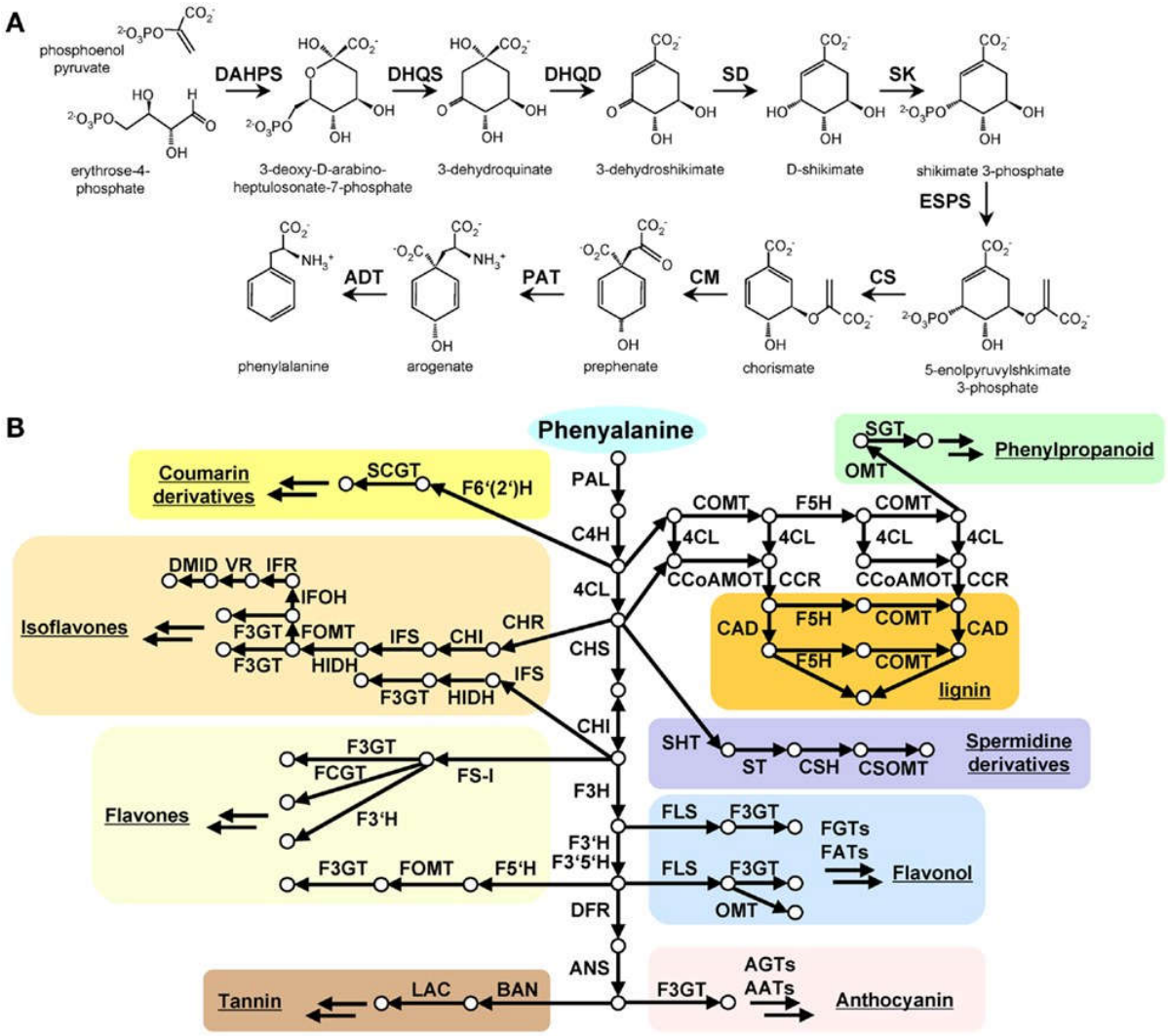

Figure - 1.8 Schematic representation of the A) Shikimate and phenylalanine biosynthesis and B) Phenylpropanoids pathway (Tohge T et al., 2013)

1.5 Release of root exudates: mechanisms and regulation

The release mechanisms of organic root exudates are still not fully understood (Mathesius and Watt, 2011). The release by plant roots was primarily thought to be a passive process mediated through three different pathways: diffusion, vesicle transport and ion channels or protein carriers (Fig. 1.9) (2007 Bertin et al., 2003; Neumann and Roemheld,). During the diffusion, small polar molecules and uncharged molecules move across the membranes and this mechanism is strictly dependent on membrane permeability (Guern et al., 1987) and cytosolic pH (Marschner, 2011). The release of compounds with high-molecular weight is usually mediated by vesicular transport

(Battey and Blackbourn, 1993). While the vesicle-mediated trafficking of proteins is well understood (Field, 2006), the mechanism of vesicle-mediated release of phytochemicals is not clearly characterized (Lin et al., 2003; Grotewold, 2004). Other compounds like amino acids, sugars, carboxylate anions are transported through protein carriers; their electrochemical gradient drives their direction movements from the cytosol of roots cells (millimolar concentration range) to the soil (micromolar concentration range). In the last years, other active transport mechanisms of root exudates have been characterized which involve ABC (ATP-Binding Cassette) transporters and multidrug and toxic compound extrusion (MATE) transporters (Yazaki 2005; Pii et al. 2015). The former mechanism involves primary transport directly energized by ATP hydrolysis while the latter depends on a H^+ gradient-dependent secondary transport. The qualitative and quantitative characteristics of root exudation are strictly dependent both on the plant species and the plant age and they are strongly influenced by biotic and abiotic factors, including stress conditions.

The plant responses to different kind of stresses produce a number of chemicals whose functions are reasonably related to protection against negative effects and promotion of positive interactions with microorganisms. In fact, environmental factors such as temperature, light and soil moisture modulate root exudation processes. Exudation of tannins and phenolic compounds in *Vicia faba* has been shown to be highly reduced at 4 °C as compared to the amounts released at 30 °C (Bekkara et al., 1998).

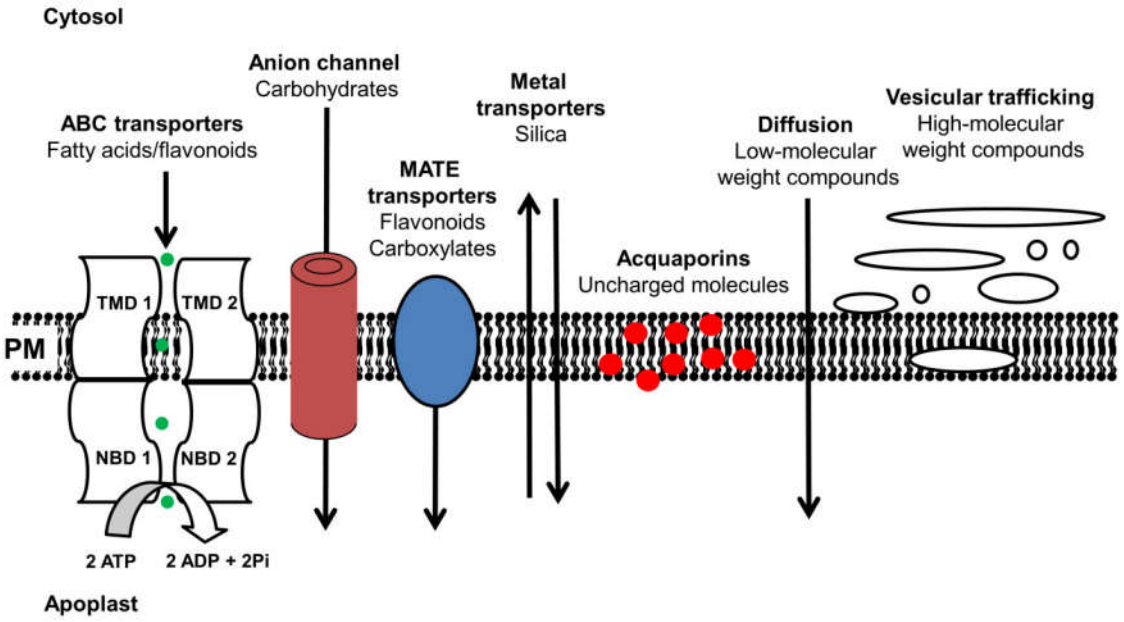

Figure 1.9 - Mechanisms of root exudation of different compounds through the plant cell membrane (Modified from Badri and Vivanco, 2009).

Similarly, light intensity can affect the exudation of secondary metabolites because of changes in photosynthesis rate (Watt and Evans, 1999). Also the availability of essential nutrients in the soil or the presence of toxic compound can greatly influence the exudation pattern (Bardi and Vivanco, 2009). Moreover, Gleba et al. (1999) proposed that the higher release of root exudates by plants in response to stresses is due to elicitors, defence signalling molecules that stimulate and influence the phytochemicals production and secretetion..In fact the elicited plants exudate compounds not found in root exudates of non- elicited plants. For example, Kneer et al. (1999) showed that roots of hydroponically cultivated *Lupinus luteus* secrete genistein, which was induced 10-fold by salicylic acid, an elicitor compound**.** In addition, a single elicitor can trigger induction of different compounds indifferent plant species (Bradi and Vivanco, 2009).

1.5.1 ABC transporters

The ATP-binding cassette transporter (ABC transporters) family include a large number of proteins identified in all phyla (Higgins, 1992). In the model plant *Arabidopsis thaliana*, the

number of ABC transporters exceeds that one reported for both yeasts (Decottignies and Goffeau, 1997) and humans (Dean et al., 2001). This is probably due to the high number of secondary metabolites produced by plants and to the necessity to excrete them from the cytoplasm (in the apoplast or other cellular compartments), avoiding toxicity (Dixon, 2005). They are classified into 13 subfamilies in relation to their size, orientation (forward or reverse), and the sequence similarity (Sanchez-Fernandez et al., 2001). Well-characterized ABC transporters in plants belong to three subfamilies (Fig. 1.10): MRP (multidrug resistance-related protein), PDR (pleiotropic drug resistance protein) and PGP (multidrug resistance P-glycoproteins). ABC transporters are primary active transporters that use the energy from nucleotide triphosphate hydrolysis to translocate solutes across cellular membranes. Loyola-Vargas et al. (2007) have shown that root exudative profiles in Arabidopsis was modified in presence of inhibitors such as cyanide, sodium orthovanadate, verapamil, nifedipine, glibenclamide, which are able to affect the cellular availability of ATP. Recently, the involvement of these ABC transporters in the processes of roots secretion was clearly demonstrated by Badri et al. (2009); using *Arabidopsis thaliana* knock-out mutants for three genes encoding ABC transporters, these authors could show the ability of those protein to transport three distinct compounds.

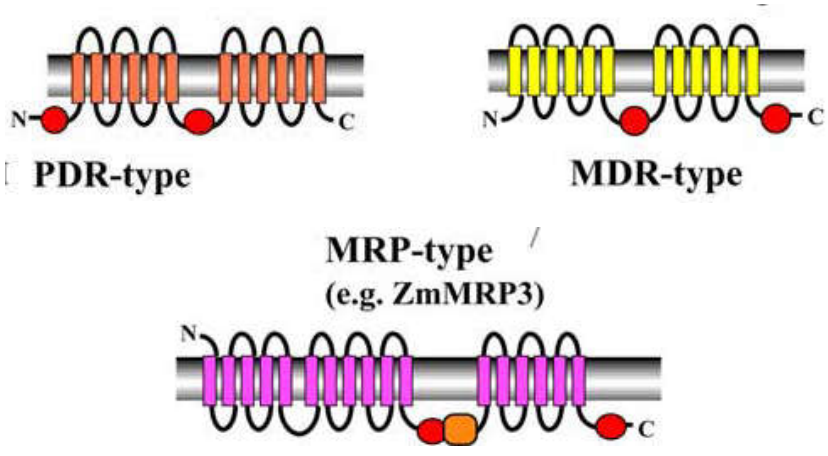

Figure 1.10 - ABC transporter topology for the PDR, MRP, PGP subfamilies. The trans-membrane hydrophobic (TMD – *Transmembrane Domain*) and ATP binding domains (NBD – *Nucleotide Binding Domain*) are represented for the different subfamilies (Yazaki, 2005).

1.5.2 MATE transporters

The Multidrug and toxic compound extrusion (MATE) transporters were firstly identified as a bacterial drug transporter family, involved in the exporting of several antimicrobial agents and thus conferring multidrug resistance (Kuroda & Tsuchiya 2009). However, these transporters are present in almost all prokaryotes and eukaryotes. In bacteria, the MATE transport activity is coupled either to the antiport of Na^+ or H^+; on the contrary, in eukaryotes only H^+-coupled antiport activity has been described. In the bacteria 9 - 13 genes encoding MATE proteins are present, while in mammalians the number is lower, with two members in humans and mice, and three in dogs (Omote et al., 2006). On the other hand, MATE transporters in plants are very abundant; in *Arabidopsis* there are 56 sequences encoding for these transporters, which localize to the plasma membrane, in the tonoplast or in the chloroplast membrane (The Arabidopsis Genome Initiative, 2000). This abundance is probably due to their involvement in the excretion of a wide array of metabolic waste products, which could be toxic for plants. In fact, the molecules transported by MATE are very different one from each other (Li et al., 2002 b). In *Arabidopsis* two MATE transporters mediate citrate excretion out of the cytosol, they are AtMATE (Liu et al., 2009) and AtFRD3 (Durrett et al., 2007). AtMATE confers aluminium tolerance allowing citrate release into the soil in response to the exposure to Al^{3+} (Magalhaes et al. 2007; Furukawa et al., 2007; Liu et al. 2009; Sbabou et al. 2010). By contrast, AtFRD3 is involved in the excretion of citrate into the xylem, and it is required for long distance Fe transport and uptake into the leaves (Durrett et al., 2007; Rogers and Guerinot, 2002; Green and Rogers, 2004). The topology of these MATE and their homologues identified in other plants presents a long cytosolic loop between the second and the third transmembrane α-helix (Fig. 1.11).

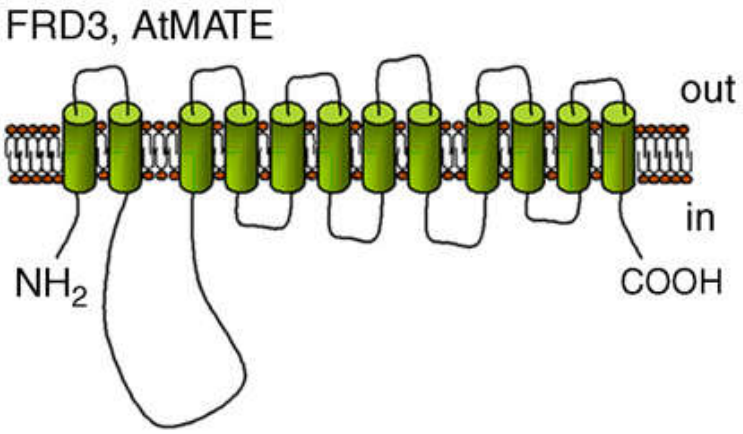

Figure 1.11 - Putative topology of a MATE transporter (Meyer et al., 2010).

1.5.3 ALMT transporters

Aluminium-activated malate transporters (ALMT) is another family of transporters which facilitates the diffusion of carboxylate compounds into the rhizosphere if toxic levels of Al^{3+} are reached in the soil. TaALMT1 has been identified in *Triticum aestivum* as the first specific channel for malate transport (Sasaki et al., 2004). *TaALMT1* encodes a hydrophobic protein formed by 6 to 7 transmembrane domains (Motoda et al., 2007) with N- and C-terminal localized in the extracellular side of the plasma membrane (Fig. 1.12). This transporter is constitutively expressed in the root tips, but it is also activated in the presence of aluminum in the apoplast, conferring resistance to wheat cultivars that possess this gene. Furthermore, in model organisms, the heterologous expression of *TaALMT1* allowed the efflux of malate activated by the presence of Al^{3+}, providing increased resistance to this metal (Delhaize et al., 2004). Homologous proteins have been identified in other plant species and numerous studies have shown that these have similar function to TaALMT1. Neverthless, *ZmALMT1*, expressed in Xenopus oocytes, was shown to have a role in the transport of anions (eg. Cl^-) rather than a specific function in the release of carboxylates in response to aluminum toxicity (Piñeros et al., 2008). In *Arabidopsis,* AtALMT protein family consists of 14 members that can be divided into three clades. AtALMT1 belongs to the same clade of TaALMT1, and it is localized on root cells plasma membrane, where it mediates the release of malate in response to aluminum toxicity (Hoekenga et al., 2006). The presence of the toxic element is required not only for the activation of AtALMT1, but also to induce its own expression. This type of mechanism is also described in *Brassica napus* for

BnALMT1 and BnALMT2 (Ligaba et al., 2006). AtALMT9 is a member of the second clade and is localized on the tonoplast in particular in the leaves mesophyll (Kovermann et al., 2007). Several studies demonstrated that AtALMT9 is more involved in the malate homeostasis than in the Al^{3+} tolerance toxicity). Recently, special attention is given to the ALMT members of the third clade, because their functionsare still uclear.

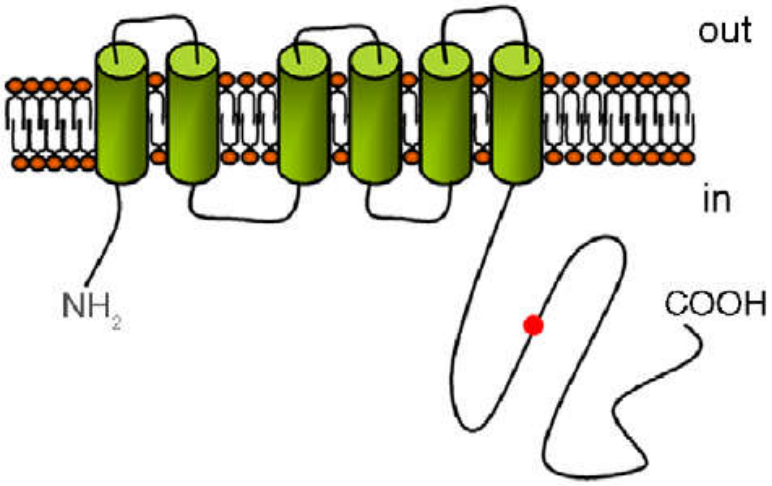

Figure 1.12 - Putative topology of an ALMT channel (Meyer et al., 2010)

2. OBJECTIVES

By 2050, the world population is predicted to increase up to 9 billion, for this reason there is a need to increase the production of food and therefore crop productivity. Up to now, obtaining a high crop yields was strongly dependent on the use of external fertilizers inputs; however even if there was a high increase in the utilization of these compounds in the last 50 years the productivity did not increase with the same trend as before. This is mainly due to the achievement of a plateau in the use efficiency of nutrients (NUE) by plants. Thus, mproving NUE is a challenge for plant breeders. To accomplish this task, a deep comprehension of soil-plant relationships and of plant mechanisms involved in nutrient acquisition is required.

It is known that phosphorus and iron are among the main nutrients responsible for determining the quality and quantity of the yield. In fact, both P and Fe are poorly available in well-aerated soils, including acid (P) and alkaline (P and Fe) soils. To address these nutritional problems, plants release in the soil a wide range of molecules, called root exudates, which modify the chemical, biological and physical characteristics of the rhizosphere, allowing the mobilization of the two nutrients.

Maize (*Zea mays*, L.), a graminaceous plant, it is one of the most widespread cereals both for human and animal consumption in the world. For this reason, this plant has been used in this PhD thesis to study the root trascrittoma of Fe-deficient maize and the capacity to take up Fe, supplied as a sparingly soluble form (Ferryhidrite) or as soluble complexing made up between Fe and natural chelating agents normally occurring in the rhizosphere (Fe-phytosiderophores (Fe-PS) or Fe-citrate). Moreover, the alterations induced by Fe deficiency on P acquisition has been studied.

Another plant used in this thesis is white lupin (*Lupinus albus* L.), which is considered a model for root exudation studies. In fact, it utilized a highly efficient strategy to mobilize sparingly available nutrients, in particular Fe and P, from soils. This strategy is based on the modification of the root architecture with the formation of cluster roots, from which organic acids and phenolic compounds are release in massive amounts. Although the response to P deficiency is generally well characterized, the mechanisms involved in the release of root exudates in Fe-deficient plants are still barely known. For this reason, the comparison of the response to Fe or P deficiency by plants has been performed studying the physiological, biochemical and transcriptional changes induced by these nutritional stresses.

The determination of the composition of root exudates is fundamental to understand how plants carry out the adaptation to specific adverse soil conditions. Through a metabolomics approach, the different exudation pattern was analysed for the different growth conditions and the root content was also investigated.

In addition, after the identification of the main compounds present in the exudates solution, like *e.g.* genistein, a molecular approach was undertaken in order to identify and functionally characterize the transporters putatively involved in their release.

Considering, for example, that calcareous soils represent one-third of the earth's surface the P- and Fe-nutritional disorders are very common and affects different plant species. In this PhD thesis, the study was extended to a fruit tree, *i.e.* apple tree. The characterization of the exudation pattern of *Malus x domestica* Borkh. plants grown under control, P- or Fe-deficient conditions was performed. Moreover, a differential gene expression analysis based on the RNA-seq technique has been undertaken in roots of these plants.

3. TRANSCRIPTIONAL AND PHYSIOLOGICAL ASPECTS OF FE DEFICIENCY IN ROOTS OF *ZEA MAYS*

Transcriptional and physiological aspects of Fe deficiency in roots of *Zea mays*

Laura Zanin[1], Silvia Venuti[1], Anita Zamboni[2], Zeno Varanini[2], Nicola Tomasi[1] and Roberto Pinton

[1] Dipartimento di Scienze Agroambientali, Alimentari e Animali, University of Udine, via delle Scienze 208, I-33100 Udine, Italy

[2] Dipartimento di Biotecnologie, University of Verona, Ca' Vignal 1- Strada Le Grazie 15, I-37134 Verona, Italy

Abstract

Plants respond to iron (Fe) deficiency using different adaptive strategies. Under limited Fe availability maize, a model species for *Strategy II* plants, improves Fe acquisition through the release of phytosiderophores (PS) into the rhizosphere and the subsequent uptake of Fe-PS complexes into root cells.Transcriptomic analysis on maize root tissues (NimbleGen microarray) revealed that the Fe-deficiency modulated the expression levels of 724 genes (508 up- and 216 downregulated, respectively). As expected, roots of Fe-deficient maize plants overexpressed genes involved in the synthesis and release of 2'-deoxymugineic acid (the main PS released by maize roots). A strong modulation of genes involved in regulatory aspects, Fe translocation, root morphological modification, in primary metabolic pathways and in hormonal metabolisms were induced by the nutritional stress.

The capability of maize plants to respond to Fe-deficiency was further evaluated exposing roots to soluble or poorly soluble Fe-sources for up to 24 hours. Real time RT-PCR analyses and ^{59}Fe uptake experiments showed that the mechanisms involved in Fe acquisition were induced by the nutritional stress; while the pathways involved in the translocation and distribution of the micronutrient within the plant were strongly activated only in Fe-sufficient plants. Moreover, the capability of Fe-deficient plants to acquire ^{32}P from readily- or scarcely-available forms was also investigated. Under Fe starvation, maize plants accumulated higher amounts of P than the Fe sufficient ones, both in roots and shoots. Consistent with this data, the root transcriptomic profile of Fe deficient plants showed that some genes encoding P transporters were positively modulated by iron starvation. Furthermore, the use of soluble Fe-sources, especially Fe-PS, allowed the acquisition and remobilization of P from poorly soluble sources.

Data here presented highlighted on the transcriptomic and physiological changes occurring in maize plats under Fe deficiency. Morover results showed that the mechanisms activated in roots

under Fe-deficiency may led to a synergistic effect in the remobilization of other nutrients than iron, like phosphorus.

3.1 Introduction

Iron deficiency is a yield-limiting factor and a worldwide problem for crop production in many agricultural regions, particularly in aerobic and calcareous soils (Mengel et al., 2001). Although the total Fe content of soils would be sufficient to meet plants requirements, most of the Fe in the soil is present in poorly available inorganic forms, especially under aerobic conditions (Lindsay, 1974). The level of plant-available Fe in the soil solution is determined by a variety of natural ligands (such as microbial siderophores, humic substances and root exudates) which are able to mobilize Fe from oxides/hydroxides forming Fe(III)-chelates (Lindsay and Schwab, 1982).

It is well known that plants react to low Fe availability using different adaptive strategies. All dicots and non-graminaceous monocots respond to Fe-deficiency by decreasing rhizosphere pH and reducing sparingly soluble ferric iron. This reductive mechanism is also known as *Strategy I* and involves the release of protons and chelating and/or reducing agents (as carboxylates and phenolic compounds) from roots into the rhizosphere. Thereafter, an enzyme at the surface of root cells (ferric chelate reductase, FRO) mediates the reduction of ferric ions to ferrous form (Chaney et al., 1972; Robinson et al., 1999). The reduced ferrous iron is then acquired by roots through a Fe^{2+} transporters belonging to the ZIP metal transporter family (iron regulated metal transporter, IRT; Eide et al., 1996).

Alternatively, graminaceous species like maize, improve Fe acquisition through the release of phytosiderophores (PS) into the rhizosphere, by the action of the PS transporter TOM1 (Nozoye et al., 2011, Nozoye et al., 2013). Iron is then taken up from the rhizosphere into the root cells as Fe(III)-PS complexes through a specific transporter, yellow stripe1 (YS1, Kobayashi and Nishizawa, 2012). Furthermore, in grasses the presence of other *Strategy I*-like mechanisms has been shown that could be involved in the Fe acquisition process (Ishimaru et al., 2006). In rice, and possibly in other monocots, the presence of IRT-like protein and natural-resistance-associated-macrophage protein (NRAMP, also known as divalent metal transporter) has been reported to play important roles in the absorption and translocation of ferrous Fe (Bughio et al., 2002; Ishimaru et al., 2006; Takahashi et al., 2011; Ishimaru et al., 2012a,b). Also in maize, homologous of OsNRAMP transporter have been identified and reported as responsive to Fe-

deficiency (Nozoye et al, 2013). Moreover, besides the efflux of phytosiderophores, rice plants (and possibly other grasses) possess an efflux transporter for phenolic compounds (phenolics efflux zero-like transporter, PEZ; Bashir et al., 2011), which is an essential component for iron solubilisation in the apoplastic space. In this way, in monocot species like maize, the low Fe-availability seems to be counteracted by the activation of some components, not exclusively relating to *Strategy II*, which might involve the acidification of the rhizosphere and the acquisition of ferrous iron forms.

Based on these assumptions, the presence of phenolic compounds and carboxylates in the rhizosphere would help the overall solubilisation of iron, which in turn might be taken up by maize roots through the Fe(III)-PS transporter (YS1) or, possibly, as ferrous form by IRT-like/NRAMP transporters.

As it might be expected, the biosynthesis in plants and the release into the rhizosphere of some root exudates interact with the uptake of other nutrients. Several studies have shown that a low Fe availability can trigger molecular responses linked to sulphur (S, for PS synthesis, Ciaffi et al., 2013) and also to phosphorus (P) metabolism (Zheng et al., 2009). While the interactions between Fe and sulphur nutrition has been well established, there is still a lack of knowledge about the effect of Fe deficiency on P nutritional status in plants. In rice seedlings, evidences have been provided about antagonistic interactions between Fe and P nutrition. A P-deficiency condition resulted in a significant increase in Fe content of plants while, on the other hand, the presence of P limits Fe concentration in plant tissues (Zheng et al., 2009). In plants, this antagonistic interaction might be due to the mechanisms used by plants to recover poorly soluble source of Fe and P from soils, *i.e.* by releasing organic acids and phenolic compounds (for review see Hirsch et al., 2006).

The aim of the present work was to study, at physiological and transcriptional level, the Fe-deficiency response in maize plants, an economically important crop. Starting from morphological observations, we characterized the maize root transcriptome. Moreover deep investigations were conducted to evaluate the capability of maize plants to use different Fe sources, such as Fe-Citrate, Fe-PS and Ferrihydrite.

3.2 Materials and methods

3.2.1 Plant material and growth conditions

Maize seeds (Zea mays L., inbred line PR33T56, Pioneer Hybrid Italia S.p.A.) were germinated over aerated 0.5mM $CaSO_4$ solution in a dark growth chamber at 25°C. Five-day-old seedlings were transferred in a continuously aerated Fe-free nutrient solution (containing, µM: NH_4NO_3 1000; $CaSO_4$ 500; $MgSO_4$ 100; KH_2PO_4 175; KCl 5; H_3BO_3 2.5; $MnSO_4$ 0.2; $ZnSO_4$ 0.2; $CuSO_4$ 0.05; Na_2MoO_4 0.05; buffered solution to pH 6.0 with 2.5 mM MES-KOH) and plants were grown for 7 days in a growth chamber under controlled climatic conditions (day/night photoperiod, 16/8 h; radiation, 220 µ Einsteins m^{-2} s^{-1}; day/night temperature, 25/20 °C; relative humidity, 70-80 %). Thereafter, some 12-day old plants were maintained for a further week under Fe-deficiency (Fe-deficient plants), while some of 12-day-old maize plants were transferred to a Fe-sufficient nutrient solution containing 100 µM Fe-EDTA (Fe-sufficient plants). Nutrient solutions were replaced every three days with fresh solutions. During the growth period, light transmittance of leaves was determined on 12 day old plants, 15-day old plants and 19-day old plants using a portable chlorophyll meter SPAD-502 (Minolta, Osaka, Japan) and presented as SPAD index values.

After 14 days of growing in Fe-free nutrient solution, 19-day-old maize plants showed visual symptoms of Fe deficiency (interveinal yellowing of the young leaves; increase in the diameter of the sub-apical zone and amplified root hair formation). The capability of Fe-deficient and Fe-sufficient plants to acidify the rhizosphere was investigated using the pH indicator bromocresol purple. Thus, whole root systems of intact plants were placed on a 3-mm-thick gel layer containing 0.9 % agar, 0.01 % bromocresol purple and buffered at pH 5.5 with 1 M KOH.

Elemental analyses were assessed on roots and shoots of 19-day old Fe-deficient and Fe-sufficient plants. Samples of roots and leaves were dried, ashed at 550° and digested with H_2O_2. Thereafter, samples were diluted with 3.75% HNO_3 and filtered through a Whatman WCN 0.2 µm membrane filter. Iron, Ca, K, Mg, Mn, Na, P, S and Zn concentrations (ppm) were then determined by ICP-OES (VISTA-MPX, Varian Inc., Palo Alto, USA).

For microarray analyses, roots of Fe-deficient and Fe-sufficient maize plants (19-day-old) were harvested three hours after the beginning of light phase. The collected roots were immediately frozen in liquid nitrogen and stored until further processing at -80°C. Sample collection was

repeated in three independent cultivations and the roots from six plants were pooled for each treatment.

3.2.2 Microarray analyses

RNA extraction was performed using the Invisorb Spin Plant RNA kit (Stratec Molecular) as reported in the manufacturer's instructions. Maize roots (70 mg) were homogenized in liquid nitrogen and the powder was mixed with 0.9 ml of DCT solution and dithiothreitol according to the supplier's instructions. The RNA quality and quantity were determined using a Bioanalyzer Chip RNA 6000 series II (Agilent).

For the microarray analyses, three independent biological replicates were used, for a total of 6 hybridizations. The cDNA synthesis, labeling, hybridization and washing reactions were performed according to the NimbleGen Arrays User's Guide (http://www.nimblegen.com/). Each hybridization was carried out on a NimbleGen microarray (Roche, NimbleGen Inc.), representing 59,756 transcripts predicted from the B73 reference genome (http://ftp.maizesequence.org/current/filtered-set/ZmB73_5b_FGS_cdna.fasta.gz). A complete description of the chip is available at the Gene Expression Omnibus (http://www.ncbi.nlm.nih.gov/geo) under the series entry (GPL17540). The microarray was scanned using an Axon GenePix 4400 (Molecular Devices) at 532nm (Cy-3 absorption peak) and GenePix Pro7 software (Molecular Devices) according to the manufacturers' instructions. Images were analyzed using NimbleScan v2.5 software (Roche), which produces Pair Files containing the raw signal intensity data for each probe and Calls Files with normalized expression data- (quantile normalization) derived probe summarization through RMA analysis (Irizzary et al. 2003). Analysis of normalized data (Calls Files) was performed using the open source software of the Bioconductor project (Gentlemen et al. 2004; http://www.bioconductor.org) with the statistical R programming language (Ihaka and Gentleman 1996; http://www.r-project.org). Differentially expressed probes were identified by linear model analysis (Smyth 2005) using the LIMMA package and applying Bayesian correction, adjusted P-value ≤ 0.05, n=3, FC $\geq |1.5|$.

Physiological and transcriptional experiments with natural Fe sources: FePS, FeCitrate and Ferrihydrite

3.2.3 Preparation of soluble sources

FePS and FeCitrate were prepared according to von Wirén et al. (1994) by mixing an aliquot of Fe-free (epi-HMA)-containing root exudates collected from Fe-deficient barley plants (Tomasi et al., 2013) or citrate (10% excess) with $FeCl_3$. Fe concentration of the Fe sources was measured by inductively coupled plasma atomic emission spectrometry (ICP-AES) before their use for plant treatments. Two different KH_2PO_4 (Sigma, Adrich) solution were prepared to a different final concentration, 10 μM or to 175 μM.

3.2.4 Preparation of poorly soluble sources

Amorphous Fe hydroxide was obtained by precipitating $^{59}Fe(NO_3)_3$ at alkaline pH, with the addition of 1 M KOH (Guzman et al. 1994). The synthetic vivianite was obtained as described in Eynard et al. (1992) through the slow neutralization of 50 mM $FeSO_4$ in 35 mM H_3PO_4 with 50 mM KOH at room temperature. The pH of the mixture was brought up to 6, where the precipitation of a blue-grey powder occurred. The powder was washed via centrifugation with distilled water to remove the presence of salt. One milliliter of suspension containing respectively or ^{59}Fe-hydroxide (2 μmol Fe) or ^{32}P-vivianite (2 μmol P) was transferred into a dialysis tube (ZelluTrans/Roth 6.0, Ø16 mm, exclusion limit of 8-10 kDa, ROTH, Karlsruhe, Germany) and mixed with 8 ml of a nutrient solution with the following composition (mM): 0.7 K_2SO_4, 0.1 KCl, 2.0 $Ca(NO_3)_2$, 0.5 $MgSO_4$, 0.1 KH_2PO_4, and 10.0 2-(N-morpholino) ethanesulfonic acid -KOH at pH 6.0.

3.2.5 Iron (^{59}Fe) uptake from soluble and poorly soluble sources by maize plants

To evaluate the capability of Fe-deficient plants to use natural Fe sources, physiological and transcriptional experiments were performed on 19-day old intact maize plants.

The day before of the experiment, roots of (18-day old) Fe-deficient and Fe-sufficient plants were washed 3 times with deionized water. Then, two intact plants were transferred to beakers containing 230 ml of a freshly prepared Fe nutrient solution. The next day, FePS, FeCitrate or Ferrihydrite were added to give a final Fe concentration of 1 μM and the treatment solutions were buffered at pH 6.0 with 10 mM MES-KOH. The photochemical reduction phenomena of Fe in the nutrient solution (Zancan et al. 2006), was limited covering the beakers with black plastic foils during the entire experiment. During the time span of 24 hours (after 1, 4, and 24 hours)

root samples were harvested, frozen in liquid nitrogen and used for the gene expression analyses. The same experimental setup was used for radiochemical analyses where the treatments were performed at a final Fe concentration of 1 μM ^{59}FePS, ^{59}FeCitrate or (^{59}Fe)Ferrihydrite and at a specific activity of 144 kBq μmol-1 Fe (Perkin Elmer, Monza, Italy). At each time-point (1 and 24 hours of treatment) plants were transferred into cold deionized water for 10 min in order to stop Fe uptake and remove the excess of ^{59}Fe at the root surface. Root apoplastic 59Fe pools were removed as described by Bienfait et al. (1985), raising roots in a solution (1.2 g l−1 sodium dithionite, 1.5 mM 2,2′-bipyridyl and 1 mM $Ca(NO_3)_2$ under N_2 bubbling gas. After roots and leaves were harvested and collected separately in vials. Root and shoot tissues were oven dried at 80°C, weighed, ashed at 550 °C, and suspended in 1 M HCl for ^{59}Fe determination by liquid scintillation counting. The ^{59}Fe accumulation was measured as nanomoles of ^{59}Fe and is presented as nmol ^{59}Fe * g^{-1} root Dry Weight.

3.2.6 Real-time RT–PCR experiments

To validate the microarray results and to analyze in a time-course the expression profile of some genes during 24 hours of Fe-source treatments, real-time RT–PCR analyses were performed. Total RNA was treated with 1 U μg-1 RNA of DNase I (Sigma Aldrich) and cDNA was synthesized from 1 μg of RNA following the application protocol of the manufacturers [42°C for 1 h with 1 pmol of oligod(T)23VN (Sigma Aldrich); 15 U of Prime RNase Inhibitor (Eppendorf); 10 U of M-MulV RNase H– (Finnzymes)]. After RNA digestion with 1 U of RNase A (USB) for 1 h at 37°C, gene expression analyses were performed by adding 0.16 μl of the cDNA to the real-time RT-PCR complete mix, FluoCycleTM sybr green (20 μl final volume; Euroclone, Pero, Italy), in a C1000 Thermal Cycler-Bio-Rad CFX96 real-time PCR detection system (Bio-Rad). The analyses of real-time RT-PCR result were performed using Bio-Rad CFX Manager v.2 software (Bio-Rad).

Real-time RT-PCRs analyses were performed to evaluate the expression level of most interesting identified by microarray and the modulation of these genes was monitored during the time span of Fe-treatments (Fig. 3.7). The primers were designed using Primer3 software (Koressaar and Remm 2007, Untergrasser et al. 2012) and they were synthesized by Sigma Aldrich (gene model ID, forward and reverse primer sequences 5'- -3'): ZmYS1 (GRMZM2G156599, AGGAGACAAGAACGCAAGGA and ACTGAACAAAGCCGCAAACT), ZmTOM1 (GRMZM2G063306, AGGAGTTCTTCTTCGTCGCA and GCACCAAGAAAACCAGCGTA),

ZmOPT7 (GRMZM2G421491, TCGTCTGGAAGGAGGAGATG and CGGTTGCTGGTTAGTGGTG), ZmNRAMP1 (GRMZM2G178190, GGAGAATTATGGCGTGAGGA and ACCACCAAACCGATCAGAAG), ZmFerritin (GRMZM2G325575, GATGCTGCTTGAGGAAGAGG and CCGACCCAGAGTTGTCAGTT), ZmPHT1;7 (GRMZM2G112377, TCCTGATGATGACGGTGTTC and GAAGTTGGCGAAGAAGAAGG).

The analyses of real-time results were performed using Bio-Rad CFX Manager v.2 software (Bio-Rad) and R (version 2.9.0; http://www.r-project.org/) with the qPCR package (version 1.1-8; http://www.dr-spiess.de/qpcR.html). Efficiencies of amplification were calculated following the authors' indications (Ritz and Spiess 2008). Real-time RT–PCR results were validated using two housekeeping genes, ZmGAPDH (GRMZM2G046804, CCTGCTTCTCATGGATGGTT and TGGTAGCAGGAAGGGAAGCA) and ZmTUA (GRMZM2G152466, AGGTCATCTCATCCCTGACG and TGAAGTGGATCCTCGGGTAG). In the Fig. 3.7, results normalized on ZmGAPDH are shown. Data were normalized with respect to the transcript level of the housekeeping genes using the 2–ΔΔCT method, where $\Delta\Delta CT = (CT_{Target} - CT_{HK})_{Time\ x} - (CT_{Target} - CT_{HK})_{Time\ 0}$ (Livak and Schmittgen, 2001).

3.2.7 Phosphorus (^{32}P) uptake from soluble and poorly soluble sources by maize plants

To investigate the effect of natural Fe-sources on the acquisition of phosphorus in plants, (19-day old) Fe deficient and Fe sufficient maize plants were treated with three unlabeled-natural Fe sources (FeCitrate, FePS and Ferrihydrite), as reported above. Moreover, nutrient solution contained also (^{32}P)-radiolabeled sources, as the soluble source (^{32}P) KH_2PO_4 or the poorly soluble source (^{32}P)Vivianite.

Before starting the assay, the roots were washed 2 times for 5 minutes in 0.5 mM $CaSO_4$, in order to remove the apoplastic component. Afterwards the plants were transferred into the uptake solution, buffered to pH 6.0 with 10 mM MES-KOH and containing phosphorus supplied as KH_2PO_4 or vivianite labeled with ^{32}P in an amount equal to 2.47 kBq μmol^{-1}. After 24 hours, root and leaves of maize plants were sampled and the phosphorus accumulation in the tissues was determined. Root samples were transferred for 5 minutes in a cold washing solution. In this way, the apoplastic radioactive component was removed and the uptake of 32P was blocked. Roots and leaves were harvested and collected separately and oven dried at 80°C, weighed,

ashed at 550 °C, and suspended in 1 M HCl. The determination of ^{32}P concentration was performed by liquid scintillation counting. The ^{32}P accumulation, measured as nanomoles of ^{32}P and is presented as nmol ^{32}P * g^{-1} root Dry Weight.

3.2.8 Statistical analysis

Physiological and transcriptomic analyses were performed on three independent biological replicates obtained from independent experiments (n = 3); for each sample a pool of six plants was used. Statistical significance was determined by one-way analysis of variance (ANOVA) using Student–Newman–Keuls test ($P < 0.05$, n = 3). Statistical analyses were performed using SigmaPlot Version 12.0 software. Statistical analysis of microarray data was performed using linear model analysis (Smyth 2005) of the LIMMA package after Bayesian correction with Bioconductor software, adjusted P-value ≤ 0.05, n=3, FC ≥ |1.5| (for details see the 'Microarray analyses' section).

3.3 Results

3.3.1 Morphological comparison between Fe-deficient and Fe-sufficient maize plants

At the end of the growing period, plants grown withut Fe supply showed typical symptoms of Fe-deficiency (Fig. 3.1, Fig. 3.2, Fig. S3.1). Indeed Fe-deficient plants showed visible interveinal yellowing of the young leaves (Fig. 3.1A, B) and a reduced chlorophyll content (SPAD index value, Fig. 3.2). The nutritional status induced changes also at the root level, with -Fe plants showing shorter roots and an increase in the diameter of the root tips (Fig. 3.1C, D). In particular, the sub-apical root zone of Fe-deprived plants showed high density of root hairs with a concomitant acidification of the external solution (Fig. S3.1). The effect of Fe deficiency was also evaluated by elemental analyses of macro and micronutrients accumulated in plants tissues (Fig. 3.3). As expected, Fe-deficient plants accumulated low amounts of Fe and, only in roots, low amounts of S. On the other hand, under Fe shortage, maize plants accumulated high amounts of manganese (Mg), zinc (Zn), P and, only in leaves, calcium (Ca) and sodium (Na, Fig. 3.3).

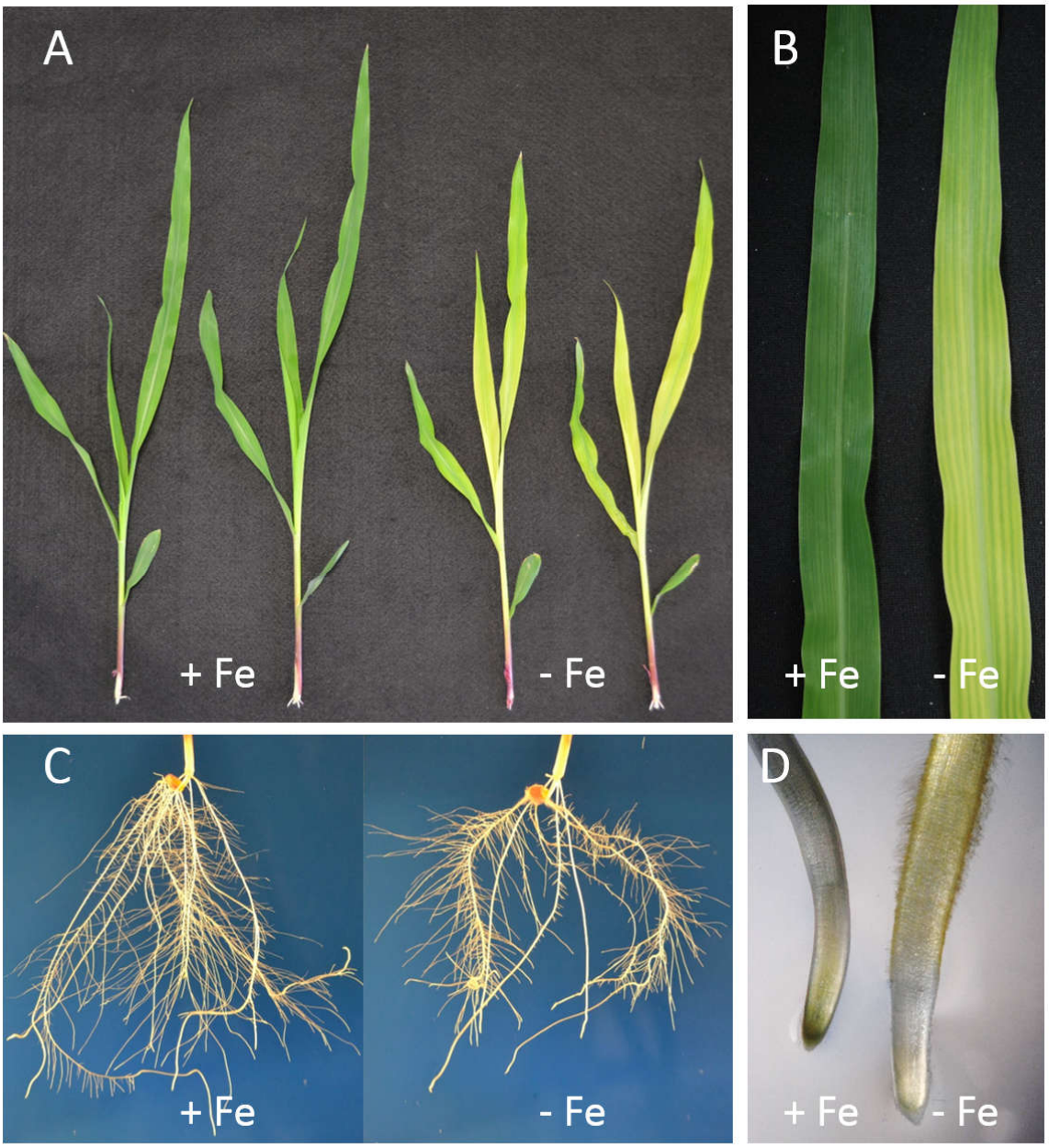

Figure 3.1 - Shoot and root apparatus of maize plants grown under different Fe-supply conditions. A, shoots of Fe-sufficient plants (left) and shoots of Fe-deficient plants (right); B, leaf details of Fe-sufficient (left) and Fe-deficient (right) plants. C, roots of Fe-sufficient plants (left) and roots of Fe-deficient plants (right); D, details of root tips of Fe-sufficient (left) and Fe-deficient (right) plants after soaking roots with pH indicator (Bromocresol purple), as indicated in materials and methods.

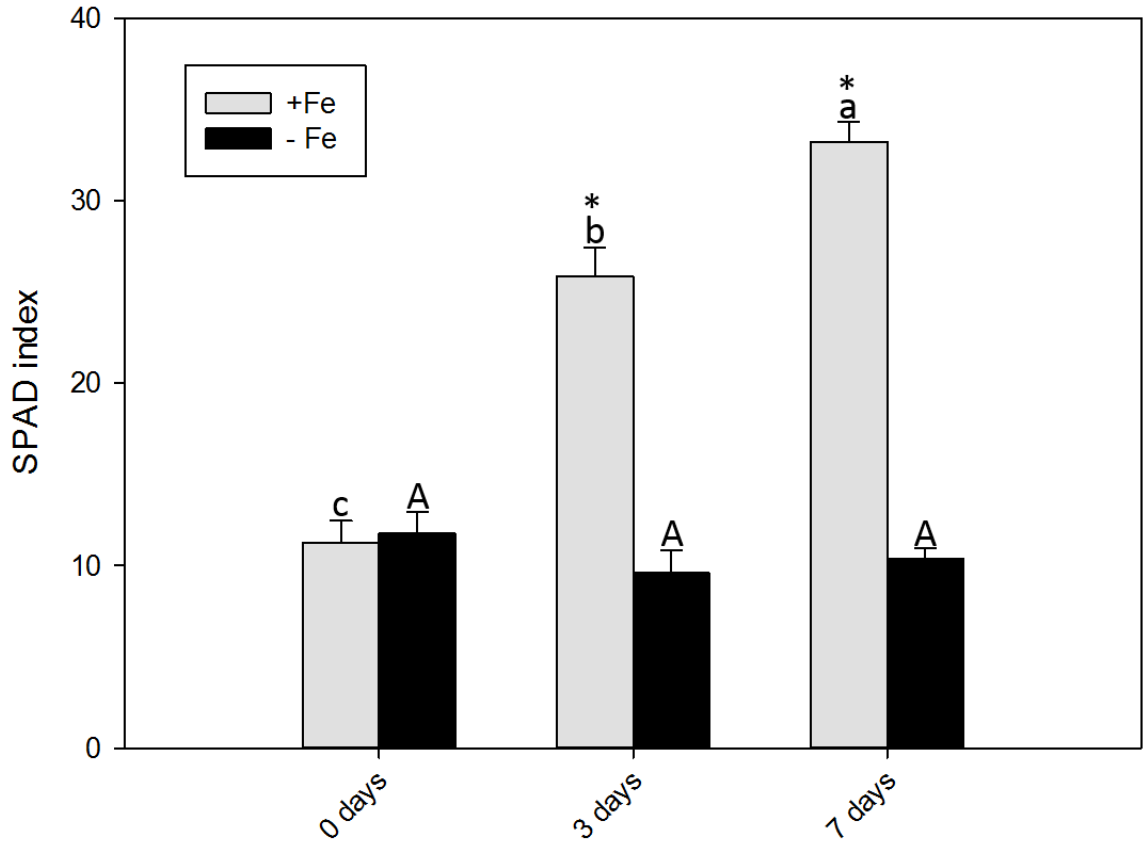

Figure 3.2 - SPAD index values of leaf tissues were measured at the beginning of the treatment (0 day), and after 7 and 14 days of Fe deficiency. Data are means ± SD of three independent experiments (capital letters refer to statistically significant differences among the mean, ANOVA Holm–Sidak, N=3, P <0.05).

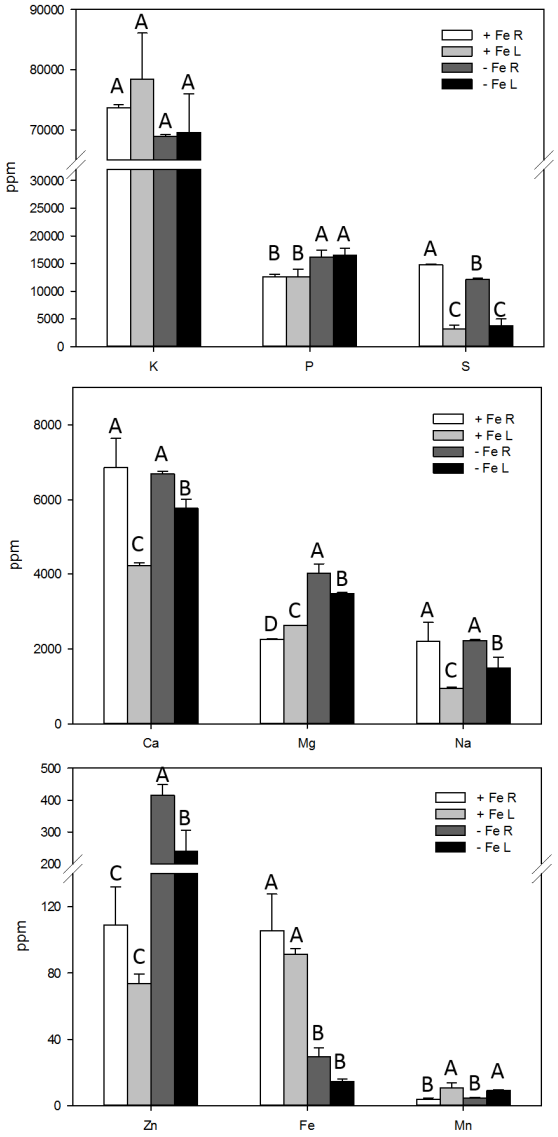

Figure 3.3 - Total content (ppm) of macro and micronutrient in shoots (L) and roots (R) of Fe-deficient (-Fe) and Fe sufficient (+Fe) maize plants. For each element, letters indicate a significant difference (ANOVA Holm-Sidak; N=3, P<0.05).

3.3.2 Root transcriptomic response to Fe-deficiency

In order to investigate at the molecular the response to Fe deficiency in maize, microarray analyses were performed on samples of Fe-deficient and Fe-sufficient roots. Analyses were performed using the maize chip 12_135K Arrays from Roche NimbleGen (http://www.nimblegen.com) which allowed the monitoring of 59,756 transcripts. Transcriptomic profiles were identified and statistically analyzed by Linear Models for MicroArray (LIMMA) (Smyth, 2005), adjusted P-value ≤ 0.05, n = 3, fold change (FC) $\geq |1.5|$. Microarray data were also validated by real-time RT–PCR analyzing the expression of five genes (Fig. 3.7).

The results indicate that Fe starvation induced changes in the root transcriptome involving 724 transcripts, 508 of which were upregulated while 216 were downregulated.

The differentially expressed transcripts were annotated based on the description file provided by Phytozome (*Zea mays* 284_6a JGI download) and clustered under functional categories according to the biological process of Gene Ontology (GO, http://www.geneontology.org). Referring to the total number of modulated transcripts, the most abundant categories were "metabolic process" (36% of modulated transcripts), "biological regulation" (11%), "localization" (10%) and "cellular process" (6%), while 33% of modulated transcripts showed unknown function. Comparing positively and negatively modulated transcripts, the main GO categories were more represented by upregulated transcripts (Fig. 3.4).

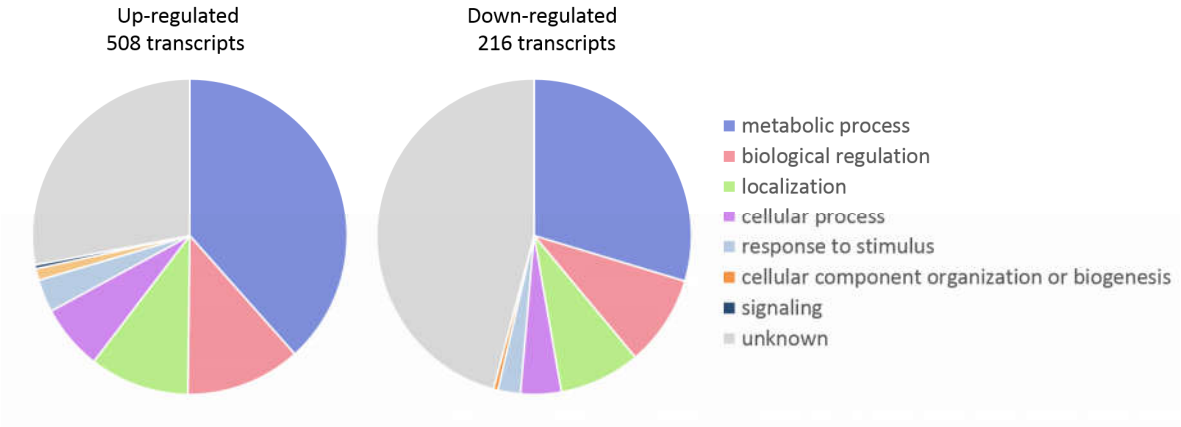

Figure 3.4 - Functional distribution among Gene Ontology (GO) categories of up- and downregulated transcripts differentially modulated by Fe deficiency (-Fe vs +Fe transcriptomic comparison). Transcripts were clustered according to the terms of "biological process" categories of GO.

Moreover, global functional analysis based on MapMan bins suggested that among those transcripts modulated by Fe deficiency there was an overrepresentation of glycolysis, mitochondrial electron transport/ATP synthesis, hormone metabolism, amino acid metabolism, abiotic stress, secondary metabolism, signaling and membrane transport functions (Fig. 3.5, Supplementary Figures S3.2). Reflecting morphological observation at the root system, several genes involved in the synthesis of lipids and in the cell wall formation were modulated by the root availability of the micronutrient (Fig. 3.5). Moreover, MapMan analyses revealed changes in several primary metabolic pathways. Some genes involved in glycolysis, fermentation and TCA cycle were upregulated under Fe starvation, namely genes coding for a glyceraldehyde-3-phosphate dehydrogenase (GADPH), phosphofructokinase (PFK), fructose-bisphosphate aldolase (FBP aldolase) and phosphoenolpyruvate carboxylase (PEPC), pyruvate decarboxylase (PDC), aldehyde dehydrogenase (ADH), lactate/malate dehydrogenase (LDH), citrate synthase (CS), isocitrate dehydrogenase (IDH), NADP-malic enzyme (NADP-ME).

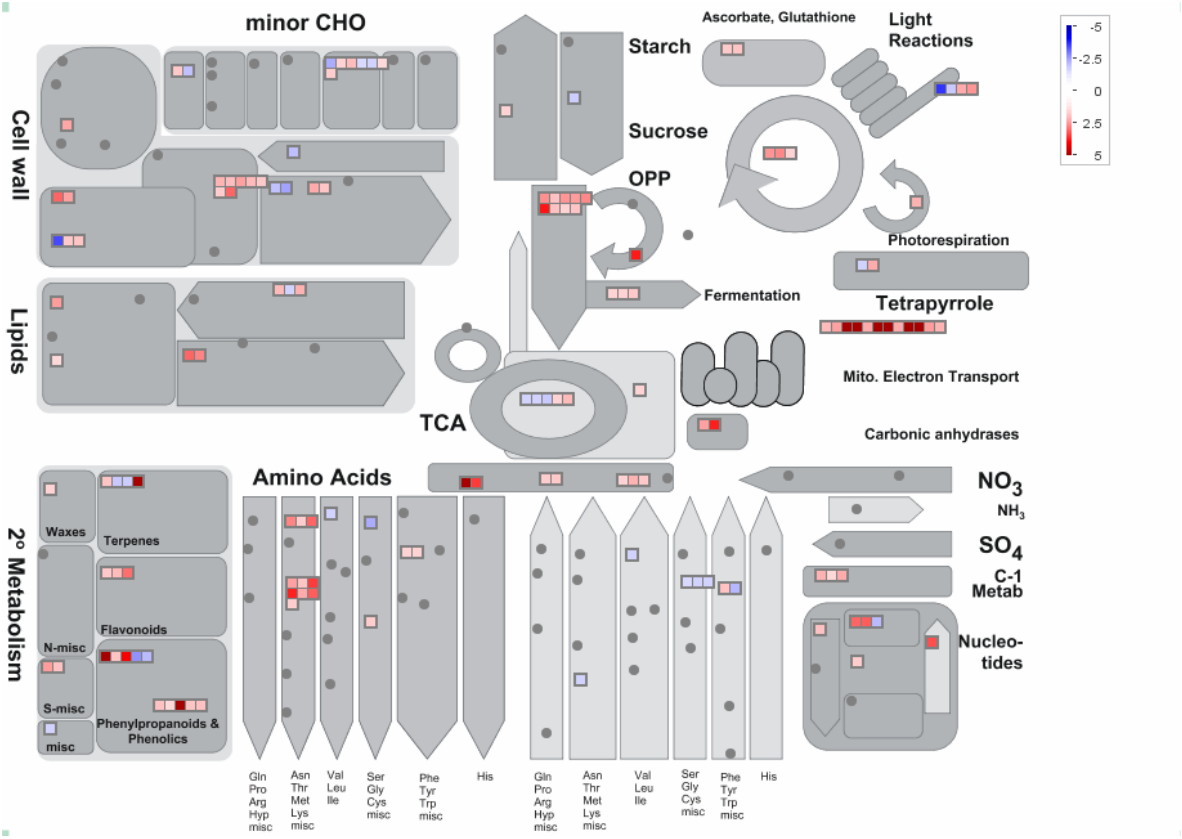

Figure 3.5 - Transcriptional modulation of genes involved in the cell metabolism by Fe deficiency. Color scale refers to the fold change values of differentially expressed transcripts: red color refers to those transcripts positively regulated by Fe deficiency, while in blue are transcripts negatively regulated by Fe deficiency.

In Fe-deficient roots, also some pathways for the synthesis of amino acids were induced, especially those for the synthesis of methionine and its derivatives (e.g. phytosyderophores), which play a crucial role in Strategy II. To provide a clear representation, the modulated genes were mapped on a custom pathway for phytosiderophore synthesis and Strategy II iron transport (Fig. 3.6 modified from Urbany et al., 2013). Iron starvation induced the expression of many genes involved in the pathway for the synthesis and release in the soil of deoxymugineic acid (DMA, Fig. 3.6).

Several transporters were modulated in response to Fe status. In particular our data identified some genes putatively involved in the acquisition/translocation of iron (encoding TOM1, VIT1, NRAMP1, OPT7 and YS-like transporters), sulphate/molybdate (MOT1), zinc (ZIFL1, ZIFL2, ZIP4) and phosphate (PHO1, PHT1;7; Tab. 3.1).

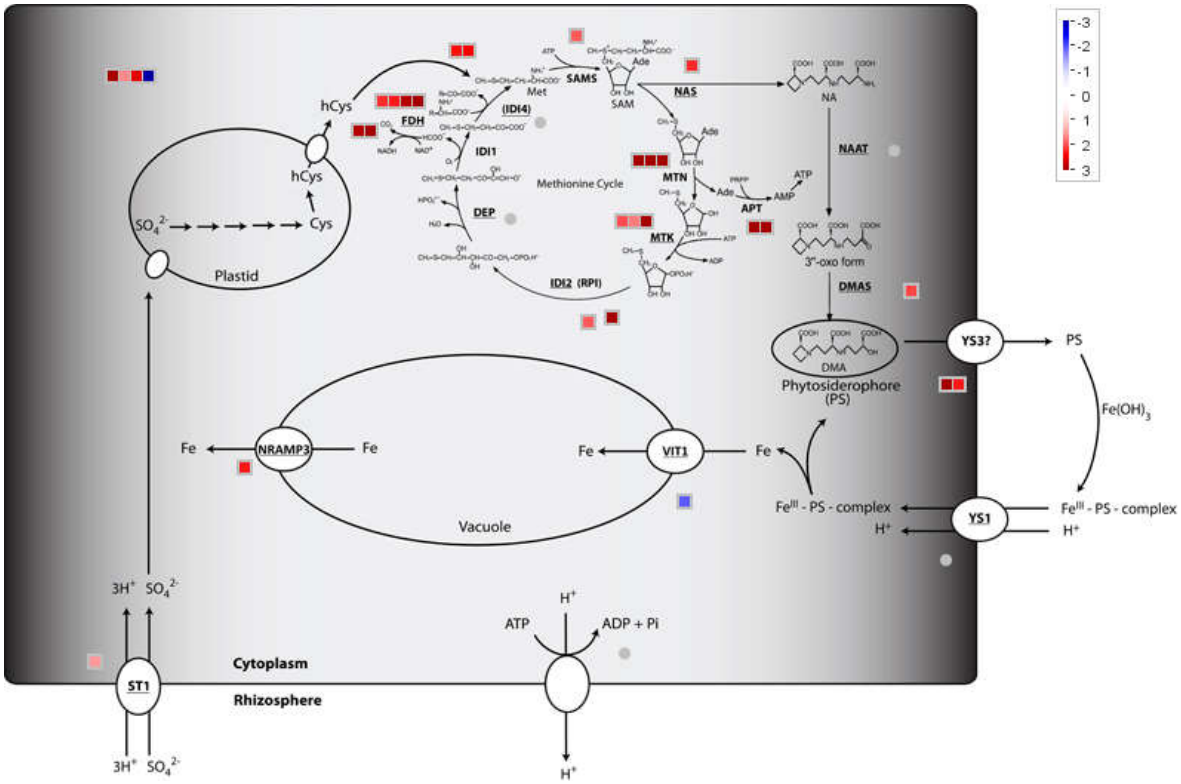

Figure 3.6 - Transcriptional changes in roots of genes involved in the Methionine cycle/DMA synthesis and Fe acquisition by Fe deficiency. Color scale refers to the fold change values of differentially expressed transcripts: red color refers to those transcripts positively regulated by Fe deficiency, while in blue are transcripts negatively regulated Fe deficiency

Table 3.1. List of modulated transcripts involving in the Fe acquisition and reported in the *Results* and *Discussion* sections by the comparison of transcriptomic profiles of Fe-deficient roots with profile of Fe sufficient ones (-*Fe* vs +*Fe* comparison). In the table are shown (starting from left column): number of transcript, transcript ID, fold change (FC), *p*-value adjusted, transcript descriprion and short name were reported for each transcript. References: *a*, Zheng et al., 2009; *b*, Urbany et al., 2013; *c*, Nozoye et al., 2015.**Error! Not a valid link.**

#	Transcript ID	FC -Fe vs +Fe	Description	protein symbol	Rice homologous gene ID	Reference
Strategy II genes						
1	GRMZM2G050108_T01	2.21	nicotianamine synthase 4	NAS	LOC_Os07g48980.1	a
2	GRMZM2G060952_T01	2.05	NAD(P)-linked oxidoreductase superfamily protein	DMAS	LOC_Os03g13390.2	a
3	GRMZM2G063306_T01	3.83	zinc induced facilitator-like 1	TOM1	LOC_Os11g04020.1	
4	GRMZM2G063306_T02	2.31	zinc induced facilitator-like 2	TOM1	LOC_Os11g04020.1	
Methionine cycle and DMA synthesis						
5	GRMZM2G049811_T01	2.20	formate dehydrogenase	FDH	LOC_Os06g29180.1	a,b,c
6	GRMZM2G054123_T01	1.94	S-adenosylmethionine synthetase family protein	SAMS3	LOC_Os01g22010.1	a,b,c
7	GRMZM2G113873_T01	1.77	cystathionine gamma-synthase, putative, expressed	CYS1	LOC_Os03g25940.4	
8	GRMZM2G131907_T01	3.24	adenine phosphoribosyl transferase 1	APT1	LOC_Os12g39860.1	a,b,c
9	GRMZM2G131907_T02	3.12	adenine phosphoribosyl transferase 1	APT1	LOC_Os12g39860.1	a,b,c
10	GRMZM2G152470_T01	2.35	homocysteine methyltransferase 2	HMT2	LOC_Os12g41390.1	
11	GRMZM2G152470_T03	2.43	homocysteine methyltransferase 2	HMT2	LOC_Os12g41390.1	
12	GRMZM2G165998_T01	2.90	RmlC-like cupins superfamily protein	ARD2	LOC_Os03g06620.1	a,b,c
13	GRMZM2G165998_T02	3.03	acireductone dioxygenase 1	ARD1	LOC_Os03g06620.1	a,b,c
14	GRMZM2G171111_T01	3.20	Phosphorylase superfamily protein	MTN2	LOC_Os06g02220.1	a,b,c
15	GRMZM2G171111_T02	3.53	methylthioadenosine	MTN1	LOC_Os06g02220.1	a,b,c

			nucleosidase 1			
16	GRMZM2G171111_T04	3.77	methylthioadenosine nucleosidase 1	MTN1	LOC_Os06g02220.1	a,b,c
17	GRMZM2G362021_T01	2.29	formate dehydrogenase	FDH	LOC_Os06g29180.1	a,b
18	GRMZM2G464137_T01	2.03	S-methyl-5-thioribose kinase	MTK	LOC_Os04g57400.1	a,b,c
19	GRMZM2G464137_T02	1.73	S-methyl-5-thioribose kinase	MTK	LOC_Os04g57400.1	a,b,c
20	GRMZM2G464137_T03	3.11	S-methyl-5-thioribose kinase	MTK	LOC_Os04g57400.1	a,b,c
21	GRMZM5G891282_T01	3.82	ribose-5-phosphate isomerase 2	RPI2	LOC_Os04g24140.1	a,b
22	GRMZM2G057506_T02	1.67			LOC_Os01g72360.1	
23	GRMZM2G131907_T02	3.12	adenine phosphoribosyl transferase 1	APT1	LOC_Os12g39860.1	a,b
24	GRMZM2G131907_T01	3.24	adenine phosphoribosyl transferase 1	APT1	LOC_Os12g39860.1	a,b
25	GRMZM2G418005_T02	1.57	formate dehydrogenase	FDH	LOC_Os06g29180.1	a,b
	Transcription factors					
26	GRMZM2G057413_T01	3.20	basic helix-loop-helix DNA-binding domain containing protein, expressed	IRO2	LOC_Os01g72370.1	a, b, c
27	GRMZM2G057413_T02	10.07	basic helix-loop-helix DNA-binding domain containing protein, expressed	IRO2	LOC_Os01g72370.1	b, c
28	AC193786.3_FGT005	2.44	basic helix-loop-helix DNA-binding domain containing protein, expressed	IRO4	LOC_Os01g72370.1	a, b, c
29	GRMZM2G350312_T01	1.63	basic helix-loop-helix DNA-binding domain containing protein, expressed	IRO3	LOC_Os03g26210.1	a, b, c
30	GRMZM2G350312_T03	1.68	basic helix-loop-helix DNA-binding domain containing protein, expressed	IRO4	LOC_Os03g26210.1	a, b, c
31	GRMZM2G350312_T04	1.62	basic helix-loop-helix DNA-binding domain containing protein, expressed	IRO5	LOC_Os03g26210.1	a, b, c
32	GRMZM2G107672_T01	2.58	FER-like regulator of iron	FER-like	LOC_Os04g31290.1	

			uptake			
33	GRMZM5G898290_T01	1.62	NAC domain containing protein 80	NAC	LOC_Os02g36880.4	a
34	GRMZM5G898290_T02	2.32	NAC domain containing protein 80	NAC	LOC_Os02g36880.4	a
	Other genes					
35	GRMZM2G029135_T01	1.62	1-aminocyclopropane-1-carboxylate synthase	ACCS	LOC_Os01g08270.1	
36	AC148152.3_FGT005	2.25	1-aminocyclopropane-1-carboxylate oxidase	AACO	LOC_Os03g48430.1	
37	GRMZM2G041418_T01	50.74	alternative NAD(P)H dehydrogenase	ADH2	LOC_Os07g37730.1	
	Transporters					
38	GRMZM2G178190_T01	2.31	NRAMP metal ion transporter	NRAMP1	LOC_Os03g11010.1	c
39	GRMZM2G112377_T01	2.30	phosphate transporter 1;7	PHT1;7	LOC_Os08g45000.1	
40	GRMZM5G891944_T01	2.19	phosphate transporter 1, putative, expressed	PHO1;H1	LOC_Os01g02000.1	
41	GRMZM2G064657_T01	2.63	phosphate transporter 1, putative, expressed	PHO1;H1	LOC_Os06g29790.1	
42	GRMZM2G421491_T01	11.76	oligopeptide transporter, putative, expressed	OPT7	LOC_Os03g54000.1	a

3.3.3 Expression pattern of transporter genes in response to Fe-treatments

The response of maize plants to Fe deficiency was further evaluated analyzing the capability of Fe-deficient roots to use three different natural Fe-sources (Fe-PS, Fe-Citrate or Ferrihydrite) provided at a Fe concentration (1 μM Fe conceivably present in soil with low availability of the micronutrient.

By real time RT-PCR, the expression of some genes related to Fe acquisition were analyzed in Fe-deficient roots treated for up to 24 hours with the Fe-sources (Fig. 3.7).

The genes coding for the PS efflux transporter and for Fe(III)-PS influx transporter, ZmTOM1 and ZmYS1 respectively, were positively modulated by Fe deficiency. When Fe-sources were supplied to Fe-deficient plants, the expression levels of these genes decreased considerably reaching after 24 hours mRNA amounts comparable to those of Fe-sufficient plants (Fig. 3.7a,b). A similar behavior was observed for *ZmOPT7* and *ZmNRAMP1*, two genes putatively involved in the response to Fe deficiency. The expression of these two genes was already modulated after 4 hours of treatment with the Fe-sources (Fig. 3.7 c, d).

Moreover changes in the expression levels were also appreciated comparing the treatments. After 24 hours of Fe-source supply, most genes were downregulated in maize roots reaching expression levels comparable to those recorded under Fe sufficiency; this was particularly evident when Fe-PS was supplied (Fig. 3.7a,b,c,d,f). Concerning *ZmOPT7*, Fe-deficient maize roots were more responsible when soluble Fe-sources (Fe-PS and Fe-Citrate) were supplied. After 24 hours of treatment, plants treated with Fe-PS and Fe-Citrate showed values comparable to those recorded in Fe-sufficient plants, while higher values were recorded when the poorly soluble source Ferrihydrite was supplied (Fig. 3.7c).

As observed by microarray analyses, Fe deficiency induced also the expression of some genes involved in phosphate transport. In particular the expression of a gene coding for an inorganic phosphate transporter (ZmPHT1;7) was analyzed when maize plants were treated with the three Fe-sources. Confirming transcriptomic data, the Fe-starved roots accumulated higher amounts of *ZmPHT1;7* transcript as compared to Fe-sufficient plants. At least up to 4 hours of treatment, high mRNA amounts were also recorded in plants treated with Fe-Citrate. On the other hand, deficient plants supplied with Fe-PS or Ferrihydrite and Fe sufficient plants show a similar expression of *ZmPHT1;7* (Fig. 3.7f).

Finally, the expression of a gene (*ZmFerritin*) highly responsive to Fe-sufficiency, encoding for a ferritin protein was evaluated. The expression of this gene was induced when Fe was available in the nutrient solution. The highest expression values were recorded in roots of Fe-sufficient plants. The addition of 1 μM soluble Fe as Fe-Citrate or Fe-PS to the Fe-free nutrient solution induced a gradual expression of the gene. On the other hand, a low expression of the gene was recorded in roots of Fe-deficient plants and Ferrihydrite-supplied plants (Fig. 3.7).

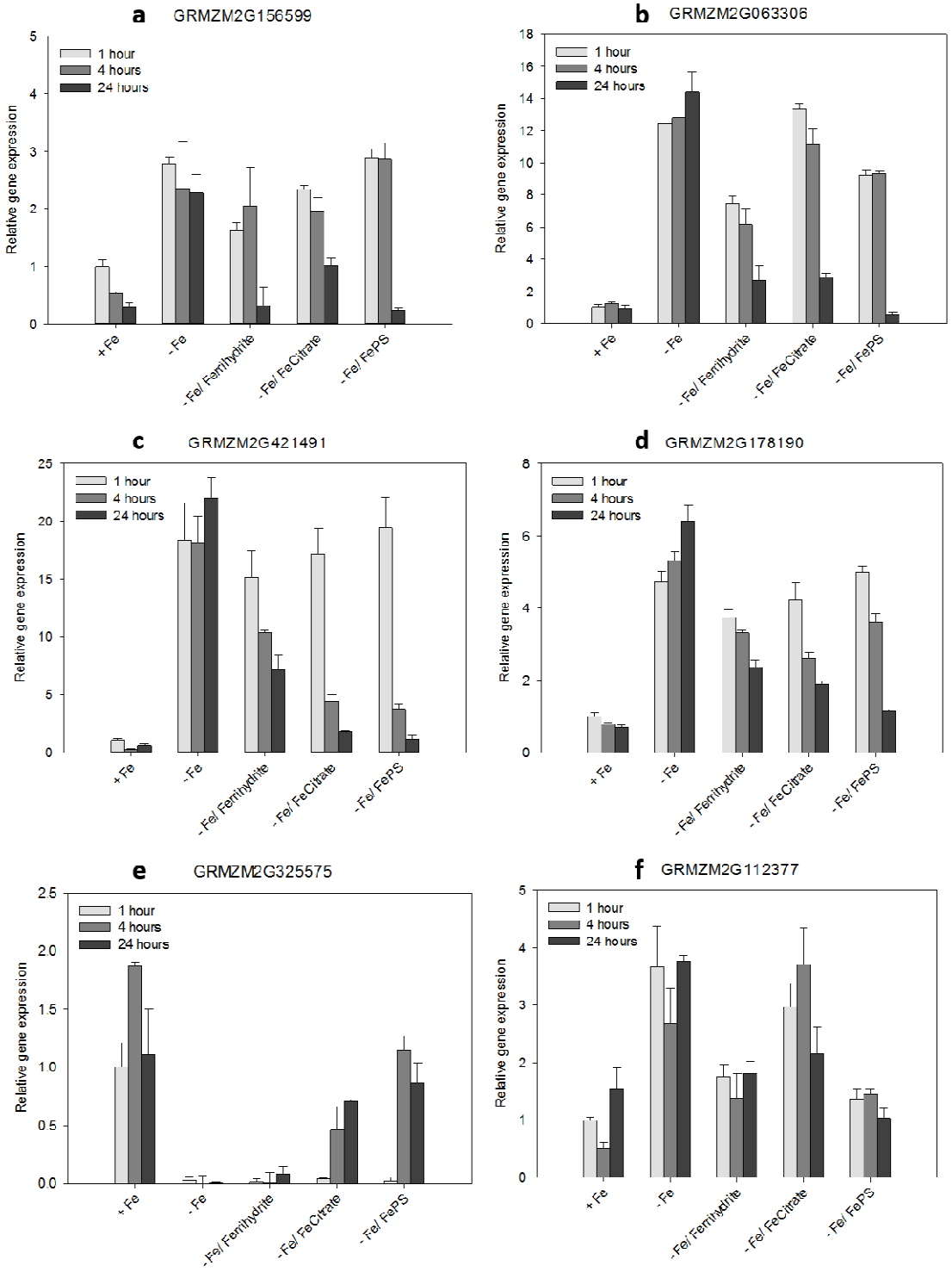

Figure 3.7. Real-time RT-PCR analyses of gene transcript levels in maize roots. 19-day-old maize plants were grown under Fe sufficiency (+Fe) or Fe deficiency (-Fe); these latter were then supplied with three different

Fe-sources (Ferrihydrite, Fe-Citrate or Fe-PS), as reported in Material and methods section. Root samples were harvested after 1, 4 and 24 hours from the beginning of the experiment. Analyzed genes: a, *ZmYS1* (GRMZM2G156599); b, *ZmTOM1* (GRMZM2G063306); c, *ZmOPT7* (GRMZM2G421491); d, *ZmNRAMP1* (GRMZM2G178190); e, *ZmFerritin* (GRMZM2G325575); f, *ZmPHT1;7* (GRMZM2G112377). Gene mRNA levels were normalized with respect to the mean transcript level of the housekeeping gene *ZmGAPDH*; relative changes in gene transcript levels were calculated on the basis of the mean transcript level of *ZmGAPDH* in Fe sufficient roots at 1 hour (relative gene expression = 1). Data are means of three independent biological replicates + SD.

3.3.4 ^{59}Fe accumulation from natural Fe sources by plants

In order to assess the ability of Fe-sufficient and Fe-deficient maize plants to use some natural Fe-sources, uptake experiments were performed using ^{59}Fe-labeled sources, as ^{59}Fe-PS, ^{59}Fe-Citrate, or as (^{59}Fe)Ferrihydrite.

After 1 hour of contact with the solution, roots of Fe-deficient maize plants accumulated more Fe than the sufficient ones when Fe was supplied as ^{59}Fe-Citrate or ^{59}Fe-PS (Fig. 3.8); the highest amount of Fe was accumulated in plants supplied with Fe-PS independently from the Fe status. After 24 hours of treatment, there was an increase in the amount of Fe accumulated in the roots, but no significant difference between the two growth conditions was observed for plants supplied with ^{59}Fe-PS. On the contrary, the Fe-deficient plants fed with ^{59}Fe-Citrate, showed a huge increase in Fe content in the roots after 24 hours of treatment, this effect being particularly evident for Fe-deficient plants. Regarding the treatment with Ferrihydrite, a sharp increase in Fe accumulation was observed after 24 hours of treatment; furthermore, only at this time asignificant difference between two Fe-nutritional status was observed.

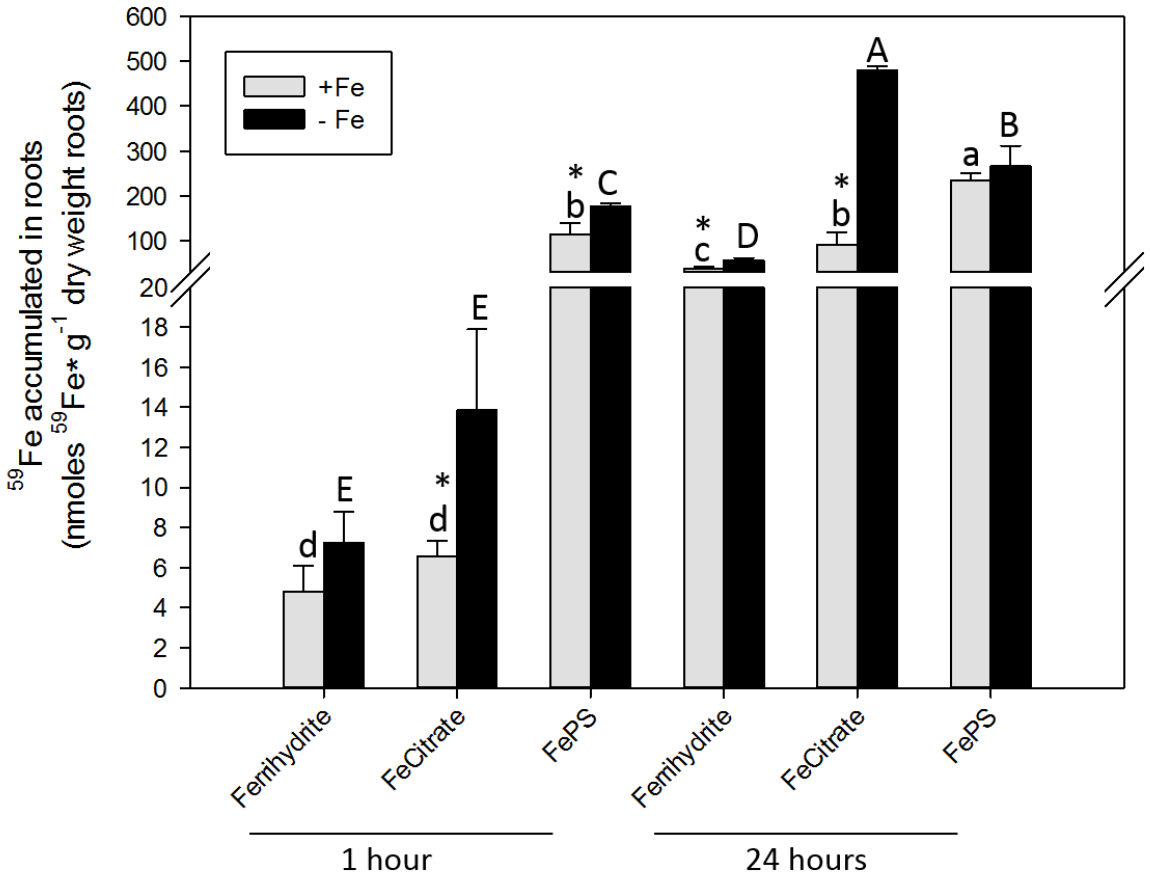

Figure 3.8 - Iron (^{59}Fe) accumulation in maize roots. The plant ability to accumulate Fe was evaluated by 59Fe uptake experiments in Fe-sufficient (+Fe, grey bars) and Fe-deficient (-Fe, black bars) plants treated for 1 and 24 hours with three labeled ^{59}Fe-sources: (^{59}Fe) Ferrihydrite, ^{59}Fe-Citrate or ^{59}Fe-PS. Iron (^{59}Fe) was added to the nutrient solution at final concentration of 1 µM. Data are means+SD of three independent experiments. Small letters, refer to statistically significant differences among Fe sufficient plants; capital letters, refer to statistically significant differences among Fe deficient plants, asterisks, refer to statistically significant differences between Fe sufficient versus Fe deficient plants. ANOVA Holm–Sidak, N=3, P <0.05). DW, dry weight.

The accumulation of ^{59}Fe by the whole plants is reported in Fig. 3.9. After 1 hour, Fe-deficient plants accumulated higher levels of ^{59}Fe than Fe-sufficient ones. Comparing the three sources, higher amount of the micronutrient was accumulated in plants when ^{59}Fe-PS was supplied.

At the end of the experiment (24 hours), the amount of Fe in plants was dependent on the nutritional status and on the Fe-source supplied.

Comparing the Fe accumulation in roots and leaves (Fig. 3.8 and Fig. S3.3) the contribution of translocation appeared to be greater in the Fe-sufficient plants.

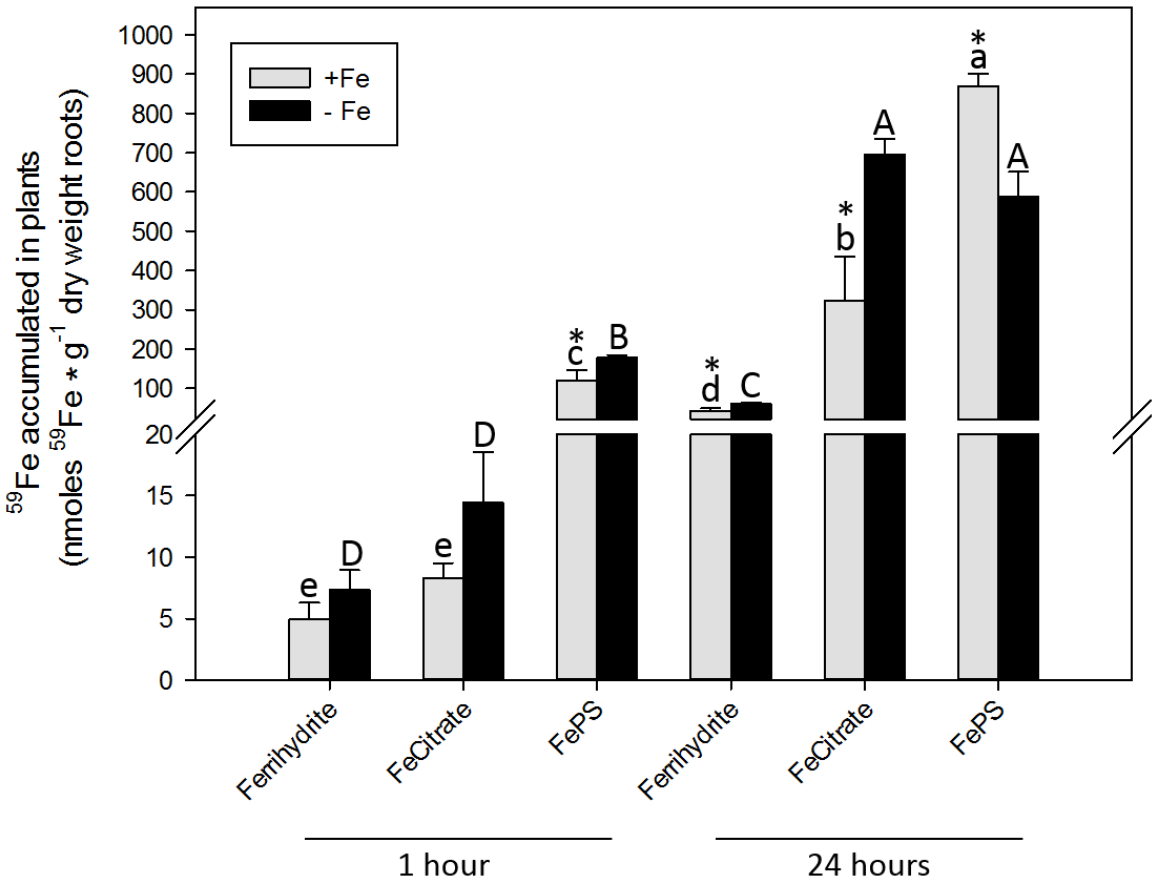

Figure 3.9 - Iron (^{59}Fe) accumulated in maize plants. The plant ability to accumulate Fe was evaluated by 59Fe uptake experiments in Fe-sufficient (+Fe, grey bars) and Fe-deficient (-Fe, black bars) plants treated for 1 and 24 hours with three labeled ^{59}Fe-sources: (^{59}Fe)Ferrihydrite, ^{59}Fe-Citrate or ^{59}Fe-PS. Iron (^{59}Fe) was added to nutrient solution at final concentration of 1 µM. Data are means+SD of three independent experiments. Small letters, refer to statistically significant differences among Fe sufficient plants; capital letters, refer to statistically significant differences among Fe deficient plants, asterisks, refer to statistically significant differences between Fe sufficient versus Fe deficient plants. ANOVA Holm–Sidak, N=3, P <0.05). DW, dry weight.

3.3.5 Phosphorus (^{32}P)-uptake in maize plants

In order to investigate a possible influence of Fe-nutritional status of plants on phosphate uptake, the measurement of ^{32}P accumulation was performed after 24 h in the same experimental conditions used for the Fe uptake experiments, except that the three Fe-sources used were not labelled with ^{59}Fe and two natural P-sources were also provided to plants: KH_2PO_4, as soluble form, and Vivianite, as a poorly soluble source. When using KH_2PO_4, the overall ^{32}P

accumulation in the root system of the Fe-sufficient plants plants fed with Fe-Ps or Ferrihydrite was significantly higher (13% and 77%, respectively) than in the deficient ones. In presence of Fe-Citrate, no differences between the two growth conditions were observed in the ^{32}P accumulated in the root tissue.

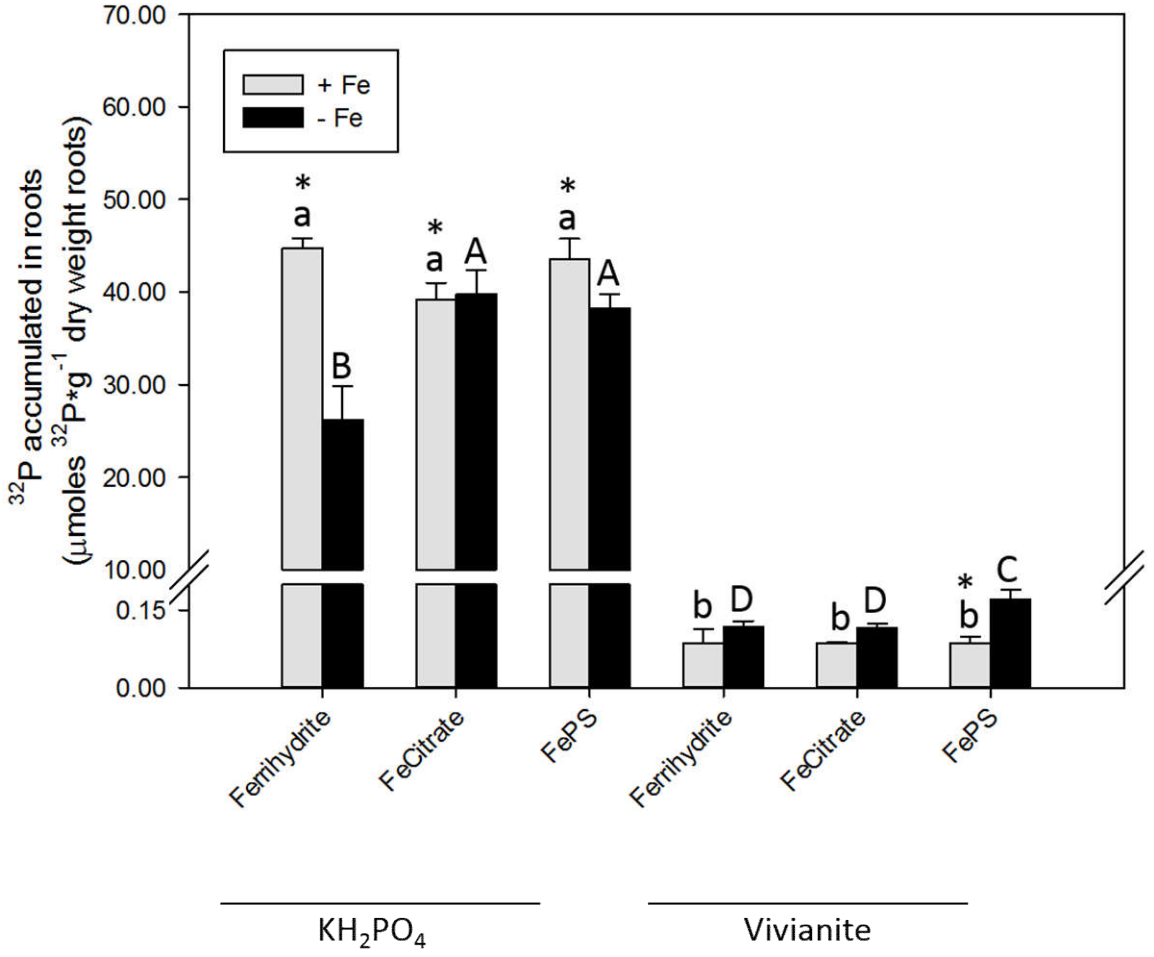

Figure 3.10 - Phosphorus-(^{32}P) accumulated in maize roots. The plant ability to accumulate P was evaluated by ^{32}P uptake experiments in Fe-sufficient (+Fe, grey bars) and Fe-deficient (-Fe, black bars) plants. -Fe and +Fe plants were treated for 24 hours with three unlabeled Fe-sources (Ferrihydrite, Fe-Citrate or Fe-PS) provided in conjunction with two different labeled ^{32}P-sources: (^{32}P)KH_2PO_4 or (^{32}P)Vivianite. Iron and phosphorus were added to the nutrient solution at a final concentration of 1 µM each. Data are means+SD of three independent experiments. Small letters, refer to statistically significant differences among Fe sufficient plants; capital letters, refer to statistically significant differences among Fe deficient plants, asterisks, refer to statistically significant differences between Fe sufficient versus Fe deficient plants. ANOVA Holm–Sidak, N=3, P <0.05). DW, dry weight.

When ^{32}P was supplied in a poorly soluble form, its accumulation slightly increased in the roots of Fe-deficient plants, the difference being significant only in plants treated with Fe-PS (Fig. 3.10). The data of ^{32}P measured in the whole plant (Fig. 3.11) shows a similar trend in the accumulation of P as in the root system. Nevertheless, in this case, Fe-sufficient plants fed with KH_2PO_4 showed a higher accumulation of P than Fe-deficient plants also when Fe-Citrate was used as Fe-source. This pattern wass mainly due to a greater amount of P in the leaves (Fig. S3.4). The accumulation levels of P from the poorly-soluble source (^{32}P-Vivianite) were slightly but significantly higher in Fe-deficient plants than those observed for Fe-sufficient plants for each Fe treatments.

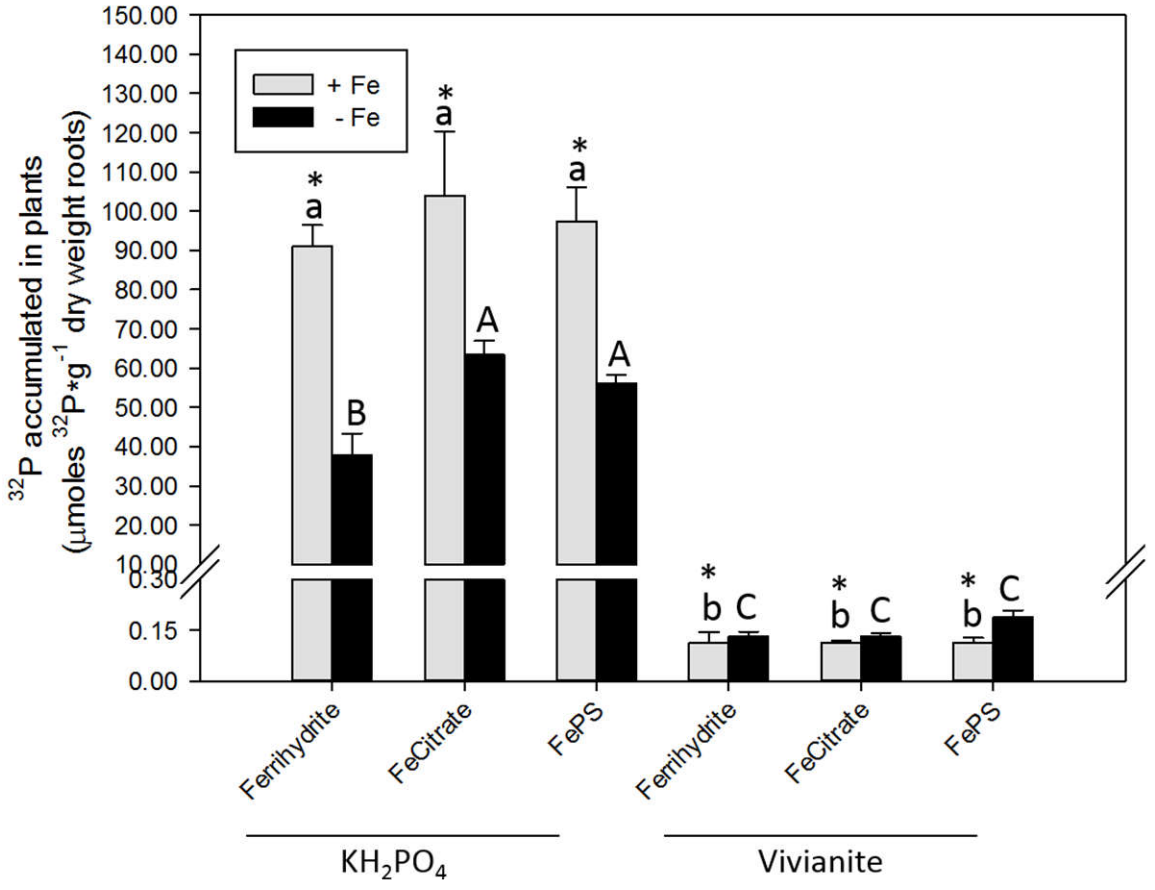

Figure 3.11 - Phosphorus (^{32}P) accumulation in maize plants. The plant ability to accumulate P was evaluated by ^{32}P uptake experiments in Fe-sufficient (+Fe, grey bars) and Fe-deficient (-Fe, black bars) plants. -Fe and +Fe plants were treated for 24 hours with three unlabeled Fe-sources (Ferrihydrite, Fe-Citrate or Fe-PS)

provided in conjunction with two different labeled ^{32}P-sources: (^{32}P)KH_2PO_4 or (^{32}P)Vivianite. Iron and phosphorus were added to the nutrient solution at a final concentration of 1 µM each. Data are means+SD of three independent experiments. *Small letters,* refer to statistically significant differences among Fe sufficient plants; *capital letters,* refer to statistically significant differences among Fe deficient plants, *asterisks*, refer to statistically significant differences between Fe sufficient versus Fe deficient plants. ANOVA Holm–Sidak, N=3, P <0.05). DW, dry weight.

3.4 Discussion

3.4.1 Characterization of response to Fe deficiency in maize roots

Morphological and transcriptomic analyses were performed on roots of 12-day-old maize plants growth under Fe-deficient or Fe-sufficient conditions. Typical symptoms of Fe deficiency were observed in maize plants, such as reduced chlorophyll content (SPAD index value, Fig. 3.2) and leaf interveinal chlorosis (Fig. 3.1A,B). However also the root apparatus was modified, since Fe-deficient roots were less developed than Fe sufficient ones (Fig. 3.1C). Moreover, as reported for dicots plants (Zamboni et al., 2012), maize roots showed thick apices with proliferation of root hairs in the subapical zone (Fig. 3.1D).

These morphological observations were then correlated with transcriptomic changes occurring in roots of Fe-deficient plants. Two nutritional status induced the differential modulation of more than 700 transcripts, 508 of which were upregulated and 216 were downregulated by Fe starvation. Although the expression of a large number of transcripts was monitored by microarray chip (more than 60,000), this result confirms that the plant response to Fe deficiency is based on the modulation of a narrow set of transcripts (Schmidt and Buckhout, 2011; Zamboni et al., 2012; Urbany et al., 2013; Li et al., 2015).

Considering the crucial role of Fe as cofactor of a wide range of enzymes, many genes encoding for cytochromes, catalase, peroxidase isozymes, ferredoxin, and isozymes of superoxide dismutase were downregulated by Fe-deficiency.

On the other hand, grasses counteract the starvation of the micronutrient by inducing the expression of those genes involved in the *Strategy II*. Consistent with this assumption microarray data showed the upregulation of several genes involved in Methionine cycle (# 5-25, Tab. 3.1), and in the synthesis and release of MAs (# 1-4 NAS, DMAS, TOM1 transporter, Tab. 3.1, Fig. 3.6). The synchronous modulation of these pathways by Fe-deficiency was reported in previous works (Nozoye et al., 2013; Urbany et al., 2013). It is widely accepted the key role of S-

adenosyl-methionine (SAM) production by Methionine-cycle to sustain the synthesis of PS. This response might be correlated with the induction by Fe deficiency of a transcription factor IRO2 (# 26-28, Tab. 3.1) which play an important role in the activation of genes involved in *Strategy II* response and can also regulate the Methionine-cycle (Ogo et al., 2007).

SAM also sustains the synthesis of an important hormone, ethylene, which is induced in Fe-deficient in plants. Among the differentially modulated transcripts, data indicated the upregulation of genes coding for ACC synthase and ACC oxidase which are directly involved in the synthesis of ethylene (# 35-36, Tab. 3.1).

Together with auxin level, ethylene content might be associated with morphological changes in roots controlling hair root proliferation under Fe deficiency (Romera et al., 2007), as observed in Fig. 3.1.

Besides the modulation of genes involved in *Strategy II* and Methionine-cycle, microarray data identified other pathways positively modulated by Fe deficiency, such as glycolysis, TCA cycle and mitochondrial chain reactions (Fig. 3.5, Fig. S3.2). During Fe deficiency, similar changes in primary metabolism have been extensively described in many species (Thimm et al., 2001; Zamboni et al., 2012; Urbany et al., 2013); our microarray data are consistent with those of previous reports.

In particular a gene coding for an alternative dehydrogenase (ADH2) was strongly induced by Fe starvation (#37, Tab. 3.1). As reported by Vigani and Zocchi (2010), the induction of this enzyme under Fe deficiency might be a valid strategy to bypass the impairment of the ubiquinone (UQ) reduction process allowing the synthesis of ATP. In this way, although mitochondria are suffering from Fe-deficiency (Mori, 1999), the activation of ADH2 might be an adaptive mechanism to sustain also under Fe starvation the ATP requirement for PS synthesis.

3.4.2 Study of Fe deficiency in maize: efficient use of natural Fe sources

Starting from transcriptomic evidence on Fe-deficient roots, we focused our study on the ability of maize plants to use three different natural Fe-sources: Fe-Citrate, Fe-PS or Ferrihydrite. These three sources were added to the external root solution mimicking field conditions of poor availability of Fe (Tomasi et al., 2013). So far, the capability of grasses to use different Fe-sources occurring at the rhizosphere has been scarcely studied.

Microarray analyses showed that Fe deficiency modulated some genes involved in the synthesis and released of PS. Therefore, by real time RT-PCR two key genes of *Strategy II* were monitored during treatment: the PS efflux transporter, *ZmTOM1,* and the Fe(III)-PS influx transporter, *ZmYS1*. While *ZmYS1* was only barely induced by Fe deficiency, *ZmTOM1* was strongly upregulated, corroborating microarray and literature data (Nozoye et al., 2013).

When Fe sources were added to the external solution, the micronutrient was taken up by plants and the genes relating to *Strategy II* were downregulated in roots (Fig. 3.7, 8, 9). These results indicate that all the three Fe-sources were used by Fe-deficient plants and triggered the downregulation of genes involving in *Strategy II* mechanisms (Fig. 3.7). Thus, depending on Fe availability, maize plants are able to rapidly adjust the mRNA amounts. Moreover, the expression pattern of *TOM1* was particularly influenced by the type of Fe-source. After 24 hours, the lowest expression values were recorded in roots treated with Fe-PS. Thus, the addition of Fe-PS determined in roots a limitation in the expression level of the gene involving in the release of PS.

In a recent study, Nozoye and coworkers (2013) hypothesized the involvement of maize ZmNRAMP1 (GRMZM2G178190) in the acquisition of external ferrous ions, as already reported for the rice homologous OsNRAMP1 and OsNRAMP5 (Takahashi et al., 2011; Ishimaru et al., 2012a,b). The gene *ZmNRAMP1* was upregulated in ys3 mutant plants defective in phytosiderophores release (Nozoye et al., 2013). This evidence suggests that roots of grasses possess an alternative mechanisms for the acquisition of Fe, which is NRAMP-mediated. In agreement with data in the literature, our results showed the induction of *ZmNRAMP1* transporter by Fe deficiency, while the treatment of Fe-deficient plants with the three Fe sources downregulated its expression. Comparing the three treatments, the supply of Fe-PS determined a more consistent reduction in the mRNA amounts. This behaviour suggests that at pH 7.5 the availability of Fe supplied by Fe-PS treatment was enough to sustain the Fe requirement of maize plants.

From microarray data, other genes involved in Fe transport and responsive to Fe deficiency were analysed by Real-Time RT PCR. Recently, a member of OPT family (OPT7) has been reported in rice to respond to Fe deficiency (Bashir et al., 2015). The same held true in maize, since microarray and real time data revealed the induction of the homologous transporter, ZmOPT7. The molecular characterization of OsOPT7 localized this transporter at the plasma membrane of

shoot and roots cells and suggested its involvement in Fe distribution and translocation to shoots (Bashir et al., 2015). In maize roots the expression of *ZmOPT7* was strongly downregulated when soluble iron sources were provided to the plants (Fig. 3.7). This pattern is also consistent with the amount of Fe translocated to the leaves. The supply of soluble sources, Fe-PS and Fe-Citrate allowed a fast recovery of Fe deficiency and, as consequence, the expression of OPT7 was limited.

Depending on the nutritional status, the ability of Fe-deficient and Fe-sufficient plants to accumulate and allocate Fe was different. Indeed, Fe-deficient roots accumulated higher amounts of Fe than Fe-sufficient ones, while opposite behaviour was detected in leaves (Fig. 3.8, Fig. S3.3). The translocation system seems to be particularly activated in the Fe-sufficient plants. Beside the nutritional status, the nature of the provided Fe-source also changed the capability of maize plants to accumulate the micronutrient. After 1 hour of treatment, roots of Fe-deficient plants acquired more efficiently ^{59}Fe when it was supplied in the form of Fe-PS than under other Fe-sources (Fig. 3.8). This behaviour fits with the mechanisms of Fe acquisition in *Strategy II* plants. Indeed, the micronutrient was already chelated by PS and, therefore, Fe-PS complex was directly taken up by plants, as substrate of YS1 transporter.

On the other hand, when Ferrihydrite or Fe-Citrate are provided, the micronutrient needs to be mobilized by PS (and other ligands) action before becoming substrate of YS1 transporter (Curie et al., 2001; Cesco et al., 2002). Nevertheless, after 24 hours of ^{59}Fe-PS treatment, there was a clear saturation of the amount of accumulated Fe by the root apparatus (Fig. 3.8). This phenomenon could be related to the maintenance of iron homeostasis and prevention of iron toxicity effect (Connolly et al., 2002).

Concerning maize leaves, Fe-sufficient plants treated with Fe-PS accumulated higher amounts of the micronutrient than Fe-deficient plants (Fig. S3.3), likely because this source of Fe can directly move into the different tissue and the mechanisms involved in the translocation are already active under this nutritional status. It has been previously demonstrated that the regulation on the capability of the *Strategy II* plants to acquire Fe is occurring at the level of the PS release and not on the Fe-PS uptake into the roots (Cesco et al., 2002).

Interestingly, after 24 hours Fe-deficient plants fed with ^{59}Fe-Citrate, showed an even higher Fe accumulation in roots than those fed with Fe-PS. On the other hand, ^{59}Fe levels were similar in both treatments due to the slightly higher translocation rate in the Fe-PS treated plants (Fig. 3.9

and Fig. S3.3). These data, suggested that maize plants are able to use directly Fe-PS and translocate this Fe-complex directly into the leaves. Indeed, some evidence showed that PS plays a key role also in the translocation of the micronutrient within plants (for a review see Kobayashi and Nishizawa, 2012).

Plants supplied with ^{59}Fe as Ferrihydrite showed the same accumulation profile as those treated with ^{59}Fe-Citrate. Nevertheless, plants under ferrihydrite treatment required more time to accumulate iron in comparison with plants treated with Fe-PS or Fe-Citrate; this is not surprising because Fe should be firstly mobilized, chelated and then taken up by the plants.

Ferritin gene is involved in Fe storage and in detoxification of Fe excess (Lescure et al., 1991). This gene could be considered as an indicator of the iron nutritional status (Itai et al., 2013); indeed *ZmFerritin* is up regulated in root system of iron sufficient maize plants (Fig. 3.7e). The Fe deficient plants fed with Fe-Citrate or Fe-PS treatments at 24h showed an upregulation of *ZmFerritin* transcript levels.

3.4.3 Antagonistic interaction between Fe and P nutrition

In rice, previous evidence reported an antagonistic interaction between Fe and P nutrition (Zheng et al., 2009). Indeed, Fe deficiency led to a wide re-programming of metabolism and regulatory networks in plants, which are linked to P nutrition. Low Fe concentration in plant tissues increased the energy demand as well the capacity of oxidative phosphorylation (Thimm et al., 2001). Moreover P is also an important element for the regulation of a wide range of proteins through post-translational modifications. Recent studies suggest that Fe deficiency induces some changes in the phosphoproteome profile of Arabidopsis roots and this modulation might be linked to a regulative mechanism for the homeostasis of the micronutrient in plants (Lan et al., 2012).

Confirming previous evidence (Zheng et al., 2009), Fe deficiency in maize determined changes in P (besides Fe) concentrations: Fe-deficient plants accumulated low levels of Fe and high amounts of P, in both shoots and roots (Fig. 3.3). As a consequence of this nutrient imbalance, Fe-deficient plants were less efficient in accumulating soluble phosphate than Fe-sufficient ones (Fig. 3.11).

At least partially, this data might be linked to gene transcriptional modulations. Indeed, microarray analyses revealed that some genes involved in P acquisition were upregulated by low Fe availability, as the inorganic phosphate transporter *ZmPHT1;7*. The rice homologous of this

latter gene (*OsPHT1;6*) plays a broad role in the acquisition of inorganic phosphorus mediating its high affinity uptake from the rhizosphere and translocation throughout the plants (Ai et al., 2009).

The addition of Fe-sources in the nutrient solution rapidly decreased in Fe-deficient roots the expression level of this transporter. The only exception to this behavior was observed when Fe-Citrate was provided to maize roots, since high amounts of mRNA were still detected even after 4 hours from the beginning of the treatment (Fig. 3.7).

It is well known that P deficiency induces in tolerant species (as white lupine) a massive release of organic acids for the solubilization of inorganic phosphate (Marschner et al., 1986) and enhance the expression of some genes coding for phosphate transporters (Liu et al., 2001; for a review see Vance , 2001).

Considering also the physiological results, the supply of citrate as Fe-Citrate might facilitate the acquisition of phosphate in Fe-deficient plants (Fig. 3.11). In a similar way, also the addition of exogenous PS (as Fe-PS source) also enhances the acquisition of inorganic phosphate and its mobilization from the poorly soluble source, vivianite (Fig. 3.10-11).

Besides the addition of exogenous PS, it should be considered that Fe-deficient plants released huge amount of endogenous PS in the nutrient solution. This observation explains the overall better use efficiency of poorly soluble source (Vivianite) by Fe-deficient plants in comparison to the Fe-sufficient ones (Fig. 3.11); which are known to release lower amount of PS). On the other hand, the supply of P-soluble source did not require a mobilization and therefore Fe-sufficient plants exceeded the P accumulation detected in Fe-deficient plants.

In this study, maize plants were grown under Fe deprivation and the plant response was analyzed performing physiological and transcriptomic analyses. In particular deep investigations were performed to underline the capability of Fe-deficient maize plants to use different Fe-sources, conceivably occurring in the rhizosphere, like Fe-Citrate, Fe-PS and Ferrihydrite. Results presented here showed a strong modulation of those pathway involved in the synthesis and release of phytosiderophores. Real time RT-PCR analyses and ^{59}Fe uptake experiments showed that the mechanisms involved in Fe acquisition were induced by the nutritional stress, while the pathways involved in the translocation and distribution of the micronutrient within the plant were not yet activated in Fe-deficient plants.

Interestingly Fe deficiency modulated also some genes involved in P acquisition. The use of soluble Fe-sources, especially Fe-PS, allowed the acquisition and remobilization of P from poorly soluble sources.

3.5 Acknowledgements

Research was supported by grants from Italian MIUR (FIRB-Programma "Futuro in Ricerca" RBFR127WJ9).
Microarray analyses were performed at the Functional Genomics Center (FGC, Department of Biotechnology) at the University of Verona.

3.6 References

Ai P, Sun S, Zhao J, Fan X, Xin W, Guo Q, Yu L, Shen Q, Wu P, Miller AJ, Xu G. (2009). Two rice phosphate transporters, OsPht1;2 and OsPht1;6, have different functions and kinetic properties in uptake and translocation. Plant J 57: 798-809.

Bashir K, Ishimaru Y, Itai RN, Senoura T, Takahashi M, An G, Oikawa T, Ueda M, Sato A, Uozumi N, Nakanishi H, Nishizawa NK. (2015). Iron deficiency regulated OsOPT7 is essential for iron homeostasis in rice. Plant Mol Biol. 88: 165-176.

Bashir K, Ishimaru Y, Shimo H, Kakei Y, Senoura T, Takahashi R, Sato Y, SatoY, Uozumi N, Nakanishi H, Nishizawa NK. (2011). Rice phenolics efflux transporter 2 (PEZ2) plays an important role in solubilizing apoplasmic iron. Soil Science and Plant Nutr 57: 803–812.

Bienfait HF, van den Briel W, Mesland-Mul NT. (1985). Free space iron pools in roots: generation and mobilization. Plant Physiol 78: 596–600.

Bughio N, Yamaguchi H, Nishizawa NK, Nakanishi H, Mori S. (2002). Cloning an iron-regulated metal transporter from rice. J Exp Bot 53: 1677–1682.

Cesco S, Nikolic M, Romheld V, Varanini Z, Pinton R. (2002). Uptake of 59Fe from soluble 59Fe–humate complexes by cucumber and barley plants. Plant Soil 241: 121–128.

ChaneyRL, Brown JC, Tiffin LO. **(**1972). Obligatory reduction of ferric chelates in iron uptake by soybeans. Plant Physiol 50**:** 208–213.

Ciaffi M, Paolacci AR, Celletti S, Catarcione G, Kopriva S, Astolfi S. (2013). Transcriptional and physiological changes in the S assimilation pathway due to single or combined S and Fe deprivation in durum wheat (Triticum durum L.) seedlings. J Exp Bot 64: 1663–1675.

Connolly EL, Fett JP, Guerinot ML. (2002). Expression of the IRT1 metal transporter is controlled by metals at the levels of transcript and protein accumulation. Plant Cell 14: 1347–1357.

Curie C, Panaviene Z, Loulergue C, Dellaporta SL, Briat JF, Walker EL. (2001). Maize yellow stripe1 encodes a membrane protein directly involved in Fe(III) uptake. Nature 409: 346–349.

Eide D, Broderius M, Fett J, Guerinot ML. **(**1996). A novel iron-regulated metal transporter from plants identified by functional expression in yeast. PNAS 93**:** 5624–5628.

Eynard A, del Campillo MC, Barrón V, Torrent J. (1992). Use of Vivianite ($Fe_3(PO_4)_2 \cdot 8H_2O$) to prevent iron chlorosis in calcareous soils. Fert Res 31: 61–67.

Gentleman, R.C., Carey, V.J., Bates, D.M., Bolstad, B., Dettling, M., Dudoit, S., Ellis, B., Gautier, L., Ge, Y., Gentry, J. (2004). Bioconductor: open software development for computational biology and bioinformatics. Genome Biol. 5: R80.

Guzman G, Alcantara E, Barron V, Torrent J. (1994). Phytoavailability of phosphate absorbed on ferrihydrite, hematite and goethite. Plant Soil 159: 219–225.

Hirsch J, Marin E, Floriani M, Chiarenza S, Richaud P, Nussaume L, Thibaud MC. (2006). Phosphate deficiency promotes modification of iron distribution in Arabidopsis plants. Biochimie 88: 1767-1771.

Ihaka R, Gentleman R. (1996). R: A language for data analysis and graphics. J Comput Graph Stat 5: 299-314.

Irizarry RA, Bolstad BM, Collin F, Cope LM, Hobbs B, Speed TP. (2003). Summaries of Affymetrix GeneChip probe level data. Nucleic Acids Res. 31: e15.

Ishimaru Y, Bashir K, Nakanishi H, Nishizawa NK. (2012a). OsNRAMP5, a major player for constitutive iron and manganese uptake in rice. Plant Signal Behav 7: 763–766.

Ishimaru Y, Takahashi R, Bashir K, Shimo H, Senoura T, Sugimoto K, Ono K, Yano M, Ishikawa S, Arao T, Nakanishi H, Nishizawa NK. (2012b). Characterizing the role of rice NRAMP5 in manganese, iron and cadmium transport. Sci Rep 2:286.

Ishimaru Y, Suzuki M, Tsukamoto T, Suzuki K, Nakazono M, Kobayashi T, Wada Y, Watanabe S, Matsuhashi S, Takahashi M, Nakanishi H, Mori S, Nishizawa NK. (2006). Rice plants take up iron as an Fe^{3+}-phytosiderophore and as Fe^{2+}. Plant J 45: 335–346.

Itai RN, Ogo Y, Kobayashi T, Nakanishi H, Nishizawa NK. (2013). Rice genes involved in phytosiderophore biosynthesis are synchronously regulated during the early stages of iron deficiency in roots. Rice 6: 1.

Kobayashi T, Nishizawa NK. (2012). Iron uptake, translocation, and regulation in higher plants. Annual Review of Plant Biology 63: 131–152.

Koressaar T, Remm M. (2007). Enhancements and modifications of primer design program Primer3. Bioinformatics 23:1289-1291.

Lan P, Li W, Wen TN, Schmidt W. (2012) Quantitative phosphoproteome profiling of iron-deficient Arabidopsis roots. Plant Physiol 159:403-17.

Lescure AM, Proudhon D, Pesey H, Ragland M, Theil EC, Briat JF. (1991). Ferritin gene transcription is regulated by iron in soybean cell cultures. PNAS 88: 8222–8226.

Li H, Wang L, Yang ZM. (2015). Co-expression analysis reveals a group of genes potentially involved in regulation of plant response to iron-deficiency. Gene 554: 16-24.

Lindsay WL, Schwab AP. (1982). The chemistry of iron in soils and its availability to plants. J Plant Nutr 5: 821–840.

Lindsay WL. (1974). Role of chelation in micronutrient availability. The plant root and its environment. University Press of Virginia, 507-524.

Liu J, Uhde-Stone C, Li A, Vance CP, Allan DL. (2001). A phosphate transporter with enhanced expression in proteoid roots of white lupine (*Lupinus albus* L.). Plant Soil 237: 257-266.

Marschner H, Romheld V, Horst WJ, Martin P. (1986). Root induced changes in the rhizosphere: importance for mineral nutrition of plants. Z Pflanzenernachr Bodenkd 149: 441–456.

Mengel K, Kirkby EA, Kosegarten H, Appel T. (2001) Principles of plant nutrition. Dordrecht: Kluwer Academic.

Mori S. (1999). Iron acquisition by plants. Curr. Opin. Plant Biol 2: 250–253.

Nozoye T, Nagasaka S, Kobayashi T, Takahashi M, Sato Y, Sato Y, Uozumi N, Nakanishi H, Nishizawa NK. (2011). Phytosiderophore efflux transporters are crucial for iron acquisition in graminaceous plants. J Biol Chem 286: 5446–5454.

Nozoye T, Nakanishi H, Nishizawa NK. (2013). Characterizing the crucial components of iron homeostasis in the maize mutants ys1 and ys3. PLoS One 8: e62567.

Nozoye T, Nakanishi H, Nishizawa NK. (2015). Transcriptomic analyses of maize ys1 and ys3 mutants reveal maize iron homeostasis. Genom. Data 5: 97-99.Ogo Y, Itai RN, Nakanishi H, Kobayashi T, Takahashi M, Mori S, Nishizawa NK. (2007). The rice bHLH protein OsIRO2 is an essential regulator of the genes involved in Fe up-take under Fe-deficient conditions. Plant J 51: 366-377.

Ritz C, Spiess AN. (2008). qpcR: an R package for sigmoidal model selection in quantitative real-time polymerase chain reaction analysis. Bioinformatics 24: 1549-1551.

Robinson NJ, Procter CM, Connolly EL, Guerinot ML. (1999). A ferric-chelate reductase for iron uptake from soil. Nature 397: 694–697.

Romera FJ, Lucena C, Alcàntara E. (2007). Plant hormones influencing iron uptake in plants. In Iron nutrition in plants and rhizospheric microorganisms. 1 edition. Edited by: Barton LL, Abadia J. Dordrecht (eds.), Springer, pp. 251-278.

Schmidt W, Buckhout TJ. (2011). A hitchhiker's guide to the Arabidopsis ferrome. Plant Physiol. Biochem 49: 462-470.

Smyth GK. (2005). Limma: linear models for microarray data. Bioinformatics and Computational Biology Solutions using R and Bioconductor. Edited by: Gentleman R, Carey V, Dudoit S, Irizarry R, Huber W (eds.), Springer, New York, pp. 397–342.

Takahashi R, Ishimaru Y, Senoura T, Shimo H, Ishikawa S, et al. (2011) The OsNRAMP1 iron transporter is involved in Cd accumulation in rice. Journal of Experimental Botany 62: 4843–4850.

Thimm O, Essigmann B, Kloska S, Altmann T, Buckhout TJ. (2001). Response of Arabidopsis to iron deficiency stress as revealed by microarray analysis. Plant Physiol 127: 1030-1043.

Tomasi N, Nobili M, Gottardi S, Zanin L, Mimmo T, Varanini Z, Römheld V, Pinton R, Cesco S. (2013). Physiological and molecular characterization of Fe acquisition by tomato plants from natural Fe complexes. Biology and Fertility of Soils 49: 187-200.

Untergrasser A, Cutcutache I, Koressaar T, Ye J, Faircloth BC, Remm M, Rozen SG. (2012). Primer3-new capabilities and interfaces. NucleicAcidsRes. 40: e115.

Urbany C, Benke A, Marsian J, Huettel B, Reinhardt R, Stich B. (2013). Ups and downs of a transcriptional landscape shape iron deficiency associated chlorosis of the maize inbreds B73 and Mo17. BMC Plant Biol 13: 213.

Vance CP. (2001). Symbiotic nitrogen fixation and phosphorus acquisition: plant nutrition in a world of declining renewable resources. Plant Physiol 127: 390–397.

Vigani G, Zocchi G. (2010). Effect of Fe deficiency on mitochondrial alternative NAD(P)H dehydrogenases in cucumber roots. J Plant Physiol 167: 666–669.

Von Wirén N, Mori S, Marschner H, Römheld V. (1994). Iron inefficiency in maize mutant ys1 (*Zea mays* L cv yellow-stripe) is caused by a defect in uptake of iron phytosiderophores. Plant Physiol 106: 71–77.

Zamboni A, Zanin L, Tomasi N, Pezzotti M, Pinton R, Varanini Z, Cesco S. (2012). Genome-wide microarray analysis of tomato roots showed defined responses to iron deficiency. BMC Genomics 13: 101.

Zancan S, Cesco S, Ghisi R. (2006). Effect of UV-B radiation on iron content and distribution in maize plants. Environ Exp Bot 55: 266–272.

Zheng L, Huang F, Narsai R, Wu J, Giraud E, He F, Cheng L, Wang F, Wu P, Whelan J, Shou H. (2009). Physiological and transcriptome analysis of iron and phosphorus interaction in rice seedlings. Plant Physiol 151: 262–274.

3.7 Supplementary Material

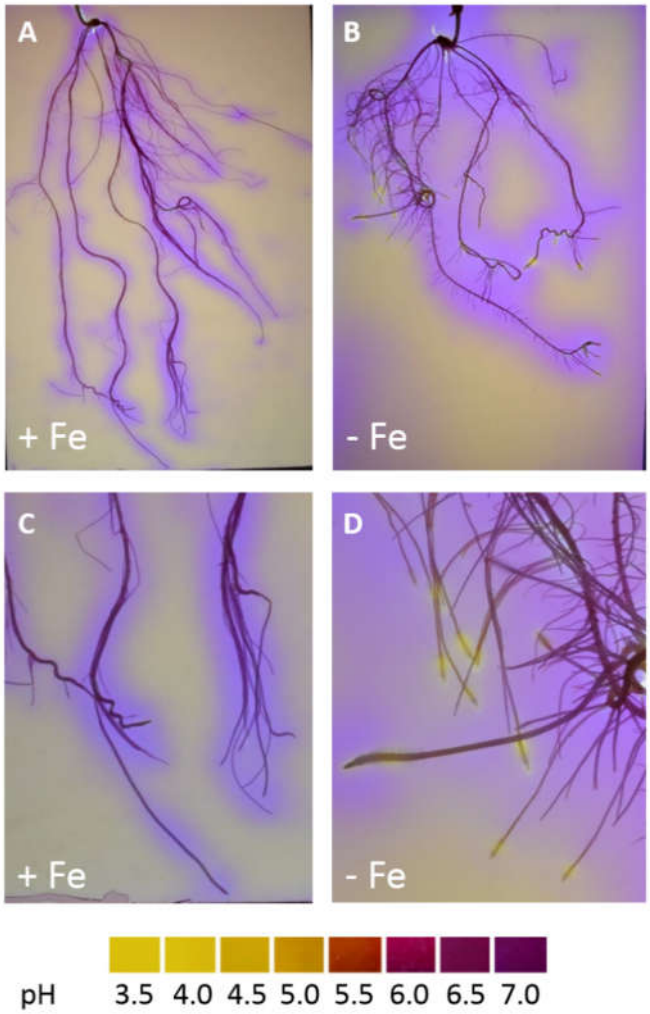

Supplementary Figure 3.1 - External acidification of maize roots under Fe deficiency (B, D) and Fe sufficiency (A, C). Maize roots were imbedded for 4 hours in agar gel containing pH indicator (Bromocresol purple); yellow indicates acidification of agar gel (pH< 5.5) and purple indicates an alkalization above pH 7.

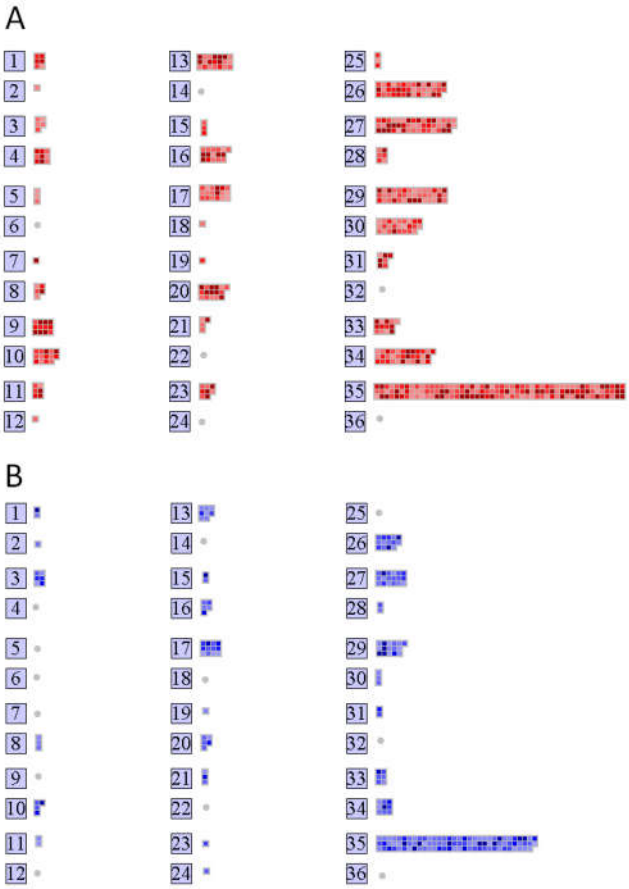

Supplementary Figure S3.2. Overview of up- (A) and down- (B) modulated transcripts in -Fe vs +Fe comparison using MapMan-bincode classification. Numbers refer to the Mapman bincode: *1*, PS; *2*, major CHO metabolism; *3*, minor CHO metabolism; *4*, glycolysis; *5*, fermentation; *6*, gluconeogenesis / glyoxylate cycle; *7*, OPP; *8*, TCA / org transformation; *9*, mitochondrial electron transport / ATP synthesis; *10*, cell wall; *11*, lipid metabolism; *12*, N-metabolism; *13*, amino acid metabolism; *14*, S-assimilation; *15*, metal handling; *16*, secondary metabolism; *17*, hormone metabolism; *18*, Co-factor and vitamine metabolism; *19*, tetrapyrrole synthesis; *20*, stress; *21*, redox; *22*, polyamine metabolism; *23*, nucleotide metabolism; *24*, Biodegradation of Xenobiotics; *25*, C1-metabolism; *26*, miscellaneous; *27*, RNA; *28*, DNA; *29*, protein; *30*, signalling; *31*, cell; *32*,micro RNA, natural antisense; *33*, development; *34*, transport; *35*, not assigned. Color scale refers to the fold change values of differentially expressed transcripts: *red* color refers to those transcripts positively regulated by Fe deficiency, while in blue are transcripts negatively regulated by Fe deficiency.

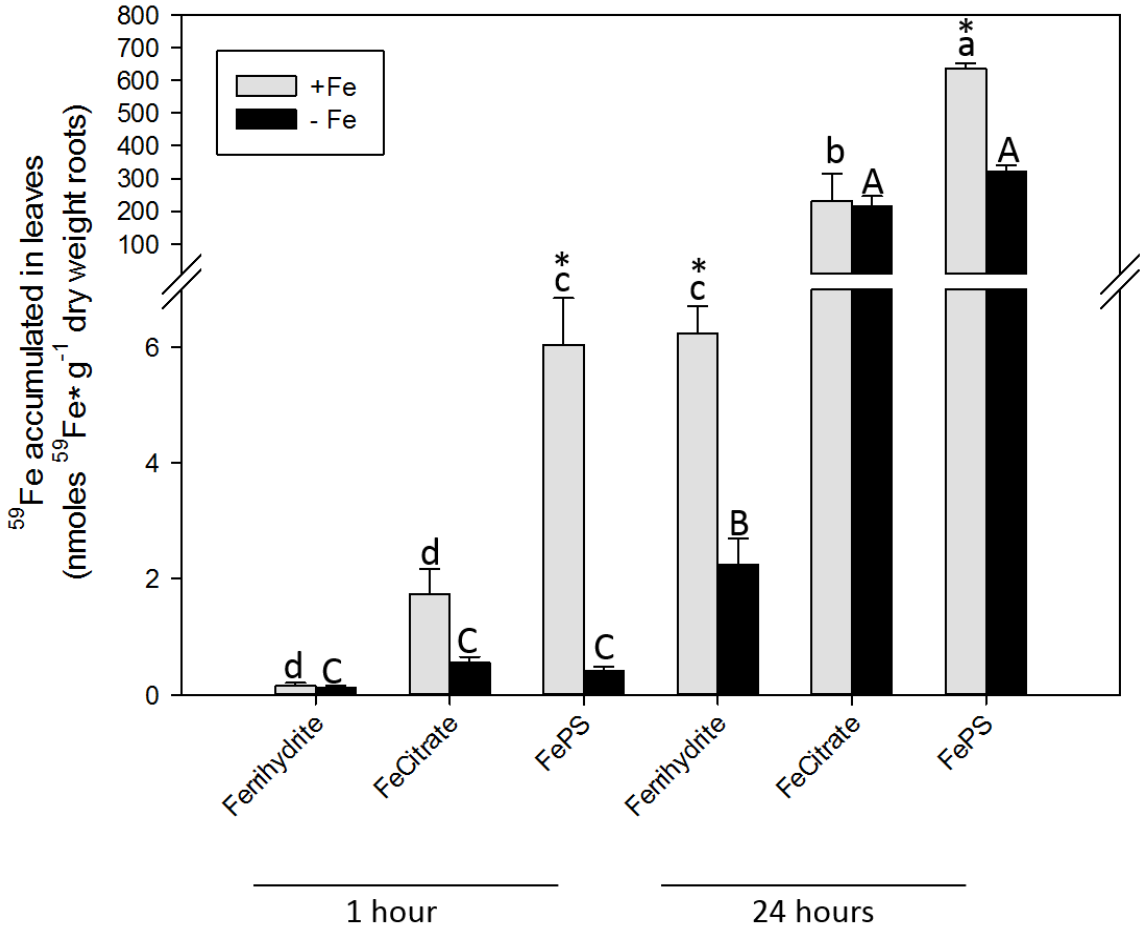

Supplementary Figure S3.3 - Iron-(^{59}Fe) accumulated in maize leaves. The plant ability to accumulate Fe was evaluated by ^{59}Fe uptake experiments on Fe-sufficient (+Fe, grey bars) and Fe-deficient (-Fe, black bars) plants treated for 1 and 24 hours with three labelled ^{59}Fe-sources: (^{59}Fe)Ferrihydrite, ^{59}FeCitrate or ^{59}FePS. Iron-(59Fe) was added to nutrient solution at final concentration of 1 µM. Data are means+SD of three independent experiments. *Small letters,* refer to statistically significant differences among Fe sufficient plants; *capital letters,* refer to statistically significant differences among Fe deficient plants, *asterisks*, refer to statistically significant differences between the two growth condition (-Fe and +Fe). ANOVA Holm–Sidak, N=3, P <0.05). DW, dry weight.

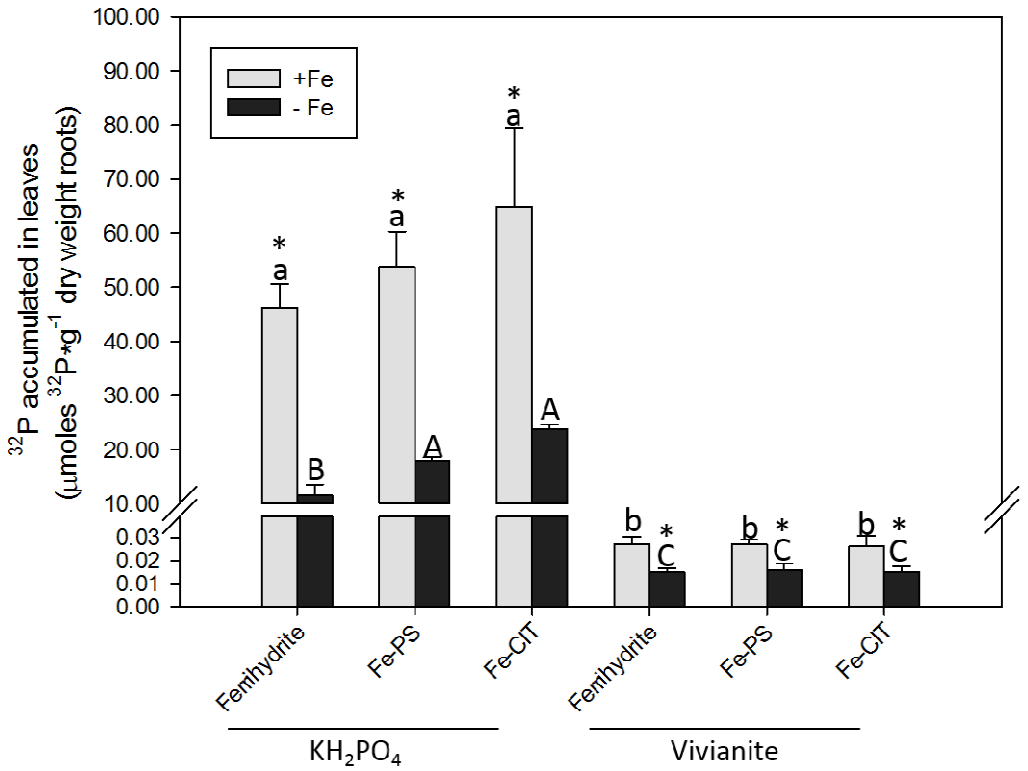

Supplementary Figure S3.4 - Phosphorus-(^{32}P) accumulated in maize leaves. The plant ability to accumulate P was evaluated by ^{32}P uptake experiments on Fe-sufficient (+Fe, grey bars) and Fe-deficient (-Fe, black bars) plants. Up to 24 hours, -Fe and +Fe plants were treated with three unlabelled Fe-sources (Ferrihydrite, FeCitrate or FePS) provided in conjunction with two different labelled ^{32}P-sources: (^{32}P)KH_2PO_4 or (^{32}P)Vivianite. Iron and phosphorus were added to nutrient solution at final concentration of 1 µM each. Data are means+SD of three independent experiments. *Small letters,* refer to statistically significant differences among Fe sufficient plants; *capital letters,* refer to statistically significant differences among Fe deficient plants, *asterisks*, refer to statistically significant differences between the two growth condition (-Fe and +Fe). ANOVA Holm–Sidak, N=3, P <0.05). DW, dry weight.

4. PHYSIOLOGICAL, TRANSCRIPTIONAL AND METABOLOMIC ANALYSES OF THE RESPONSE TO IRON AND PHOSPHORUS DEFICIENCY IN WHITE LUPINE

Physiological, transcriptional and metabolomics analyses of the response to iron and phosphorus deficiency in white lupine

Silvia Venuti[1], Laura Zanin[1], Fabio Marroni[1], Michele Morgante[1], Javier Abadia[2], Ana Maria Àlvarez-Fernandez[2], Nicola Tomasi[1] and Roberto Pinton[1]

[1] Dipartimento di Scienze Agroambientali, Alimentari e Animali, University of Udine, via delle Scienze 208, I-33100 Udine, Italy

[2] Department of Plant Nutrition, Estacion Experimetal de Aula Dei, Avda Montanana, Zaragoza, Spain

Abstract

Iron (Fe) and phosphorus (P) are essential nutrients for plants growth. Despite their abundance in soils, they are barely available for plants. In order to overcome these nutritional stresses, plants have evolved many strategies including physiological, biochemical and morphological adaptations. Low molecular weight compounds released from the roots, generally called exudates, play a crucial role in P and Fe mobilization. White lupine (*Lupinus albus* L.) is considered a model plant for studying root exudates. In fact, this plant is able to markedly modify its root architecture by forming special structures called cluster roots, which release huge amounts of exudates in the rhizosphere soil.

This work aimed to compare the physiological, metabolomic and transcriptomic responses of – P and – Fe white lupine plants, in the attempt to clarify how the mechanisms involved in the acquisition of Fe might be affected by the P-deficient nutritional status and *vice versa*.

The results highlighted a physiological and transcriptional link between the responses to Fe and P deficiency in white lupine. Phosphorus-deficient plants activated the Strategy I Fe acquisition mechanisms, leading to an enhanced Fe mobilization and translocation. On the other hand, Fe deficiency also induced the transcription of some P deficiency-responsive genes. Iron and P deficiency determined the release of scopoletin and genistein derivatives. Furthermore, in –Fe plants the variety of coumarins compounds released were wider than in – P plants, which released mostly isoflavonoids. The analysis of the root contents showed that white lupine synthesises a set of constitutive compounds, which are found as malonyl-derivatives forms independently of the nutritional status of plants; these compounds are then released in aglycon-forms when plants are experiencing P or Fe deficiency conditions.

4.1 Introduction

Iron (Fe) and phosphorus (P) are essential nutrients for plant growth and yield quality. Even if they can be present in sufficient amounts in soils, they are poorly available for plant acquisition. In alkaline soils, which represented one-third of the earth's surface, both Fe and P are even less soluble due to their precipitation with hydroxides and Mg and Ca ions, respectively (Hansen et al. 2006). These deficiency-inducing conditions can be prevented by the use of organic or mineral fertilizers for P or using synthetic chelate molecules for Fe. Nevertheless, these applications are often costly both at the economical and environmental levels. For these reason, alternative agronomical practices are needed for a more sustainable agriculture.

A deeper understanding of mechanisms used by plants to overcome low P or Fe availability are necessary in order to increase their nutrient use efficiency. Plants have developed two mechanisms for Fe acquisition, called *Strategy I* and *Strategy II*. In *Strategy I*, used by non-graminaceous monocots and dicots, plants acidify the rhizosphere increasing the solubility of Fe. Roots also release different molecules, like carboxylates and phenolic compounds, in order to chelate Fe (III) present in the soil (Marschner and Römheld 1994). Chelated Fe(III) is reduced by a specific oxidoreductase (FRO2, Robinson NJ et al., 1999) and Fe^{2+} is taken up by root cells, *via* a specific transporter known as Iron regulated transporter1 (IRT1, Eide et al., 1996). In *Strategy II*, confined to grasses, plants release phytosiderophores (PS), which strongly chelate Fe (III). The absorption of the complex Fe (III)-PS inside root cells is mediated by an oligopeptide transporter, called Yellow stripe 1 (YLS1; Curie et al., 2001; Le Jean et al., 2005). Transcriptional regulation of the responses in both strategies has been widely demonstrated.

To increase the P availability, plants induce physiological, biochemical and morphological adaptations, generally called phosphate starvation response (PSR) (Vance et al., 2003; Secco et al., 2014). This plant response determine the release of carboxylates and phenolic compounds and lead to transcriptional induction of genes coding for high-affinity phosphate transporters (PHT), phosphatases and regulatory components (e.g. transcription factors, hormones, epigenetic modifications). These changes lead to an increased mobilization of Pi and to a modulation of P homeostasis. In both nutritional stresses, the release in the rhizosphere of a wide range of molecules, called root exudates, is crucial for the effectiveness of the response. Root exudates act by mobilizing the sparingly available nutrients in soils mainly via complexation, ligand exchange

and, in the case of phenolic compounds, reduction; they can also affect soil microbial activities. White lupine (*Lupinus albus* L.) is considered a model plant for studying on root exudates. In soils with low nutrient availability, this plant strongly modifies the root architecture with the formation of bottlebrush like structures, called cluster or proteiod roots (Vance et al., 2003). These latter are able to release huge amounts of root exudates in soil, which strongly modify the biological, chemical and physical characteristics of the rhizosphere and therefore mobilize Fe and P. Although the response of white lupine plants to P deficiency is quite well characterized, that to Fe deficiency is still barely known. The aim of this work was to characterize the Fe-deficiency response in white lupine plants. Moreover, comparing the physiological, metabolomic and transcriptomic data of the – P and – Fe plants it was tempted to clarify how the mechanisms involved in the acquisition of Fe were affected by the P-deficient nutritional status and *vice versa*.Our aim was to investigate the common feature and differences between the two types of responses.

4.2 Materials and methods

4.2.1 Plant growth

White lupine seeds (*Lupinus albus* L. cv. Amiga; Südwestdeutsche Saatzucht, Rastatt, Germany) were soaked for 24 hours in aerated water and germinated on a plastic net placed at the surface of an aerated 0.5 mM $CaSO_4$ solution in a growth chamber at 25 °C in the dark. Thereafter, 4-day-old seedlings were transferred in a hydroponic system, containing a complete nutrient solution with the following composition: [mM] 0.25 KH_2PO_4, 5 $Ca(NO_3)_2$ $4H_2O$, 1.25 $MgSO_4$, 1.75 K_2SO_4, 0.25 KCl; [µM]: 20 Fe(III)EDTA, 25 H_3BO_4, 1.25 $MnSO_4$ $7H_2O$, 1.5 $ZnSO_4$ $7H_2O$, 0.5 $CuSO_4$ $5H_2O$, 0.025 $(NH_4)_6Mo_7O_{24}$ $4H_2O$, or in a P-free or Fe-free nutrient solution. The nutrient solution was renewed every 3 days. Plants were grown in a growth chamber under controlled conditions for 4 weeks (day/night photoperiod, 16/8 h; radiation, 220 µ Einsteins $m^{-2}s^{-1}$; day/night temperature, 25/20 °C; relative humidity, 70-80 %). During the growth period, light transmittance of leaves was determined every 4-5 days using a portable chlorophyll meter SPAD-502 (Minolta, Osaka, Japan) and presented as SPAD index values. The shoot and root materials were collected and stored at -80°C for the further molecular analysis only on the root apices (1-cm length) for sufficient plants and apices and cluster roots for P- and Fe-deficient plants. Experiments were repeated three times.

4.2.2 Acidification capability of the whole root system

The potential difference in acidification among control, - P and – Fe white lupine plants were visually investigated. After grown for 32 days in treatment solution, the intact plants were taken from the pots and rinsed in distilled water. Afterward, the whole plant roots were placed on a 3-mm-thick agar gel (9.0 g/liter) layer with pH 5.5 containing 0.1 g/liter pH indicator (bromocresol purple). To separate the root, was used a nipper and a transparent film; afterwards the root surface was placed in agar. The transparent film was removed and a glass plate was located above the agar gel film 3 mm surface in order to provide aeration to the root. The agar gel film was wrapped with an aluminum foil to avoid light penetration into the root zone and placed in the grow chamber for 4 hours before visualization.

4.2.3 Fe-reduction capability of the whole root system

Similarly to acidification gel, the reduction capability among the different treatment were compared using a gel containing a chelating agent for Fe(II). The experimental setup is the same as previously described except for the gel composition (1.0% w/v), 100 μM Fe-III-EDTA and 300 μM BPDS (bathophenantroline-disulfonic acid).

4.2.4 Preparation of soluble and poorly soluble sources of Fe or Pi

Fe-EDTA was prepared according to von Wirén et al. (1994) by mixing EDTA (10% excess) with $FeCl_3$. Fe concentration of the Fe sources was measured by inductively coupled plasma atomic emission spectrometry (ICP-AES) before its use for plant treatments. The KH_2PO_4 (Sigma Aldrich) solution was prepared to a final concentration of 250 μM.

Amorphous Fe hydroxide was obtained by precipitating $^{59}Fe(NO_3)_3$ at alkaline pH, with the addition of 1 M KOH (Guzman et al., 1994). The Synthetic Vivianite was obtained as described in Eynard et al. (1992) through the slow neutralization of $FeSO_4$ (0.05 M) in H_3PO_4 (0.035 M, 250 mL) with KOH (0.05M) at room temperature. The pH of the mixture was brought up to 6, where the precipitation of a blue-grey powder occurred. The powder was washed via centrifugation with Milli-Q water to remove the presence of salt. One milliliter of suspension containing respectively either ^{59}Fe hydroxide (2 μmol Fe) or ^{32}P Vivianite (2 μmol P) was transferred into a dialysis tube (ZelluTrans/Roth 6.0, Ø16 mm, exclusion limit of 8–10 kDa, ROTH, Karlsruhe, Germany) and mixed with 8 mL of a nutrient solution with the following

composition (in millimolar): K_2SO_4 0.7, KCl 0.1, $Ca(NO_3)_2$ 2.0, $MgSO_4$ 0.5, KH_2PO_4 0.25, and MES-KOH 10 (pH 6).

4.2.5 Iron (^{59}Fe) uptake from soluble and poorly soluble sources by white lupine plants

The day before of the experiment, roots of Control, P-deficient and Fe-deficient plants were washed 3 times with deionized water and then transferred into beakers containing 230 mL of a freshly prepared Fe nutrient solution. The next day ^{59}Fe-EDTA, (^{59}Fe)Ferrihydrite at a specific activity of 144 kBq μmol^{-1} Fe (Perkin Elmer, Monza, Italy) were added to give a final Fe concentration of 1 μM. The photochemical reduction phenomena of Fe in the nutrient solution (Zancan et al. 2006), was limited covering the beakers with black plastic foils during the entire experiment The ^{59}Fe uptake analysis were performed after 1, 4, 8 and 24 h of treatments. At each time point plants were transferred into cold deionized water for 10 min in order to stop Fe uptake and remove the excess of ^{59}Fe at the root surface. Root apoplastic ^{59}Fe pools were removed by 1.2 g L^{-1} sodium dithionite and 1.5 mM 2,2′-bipyridyl in 1 mM $Ca(NO_3)_2$ under N_2 bubbling gas described by Bienfait et al. (1985). After roots and leaves were harvested and collected separately in vials. Root and shoot tissues were dried in a oven at 80°C, weighed, ashed at 550 °C, and suspended in 1 M HCl for ^{59}Fe determination by liquid scintillation counting. The ^{59}Fe uptake rate, measured as nanomoles of ^{59}Fe, is referred to root and is presented as g^{-1}*root Dry Weight for 1, 8, 4 or 24 h.

4.2.6 Phosphorus (^{32}P) uptake from soluble and poorly soluble sources by white lupine plants

Before starting the assay, the roots were washed twice for 5 minutes in 0.5 mM $CaSO_4$, in order to remove the apoplastic component. Afterwards the plants were transferred into the uptake solution, buffered to pH 6.0 with 10 mM MES-KOH and containing phosphorus supplied as KH_2PO_4 or Vivianite labeled with ^{32}P in an amount equal to 2.47 kBq μmol^{-1}. The uptake was performed at 1, 4, 8 and 24 hours. At the end, samples were transferred for 5 minutes in a cold washing solution. This operation was repeated twice. In this way, the apoplastic radioactive component was removed and the uptake of ^{32}P was blocked. After roots and leaves were harvested and collected separately in vials. Root and shoot tissues were oven dried at 80 °C, weighed, ashed at 550 °C, and suspended in 1 M HCl for ^{32}P determination by liquid scintillation counting. The ^{32}P uptake rate, measured as nanomoles of ^{32}P, is referred to root plants and is

presented as g^{-1}*Root Dry Weight for 1, 4, 8 or 24 h. The same experiment setup was used on excised root tissues, *i.e.* root apices and cluster roots, up to 1 h.

4.2.7 RNA Extraction, cDNA Library Preparation and Sequencing for RNA-Seq

Total RNA was extracted from three biological replicates of 12 root samples apices for control plants and apices and cluster root for Pi and Fe deficient plants using the Spectrum™ Plant Total RNA Kit (Sigma Aldrich). RNA samples were quantified using *Qubit*™ 2.0 Fluorometer (Life Technology), and RNA integrity was checked with the RNA6000 Nano Assay using the Agilent 2100 Bioanalyzer (Agilent Technologies). cDNA library preparation and sequencing reactions were performed by IGA Technology Services s.r.l. (Udine, Italy). An amount of 2 µg of total RNA was used for library preparation following the Illumina protocol TrueSeq 2.0. Briefly, RNA was fragmented into fragment with an average of 500 bp. Then, mRNA was purified using poly-T beads. The first- and second-strand cDNAs were synthesized and end repaired. Adaptors were ligated after adenylation at the 3' ends and cDNA templates were enriched by PCR. The 50 bp single end reads were obtained using an Illumina Hiseq2000 platform.

4.2.8 Sequence processing

Adapters were removed using cutadapt (http://code.google.com/p/cutadapt/) and the reads were trimmed for quality with ERNE-FILTER (http://erne.sourceforge.net). Alignment against the transcriptome [Lupinus albus Gene Index Version 2 (LAGI02, Secco *et al*., 2014)] was performed with TopHat version 2.0.5 (Kim et al, 2013) with default parameters. Transcript expression was estimated using cufflinks (Trapnell *et al*, 2010), and differential expression evaluated using cuffdiff software (P-value ≤ 0.05, n=3; Trapnell *et al*., 2012). Differentially expressed genes were assigned to functional categories using BlastX and Blast2GO and to metabolic pathways using MapMan.

4.2.9 Statistical analyses

Physiological and transcriptomic analyses were performed on three independent biological replicates obtained from independent experiments (n = 3), a pool of six plants was used for each sample. Statistical significance was determined by one-way analysis of variance (ANOVA) using Holm–Sidak test ($P < 0.05$, n = 3). Statistical analyses were performed using SigmaPlot Version 12.0 software.

4.2.10 Extraction of phenolics from roots and nutrient solutions

Phenolic compound were extracted from roots and nutrient solutions as described by Fourcroy et al. (2014), with some modifications. For each sample, the extraction was done twice. The first extraction was aimed to identify relevant compounds in the samples (those increased with Fe and P deficiency). The second extraction of phenolics was carried out with the addition of internal standards (ISs) to the samples (see below) and aimed at the quantification of the compounds of interest.

Frozen roots (100 mg) were ground with 1 mL of 100 % LC-MS grade methanol in a Retsch M301 ball mill (Restch, Düsseldorf, Germany) for 5 min. The supernatant was recovered by centrifugation (12,000 g, 4 ºC and 5 min) and stored at -20 °C, and the pellet was resuspended with 1 mL of 100% methanol and with or without 33 µL of a solution of the internal standards (6.6 µM esculetin, 3.3 µM, artemicapin C, 6.6 µM isofraxidin and 43.4 µM myrecitrin, 13.7 µM quercetin malonyl-O-glucoside and 43.4 naringenin), homogenised for 5 min and the supernatant recovered again. This step was repeated without the addition of internal standards. All three supernatants per sample were pooled, vacuum concentrated and diluted with a solution of 15% methanol and 0.1% formic acid to a final volume of 250 µl. Extracts were filtered through polyvinylidene fluoride (PVDF) 0.45 µm ultrafree-MC centrifugal filter devices (Millipore, Billerica, MA, USA) and stored at -80 °C until analysis.
Phenolics of nutrient solutions (500 mL of solution used for the growth of 6 plants) were retained in a SepPack C18 cartridge (Waters), eluted from the cartridge with 2 mL of 100 % LC-MS grade methanol, and the eluates stored at -80 ºC. One day before phenolics analyses, the eluates were thawed and an aliquot of 400 µl were vacuum dried with and without 20 µl of a solution of internal standards (2.6 µM esculin, 13.4 µM esculetin, 13.4 µM artemicapin C, 2.6 µM myrecitrin and 5.3 µM naringenin). The dried samples were dissolved with a solution of 15% methanol and 0.1% formic acid to a final volume of 100 µl, and then analyzed for phenolics.

4.2.11 Phenolics analysis by HPLC-UV/VIS-ESI-MS (TOF)

HPLC-UV/VIS-ESI-MS (TOF) analysis was carried out using the method of Fourcroy et al. (2014) with some modifications. An Alliance 2795 HPLC system (Waters) coupled to a UV/VIS (Waters PDA 2996) detector and a time-of-flight mass spectrometer [MS(TOF); MicrOTOF, Bruker Daltonics, Bremen, Germany] equipped with an electrospray (ESI) source were used.

Separations were performed using an analytical HPLC column (Symmetry® C18, 15 cm x 2.1 mm i.d., 5 µm spherical particle size, Waters) protected by a guard column (Symmetry® C18, 10 mm x 2.1 mm i.d., 3.5 µm spherical particle size, Waters) with a gradient mobile phase built with 0.1% (v/v) formic acid in water and 0.1% (v/v) formic acid in methanol. Table 4.1 shows the elution program. The flow rate and injection volume were 0.2 ml min^{-1} and 20 µl, respectively.
The ESI-MS(TOF) operating conditions and software were those described in Fourcroy et al. (2014). Mass spectra were acquired in positive and/or negative ion mode in the range of 50-1000 mass-to-charge ratio (*m/z*) units. The mass axis was calibrated externally and internally using Li-formate adducts [10 mM LiOH, 0.2% (v/v) formic acid and 50% (v/v) 2-propanol]. The internal mass axis calibration was carried out by introducing the calibration solution with a divert valve at in the first and last three minutes of each HPLC run. Molecular formulae were assigned based on exact molecular mass with errors <5 ppm (Bristow, 2006).. Concentrations of phenolics were quantified by external calibration with internal standardization. For analytes and internal standards, the peak areas were obtained from chromatograms extracted at the *m/z* (± 0.02) ratios corresponding to $[M+H]^+$ ions, with the exception of glycosides, for which the *m/z* ratios corresponding to $[M\text{-hexose}+H]^+$ ions were used.

4.2.12 Phenolics analysis by HPLC/ESI MS/MS(ion trap)

HPLC-ESI-MS/MS (ion trap) analysis was carried out with the Alliance 2795 HPLC system (Waters) coupled to a spherical ion-trap mass spectrometer (HCT Ultra, BrukerDaltonics) equipped with an ESI source. The HPLC conditions were those described above. ESI-ion trap-MS analysis was carried out in positive and/or negative ion mode, the MS spectra were acquired in the standard/normal mass range mode and the mass axis was externally calibrated with a tuning mix (from Agilent Technologies). The HCT Ultra was operated with settings shown in Table 4.2. The protonated ions of interest $[M+H]^+$ were subjected to collision induced dissociation (CID; using the He background gas present in the trap for 60 ms) to produce a first set of fragment ions, MS/MS or MS^2. Subsequently, one of the fragment ions was isolated and fragmented to give the next set of fragment ions, MS^3 and so on. For each precursor ion, the fragmentation steps were optimized by visualizing the intensity changes of the fragmented ions.

Table 4.1 - Elution program used for HPLC based separation of phenolics. The mobile phase was built with two solvents: 0.1% of formic in water (A) and 0.1% formic acid in methanol (B).

Time (min)	% solvent B
0	15
45	50
48	55
50	55
53	15
60	15

Table 4.2 - Operating conditions of the HCT Ultra ion trap mass spectrometer used for identification of phenolics.

Nebulizer gas	N_2
Nebulizer gas pressure	40 psi
Drying gas	N_2
Drying gas (N_2) flow rate	9.0 l min^{-1}
Drying gas temperature	350 ºC and 200 ºC
Operation mode	Full scan and Multiple Reaction Monitoring (MRM)
Target for full scan mode	30,000
Maximum accumulation time for full scan mode	200 ms
Mass-to-charge ratio (*m/z*) range for full scan mode	50-1200 u
Target for MRM mode	30,000
Maximum accumulation time for MRM mode	200 ms
Mass-to-charge ratio (m/z) range for MRM mode	50-500 u
Fragmentation amplitude for MS2 and MS3	1.0 V
Isolation width for MS2 and MS3	1.0 and 2.0 u
Cutoff selection to precursor mass for MS2 and	27.0%

4.3 Results

4.3.1 Morphological and physiological changes in P-deficient and Fe-deficient plants

To study the molecular and physiological response of white lupine plants to P- and Fe-starvation, plants were grown for 32 days under hydroponic conditions in a complete nutrient solution (+P, +Fe) or maintained in a nutrient solution depleted in P or Fe. At the end of the growing period typical symptoms of P and Fe deficiency were observed (Fig. 4.1**).**

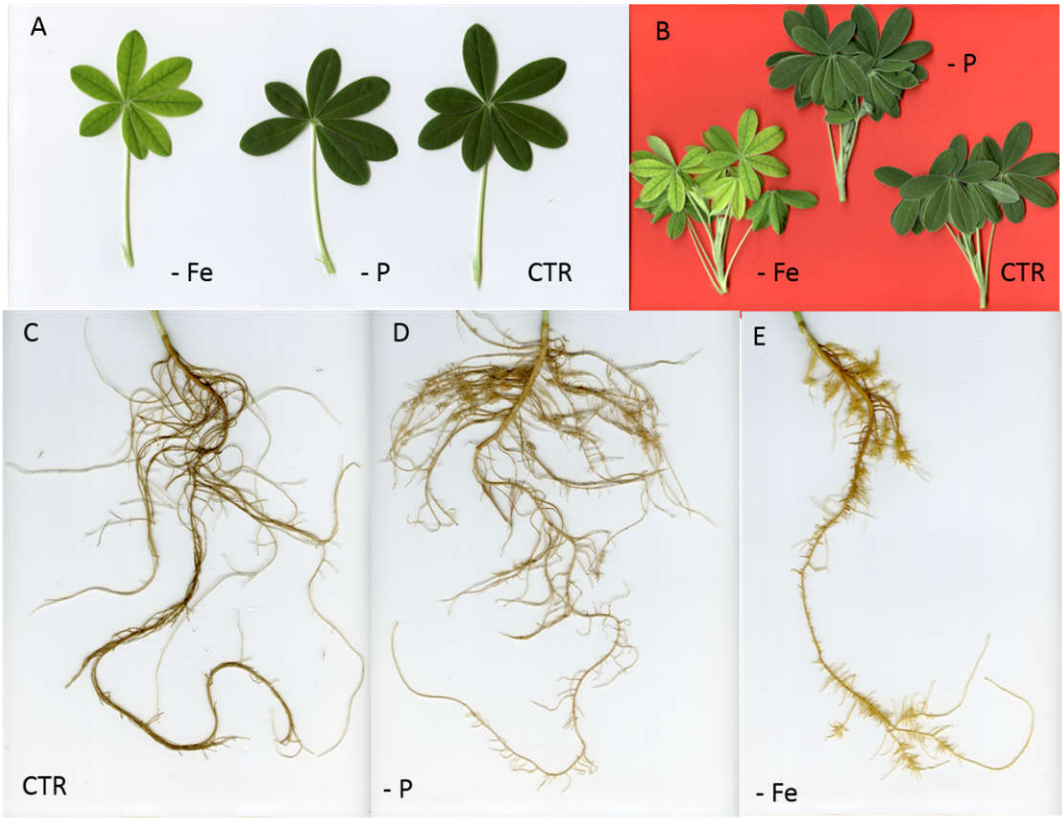

Figure 4.1 - Shoot (A-B) and root (C-E) system of plants grown in phosphorus (P) or iron (Fe) starvation or in complete nutrient solution (CTR).

The leaves of P-deficient plants showed a dark blue-green color while Fe-deficient plants had chlorotic leaves (Fig. 4.1, A and B) indicating a decrease in the chlorophyll content (see also values of SPAD index, Fig. 4.2). No significant variations in the SPAD index values were instead detected in leaves of P-deficient plants as compared to control plants. The nutritional status also induced morphological changes in the root architecture. In P- and Fe-starved plants,

the production of proteoid roots (cluster roots) was enhanced (Fig. 4.1, D and E). These tertiary root structures were completely absent in plants grown in a complete nutrient solution (Fig. 4.1, C). As compared to Fe-deficient plants, P-deficient ones showed a much bigger development of the roots, with longer lateral roots; furthermore, the number of cluster roots was higher in these plants and distributed in the upper part of the root system.

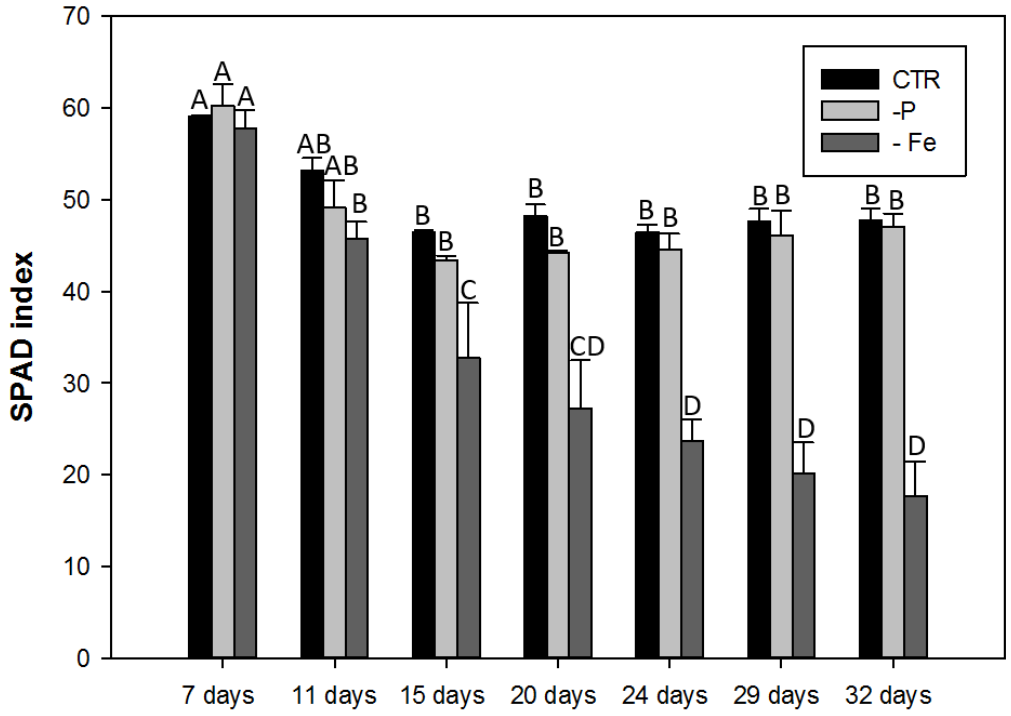

Figure 4.2 - SPAD index values of leaf tissues were measured at the beginning of the treatment (7 day), and after every-3-4 days of Fe and P deficiency.

The capability of the root system to acidify the rhizosphere was observed using an acidification gel, containing bromocresol purple as pH indicator. In the figure 4.3, A, the control plant showed an alkalinization of the substrate, in particular at the root apex. On the other hand, under P deficiency a clear acidification was observed at the level of cluster roots (Fig. 4.3, B). Acidification of the external medium was observed also for Fe-starved plants, involving the whole root apparatus (Fig. 4.3, C).

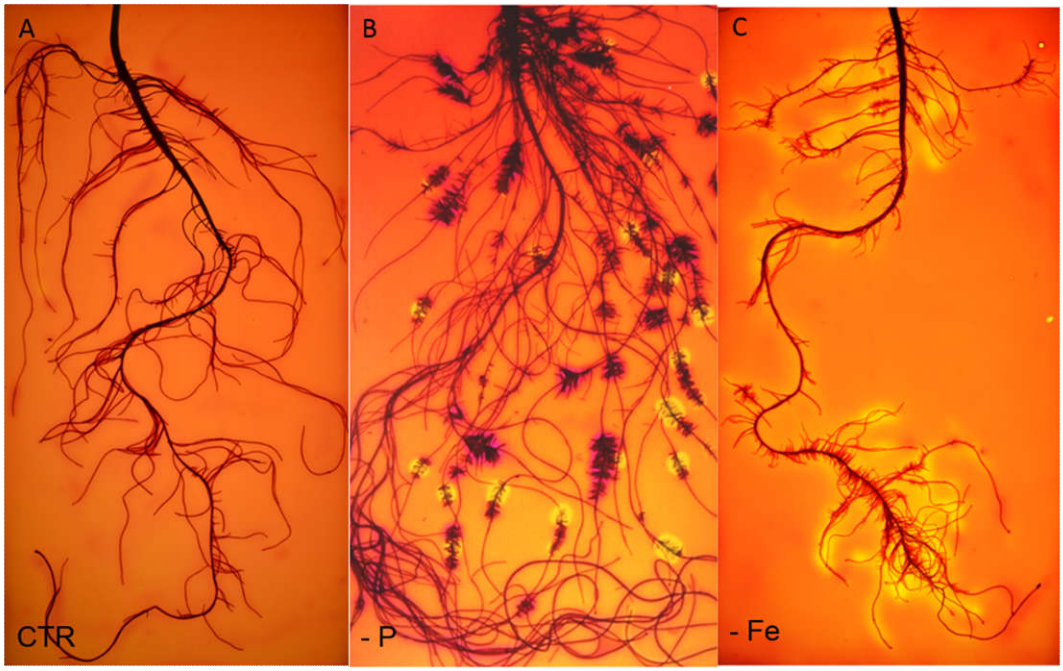

Figure 4.3 - Visualization of rhizosphere acidification by the root system of control (A), P-deficient (B), or Fe-deficient (C) plants. The roots (32-day-old plants) were placed for 6 h in agar gel containing bromocresol purple as pH indicator. Yellow indicates acidification, purple indicates alkalinization.

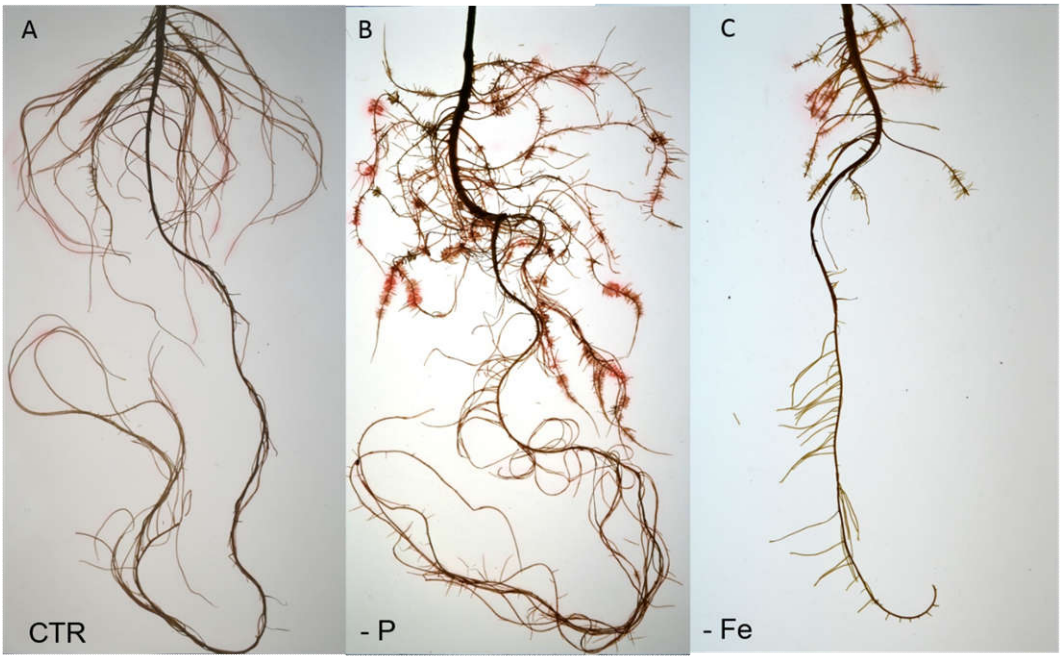

Figure 4.4 - Visualization of Fe(III)-reductive activity by the root system of control (A), P-deficient (B), or Fe-deficient (C) plants. The roots (32-day-old plants) were placed for 6 hour in agar gel containing 100 µM Fe (III)-EDTA and 300 µM BPDS; the formation of Fe(II)-BPDS determines the reddish color.

Fe(III)-chelate (Fe(III)-EDTA) reductase activity of white lupine was detected for all the three plant growth conditions (CTR, - P, - Fe). While control plants showed a weak reduction activity, Fe- and P-deficient plants showed a strong reduction activity, especially at the level of cluster roots (Fig. 4.5).

4.3.2 Overview of transcriptomic data

The transcriptomic analysis of white lupine was performed on roots tissue, which include: root apices or cluster root of Fe-deficient plants, (-Fe RA or –Fe CR, respectively), cluster root of P-deficient plants (-P CR) and root apices of plants grown in a complete nutrient solution (CTR RA). For each thesis, three independent biological replicates were used and the generated RNA-seq libraries were then single–end sequenced. After filtering, reads (length above 50 bp) were aligned against a reference transcriptome of lupin [*Lupinus albus* Gene Index Version 2 (LAGI02, Secco et al., 2014)]. Four transcriptomic profiles were obtained (-Fe RA, -Fe CR, -P CR, CTR RA) and were then compared with each other (Table 4.3).

Table 4.3 - Number of up- and downregulated genes for each transcriptomic comparison. –Fe RA, root apices of Fe-deficient plants; -Fe CR, cluster roots of Fe-deficient plants; -P CR, cluster roots of P-deficient plants; CTR RA, root apices of control plants

Comparison	Upregulated genes	Downregulated genes
- Fe RA vs Control RA	924	717
- Fe CR vs Control RA	2084	3388
- Fe CR vs - Fe RA	893	700
- P CR vs - Fe CR	1212	701
- P CR vs Control RA	1129	932

In the comparison - Fe RA vs CTR RA the amount of genes up regulated was higher than the genes repressed, 924 and 717, respectively. In proteoid roots (CR) of Fe-deficient plants, the number of up- and downregulated transcripts was much higher than that of the comparison -Fe RA vs Control RA. Indeed, there were about 1600 modulated genes when comparing cluster roots with root apices of -Fe plants (- Fe CR vs - Fe RA). When comparing the cluster roots of -P and -Fe plants, the amount of upregulated genes in -P CR was even higher with a comparable number of repressed ones. Also in the comparison -P CR versus the apices of control plants an up- and down-regulation of 1129 and 932 genes, respectively, has been observed.

4.3.3 Iron deficiency responsive genes

In the five comparisons, the expression of those genes known to be involved in the response to Fe-deficiency was checked and reported in Tab. 4.4. Particular attention was paid to those transcripts involved in the Fe acquisition by *Strategy I* mechanism. Most of identified transcripts code for only putative proteins, which showed sequence similarity with known proteins of Arabidopsis (Tab. 4.4).

In the root apices and cluster roots of Fe-starved plants compared with control plants, several Fe-responsive genes were found to be induced by Fe deficiency, such as *FRO2* and its isoform *FRO3*, the oxidoreductases putatively involved in the Fe(III) reduction at the root cell-rhizosphere interface. Another protein involved in Fe-deficiency response, the H^+ATPase isoform AHA2 presumably responsible for rhizosphere acidification, was upregulated in CR and apices of –Fe plants; other AHA gene isoforms such as *AHA1, AHA3* and *AHA6* showed an

increase in their transcript levels. Transcription of a gene coding for putative transporter for phenolic compounds *PDR9* was induced. Other regulatory genes with crucial functions in Fe acquisition, like *FIT* (Fe-deficiency induced transcription factor), *bHLH38* and *IREG2* (*iron regulated protein*), were all upregulated. *IREG2* is co-regulated with *IRT1*, the Fe^{2+} transporter, by the transcription factor FIT bound to bHlH38. In addition, oligopeptide transporters (OPT3, OPT7), essential for systemic iron signaling and redistribution, were positively modulated. Higher transcript levels due to Fe deficiency are also detected for the gene coding for transporter like *Nramp1*. Another marker gene for Fe-deficiency response is *FRD3*, encoding a citrate efflux transporter putatively involved in the xylem citrate loading for Fe translocation to the shoot**,** is massively upregulated. Genes coding for ferritin isoforms (*FER1*, *FER2*, *FER4*) involved in Fe storage were negatively modulated by Fe deficiency.

Comparing CR of P-deficient plants *versus* RA of sufficient plants, the modulation of some of Fe-deficiency-related genes was also observed. The upregulation involved transcripts of the following genes: *FIT, FRO2, FDR3, PDR9, AHA2, ATIREG2, ZIP1,NRAMP1* and *PEZ1*. The transcript factor *FIT*, and the transporter *FDR3* showed a great upregulation compared with the control. Also *FER1* and *FER4*, coding for the major intracellular Fe storage protein, exhibited an increase in their transcript levels.

Table 4.4 – List of modulated transcripts involved in the Fe acquisition . FC, fold change.

White Lupine Gene ID	Arabidopsis Gene ID	Symbol	Description	Comparisons (Log_2 FC)				
				- Fe CR vs CTR RA	-Fe RA vs CTR RA	-Fe CR vs -Fe RA	- P CR vs -Fe CR	-P CR vs CTR RA
LAGI02_24785|Glyma07g07380.1	AT1G01580	*FRO2*	*Ferric reduction oxidase 2*	2.84	1.39	1.45		1.65
LAGI02_71934|Glyma18g47060.1	AT1G23020	*FRO3*	*Ferric reduction oxidase 3*	6.45	6.01		-7.28	
LAGI02_20003|Glyma14g17360.1	AT2G18960	*AHA1*	*H+-ATPases*	0.76				
LAGI02_5677|Glyma13g00840.1	AT2G18960	*AHA1*	*H+-ATPases*	3.85	3.34		-1.81	
LAGI02_1528|Glyma15g17530.1	AT4G30190	*AHA2*	*H+-ATPases*	3.34	2.36			3.49
LAGI02_7700|Glyma09g06250.3	AT4G30190	*AHA2*	*H+-ATPases*	1.72				
LAGI02_67194|Glyma17g29370.1	AT5G57350	*AHA3*	*H+-ATPases*	1.94		1.63	-1.54	
LAGI02_77609|Glyma17g29370.1	AT2G07560	*AHA6*	*H+-ATPases*	1.58		1.30		
LAGI02_47307|Glyma15g41620.1	AT3G12750	*ZIP1*	*Zinc/iron transporter*	2.33				
LAGI02_49105|Glyma15g41620.1	AT3G12751	*ZIP1*	*Zinc/iron transporter*	2.34		1.74		2.26
LAGI02_30907|Glyma06g12190.2	AT2G30080	*ZIP6*	*Zinc/iron transporter*	1.34	1.19			
LAGI02_30907|Glyma06g12190.1	AT1G80830	*NRAMP1*	*Metal transporter Nramp*	3.40	2.79		-2.04	1.36
LAGI02_24152|Glyma17g01000.1	AT4G1637034	*OPT3*	*Oligopeptide transporter 3*	2.89	2.32		-3.04	
LAGI02_77211|Glyma07g39780.1	AT4G1637034	*OPT3*	*Oligopeptide transporter 3*	7.20	6.89		-7.98	
LAGI02_22531|Glyma02g05300.2	AT4G10770	*OPT7*	*Oligopeptide transporter 7*	1.18	0.94			
LAGI02_17601|Glyma17g04360.1	AT3G53480	*PDR9*	*Pleiotropic drug resistance 9*	3.32	3.01			2.03
LAGI02_29515|Glyma09g15550.2	AT3G08040	*FRD3*	*Ferric reductase defective 3*	8.14	6.63	1.50	-1.81	6.33
LAGI02_34857|Glyma12g10620.2	AT3G21690	*PEZ1*	*Phenolics efflux transporter*	2.29	2.06			2.18
LAGI02_7500|Glyma07g19060.1	AT5G01600	*ATFER1*	*Ferric iron binding*	-5.39	-2.63		5.04	
LAGI02_1167|Glyma03g06420.1	AT5G01601	*ATFER1*	*Ferric iron binding*	-5.01	-3.00	-2.01	4.54	
LAGI02_4939|Glyma03g06420.1	AT5G01600	*ATFER1*	*Ferric iron binding*	-1.25	-1.26		3.22	1.98
LAGI02_4586|Glyma03g06420.1	AT5G01601	*ATFER1*	*Ferric iron binding*	-3.71	-2.94		3.84	

LAGI02_6371|Glyma03g06420.1	AT5G01601	*ATFER1*	*Ferric iron binding*			2.05	
LAGI02_73969|Glyma07g19060.1	AT3G11050	*ATFER2*	*Ferric iron binding*	-4.68	-2.78	4.41	
LAGI02_46164|Glyma03g06420.1	AT2G40300	*ATFER4*	*Ferric iron binding*	-4.45	-2.31	3.81	
LAGI02_73880|Glyma18g43650.2	AT2G40300	*ATFER4*	*Ferric iron binding*	-3.75			
LAGI02_61735|Glyma03g06420.2	AT2G40300	*ATFER4*	*Ferric iron binding*	-1.59		3.13	1.54
LAGI02_5567|Glyma18g43650.2	AT2G40300	*ATFER4*	*Ferric iron binding*			2.09	
LAGI02_62529|Glyma18g43650.2	AT2G40300	*ATFER4*	*Ferric iron binding*			3.44	1.69
LAGI02_43087|Glyma03g28611.1	AT3G56970	*BHLH038*	*Basic Helix-Loop-Helix*	3.03	2.88	-2.20	
LAGI02_8637|Glyma03g28611.1	AT3G56970	*BHLH038*	*Basic Helix-Loop-Helix*	3.21	2.91	-2.34	
LAGI02_37557|Glyma11g19850.1	AT2G28160	*FIT*	*Fer-like regulator of iron*	6.38	6.06		6.53
LAGI02_29706|Glyma03g05190.1	AT5G03570	*ATIREG2*	*Iron-regulated protein 2*	2.62	1.98	-1.34	1.29
LAGI02_46167|Glyma08g18000.1	AT3G12900		*oxidoreductase, 2OG-Fe(II)*	4.20	3.62	-2.67	1.53
LAGI02_40537|Glyma10g22680.3	AT4G25100	*FSD1*	*Fe superoxide dismutase 1*	-2.16			-1.38
LAGI02_1138|Glyma04g41990.1	AT1G77120	*ADH1*	*Alchol dehydrogenase1*	1.11	1.19		1.85
LAGI02_12480|Glyma06g12780.1	AT1G77120	*ADH1*	*misc.alcohol dehydrogenases*	1.90			

4.3.4 Phosphorus-deficiency responsive genes

Plant adaptation to P deficiency was accompanied by wide changes in gene expression. In our genome-wide transcriptomic study, the expression of several phosphate-starvation induced (PSI) genes was significantly modified: genes coding for high-affinity phosphate transporters (PHTs) or purple acid phosphatases (PAPs); genes belonging to the family of the SPX domain containing protein (e.g. PHO1, SPX-MFS,) involved in Pi homeostasis (Tab. 4.5).

Analyzing the gene expression in the comparison -Fe CR versus control apices, several isoforms of phosphate transporters (PHT/PT) such as PHT1;4 and PTH1;9, were upregulated. In addition, numerous transcripts of *PAP10* and *PAP9* were upregulated in this comparison. The upregulation involved also transcripts coding for SPX proteins, such as SPX1 and PHO1. In particular, a transcription factor (bHlH32) and a phosphate starvation induced gene (PS2), known to be involved in the P-deficiency response, showed a high expression level. Moreover, the *low phosphate root* paralogue gene (*LPR2*), involved in plant root development in response to low-P conditions, was positively modulated. In the comparison between the apices of -Fe *vs* control plants, few genes were positively modulated: *PAP10, PS2*, *PHT1;9* and *PHT1;4* and *LPR2*. Phosphorus deficiency caused a stronger modulation of P-deficiency responsive genes as compared to Fe starvation. In –P CR *vs* control apices, Pi transporters were dramatically upregulated. For example, *PHT1;9, PHT1;4* and *PHT1;5* showed a transcript level more than 3 times higher -P CR than in the control root tips. Transcript levels of other transporters, such as the *phosphate transport traffic facilitator* (*PHF1*) and the ABC transporter *PDR2* showed an increased gene expression. Also the different *SPX* and *PAP* isoforms responded to P starvation, increasing the amount of their transcripts. A strong upregulation was observed for *PS2* and *bHLH32* genes, which showed, respectively, 8- and 6-fold change in comparison with the control apices. Trancripts coding for enzymes related to re-modelling membrane lipid composition, in order to remobilize Pi from phospholipids, such as monogalactosyl diacylglycerol synthases (MGDs), sulfoquinovosyltransferase (SQD2) and the phospholipase C2, were also highly expressed in –P CR tissues.

Table 4.5 - – List of modulated transcripts known to be responsive to P-deficiency. FC, fold change.

White Lupine Gene ID	Arabidopsis Gene ID	Symbol	Description	Comparisons (Log_2 FC)				
				-Fe CR vs CTR RA	-Fe RA vs CTR RA	- Fe CR vs - Fe RA	- P CR vs -Fe CR	- P Cl vs CTR RA
LAGI02_2960|Glyma19g34710.1	AT2G38940	*ATPT2/PHT1;4*	*Phosphate transporter 1;4*	2.54		2.15	1.41	3.95
LAGI02_2933|Glyma02g00840.2	AT2G38940	*ATPT2/PHT1;4*	*Phosphate transporter 1;4*	6.59	5.78	0.81	-1.41	5.18
LAGI02_3318|Glyma10g04230.1	AT2G38940	*ATPT2/ PHT1;4*	*Phosphate transporter 1;4*				5.82	3.56
LAGI02_9996|Glyma07g34870.1	AT1G76430	*PHT1;9*	*Phosphate transporter 1;9*	1.46	1.05			
LAGI02_5995|Glyma07g01410.1	AT1G73010	*PS2*	*Phosphate starvation-induced gene*	2.16	1.95		6.01	8.18
LAGI02_26523|Glyma20g03260.1	AT2G03450	*PAP9*	*Purple acid phosphatase 9*	0.84				1.28
LAGI02_1618|Glyma06g03091.1	AT2G27190	*PAP12*	*Purple acid phosphatase 12*				6.49	5.86
LAGI02_2421|Glyma12g01000.1	AT2G16430	*PAP22*	*Purple acid phosphatase22*	4.09	1.88	2.21	5.99	10.08
LAGI02_29629|Glyma19g39040.4	AT2G38920	*SPX*	*SYG1/Pho81/XPRdomain-containing*				1.56	1.11
LAGI02_12786|Glyma06g07260.3	AT5G20150	*SPX1*	*SPX domain gene 1*	0.85			1.42	2.27
LAGI02_46487|Glyma03g03820.1	AT5G20150	*SPX1*	*SPX domain gene 1*				6.92	7.63
LAGI02_11740|Glyma03g03820.2	AT2G45130	*SPX3*	*SPX domain gene 3*				7.39	6.73
LAGI02_11675|Glyma07g32690.1	AT3G25710	*BHLH32*	*Basic helix-loop-helix 32*	4.56			4.68	9.24
LAGI02_4954|Glyma02g00640.1	AT3G23430	*PHO1*	*Phosphate 1*	1.12				1.04
LAGI02_4530|Glyma02g00640.1	AT3G23430	*PHO1*	*Phosphate 1*	1.32				1.41
LAGI02_31505|Glyma10g34380.1	AT3G52190	*PHF1*	*Phosphate transporter traffic*					1.68
LAGI02_438|Glyma20g33180.1	AT3G52190	*PHF1*	*Phosphate transporter traffic*				1.66	1.60
LAGI02_438|Glyma20g33180.1	AT3G52190	*PHF1*	*Phosphate transporter traffic*				1.62	1.60
LAGI02_4506|Glyma20g33180.1	AT3G52190	*PHF1*	*Phosphate transporter traffic*				2.06	2.15
LAGI02_32329|Glyma20g33180.2	AT3G52190	*PHF1*	*Phosphate transporter traffic*				1.91	2.47

LAGI02_32329|Glyma20g33180.2	AT3G52190	*PHF1*	*Phosphate transporter traffic*				1.93	2.47
LAGI02_8534|Glyma20g32870.2	AT4G15230	*PDR2*	*Transport ABC/ Transporters and*				4.67	7.60
LAGI02_31783|Glyma17g11720.1	AT5G20410	*MGD2*	*Monogalactosyl diacylglcerol*			4.42	5.04	
LAGI02_31783|Glyma17g11720.1	AT5G20410	*MGD2*	*Monogalactosyl diacylglcerol*			4.82	5.04	
LAGI02_9404|Glyma03g14200.1	AT5G01220	*SQD2*	*Sulfoquinovosyldiacylglycerol 2*				1.62	2.20
LAGI02_63041|Glyma07g17680.2	AT5G01220	*SQD2*	*Sulfoquinovosyldiacylglycerol 2*				2.22	2.74
LAGI02_27804|Glyma18g42540.1	AT5G01220	*SQD2*	*Sulfoquinovosyldiacylglycerol 2*				3.26	3.26
LAGI02_31045|Glyma19g31430.1	AT4G33030	*SQD1*	*Sulfoquinovosyldiacylglycerol 1*				1.31	1.20
LAGI02_4158|Glyma14g06450.1		*PLC2*	*Phospholipase C 2*	-1.60			2.98	1.38
LAGI02_41880|Glyma20g25640.1	AT2G01180	*LPP1*	*Phosphatidic acid phosphatase 1*	1.18	0.99		-1.15	
LAGI02_11538|Glyma20g25650.1	AT1G15080	*LPP2*	*Phosphatidic acid phosphatase 2*	1.29				
LAGI02_2718|Glyma10g41010.1	AT1G71040	*LPR2*	*Low Phosphate Root2*	1.31	0.86			2.26
LAGI02_30767|Glyma10g41010.1	AT1G23010	*LPR1*	*Low Phosphate Root1*				-1.02	

4.3.5 Phenylprophanoid metabolism

The phenylpropanoid pathway (PPP) leads to the production of molecules like flavonoids, coumarins, hydroxycinnamic acid conjugates and lignins, starting from the carbon skeleton of phenylalanine. Several genes of the PPP and shikimate pathway were differentially modulated under Fe starvation (Tab. 4.6). In the comparison between -Fe CR and the RA of control plants, the chorismate mutase (CM) and arogenate dehydratase 3 (ADT3), which lead to the phenylalanine production, were respectively down- and upregulated. The PAL1 (Phenylalanine ammonia lyase1) and another isoform (PAL2), which catalyze the conversion of L-phenylalanine to trans-cinnamic acid, were upregulated. Other genes that showed a positive modulation of their transcript level in the phenylpropanoid biosynthetic pathway were *4CL* (*4-coumarate-CoA ligase*), *F6'H1* (*Feruloyl-CoA 6'-Hydroxylase1*) and *HCT* (*shikimate O-hydroxycinnamoyltransferase*). The first two enzymes are responsible for the production respectively of 4-coumaroyl-CoA and 6'-hydroxyferuloyl CoA, meanwhile HCT catalyzes the production of p-coumaroyl shikimate or of caffeoyl-CoA. Also an increased expression of the gene *FH3* (*flavanone 3-hydroxylase*) and *flavanone 3-deoxygenase hydroxylase*, both linked with flavonoid synthesis, were detected.

Positively modulated genes were also *FAH* (*Ferulic acid hydroxylate*) and *CCR* (*Cinnamoyl-CoA reductase*), which code for enzymes involved in lignin biosynthesis. On the other hand, two *CAD* (*cinnamoyl-alcohol dehydrogenase*) isoforms showed an opposite behavior. Moreover, some enzymes which add methyl or malonyl groups to phenylpropanoid compounds were upregulated (Caffeate O-methyltransferase (COMT1), Caffeoyl-CoA 3-O-methyltransferase (CCoAOMT1) and Flavonoid glucoside malonyl transferase (Mat4). A lower transcript abundance was detected for *CHS* and *CHI* genes, which encode respectively for chalcone synthase and chalcone-flavonone isomerase.

Comparing -Fe RA *versus* the control RA, the gene modulation was comparable with that occurring in -Fe CR vs control RA, even if the number of genes and the changes in transcript abundance were smaller. In -P cluster roots versus control apices, upregulated genes were the *feruloyl-CoA 6'-Hydroxylase1* (*F6'H1*), *chalcone synthase* and *flavonone 3-dioxygenase* (*F3H*) and *dihydroflavonol-4-reductase* (*DFR*). Feruloyl-CoA 6'-Hydroxylase1 is a key enzyme in the production of coumarins, while F3H is an enzyme involved either in the flavones or flavonols production. The DFR enzyme is involved in the anthocyanins' synthesis. Highly abundant were

the transcripts of a *cinnamoyl CoA-reductase* isoform (*CCR*). This gene, together with *ferulic acid 5-hydroxylase*, which is upregulated, are involved in lignin synthesis.

Expression profile of the comparison –P CR vs –Fe CR showed a positive modulation of the arogenate dehydratase 6 and of the *flavonol synthase* (*FLS*) emerged; interestingly this modulation occurred only in this comparison.

Table 4.6 - Transcripts encoding for enzymes involved in the phenylpropanoid pathway.Fc, fold change.

White Lupine Gene ID	Arabidopsis Gene ID	Symbol	Description	Comparisons (Log_2 FC) -Fe CR vs CTR RA	-Fe RA vs CTR RA	-Fe CR vs Fe A	-P CR vs Fe CR	-P CR vs -Fe RA	-P CR vs Ctr
LAGI02_11537|Glyma12g30660.1	AT2G27820	*ADT3*	*Arogenate dehydratase 3*	1.79	2.19				
LAGI02_25407|Glyma17g05290.1	AT1G08250	*ADT6*	*Arogenate dehydratase 6*				1.43		
LAGI02_12967|Glyma14g11870.1	AT5G10870	*CM2*	*Chorismate mutase 2*	-0.84					
LAGI02_8562|Glyma03g33880.1	AT2G37040	*PAL1*	*Phe ammonia lyase 1*	1.22					
LAGI02_52749|Glyma03g33880.1	AT3G53260	*PAL2*	*Phe ammonia lyase 2*	1.07					
LAGI02_54629|Glyma14g39840.1	AT1G20510	*OPCL1*		-1.31			1.68		
LAGI02_35534|Glyma17g07190.2	AT1G51680	*4-CL*	*4-coumarate--CoA ligase*	2.70					
LAGI02_43005|Glyma03g23770.1	AT3G13610	*F6'H1*	*Feruloyl-Coa 6'-Hydroxylase1*	5.80	5.07		-4.86	-4.13	1.53
LAGI02_37850|Glyma07g02460.1	AT5G48930	*HCT*	*Shikimate O-hydroxycinnamoyltransferase*	1.84	1.34		-1.54	-1.04	
LAGI02_47911|Glyma13g33730.1	AT1G53520	*CHI*	*Chalcone-flavanone isomerase*	-1.44					
LAGI02_66480|Glyma01g43880.1	AT5G13930	*CHS*	*Chalcone synthase*	-1.03		-0.96	2.24	1.28	1.21
LAGI02_33551|Glyma01g43880.1	AT5G13930	*CHS*	*Chalcone synthase*				1.29		
LAGI02_66592|Glyma13g02740.1	AT5G08640	*FLS*	*Flavonol synthase SYNTHASE*				1.19		
LAGI02_42000|Glyma20g01200.1	AT3G19000	*FH3*	*Flavanone 3-hydroxylase*	1.06	0.87				
LAGI02_1980|Glyma07g18280.1	AT5G05600		*Flavanone 3-dioxygenase.*	1.14				1.57	2.13
LAGI02_44578|Glyma07g02690.1	AT1G15950	*CCR1*	*Cinnamoyl-CoA reductase 1*	2.60	1.74	0.86	-2.23	-1.37	
LAGI02_44670|Glyma11g29460.1	AT5G58490	*CCR*	*Cinnamoyl-CoA reductase family*	2.87	3.48		-4.04	-4.65	
LAGI02_64149|Glyma07g02690.1	AT5G58490	*CCR*	*Cinnamoyl-CoA reductase family*	1.26					
LAGI02_47036|Glyma11g29460.2	AT5G58490	*CCR*	*Cinnamoyl-CoA reductase family*				2.87	4.3	8
LAGI02_61811|Glyma12g02230.3	AT5G19440	*CAD*	*Cinnamyl-alcohol dehydrogenase*	-2.01	-1.08				-1.28
LAGI02_34774|Glyma12g02230.3	AT5G19440	*CAD*	*Cinnamyl-alcohol dehydrogenase*	2.06	2.59				2.140

LAGI02_75037|Glyma09g33820.1	AT2G23910		*Dihydroflavonol-4-reductase*					1.93
LAGI02_37597|Glyma19g02150.1	AT4G36220	*FAH1*	*Ferulic acid 5-hydroxilase 1*	1.16		1.15	1.45	2.32
LAGI02_483|Glyma19g02150.1	AT4G36220	*FAH1*	*Ferulic acid 5-hydroxilase 1*	1.24	1.19	1.19	1.24	2.43
LAGI02_26299|Glyma04g40580.1	AT5G54160	*COMT1*	*Caffeate O-methyltransferase*	0.79				
LAGI02_43452|Glyma06g14200.1	AT5G54160	*COMT1*	*Caffeate O-methyltransferase*	1.08				1.02
LAGI02_40545|Glyma06g14200.1	AT5G54160	*COMT1*	*Caffeate O-methyltransferase*	1.42				
LAGI02_43183|Glyma07g05470.1	AT5G54160	*COMT1*	*Caffeate O-methyltransferase*	3.26	2.63	-2.58	-1.96	
LAGI02_5715|Glyma11g05800.2	AT4G34050	*CCoAOMT1*	*Caffeoyl-CoA 3-O-methyltransferase*	0.89				
LAGI02_856|Glyma07g33780.1	AT4G34050	*CCoAOMT1*	*Caffeoyl-CoA 3-O-methyltransferase*	2.21	1.83	-1.87	-1.49	
LAGI02_50654|Glyma17g18800.1	AT4G34051	*CCoAOMT2*	*Caffeoyl-CoA 3-O-methyltransferase*			1.19		

4.3.6 Methionine Cycle

The methionine-derivative, S-adenosyl methionine (SAM), is required for methyl group transfer. Its cycle is known to be affected by the plant nutritional status of plant as Fe deficiency determine a positively modulation in the invoved enzymes. S-adenosyl methionine is synthesized from L-Met by S-Met adenosyltransferase (MAT). The most important proteins of the Met cycle are the SAM synthases (MAT1, MAT2, MAT3, and MAT4), the cobalmine-independent Met synthase (ATMS1), and the S-adenosyl-L-homo-Cys hydrolase (SAHH1). S-adenosyl methionine is also the substrate for the biosynthesis of nicotinamine (NA) by nicotianamine synthase (NAS). Moreover, ARD2 **(**acidoreductone oxygenase**)** protein seem to be involved in the recovery of L-Met from methylthioadenosine. Some of these genes were found to be modulated under Fe deficiency (Tab. 4.7). In apices and cluster root of -Fe plants the transcript level of *MAT1* was almost 4 times higher than in root tips of control plants. On the contrary, *MAT3*, *ATMS1* and *SAHH1* genes were repressed in -Fe CR. *Acidoreductone oxygenase (ARD2)* transcript was induced in both -Fe CR and RA. The transcript levels of two *Nicotianamine synthase* isoforms, *NAS2* and *NAS3,* were strongly modulated by Fe deficiency in both root structures. *Nicotianamine synthase 2* was upregulated meanwhile *NAS3* downregulated**.** In the comparison between -P CR and control roots the only genes affected were *MAT1* and *NAS3*, which were downregulated, and *ARD2* which showed an increase in its transcript level.

Table 4.7 - List of transcripts encoding enzymes of the methionine cycle. Fc, fold change.

White Lupine Gene ID	Arabidopsis Gene ID	Symbol	Description	Comparisons (Log_2 FC)				
				- Fe CR vs CTR RA	-Fe RA vs CTR RA	- Fe CR vs - Fe RA	- P CR vs -Fe CR	- P CR vs CTR RA
LAGI02_36793|Glyma10g28500.1	AT1G02500	*MAT1*	*S-adenosylmethionine synthetase 1*	3.91	3.52		-2.97	-2.58
LAGI02_26338|Glyma03g34120.1	AT2G36880	*MAT3*	*Methionine adenosyltransferase 3*	-2.13		-1.25		
LAGI02_13662|Glyma03g34120.1	AT2G36880	*MAT3*	*Methionine adenosyltransferase 4*	-1.31				
LAGI02_7753|Glyma19g29180.4	AT5G17920	*ATMS1*	*Cobalamin-independent synthase family protein*	-1.37		-0.82		
LAGI02_8521|Glyma08g11480.1	AT4G13940	*SAHH1*	*S-adenosyl-L-homocysteine hydrolase*	-1.62		-0.87		
LAGI02_933|Glyma10g38940.1	AT4G14710	*ATARD2*	*Acireductone dioxygenase [iron(II)-requiring]*	1.09	0.99			1.22
LAGI02_1177|Glyma20g28860.1	AT4G14710	*ATARD2*	*Acireductone dioxygenase [iron(II)-requiring]*	1.25	0.93			1.40
LAGI02_552|Glyma10g38940.1	AT4G14710	*ATARD2*	*Acireductone dioxygenase [iron(II)-requiring]*	1.33				
LAGI02_49258|Glyma19g41630.1	AT1G09240	*NAS3*	*Nicotianamine synthase 3*	-3.58	-1.42	-2.16		-4.47
LAGI02_63575|Glyma03g39050.1	AT5G56080	*NAS2*	*Nicotianamine synthase 2*	7.61	7.22		-7.29	
LAGI02_69941|Glyma19g41630.1	AT5G56080	*NAS2*	*Nicotianamine synthase 2*	7.87	7.42		-6.53	

Table 4.8 - Transcripts encoding for enzymes involve in pH modification or homeostasis that were significantly modulated in roots of white lupine grown in Fe or P deficiency or in control condition. Fc, fold change.

White lupine Gene ID	Arabidopsis Gene ID	Symbol	Description	Comparisons (Log_2 FC)				
				- Fe CR vs CTR RA	-Fe RA vs CTR RA	- Fe CR vs - Fe RA	- P CR vs -Fe CR	- P Cl vs CTR RA
LAGI02_1528|Glyma15g17530.1	AT4G30190	*AHA2*	*H+-ATPases*	3.34	2.36			3.49
LAGI02_7700|Glyma09g06250.3	AT4G30190	*AHA2*	*H+-ATPases*	1.72				
LAGI02_23873|Glyma07g03220.2	AT1G15690	*ATAVP3*	*Proton transport*	-1.74	-1.08			-1.91
LAGI02_5317|Glyma07g00430.1	AT1G78900	*VHA-A*	*Vacuolar ATP synthase subunit A*	-1.15			1.04	
LAGI02_29045|Glyma01g41930.1	AT1G12110	*NRT1.1*	*Nitrate transmembrane transporter*	-1.59	-1.66			-1.32
LAGI02_60692|Glyma12g30750.1	AT4G21105		*Cytochrome-c oxidase*	1.43			3.22	4.70

4.3.7 Genes involve in the pH modification of the rhizosphere or cell pH homeostasis

Several genes are known to be involved in the pH modification of the cell sap and/or of the rhizosphere. In the gene expression profile reported in Table 4.8, some of these genes, such as *AHA2, AtNRT1, AtAVP3* and *VHA-A2* were transcriptionally modulated.

The *AHA2* transcript was upregulated in the CR and AR of -Fe plants compared with the control apices, while *AtNRT1* was downregulated (Tab. 4.9). In addition to the downregulation of *AtNRT1*, two vacuolar proton ATPases, *AtAVP3* and *VHA-A2*, were downregulated under Fe deficiency. Moreover, the mitochondrial cytochrome *c* oxidase transcript level was increased in cluster roots of Fe-deficient plants. However, in the root tips no modulation of *VHA-A2* or of the cytochrome c oxidase was detected.

Also in the CR of P-deficient plants, the transcript abundance of *AHA2*, *AtNRT1*, *AtAVP3* were higher compared to the control tissues. The transcript level of the *cytochrome c oxidase* was strongly induced, being almost 5 times higher than in the apices of control plants. Comparing the two cluster root structures in –P and –Fe plants, the only detectable variation in transcript level referred to the *VHA-A* and *cytochrome c oxidase*, which were more abundant in the -P tissue.

4.3.8 Detection and quantification of phenolic compounds in root exudates and root tissues

The composition and rate of release of phenolic compounds was evaluated via a metabolomic approach. Using HPLC-MS, the phenolic compounds released from the whole root system of -P, -Fe and control lupine plants were characterized and quantified. Analyses of phenolic compounds were also performed using root cluster roots or root apices of those plants.

Fifty different compounds were identified in the root samples and were reported in the Table 4.10. The analysis revealed that the main compounds identified in the root tissues were scopoletin and genistein derivatives, belonging to the families of coumarins and flavonoids, respectively. The types of derivatizations were mostly hydroxylation and methoxylation and the resulting compounds were often conjugated with glucosyl and malonyl residues.

The compounds ubiquitously present in all the analysed tissues were the followings: coumarins: Glycoside of methoxyscopoletin (R3 and R4), Hydroxymethoxyscopoletin-O-malonyl glycoside (R8 and R9), Hydroxy-5-methoxyscopoletin (R10); flavonoids: Genistein isomer-O-malonyl-diglucoside (R15), Diglycoside of hydroxigenistein (R16), Genestein 7-glucoside and its isomers (R18, R21and R24), Apigenin-7-glucoside (R35), Glycoside of hydroxygenistein (R19 and R28, R36, R38), Hydroxygenistein-O-malonyl-glycoside (R20, R22, R30, R32, R34, R37, R41, R43, R46), Dihydroxygenistein malonyl glucoside (R25 and R26), Methoxyhydroxygenistein (R44, R39), Genistein-O-malonyl-glycoside (R45), Methoxygenistein isomers (R49, R50, R51), Hydroxygenistein (R40, R42), and Genistein (R48). Several compounds were detected specifically in –Fe CR and RA: Glycoside of methoxyscopoletin (R5), Hydroxyscopoletin isomers (R6 and R7) different isomers of methoxyscopoletin (R11, R14, R17), Glycoside of methoxyscopoletin (R12), Dimethoxyscopoletin-O-malonylglycoside (R51), Ferulic acid (R15).

Table 4.10 - Phenolic compounds accumulated by roots of white lupine plants in response to Fe and P deficiency. Retention times (RT), $[M+H]^+$ and/or $[M-H]^-$ exact mass-to-charge ratios (*m/z*), molecular formulae, error *Denotes fragmentations with 0.2 amplitude

#	R.T. (min)	Measured *m/z*	Molecular formula	Calculated *m/z*	Error *m/z* (ppm)	Name (Common name)	-Fe CR	-Fe RA	-P CR	-P RA	CTR RA
R1	9.3	409.0521	$C_{16}H_{18}O_{10}K^+$	409.0531	2.4	Glycoside of hydroxyscopoletin	+	+			
R2	11.6	225.0386	$C_{10}H_9O_6^+$	225.0394	3.6	Dihydroxyscopoletin	+	+			
R3	12.2	401.1063	$C_{17}H_{21}O_{11}^+$	401.1078	3.7	Glycoside of hydroxymethoxyscopoletin	+	+	+	+	+
R4	12.9	401.1069	$C_{17}H_{21}O_{11}^+$	401.1078	2.2	Glycoside of hydroxymethoxyscopoletin	+	+			
R5	14.5	407.0938	$C_{17}H_{20}O_{10}Na^+$	407.0949	2.7	Glycoside of methoxyscopoletin	+	+			
R6	15.8	209.0447	$C_{10}H_9O_5^+$	209.0445	-1	Hydroxiscopoletin isomer	+	+			
R7	16.5	209.0449	$C_{10}H_9O_5^+$	209.0445	-1.9	8-Hydroxiscopoletin (Fraxetin)	+	+			
R8	18.1	487.1059	$C_{20}H_{23}O_{14}^+$	487.1082	4.7	Hydroxymethoxyscopoletin-O-malonyl-glycoside	+	+	+	+	+
R9	19.5	487.1058	$C_{20}H_{23}O_{14}^+$	487.1082	4.9	Hydroxymethoxyscopoletin-O-malonyl-glycoside	+	+	+	+	+
R10	20.1	239.0538	$C_{11}H_{11}O_6^+$	239.055	5	Hydroxy-5-methoxyscopoletin (Hydroxyfraxinol)	+	+	+	+	+
R11	21.7	223.0595	$C_{11}H_{11}O_5^+$	223.0601	2.7	8-Methoxyscopoletin (Isofraxidin)	+	+			
R12	21.9	415.1229	$C_{18}H_{23}O_{11}^+$	415.1235	1.4	Glycoside of dimethoxyscopoletin	+	+			
R13	22.7	223.0596	$C_{11}H_{11}O_5^+$	223.0601	2.2	Isomer of methoxyscopoletin	+	+			
R14	23	195.0642	$C_{10}H_{11}O_4^+$	195.0651	4.6	Feulic acid	+	+			
		193.0505	$C_{10}H_9O_4^-$	193.0506	0.5						
R15	23	681.1633	$C_{30}H_{33}O_{18}^+$	681.1661	4.1	Genistein isomer-O-malonyl-diglucoside	+	+	+	+	+
R16	24	611.1594	$C_{27}H_{31}O_{16}^+$	611.1607	2.1	Diglycoside of hydroxygenistein	+	+	+	+	+
R17	24.2	223.0599	$C_{11}H_{11}O_5^+$	223.0601	0.9	5-Methoxyscopoletin (Fraxinol)	+	+			
R18	26.9	433.1142	$C_{21}H_{21}O_{10}^+$	433.1129	-3	Genistein 7-glucoside (Genistin)	+	+	+	+	+
R19	27.4	449.1071	$C_{21}H_{21}O_{11}^+$	449.1078	01-giu	Glycoside of hydroxygenistein	+	+	+	+	+
R20	28	535.1066	$C_{24}H_{23}O_{14}^+$	535.1082	1.5	Hydroxygenistein-O-malonyl-glycoside	+	+	+	+	+
R21	28.5	501.1217	$C_{21}H_{25}O_{14}^+$	501.1239	4.4	Dimethoxyscopoletin-O-malonylglycoside	+	+	+	+	+
R22	28.6	535.1066	$C_{24}H_{23}O_{14}^+$	535.1082	3	Hydroxygenistein-O-malonyl-glycoside	+	+	+	+	+

R23	28.6	223.0593	$C_{11}H_{11}O_5^+$	223.0601	3.6	Isomer of methoxyscopoletin (Umckalin isomer)	+	+			
R24	28.7	433.1124	$C_{21}H_{21}O_{10}^+$	433.1129	1.2	Glycoside of genistein	+	+	+	+	+
R25	28.7	551.1012	$C_{24}H_{22}O_{15}^+$	551.1032	3.1	Dihydroxygenistein malonyl glucoside	+	+	+	+	+
R26	30.6	551.1012	$C_{24}H_{22}O_{15}^+$	551.1032	3.6	Dihydroxygenistein malonyl glucoside	+	+	+	+	+
R27	31	253.0693	$C_{12}H_{13}O_6^+$	253.0707	5	Dimethoxyscopoletin	+	+	+	+	+
R28	31.1	449.1059	$C_{21}H_{21}O_{11}^+$	449.1078	4.2	Glycoside of hydroxygenistein	+	+	+	+	+
R29	31.9	253.0699	$C_{12}H_{13}O_6^+$	253.0707	3.2	Dimethoxyscopoletin	+	+			
R30	32.4	535.1055	$C_{24}H_{23}O_{14}^+$	535.1082	5	Hydroxygenistein-O-malonyl-glycoside	+	+	+	+	+
R31	32.7	433.1111	$C_{21}H_{21}O_{10}^+$	433.1129	4.2	Glycoside of genistein	+	+	+	+	+
R32	33.2	535.1076	$C_{24}H_{23}O_{14}^+$	535.1082	1.1	Hydroxygenistein-O-malonyl-glycoside	+	+	+	+	+
R33	34.2	463.1255	$C_{22}H_{23}O_{11}^+$	463.1235	-4.3	Glycoside of methoxygenistein	+	+	+	+	+
R34	35	535.107	$C_{24}H_{23}O_{14}^+$	535.1082	2.2	Hydroxygenistein-O-malonyl-glycoside	+	+	+	+	+
R35	35.5	433.1124	$C_{21}H_{21}O_{10}^+$	433.1129	1.2	Apigenin 7 glucoside	+	+	+	+	+
R36	35.5	449.1064	$C_{21}H_{21}O_{11}^+$	449.1078	3.1	Glycoside of hydroxigenistein	+	+	+	+	+
R37	36.6	535.1089	$C_{24}H_{23}O_{14}^+$	535.1082	-1.3	Hydroxygenistein or hydroxyapigenin -O-malonyl-	+	+	+	+	+
R38	37.1	449.1066	$C_{21}H_{21}O_{11}^+$	449.1078	2.7	Glycoside of hydroxigenistein	+	+	+	+	+
R39	38.6	317.0643	$C_{16}H_{13}O_7^+$	317.0656	4.1	Methoxyhydroxygenistein	+	+	+	+	+
R40	38.9	287.0539	$C_{15}H_{11}O_6^+$	287.055	3.8	hydroxygenistein or hydroxyapigenin	+	+	+	+	+
R41	39.4	535.1062	$C_{24}H_{23}O_{14}^+$	535.1082	3.7	Hydroxygenistein-O-malonyl-glycoside	+	+	+	+	+
R42	39.6	287.0537	$C_{15}H_{11}O_6^+$	287.055	4.5	Hydroxygenistein	+	+	+	+	+
R43	40.4	535.1076	$C_{24}H_{23}O_{14}^+$	535.1082	1.1	Hydroxygenistein or hydroxyapigenin -O-malonyl-	+	+	+	+	+
R44	40.7	317.0655	$C_{16}H_{13}O_7^+$	317.0656	0.3	Methoxyhydroxygenistein	+	+	+	+	+
R45	41.5	519.1133	$C_{24}H_{23}O_{13}^+$	519.1133	4.6	Genistein-O-malonyl-glycoside	+	+	+	+	+
R46	41.9	535.1059	$C_{24}H_{23}O_{14}^+$	535.1082	4.3	Hydroxygenistein-O-malonyl-glycoside	+	+	+	+	+
R47	44.3	303.0497	$C_{15}H_{11}O_7^+$	303.0497	0	Quercitin	+	+	+	+	+
R48	46.9	271.0596	$C_{15}H_{11}O_5^+$	271.0601	1.8	Genistein	+	+	+	+	+
R49	47.6	301.0716	$C_{16}H_{13}O_6^+$	301.0707	-3	Methoxygenistein	+	+	+	+	+
R50	52.2	301.0706	$C_{16}H_{13}O_6^+$	301.0707	0.3	Methoxygenistein	+	+	+	+	+
R51	53.5	301.0705	$C_{16}H_{13}O_6^+$	301.0707	0.7	Methoxygenistein		+		+	

Also in the root exudates the identified molecules were mainly scopoletin and genistein derivatives. In –Fe exudates great amounts of hydroxyscopoletin (fraxetin) and of the two isomers of dihydroxy scopoletin were identified. Several isomers of methoxyscopoletin and of methoxyhydroxy scopoletin such as hydroxyisofraxidin and hydroxyfraxinol were also detected in high amount. Moreover, one glycoside and two malonylglucoside coumarin were identified.

The main flavonoid detected was genistein. This compound was the target of the same kind of modifications.The genistein aglycon and many isomers of hydroxyl- and metoxy-genistein were released by Fe-deficient plants. Only one flavonoid glycoside, Apigenin 7-glucoside, was found.

In the -P root exudates, the detected compounds were for coumarins: hydroxyscopoletin, two isomers of methoxyscopoletin (known as Isofraxidin and Fraxinol) and a dimethoxyscopoletin. Moreover two isomers of hydroxymethoxyscopoletin malonyl glucoside were found. Regarding the flavonoid compounds, high level of genistein, hydroxyl-, methoxy- and hydroxymethoxy-genistein were released by the – P roots.

The amount of these compounds in the root exudates of control plants were below the limit of detection. Quantification of the different compounds are under way.

Table 4.11 - Compounds identified in root exudates released by Control, – Fe and –P of white lupine plants. Retention times (RT), $[M+H]^+$ and/or $[M-H]^-$ exact mass-to-charge ratios (*m/z*), molecular formulae, error. * Denotes the negative mode

#	R. T. (min)	Measured *m/z*	Molecular formula	Calculated *m/z*	Error *m/z* (ppm)	Name (common name)	CTR	-Fe	- P
E1	9.2	225.0405	$C_{10}H_9O_6^+$	225.0394	-4.9	Dihydroxyscopoletin		+	
E2	11.3	225.0399	$C_{10}H_9O_6^+$	225.0394	-2.2	Dihydroxyscopoletin		+	
E3	12.1	423.0877	$C_{17}H_{20}O_{11}Na^+$	423.0897	4.7	Glycoside hydroxymetoxyscopoletin		+	+
			$^*C_{17}H_{19}O_{11}^-$	399.0922	-1.8				
E4	15.8	209.0448	$C_{10}H_9O_5^+$	209.0445	-1.4	Hydroxyscopoletin		+	
E5	16.5	209.0448	$C_{10}H_9O_5^+$	209.0445	-1.4	8-Hydroxyscopoletin (Fraxetin)		+	
E6	17.2	237.0398	$C_{11}H_9O_6^+$	237.0394	-1.7	oxidateshydroxyfraxinol		+	
E7	17.4	239.0541	$C_{11}H_{11}O_6^+$	239.055	3.8	Hydroxy-8-methoxyscopoletin (Hydroxyisofraxidin)		+	
E8	18	487.1068	$C_{20}H_{23}O_{14}^+$	487.1082	2.9	Hydroxymethoxyscopoletin-O-malonyl-glycoside		+	+
E9	19.4	487.1069	$C_{20}H_{23}O_{14}^+$	487.1082	2.7	Hydroxymethoxyscopoletin-O-malonyl-glycoside		+	+
E10	19.9	239.0556	$C_{11}H_{11}O_6^+$	239.055	-2.5	Hydroxy-5-methoxyscopoletin (Hydroxyfraxinol)		+	
E11	21.4	239.0558	$C_{11}H_{11}O_6^+$	239.055	-3.3	Hydroxymethoxyscopoletin		+	
E12	21.6	223.0604	$C_{11}H_{11}O_5^+$	223.0601	-1.3	8-Methoxyscopoletin (Isofraxidin)		+	+
E13	22.5	223.0605	$C_{11}H_{11}O_5^+$	223.0601	-1.8	Methoxyscopoletin isomer		+	
E14	24.2	223.0603	$C_{11}H_{11}O_5^+$	223.0601	-0.9	5-Methoxyscopoletin (Fraxinol)		+	+
E15	28.5	223.0606	$C_{11}H_{11}O_5^+$	223.0601	-2.2	Methoxyscopoletin		+	
E16	28.5	501.1216	$C_{21}H_{25}O_{14}^+$	501.1239	4.6	Dimethoxyscopoletin-O-malonylglycoside		+	
E17	30.6	281.066	$C_{13}H_{13}O_7^+$	281.0656	-1.4	Modified with C2H2O Hydroxymethoxyscopoletin		+	
E18	30.7	253.0714	$C_{12}H_{13}O_6^+$	253.0707	-2.8	Dimethoxiscopoletin		+	+
E19	31.8	253.0711	$C_{12}H_{13}O_6^+$	253.0707	-1.6	Dimethoxiscopoletin		+	
E20	32.9	303.0486	$C_{15}H_{11}O_7^+$	303.0499	4.3	Dihydroxygenistein		+	

E21	34.5	281.0658	$C_{13}H_{13}O_7^+$	281.0656	-0.7	Modified with C2H2O Hydroxymethoxyscopoletin	+	
E22	35.5	433.1125	$C_{21}H_{21}O_{10}^+$	433.1129	0.9	Apigenin 7-glucoside	+	
E23	38.6	317.0658	$C_{16}H_{13}O_7^+$	317.0656	-0.6	Metoxyhydroxygenistein	+	+
E24	39	287.0552	$C_{15}H_{11}O_6^+$	287.055	-0.7	Hydroxygenistein	+	+
E25	39.5	287.0559	$C_{15}H_{11}O_6^+$	287.055	-3.1	Hydroxygenistein	+	+
E26	40.7	317.0656	$C_{16}H_{13}O_7^+$	317.0656	0	Metoxyhydroxygenistein	+	+
E27	46.7	331.0823	$C_{17}H_{15}O_7^+$	331.0812	-3.3	Dimetoxygenistein	+	+
E28	46.8	271.0605	$C_{15}H_{11}O_5^+$	271.0601	-1.5	Genistein	+	+
E29	47.5	301.0706	$C_{16}H_{13}O_6^+$	301.0707	0.3	Metoxy genistein	+	+
E30	52.2	301.071	$C_{16}H_{13}O_6^+$	301.0707	-1	Metoxy genistein	+	+
E31	53.4	301.0705	$C_{16}H_{13}O_6^+$	301.0707	0.7	Metoxy genistein	+	+
E32	53.9	331.0814	$C_{17}H_{15}O_7^+$	331.0812	-0.6	Dimetoxygenistein	+	+

4.3.9 ^{59}Fe accumulation from soluble and poorly soluble Fe-sources

In order to investigate how the plant nutritional status affects the capacity of plants in acquiring Fe, were performed time-course experiments (1, 4, 8, 24 hours) of ^{59}Fe uptake using (^{59}Fe)Fe-EDTA (soluble source) or (^{59}Fe)Ferrihydrite (poorly soluble). Concerning the accumulation of ^{59}Fe supplied as Fe-EDTA, figure 4.5 shows that roots of Fe-deficient plants, accumulated more Fe- than P-deficient or control plants already after 1 hour of treatment, reaching a peak at 8 hours. Phosphorus-starved and control plants accumulated ^{59}Fe with the same trend as Fe-deficient plants but at levels about 14- and 30-times lower, respectively. A much lower ^{59}Fe accumulation occurred in plants fed with Ferrihydrite in comparison with plants treated with the soluble source. Indeed only after 24 hour of treatment, roots of Fe-deficient plants showed a significant increaset of ^{59}Fe with respect to plants grown in a complete nutrient solution or in a P-free solution.

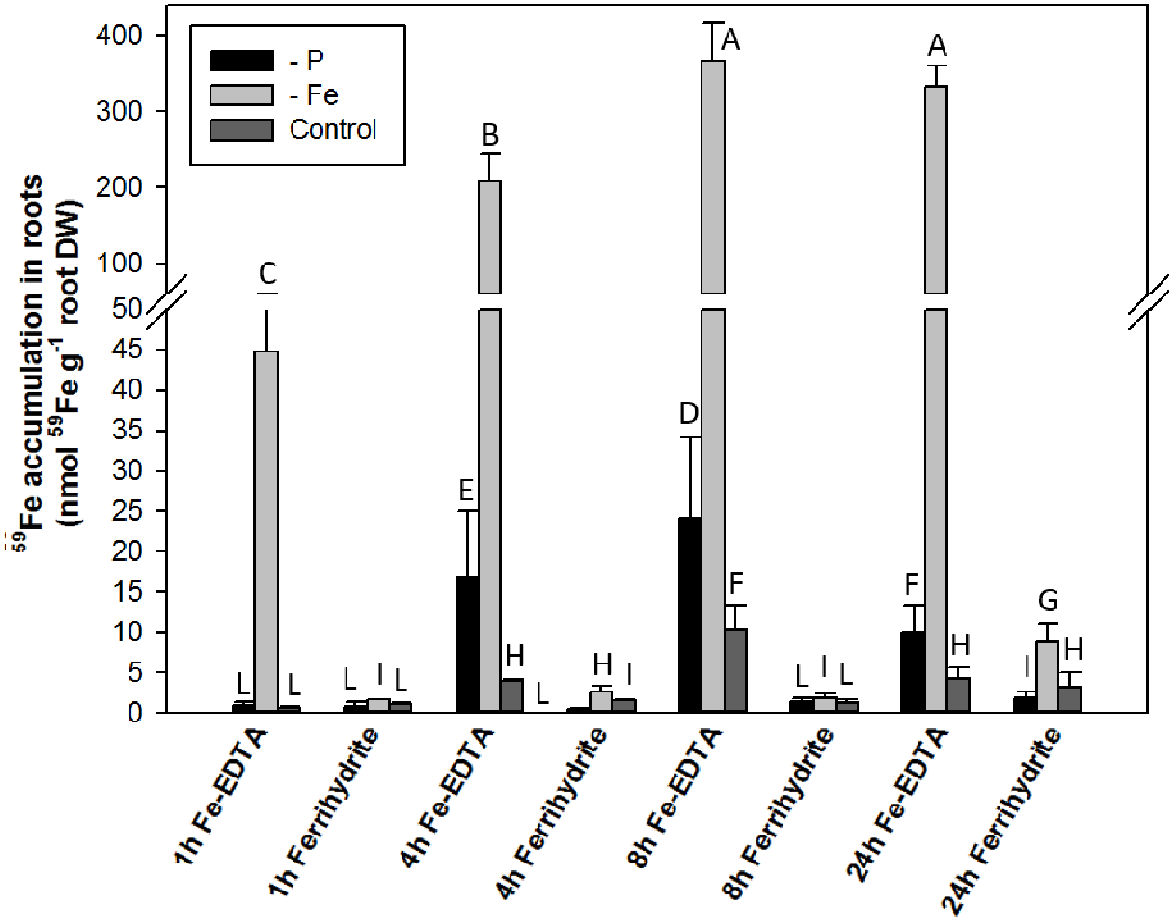

Figure 4.5 - Accumulation of ^{59}Fe in roots of white lupine plants grown in a complete, P- or Fe-free nutrient solution. Plants were treated respectively with (^{59}Fe)Fe-EDTA (soluble source) or with (^{59}Fe)Ferrihydrite for

1, 4, 8 and 24 hours. Data are means + SD of three independent experiments (capital letters refer to statistically significant differences among the mean, ANOVA Holm–Sidak, N = 3, *P* < 0.05). DW, dry weight.

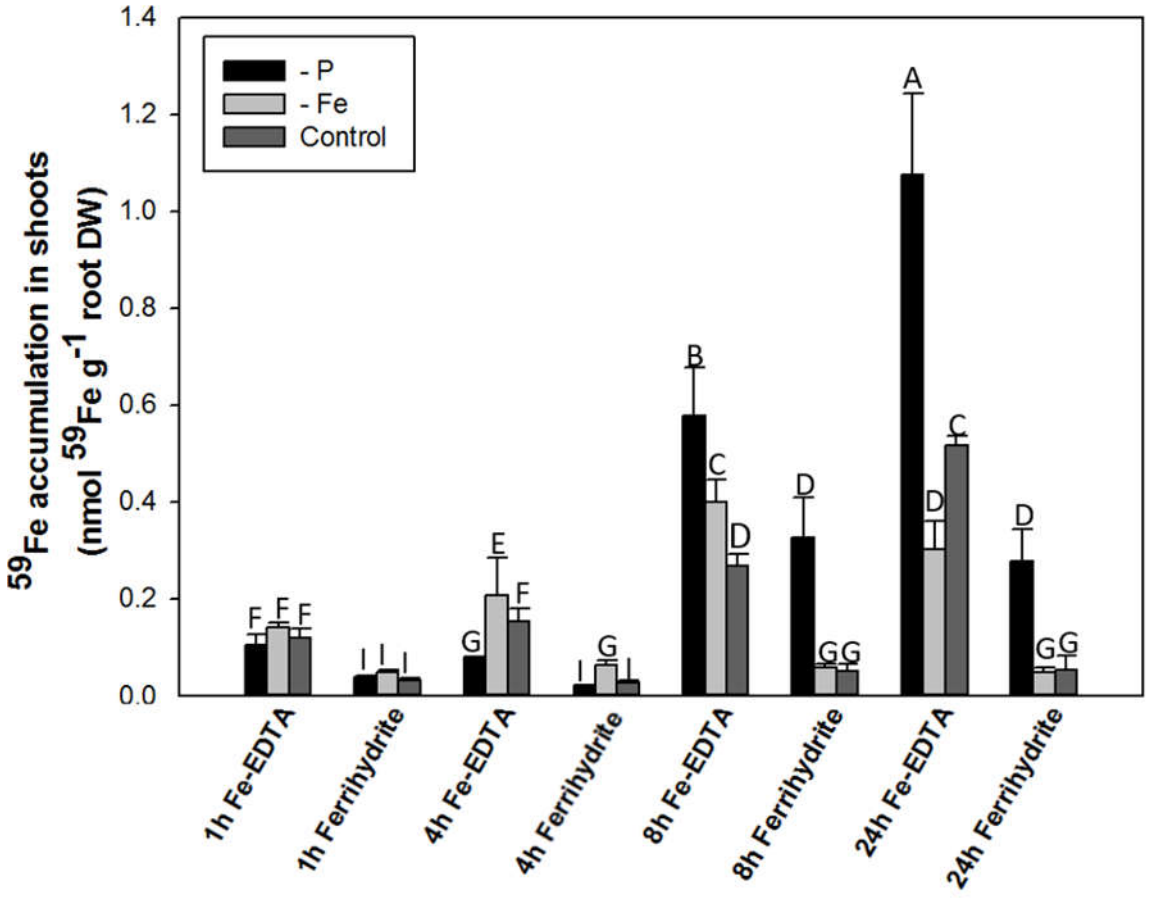

Figure 4.6 - Accumulation of ^{59}Fe in shoots of white lupine plants grown in a complete, P- or Fe-free nutrient solution. Plants were treated respectively with (^{59}Fe)Fe-EDTA (soluble source) or with (^{59}Fe)Ferrihydrite for 1, 4, 8 and 24 hours. Data are means + SD of three independent experiments (capital letters refer to statistically significant differences among the mean, ANOVA Holm–Sidak, N = 3, *P* < 0.05). DW, dry weight.

Fig. 4.6 showed accumulation of ^{59}Fe in shoots. It is clear how the contribution of translocation is greater in P-deficient plants under both treatments in comparison with the other growth conditions. In the Fe-deficient and control plants there were no significant differences in the amount of ^{59}Fe accumulated in shoots.

The accumulation of ^{59}Fe in specific excised root tissues (apices and cluster roots) of plants

treated with the different Fe-sources has also been measured. The accumulation of ^{59}Fe was higher in both apex or cluster root tissue of Fe-deficient plants then in control and P-deficient plants, independently of the source supplied. Using (^{59}Fe)Fe-EDTA, the amount of the micronutrient accumulated in cluster roots was about 40 % higher than in apices; on the other hand when (^{59}Fe)Ferrihydrite was supplied, apices showed an almost 70 % higher accumulation than cluster roots. Regarding P-deficient plants, no difference occurred in the uptake between the two different tissues; however the accumulation in the cluster roots and apices tissues was higher when Fe was supplied as (^{59}Fe)Fe-EDTA.

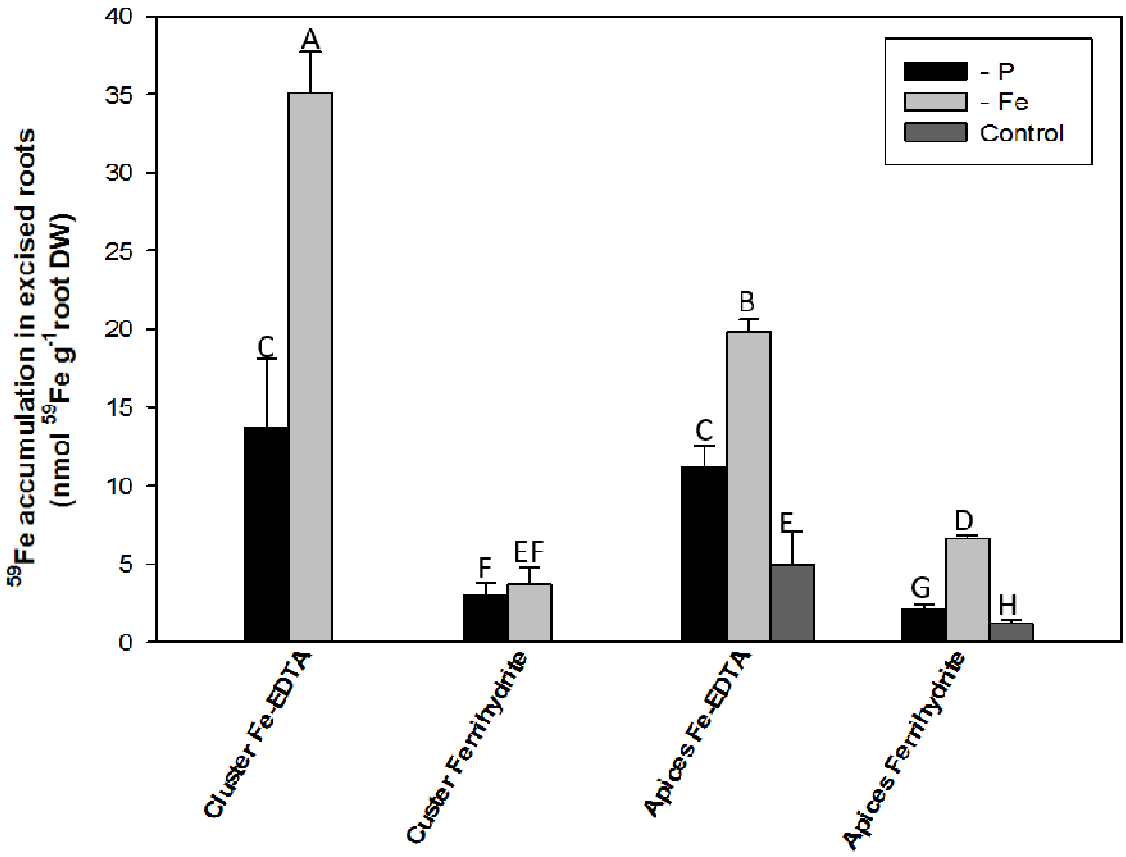

Fig 4.7 - Accumulation of ^{59}Fe in different root tissues (apices and cluster roots) of white lupine plants grown in a complete, P- or Fe-free nutrient solution. Plants were treated for 1 hour with (^{59}Fe)Fe-EDTA (soluble source) or (^{59}Fe)Ferrihydrite. Data are means + SD of three independent experiments (capital letters refer to statistically significant differences among the mean, ANOVA Holm–Sidak, N = 3, P < 0.05). DW, dry weight.

4.3.10 ^{32}P accumulation from soluble and poorly soluble P sources

The same experimental setup described in the previous paragraph was used to investigate the accumulation of ^{32}P in control, P- and Fe-deficient plants. The plants were treated with (^{32}P)KH_2PO_4 (soluble source) or with (^{32}P)Vivianite for 1, 4, 8 and 24 hours. Data reported in Figure 4.8 show that P-deficient plants accumulated greater amounts of (^{32}P)KH_2PO_4 as compared to plants grown in a complete nutrient solution or in a Fe-free one. The amount of ^{32}P increased with time until reaching a peak 24 hours after the beginning of the treatment. However, plants displayed a higher capability to accumulate ^{32}P from the soluble source than from the poorly soluble one. No significant differences were observed in the accumulation of the macronutrient between Fe-deficient and control plants, when P was supplied as (^{32}P)KH_2PO_4. In contrast, Fe-deficient plants fed with (^{32}P)Vivianite acquired a greater amount of ^{32}P with respect to the control plants.

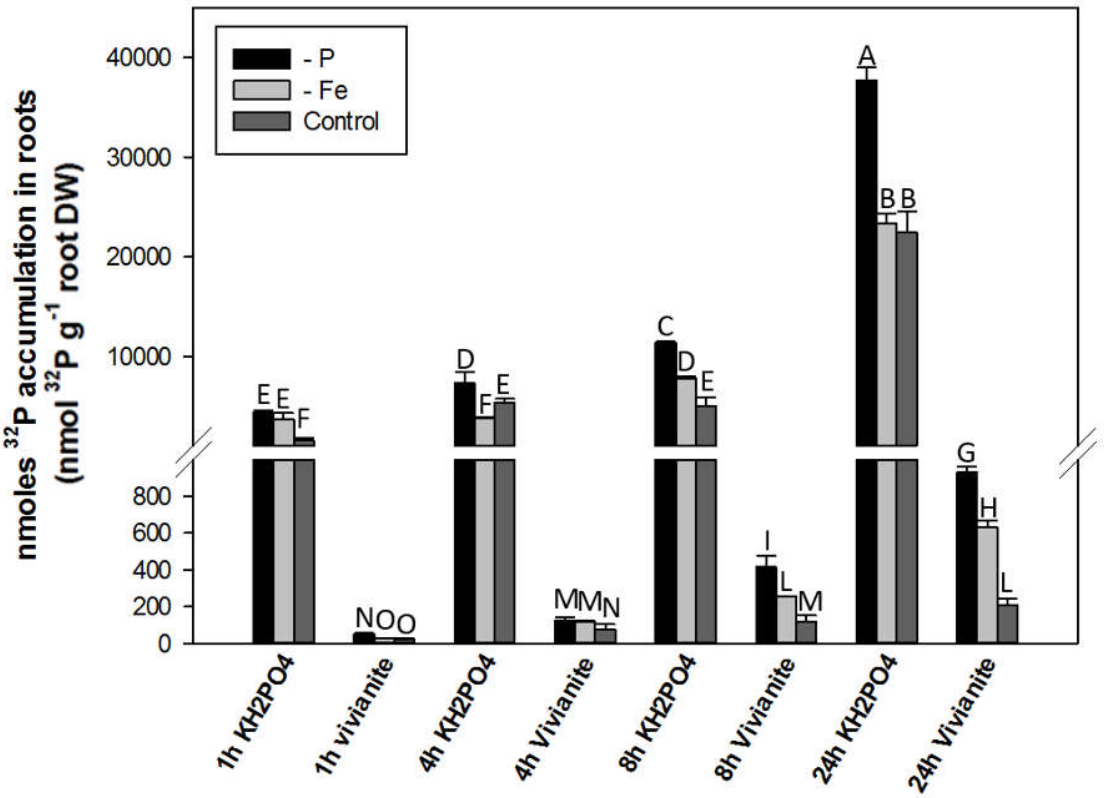

Fig 4.8 - Accumulation of ^{32}P in roots of white lupine plants grown in a complete, P- or Fe-free nutrient

solution. Plants were treated with (^{32}P)KH_2PO_4 (soluble source) or with (^{32}P)Vivianite for 1, 4, 8 and 24 hours. Data are means + SD of three independent experiments (capital letters refer to statistically significant differences among the mean, ANOVA Holm–Sidak, N = 3, P < 0.05). DW, dry weight.

Figure 4.9 shows ^{32}P accumulation in shoots of plants grown in the three different nutritional conditions. As observed in the roots, the P-deficient plants presented a higher translocation of the nutrient, irrespective of the Fe-source. No difference in the the amount of P accumulated was observed comapring the Fe-deficient plants with the control ones.

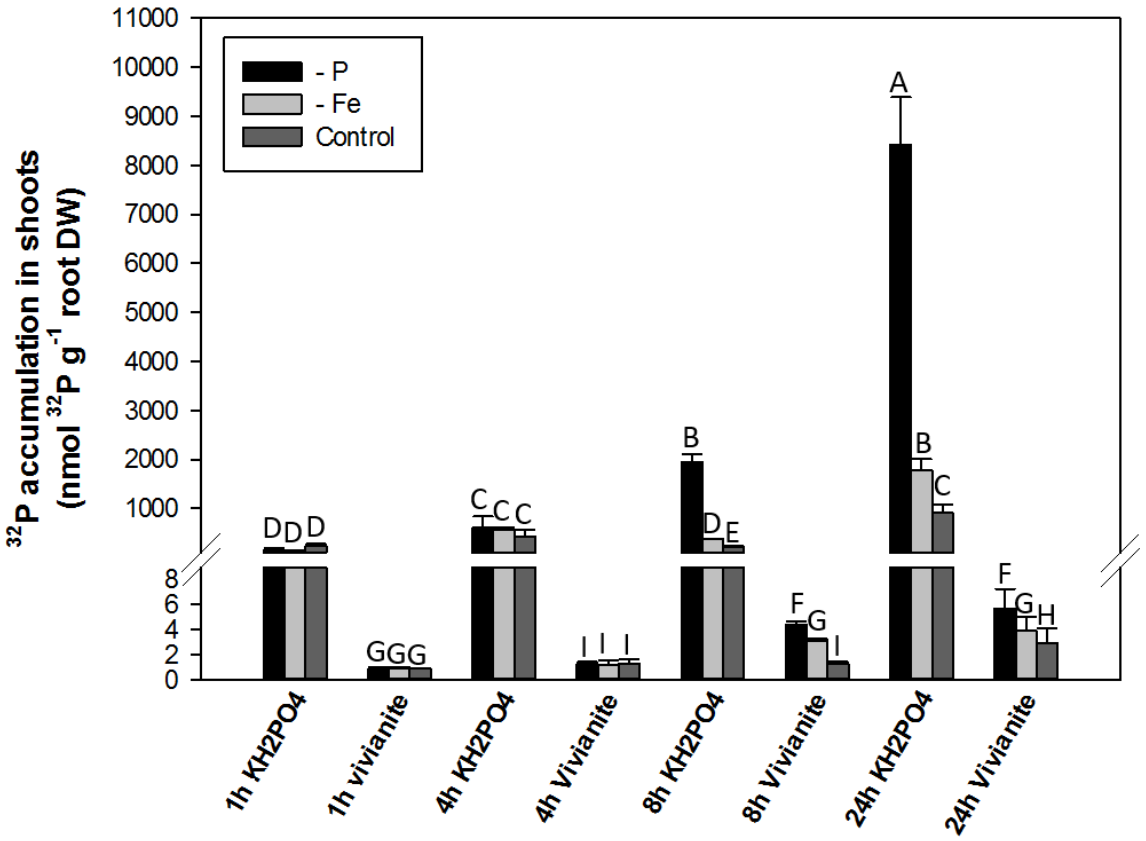

Figure 4.9 - Accumulation of ^{32}P in shoots of white lupine plants grown in a complete, P- or Fe-free nutrient solution. Plants were treated with (^{32}P)KH_2PO_4 (soluble source) or with (^{32}P)Vivianite for 1, 4, 8 and 24 hours. Data are means + SD of three independent experiments (capital letters refer to statistically significant differences among the mean, ANOVA Holm–Sidak, N = 3, P < 0.05). DW, dry weight.

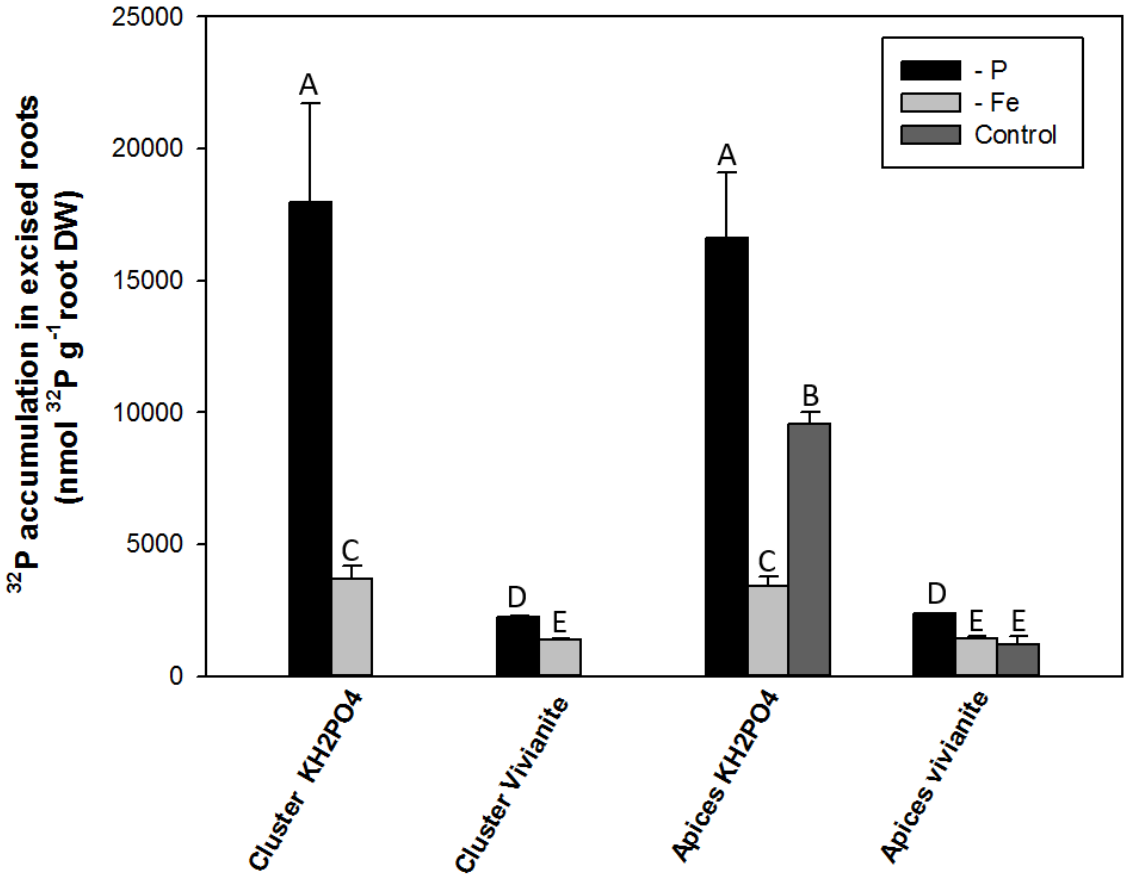

Figure 4.10 - Accumulation of ^{32}P in different root tissues (apices and cluster roots) of white lupine plants grown in a complete, P- or Fe-free nutrient solution. Plants were treated with (^{32}P)KH_2PO_4 (soluble source) or with (^{32}P)Vivianite for 1 hour. Data are means + SD of three independent experiments (capital letters refer to statistically significant differences among the mean, ANOVA Holm–Sidak, N = 3, P < 0.05). DW, dry weight.

The same experiment was performed using excised root tissues: apices and cluster roots (Fig.4.10) were treated for 1 hour with (^{32}P)KH_2PO_4 (soluble source) or with (^{32}P)Vivianite. The highest accumulation of ^{32}P was observed in the P-deficient plants; no significant difference in the amount of P accumulated into the two different root structures was observed. The same behavior occurred when ^{32}P was taken up from (^{32}P)Vivianite, although the amount of the macronutrient accumulated from this source was almost 70 % lower than that accumulated from the soluble source. In the apices and cluster roots of Fe-deficient plants the accumulation of ^{32}P

in both root structure was comparable, although the amount coming from (^{32}P)KH_2PO_4 was 50 % higher than that supplied by (^{32}P)Vivianite. Control plants also accumulate more ^{32}P when treated with the soluble source in comparison with Vivianite.

4.4 Discussion

Iron (Fe) and phosphorus (P) are essential nutrients for plant and their shortage can severely affect plant growth and crop productivity. Although both nutrients are abundant in the soil, their solubility in the soil solution is often scarce and not adequate to sustain the nutritional requirement of plants. To counteract the low availability of P and Fe, plants respond activating different strategies which might cooperate in the root acquisition of both nutrients (Hirsch et al., 2006; Ward et al., 2008).

4.4.1 Response to Fe deficiency in white lupine plants

In the present work, Fe-deficient plants showed the characteristic symptoms of Fe starvation in both leaves and roots. Indeed, Fe-deficient plants displayed clear interveinal leaf chlorosis and particular morphological structures at the root level, called *cluster roots*. It is well known as, under Fe starvation, dicots (like white lupine) induce a specific response, called *Strategy I*, which facilitate Fe acquisition in roots. As expected, transcriptomic analysis revealed that the typical responsive genes to Fe starvation, (like *AHA2*, *FRO2*, *IRT1, FIT* and *BHLH39*; Connolly and Guerinot, 2002; Schmidt, 2003; Santi and Schmidt, 2009; Rodiguez-Celma et al., 2013) were upupregulated in Fe-deficient lupine, in both cluster roots (CR) and root apices (RA; Tab. 4.4). Accordingly with the upregulation of *FRO2*, a strong activity of Fe(III) reduction was observed at the level of CR tissues (Fig. 4.4). Moreover, the increased expression of the *AHA2* and *IRT1* genes correlated with the capability of Fe-deficient plants to acidify the rhizosphere (Fig. 4.3) and to accumulate ^{59}Fe into excised roots (Fig. 4.7). The response to Fe shortage caused an increase in the expression of different genes coding for transporters involved in iron homeostasis. In particular, the citrate efflux transporter FDR3 (Ferric reductase defective 3; Rogers and Guerinot, 2002), which loads citrate into the xylem, was positively modulated. This transporter has been shown to be essential for Fe chelation of in the xylem sap and thus for Fe translocation. Moreover, three genes coding for two oligopeptide transporters and a NRAMP transporter (*OPT3*, *OPT7* and *NRAMP1*) were positively modulated by Fe shortage in CR and RA of lupin

plants which are probably involved in Fe translocation, redistribution and homeostasis (Curie et al. 2000; Zhai et al., 2014; Bashir K et al., 2015). Data reveal that Fe deficient condition also induced the expression of a gene homologous to *PEZ* transporters of *Oryza sativa* (*PEZ1* and *PEZ2*), which are involved in the apoplastic Fe mobilization (Bashir et al., 2011; Kobayashi, 2012). Another Fe-responsive gene is the *pleiotropic drug resistance 9* gene (*PDR9/ABCG37*), which was upregulated in Fe-deficient white lupine roots. Recently, Fourcroy et al., (2014) functionally characterized this transporter, showing its involvement in the export of coumarins. These exudates participate in the mobilization of Fe in the rhizosphere of *Strategy I* plants (Schmid et al., 2014; Fourcroy et al., 2014). On the contrary, *Ferritin* isoform genes (*FER1*, *FER2* and *FER4*) involved in Fe storage (Connolly and Guerinot, 2002, Buckhout et al, 2009) showed a strong downregulation of transcript levels, confirming the condition of the shortage of the micronutrients under the imposed stress.

It is known that in *Arabidopsis,* Fe deficiency determine an upregulation of genes involved in the methionine cycle, in which SAM (S-adenosyl-methionine) plays a key role. In the research by Fernandez-Celma et al. (2013), the *MAT1*, *MAT3*, *MS1* and *SAHH1* genes exhibited an increased amount of these transcripts in –Fe *Arabidopsis* plants; on the other hand, in *Medicago truncatula*, all these genes, except *MAT1*, resulted downregulated. A similar behavior was observed only in –Fe CR, and not in –Fe RA. The *ARD2* gene*,* coding for an enzyme with a putative function in the recovery of L-Met from methylthioadenosine, was also induced by Fe starvation in CR and RA of white lupine, as reported in *Arabidopsis* and *Medicago truncatula* (Fernandez-Celma et al., 2013). Moreover, SAM (S-adenosyl methionine) is the substrate for the biosynthesis of nicotianamine, an important cellular Fe chelator, catalyzed by the nicotianamine synthase (NAS). This enzyme is coded by four isogenes in *Arabidopsis* (Shojima et al., 1990; Herbik et al., 1999). The gene *NAS2*, which homologous was upregulated in Fe-deficient *Arabidopsis*, was also strongly induced in CR and RA of –Fe lupine roots. An opposite behavior was observed for the *NAS3* gene. The encoded protein is known to be exclusively present under Fe-sufficient growth conditions (Mizuno et al., 2003).

Under Fe deficiency, Santi and Schmidt (2009) showed that a gene coding for a plasma membrane proton pump (AHA2), which is involved in rhizosphere acidification, was upregulated in Arabidopsis. Moreover, its activity promotes nitrate uptake into root cells *via* a nitrate-proton cotransporter (AtNRT1.1); these activities, in combination with those involved in

nitrate assimilation, are responsible for the alkalinisation of the cytosol and of the rhizosphere (Miller et al., 2007; Krouk et al., 2010). A high proton extrusion activity in *Arabidopsis* under Fe-deficient conditions was observed concomitant with a lower expression of AtNRT1.1 (Santi and Schmidt, 2009). Moreover, high nitrate concentration can determine Fe chlorosis, probably due to an increase of apoplasmic pH (Smolders et al., 1997). In agreement with these observations, the *NRT1* gene was downregulated in roots (CR and RA) of Fe-deficient lupine plants. Furthermore, two vascular ATPase genes, AVP3 and VHA-A, were both downregulated.
Genes belonging to the phenylpropanoid pathway (PPP) are modulated by the nutritional status of plants as in Fe deficiency. Recently many transcriptomic (Yang et al., 2010; Rodríguez-Celma *et al*., 2013) and proteomic (Lan et al., 2011) studies have focused on the upregulation of a set of genes involved in the PPP in *Arabidopsis* roots. As reported in *Arabidopsis*, also in CR and RA of Fe-deficient white lupine plants, a set of these genes was modulated. The upregulation of the gene coding for ADT3 (arogenate dehydratase 3) enzyme, which leads to the biosynthesis of phenylalanine, was observed. The genes coding for phenylalanine-ammonia lyase isoforms PAL1 and PAL2*,* and for the coumarate:CoA ligases (4CL), were induced by Fe deficiency in CR. The same held true for genes encoding caffeoyl-CoA O-methyltransferase and F6′H1, which mediate the conversion of caffeoyl-CoA to feruloyl-CoA and the subsequent production of 6′hydroxy-feruloyl-CoA, respectively. This intermediate is foundamental for the coumarins synthesis. The conversion of caffeoyl-CoA to feruloyl-CoA is dependent on S-adenosyl-L-Met synthase (MAT1) which genes was upregulated as reported above. This study showed that gene encoding the enzyme chalcone synthase (CHS) and chalcone isomerase CHI), which are involved in the first steps of flavonols synthesis are down regulated.

4.4.2 Response to P deficiency in white lupine plants

Plants under P-deficiency developed leaves with a dark blue-green coloration and numerous cluster root structures were present in the root apparatus, which are characteristics of the P-nutritional stress response (Marschner, 2011).
Some genes commonly expressed under P deficiency were found in the transcriptomic data. Among these, some genes belong to *PS2* (*P-starvation induced gene 2*), *PHT*, *SPX* and *PAP* families. Three genes encoding SPX domain-containing proteins, were upregulated in P-deficient roots. These proteins are essential for maintaining Pi homeostasis (Secco et al., 2012) and have

been suggested to be involved in P signaling (Duan et al., 2008; Chiou and Lin, 2011). Phosphorus-deficient plants showed an increased uptake of Pi compared with P-sufficient plants (Liu et al., 2001). In our dataset, three *plasma membrane high affinity transporter* (*PHT)* gene were found to be upregulated (Tab. 4.5) supporting the high accumulation of ^{32}P in root of –P plants (Fig. 4.8). Another upregulated gene is *PHF1,* which encodes a protein located in the endoplasmic reticulum that is required for the correct targeting of the PHT transporters to the plasmalemma (Bayle et al., 2011). Other candidate genes used as P-shortage indicators such as *bHlH32, MGD2, SQD*, *phospholipase C2* showed an increase in their transcript levels. In addition, the increased transcription of *PHO1* gene, which encode for a protein involved in the loading the Pi into the xylem (Hamburger, 2002), could explain the higher allocation of P in –P shoots (Fig. 4.9).

4.4.3 Relationships between plant responses to P and Fe deficiency

Transcriptomic data showed that both Fe and P deficiency were able to activate pathways in the acquisition of the other nutrient. Indeed, in the gene expression profiles of P-deficient plants, genes involved in the mobilization of Fe, like *IRT1, FRO2* and *AHA2*, and their regulator *FIT*, were upregulated, indicating that in P shortage, white lupine activate also the typical *Strategy I* mechanisms involved in Fe acquisition (Ward et al., 2008). The gels exhibiting the Fe(III)-reduction activity and the rhizosphere acidification confirmed the higher capability of –P CR to reduce Fe(III) chelates (Fig. 4.3; 4.4), and that the main tissue involved in the acidification was the CR, supporting the transcriptional data, which showed an upregulation of *FRO2 and AHA2* in roots of P-deficient plants. Also at the physiological level, ^{59}Fe accumulation was enhanced in the –P plants as compared to the control ones both in root and leaf tissues (Fig. 4.5; 4.6). The activation of these common mechanisms could be functional to the mobilization of P from P-Fe precipitates. In addition, genes involved in Fe homeostasis as *FRD3*, *PDR9* and *NRAMP1* resulted to be also upregulated in –P plants. Regarding *FRD3*, its increased expression could explain the enhanced accumulation of ^{59}Fe in leaves (Fig. 4.6). The putative gene *PEZ1/2* which share high sequence similarity with *AtPEZ1/2* was strongly upregulated suggesting that the –P plants enhanced their capability to mobilize Fe from the apoplast and/or translocate it *via* xylem sap. In accordance with the previous work of O'Rourke (2003), *FER1* and *FER4* transcript levels were abundant in roots of P-deficient plants. This author suggested that increased root exudation of Fe-chelating compounds might facilitate a greater Fe^{2+} uptake under P-deficient condition,

thus reducing Fe-P precipitation in the rhizosphere. Bournier et al. (2013) demonstrated that the upregulation of *FER1* in Arabidopsis is involved in the P-starvation response and that it is not linked to the Fe status of plants and is specifically initiated by P deficiency condition. Also in –Fe CR and RA some genes specific to the P-deficiency response were modulated, such as the *PHT transporters*, two isoforms of *PAPs*, the *PS2* and *PHO1*. These results suggest that the Pi uptake is also potentiated in Fe-deficient plants. Indeed, in our physiological experiments the mobilization and uptake of Pi was enhanced in –Fe plants as compared to the control ones.

Iron and P deficiency determines a wide number of changes in plant metabolism. As reported above Fe shortage in *Arabidopsis* induce an upregulation of genes involved in the Met cycle. Few genes belonging to this cycle were also influenced by the P deficiency. Contrary to Fe deficiency, P deficiency induced the downregulation of *MAT1*. On the other hand, *ARD2* and the *NAS3* were respectively up- and down-regulated as in Fe starvation.

Both Fe and P shortage can influence the proton pumping activity. The same response was observed in the CR of white lupine plants under P deficiency compared with Fe deficiency (Tab.4.8). This suggest that plants through the modulation of the nitrate uptake, try to increase the efficiency of nutrient mobilization, enhancing the rhizosphere acidification.

The comparison of the effect of both P and Fe deficiency on PPP highlighted some similarities. Both deficiencies showed an increased expression of the *FH'6* gene which lead to coumarin production. On the contrary, in P-starved plants activated enzymes involved in the flavone syntheses, as CHS and FLS; meanwhile in Fe-deficient plants, the CHS and CHI isomerase were downregulated, probably to promote the production of coumarins, even if a gene involved in flavonoid synthesis (*FH3*) was upregulated. Furthermore, in according with other studies, both P and Fe deficiency modulated positively the enzymes involved in the lignin synthesis (Donnini et al., 2011; O'Rourke et al., 2013).

4.4.4 Metabolomics approach to identify the exudation pattern

Several studies indicated that one aspect of the response to Fe and P deficiency by plants is the released of significant amounts of root exudates, containing organic acids and flavonoids. To lend support to our transcriptomic data, we also investigated the biosynthesis and release of phenolics, analysing the phenolics' content inside the roots and in the root exudates under the

different nutritional conditions. In the root tissues, the main molecules detected were scopoletin (coumarin subfamily) and genistein (flavonoid) derivatives, conjugated with malonate and/or glucoside molecules. Under Fe deficiency both in CR and RA, a high variety of coumarins was identified, in accordance with the transcriptomic data showing a high increase of the transcript abundance of *F6'H* gene and of the specific transporter *PDR9*. In –P conditions, scopoletin derivatives were detected but with a lower variety of compounds and in lower amounts.
On the other hand, many genistein derivatives were found in all the tissues under each growth condition. Recently it has been suggested that the chemical modifications of flavonoids, which include methylation, glycosylation and malonylation have specific function in flavonoid targeting (Zhao, 2011). Most studies demonstrated that glycosylation is a prerequisite for flavonoids in order to be transported into the vacuoles, while the aglycone forms could be transported outside the cell. Furthermore, Zhao et al. (2011) characterized a MATE2 transporter in *Medicago truncatula*, which mediates the vacuolar sequestration of flavonoids' glycoside and glycosate malonates. This research suggest, that the glycoside-malonyl genistein and scopoletin that we identified in the root tissues were presumabily stored in the vacuoles. Moreover, the aglycone form of scopoletin and genistein derivatives were detected in the root exudates of Fe- and P-deficient plants but not in the control plants, as expected from the research by Zhao et al. (2011). The observation that some compounds are present in the roots but not in the root exudates, under control conditions might suggest that plants have a basal production of these compounds that are probably stored in the cell and then promptly released only when this kind of nutritional stress takes place.

In conclusion these results showed a physiological and transcriptional link between the responses to Fe and P deficiency in white lupine roots. Phosphorus-deficient plants activated the *Strategy I* Fe acquisition mechanisms that lead to an enhanced Fe mobilization and translocation and that might help the P acquisition process. On the other hand, also the Fe deficiency induced the transcription of some P-deficient-responsive genes even if the mobilization of Pi by the –Fe plants remained limited.
In both the nutritional conditions, the release of root exudates appear to be a crucial step for an effective response. Iron and P deficiency determined the release of scopoletin and genistein derivatives. Furthermore, in –Fe plants the variety of coumarins compounds released was wider

than in –P plants, which, on the other hand, released mostly isoflavonoids. The analysis of the root contents showed that plants constitutively synthetise a set of compounds, which are found in malonyl-derivatives forms independently of the nutritional status of plants; these compounds are then released in aglycon-forms when plants are experiencing P- or Fe-deficiency conditions.

4.5 Acknowledgements

Research was supported by grants from Italian MIUR (FIRB-Programma “Futuro in Ricerca” RBFR127WJ9).

RNA sequencing analysis analyses were performed at the Institute of Applied Genomics (IGA, Udine) and the LC-MS analyses at the CSIC (Zaragoza, Spain).

4.6 References

Bashir K, Ishimaru Y, Shimo H, Kakei Y, Senoura T, Takahashi R, Sato Y, SatoY, Uozumi N, Nakanishi H, Nishizawa NK. (2011). Rice phenolics efflux transporter 2 (PEZ2) plays an important role in solubilizing apoplasmic iron. Soil Science and Plant Nutr 57: 803–812.

Bashir K, Ishimaru Y, Itai RN, Senoura T, Takahashi M, An G, Oikawa T, Ueda M, Sato A, Uozumi N, Nakanishi H, Nishizawa NK. (2015). Iron deficiency regulated OsOPT7 is essential for iron homeostasis in rice. Plant Mol Biol 88:165-176.

Bayle V, Arrighi JF, Creff A, Nespoulous C, Vialaret J, Rossignol M, Gonzalez E, Paz-Ares J, Nussaume L. (2011). Arabidopsis thaliana high-affinity phosphate transporters exhibit multiple levels of posttranslational regulation. Plant Cell 23:1523-1535.

Bienfait HF, van den Briel W, Mesland-Mul NT. (1985). Free space iron pools in roots: generation and mobilization. Plant Physiol 78: 596–600.

Bournier M, Tissot N, Mari S, Boucherez J, Lacombe E, Briat JF, Gaymard F.(2013). Arabidopsis ferritin 1 (AtFer1) gene regulation by the phosphate starvation response 1 (AtPHR1)

transcription factor reveals a direct molecular link between iron and phosphate homeostasis. J Biol Chem 288:22670-22680.

Briat JF, Rouached H, Tissot N, Gaymard F, Dubos C. (2015). Integration of P, S, Fe, and Zn nutrition signals in Arabidopsis thaliana: potential involvement of phosphate starvation response1 (PHR1). Front Plant Sci 6:290.

Bristow AWT. (2006). Accurate mass measurement for the determination of elemental formula-a tutorial. Mass Spectrometry Reviews 25:99 – 111.

Buckhout TJ, Yang TJ, Schmidt W. (2009). Early iron-deficiency-induced transcriptional changes in Arabidopsis roots as revealed by microarray analyses. BMC Genomics 10:147.

Chiou TJ, Lin SI. (2011). Signaling network in sensing phosphate availability in plants. Annu Rev Plant Biol 62:185-206.

Connolly EL, Guerinot M. (2002). Iron stress in plants. Genome Biol 3- 4.

Curie C, Alonso JM, Le Jean M, Ecker JR, Briat JF. (2000). Involvement of NRAMP1 from Arabidopsis thaliana in iron transport. Biochem J 347: 749-755.

Curie C, Panaviene Z, Loulergue C, Dellaporta SL, Briat JF, Walker EL. (2001). Maize yellow stripe1 encodes a membrane protein directly involved in Fe(III) uptake. Nature. 409:346-349.

Donnini, S., Dell'Orto, M., Zocchi, G. (2011). Oxidative stress responses and root lignification induced by Fe deficiency conditions in pear and quince genotypes. Tree physiology 31: 102-113.

Duan K, Yi K, Dang L, Huang H, Wu W, Wu P. (2008). Characterization of a sub-family of Arabidopsis genes with the SPX domain reveals their diverse functions in plant tolerance to phosphorus starvation. The Plant Journal 54: 965–975.

Eide D, Broderius M, Fett J, Guerinot ML (1996). A novel iron-regulated metal transporter from plants identified by functional expression in yeast. Proc Natl Acad Sci U S A. 93:5624-5628.

Fourcroy P, Sisó-Terraza P, Sudre D, Savirón M, Reyt G, Gaymard F, Abadía A, Abadia J, Alvarez-Fernández A, Briat JF (2014). Involvement of the ABCG37 transporter in secretion of scopoletin and derivatives by Arabidopsis roots in response to iron deficiency. New Phytol 201: 155-167.

Hagström J, James WM, Skene KR. A.(2001). Comparison of structure, development and function in cluster roots of Lupinus albus L. under phosphate and iron stress. Plant Soil 232: 81-90.

Hamburger D, Rezzonico E, MacDonald-Comber Petetot J, Somerville C, Poirier Y. (2002) Identification and characterization of the Arabidopsis PHO1 gene involved in phosphate loading to the xylem. Plant Cell 14: 889–902.

Hansen, N. et al., 2006. Iron Nutrition in Field Crops. In L. L. Barton & J. Abadia, eds. *Iron Nutrition in Plants and Rhizospheric Microorganisms*. Springer Netherlands, pp. 61–83.

Herbik A, Koch G, Mock HP, Dushkov D, Czihal A, Thielmann J, Stephan UW, Bäumlein H . (1999). Isolation, characterization and cDNA cloning of nicotianamine synthase from barley. A key enzyme for iron homeostasis in plants. Eur J Biochem 265: 231-239.

Hirsch, J., Marin, E., Floriani, M., Chiarenza, S., Richaud, P., Nussaume, L., et al. (2006). Phosphate deficiency promotes modification of iron distribution in Arabidopsis plants. Biochimie 88: 1767–1771.

Kim D, Pertea G, Trapnell C, Pimentel H, Kelley R, Salzberg SL.(2013). TopHat2: accurate alignment of transcriptomes in the presence of insertions, deletions and gene fusions. Genome Biol 14: R36.

Kobayashi T, Nishizawa NK. (2012). Iron uptake, translocation, and regulation in higher plants. Annual Review of Plant Biology 63: 131–152.

Krouk G, Mirowski P, LeCun Y, Shasha DE, Coruzzi GM. (2010). Predictive network modeling of the high-resolution dynamic plant transcriptome in response to nitrate. Genome Biol 11:R123.

Lan P, Li W, Wen TN, Shiau JY, Wu YC, Lin W, Schmidt W .(2011). iTRAQ protein profile analysis of Arabidopsis roots reveals new aspects critical for iron homeostasis. Plant Physiol 155: 821–834.

Le Jean M, Schikora A, Mari S, Briat JF, Curie C. (2005). A loss-of-function mutation in AtYSL1 reveals its role in iron and nicotianamine seed loading. Plant J 44(5):769-782.

Liu J, Uhde-Stone C, Li A, Vance CP, Allan DL. (2001). A phosphate transporter with enhanced expression in proteoid roots of white lupine (Lupinus albus L.). Plant and Soil 237: 257 – 266.

Marinova K, Pourcel L, Weder B, Schwarz M, Barron D, Routaboul JM, Debeaujon I, Klein M. (2007). The Arabidopsis MATE transporter TT12 acts as a vacuolar flavonoid/H+ -antiporter active in proanthocyanidin-accumulating cells of the seed coat. Plant Cell 19: 2023-2038.

Marschner H, Römheld V. (1994). Strategies of plants for acquisition of iron. Plant Soil 165: 261-274.

Miller AJ, Fan X, Orsel M, Smith SJ, Wells DM. (2007). Nitrate transport and signalling. J Exp Bot 58: 2297–2306.

Mizuno D, Higuchi K, Sakamoto T, Nakanishi H, Mori S, Nishizawa NK: (2003). Three nicotianamine synthase genes isolated from maize are differentially regulated by iron nutritional status. Plant Physiol 132: 1989–1997.

O'Rourke JA, Yang SS, Miller SS, et al. (2013). An RNA-Seq transcriptome analysis of orthophosphate-deficient white lupine reveals novel insights into phosphorus acclimation in plants. Plant Physiology. 161: 705 – 724.

Rellán-Alvarez R, Andaluz S, Rodríguez-Celma J, Wohlgemuth G, Zocchi G, Alvarez-Fernández A, Fiehn O, López-Millán AF, Abadía J.(2010). Changes in the proteomic and metabolic profiles of Beta vulgaris root tips in response to iron deficiency and resupply. BMC Plant Biol 10:120.

Robinson NJ, Procter CM, Connolly EL, Guerinot ML. (1999). A ferric-chelate reductase for iron uptake from soil. Nature 397: 694–697.

Rodríguez-Celma J, Lin WD, Fu GM, Abadía J, López-Millán AF, Schmidt W. (2013). Mutually exclusive alterations in secondary metabolism are critical for the uptake of insoluble iron compounds by Arabidopsis and *Medicago truncatula*. Plant Physiol 162:1473-1485.

Rogers EE, Guerinot ML. (2002). FRD3, a member of the multidrug and toxin efflux family, controls iron deficiency responses in Arabidopsis. Plant Cell 14:1787-1799.

Santi S, Schmidt W. (2009). Dissecting iron deficiency-induced proton extrusion in Arabidopsis roots. New Phytol 183:1072-1084.

Schmidt, W. (2003). Iron solutions: acquisition strategies and signaling pathways in plants, Trends Plant Sci. 8: 188-193.

Schmid NB, Giehl RF, Döll S, Mock HP, Strehmel N, Scheel D, Kong X, Hider RC, von Wirén N .(2014). Feruloyl-CoA 6'-Hydroxylase1-dependent coumarins mediate iron acquisition from alkaline substrates in Arabidopsis. Plant Physiol 164:160-172.

Secco D, Shou H, Whelan J, Berkowitz O. (2014). RNA-seq analysis identifies an intricate regulatory network controlling cluster root development in white lupine. BMC Genomics 15:230.

Secco D, Wang C, Arpat BA, Wang Z, Poirier Y, Tyerman SD, Wu P, Shou H, Whelan J. (2012). The emerging importance of the SPX domain-containing proteins in phosphate homeostasis. New Phytol 193:842-851.

Secco D, Whelan J. (2014). Toward deciphering the genome-wide transcriptional responses of rice to phosphate starvation and recovery. Plant Signal Behav 9:e28319.Shojima, S., Nishizawa, N.K., Fushiya, S., Nozoe, S., Irifune, T. and Mori, S. (1990). Biosynthesis of phytosiderophores. Plant Physiol. 93: 149-1503.

Smolders AJP, Hendriks RJJ, Campschreur HM, Roelofs JGM. (1997). Nitrate induced iron

deficiency chlorosis in Juncus acutiflorus. Plant Soil 196: 37–45.

Trapnell C, Roberts A, Goff L, Pertea G, Kim D, Kelley DR, Pimentel H, Salzberg SL, Rinn JL, Pachter L. (2012). Differential gene and transcript expression analysis of RNA-seq experiments with TopHat and Cufflinks. Nat Protoc 7:562-78.

Trapnell C, Williams BA, Pertea G, Mortazavi A, Kwan G, van Baren MJ, Salzberg SL, Wold BJ, Pachter L. (2010). Transcript assembly and quantification by RNA-Seq reveals unannotated transcripts and isoform switching during cell differentiation. Nat Biotechnol 28:511-5.

Uhde-Stone C, Zinn KE, Ramirez-Yáñez M, Li A, Vance CP, Allan DL. (2003). Nylon filter arrays reveal differential gene expression in proteoid roots of white lupine in response to phosphorus deficiency. Plant Physiol 131:1064-1079.

Vance CP, Uhde-Stone C, Allan DL. (2003). Phosphorus acquisition and use: critical adaptations by plants for securing a nonrenewable resource. New Phytol 157:423–447.

Ward, J. T., Lahner, B., Yakubova, E., Salt, D. E., and Raghothama, K. G.(2008). The effect of iron on the primary root elongation of Arabidopsis during phosphate deficiency. Plant Physiol. 147:1181–1191.

Yang K, Jeong N, Moon J-K, Lee Y-H, Lee S-H, Kim HM, Hwang CH, Back K, Palmer RG, Jeong S-C. (2010). Genetic analysis of genes controlling natural variation of seed coat and flower colors in soybean. J Hered 101:757–768.

Zancan S, Cesco S, Ghisi R. (2006). Effect of UV-B radiation on iron content and distribution in maize plants. Environ Exp Bot 55: 266–272.

Zhai Z, Gayomba SR, Jung HI, Vimalakumari NK, Piñeros M, Craft E, Rutzke MA, Danku J, Lahner B, Punshon T, Guerinot ML, Salt DE, Kochian LV, Vatamaniuk OK.(2014). OPT3 Is a Phloem-Specific Iron Transporter That Is Essential for Systemic Iron Signaling and Redistribution of Iron and Cadmium in Arabidopsis. Plant Cell 26:2249-2264.

Zhao J, Huhman D, Shadle G, He XZ, Sumner LW, Tang Y, Dixon RA.(2011). MATE2 mediates vacuolar sequestration of flavonoid glycosides and glycoside malonates in Medicago truncatula. Plant Cell 23:1536-1555.

5. RELEASE OF GENISTEIN FROM WHITE LUPINE CLUSTER ROOTS IS CATALYSED BY A MULTI DRUG EXTRUSION PROTEIN

Release of genistein from white lupine cluster roots is catalysed by a multi drug extrusion protein

Stefano Gottardi[1], Venuti Silvia[1], Laura Zanin[1], Fabio Valentinuzzi[1,2], Tanja Mimmo[2], Stefano Cesco[1], Rita Francisco De Brito[3], Enrico Martinoia[3], Roberto Pinton[1], Nicola Tomasi[1]

[1] Department of Agricultural and Environmental Sciences, University of Udine, Udine, Italy

[2] Faculty of Science and Technology, Free University of Bolzano, Bolzano, Italy

[3] Institute of Plant Biology, University of Zurich, Zurich, Switzerland

Abstract

White lupin (*Lupinus albus* L.) has developed a complex strategy to survive in low nutrient soils. This behavior involves the modification of root architecture with the formation of cluster roots and the release of root exudates, mainly organic acids and phenolic compounds. These molecules can mobilize sparingly available nutrients in soils, such as phosphorus, *via* complexation and/or ligand exchange.

It is well-known that genistein is a flavonoid released in high amounts from P-deficient white lupin roots; this compound is exuded mainly from the juvenile and immature cluster roots. To our knowledge, there are no data on proteins involved in this processes, although MATE-mediated transmembrane flavonoid transport has been characterized in other plant species.

Aim of this study was to functionally characterize a MATE transporter (LaMATE2) involved in the release of genistein from roots of white lupin plants. The complete sequences of the gene was isolated and the expression study was performed in tissues of P-deficient and sufficient white lupin plants; via a silencing approach the involvement of LaMATE2 in the root release of genistein was evaluated. The localization of the LaMATE2 protein was performed in *Arabidopsis thaliana* protoplast and its transport activity was characterized in yeast vesicles.

5.1 Introduction

The concentration of available phosphate (Pi) for plant nutrition in soil seldom exceeds 10 μM (Bieleski, 1973). Therefore the scarce availability of this nutrient is one of the most common growth-limiting factors in many ecosystems and in particular in acidic soils

(Raghothama & Karthikeyan, 2005; Marschner, 2012). To cope with this problem, plants have evolved several adaptation mechanisms (Schachtman et al., 1998; Lambers et al., 2015). Two main adaptation responses are the association with mycorrhizal fungi or the formation of particular root structures, called cluster roots or proteoid roots (Purnell, 1960). From the latter tissue, an abundant release of root exudates into the rhizosphere is occurring in P-deficient plants (Dinkelaker et al., 1989; Neumann et al., 1999). These root exudations are mainly composed of citrate, malate and other carboxylates and of phenolic compounds (Neumann et al., 1999). These latter are mainly genistein and its derivatives, like e.g. glycosylated and/or hydroxylated genistein (Weisskopf et al., 2006b). These molecules have been shown to be involved both in the mobilization of nutrients, such as Fe via the reduction and complexation, and in the modulation of soil microorganism activities (Tomasi et al., 2008; Cesco et al., 2010).

Up to now the mechanisms involved in the release of root exudates is still scarce (Weston et al., 2012; Baetz & Martinoia, 2014; Pii et al., 2015), with some quite well characterized exceptions, such as the Al-induced release of carboxylates (Kochian et al., 2015). Concerning the release of phenylpropanoid compounds, recently, a transporter of coumarins has been functionally characterized in Fe-deficient Arabidopsis roots (Fourcroy et al., 2013; Rodriguez-Celma et al., 2013). However, the mechanisms involved in the release of flavonoids from roots is still unknown. Some members from the family of the multidrug and toxic compound extrusion (MATE) have been shown to be able to transport these molecules. Marinova and coworkers (Marinova et al., 2007) demonstrated that Transparent Testa12 protein catalyzes the transmembrane transport of some glycosylated proantocyanins through the tonoplast of *Arabidopsis* seeds. Another MATE protein (MATE2) from Medicago truncatula transports either anthocyanins, glucosidated flavonoids or malonate-glucoside flavonoids into the vacuole of flowers and other tissues (Zhao et al., 2011). Since then, some other MATEs have been shown to be involved mostly in anthocyanins accumulation in fruits, leaves and flowers (for review see Takanashi et al., 2014).

In this work we functionally characterized a MATE transporter (LaMATE2) involved in the release of genistein from roots of white lupine plants. The complete sequences of the gene was isolated and expression study was performed in tissues of P-deficient and sufficient white lupine plants; via a silencing approach the involvement of LaMATE2 in the root release of genistein

was evaluated. The localization of the LaMATE2 protein was performed in *Arabidopsis* protoplast and its transport activity was characterized in yeast vesicles.

5.2 Materials and methods

5.2.1 Plant growth

White lupine seeds (*Lupinus albus* L. cv. Amiga; Südwestdeutsche Saatzucht, Rastatt, Germany) were soaked for 24 hours in aerated water and germinated on a plastic net placed at the surface of an aerated 0.5 mM $CaSO_4$ solution in a growth chamber at 25 °C in the dark. Thereafter, 4 day-old seedlings were transferred under hydroponic system, containing a complete nutrient solution with the following composition: [mM] 5 $Ca(NO_3)_2$ $4H_2O$, 1.25 $MgSO_4$, 1.75 K_2SO_4, 0.25 KCl; [µM]: 20 Fe(III)EDTA, 25 H_3BO_4, 1.25 $MnSO_4$ $7H_2O$, 1.5 $ZnSO_4$ $7H_2O$, 0.5 $CuSO_4$ $5H_2O$, 0.025 $(NH_4)_6Mo_7O_{24}$ $4H_2O$; with or without 0.25 mM KH_2PO_4 in control (P-sufficient) or P-deficiency. Plants were grown in a growth chamber under controlled conditions for 4 weeks (day/night photoperiod, 16/8 h; radiation, 220 µ Einsteins $m^{-2}s^{-1}$; day/night temperature, 25/20 °C; relative humidity, 70-80 %). Experiments were repeated three times.

5.2.2 Harvest of cluster roots at different developmental stage

In P-deficiency, lupine plants after 3-4 weeks of growth, modify the root architecture developing particularly root structures, called cluster roots or proteoid roots. In order to differentiate the developmental stages of root clusters, the root system was immerged in a pH-indicator solution (Bromocresol purple 0.04%). Depending on their ability to acidify the solution, different cluster regions were identified (juvenile, immature, mature, senescent), as described by Massonneau et al. (2001). The different stages of cluster root and apices for P-deficient plants and only apices for P-sufficient plants were collected and they were used immediately for physiological experiments while for molecular analysis samples were stored at -80 °C.

5.2.3 Collection of root exudates

The root material was washed for 10 minutes in $CaSO_4$ 0.5 mM, and later transferred in 0.5 mM $CaSO_4$; 10 mM MES-KOH solution at pH 6.0 and shook for 1 hour at 120 rpm. The solutions were collected in order to measure the release of flavonoids. The fresh weight was measured.

5.2.4 Flavonoids analysis

Flavonoids separation was performed by HPLC instrument with a X-Bridge Shield-C18 column (5 mm, 4.6 x 200 mm, Waters, Milano, Italy Waters) using an isocratic elution with 60% of solvent A (Acetonitrile 60%) and 40 % of solvent B (H_2SO_4 1%) as mobile phases at a flow rate of 1 mL min^{-1} and detected at 254 nm (PDA 2998 Waters Spa, Italy).

5.2.5 RNA extraction and cDNA synthesis

RNA extractions were performed using the InviTrap Spin Plant RNA Mini Kit (Stratec Molecular, Berlin, Germany) following manufacturer's instructions and contaminant genomic DNA was removed using 10 U of DNase I (GE Healthcare, Munich, Germany). The quantity and the quality of RNA was checked using a spectrophotometer, followed by a migration in a 1 % agarose gel. One microgram of total RNA for each sample was retrotranscribed using 1 pmol Oligo $d(T)_{23}$ (Sigma Aldrich, Saint Louis, USA) and 10 U M-MulV RNase H (Finnzymes, Helsinki, Finland) following manufacturers' instruction. cDNA obtained was kept at -20 °C for the following molecular analyses.

5.2.6 Gene expression analysis

Real-time RT-PCR analyses were performed in triplicates on the three biological samples. The reaction was performed adding 0.1 µl of cDNA to RT complete reaction mix, Fluocycle^{TM} sybr green (20 µl final volume; Euroclone, Pero, Italy) using the DNA Engine OPTICON2 *Continuous* Fluorescence Detector system (Biorad). Specific primers were designed for the target and the housekeeping gene using Primer3 software (Koressaar & Remm, 2007; Untergasser *et al.*, 2012) and they were synthesized by Sigma Aldrich Srl (Milan, Italy; Supplementary Table 1). The gene expression analysis of real-time result were performed using Opticon Monitor 2 software (Biorad). Data were normalized respect to the transcript level of the housekeeping gene (Ubiquitin gene) using the $2^{-\Delta\Delta CT}$ method, where $\Delta\Delta C_T = (C_{T,Target} - C_{T,HK})_{sample} - (C_{T,Target} - C_{T,HK})_{control}$ ($livak_{Time\ 0}$ (Livak & Schmittgen, 2001)). The efficiency of amplification was calculated using R program (version 2.9.0; http://www.r-project.org/) with the qPCR package (version 1.1-8), following the authors' indications.

5.2.7 Isolation of the LaMATE2 sequence

The partial sequence was isolated via a cDNA-AFLP approach starting from RNA extracted from juvenile cluster roots compared to mature and senescent ones, for details see Massonneau et al. (2001). The full open reading frame (ORF) was isolated using the 5'/3' RACE Kit (2nd generation, Roche Diagnostics S.p.a., Monza, Italy) following the manufacturer's instructions. Thereafter the complete ORF was amplified from the cDNA of juvenile cluster root tissues from P-deficient plants and cloned in pGEMT easy vector (Promega Italia Srl, Milan, Italy) and sequenced. The *LaMATE2* full sequence has been deposited in the NCBI database (XXXX).

5.2.8 Silencing: pRedRoot:LaMATE2 cloning

LaMATE2 silencing was performed using binary transformation vectors, *pRNAi* and *pRedRoot* (Limpens et al., 2004). Target regions were first amplified with PCR, and subsequently cloned into pRNAi vector between the restriction sites *NcoI –SwaI* and *BamHI–SpeI*. The cloned sequences were regulated by a double CaMV 35S promoter and OCS 3' terminator. The resulting inverted repeated construct *KpnI–PacI* was inserted into the pRedRoot binary vector, as pRedRoot::*LaMATE2*. Target regions were amplified using the primer combinations including the folowing restriction sites: *SpeI–AscI* and *BamHI–SwaI*.

5.2.9 Agrobacterium rhizogenes-mediated transformation

Agrobacterium rhizogenes, ARqua1 strain (Quandt *et al.*) competent cells were transformed either with 1 µg of empty vector pRedRoot (pRR) or 1 µg of the construct pRedroot::*LaMATE2*. Bacteria were grown on LB Agar under Kanamycin and Streptomycin selection and the positively transformed bacteria were selected.

Lupine seedlings (4-day-old) were transformed using *Agrobacterium rhizogenes* harbouring the construct pRR::*LaMATE2*. A positive colony of *Agrobacterium* was selected and grown in LB liquid culture overnight. Five-hundred µL of the bacterial suspension was infiltrated below the cotyledon of either the empty pRR vector (control plants) or pRR::*LaMATE2*. Three transformed seedlings of each treatment were then transferred in pots filled for ¾ with perlite and the P-free nutrient solution previously described. After 3 weeks white lupine plants were moved in hydroponic solutions (with the same composition) and grown for additional 3 weeks in hydroponics. At harvest root exudate and plant material were collected and freezed at -80°C.

5.2.10 pNEV Cloning

Construction of yeast expression vector pNEV (Sauer & Stolz, 1994) containing *LaMATE2*$_{ORF}$ was performed by amplifying *LaMATE2*$_{ORF}$ sequence with primers having both a *NotI* restriction sites at the 5'end. The subcloning of the PCR product (*LaMATE2*) was performed into the *NotI* site of pNEV, the orientation was verified by sequencing and resulting in pNEV::*LaMATE2*$_{ORF}$. The transformation of competent yeast cells (*Saccharomyces cerevisiae* YPH499 strain) was performed following a standard procedure (Gietz & Woods, 2002) and transformants were selected on synthetic dextrose minimal medium (Burke et al., 2000) with Oxoid agar (Difco, Detroit, USA) lacking uracil (Synthetic Defined (SD)-Ura medium).

5.2.11 Isolation of Membrane Vesicles from Yeast and Transport Assays

YPH499 yeast cells transformed with the empty pNEV vector or pNEV::*LaMATE2*$_{ORF}$ were grown on SD-Ura liquid medium and harvested by centrifugation. Cells were incubated in YPD medium for 30 min, collected by centrifugation, and digested with lyticase (1,000 U g^{-1} fresh weight cells; Sigma Aldrich), and then microsomal vesicles were isolated as described by Tommasini and coworkers (1996) with the modifications reported by Klein et al. (2002). A transport assay was performed in order to study the genistein transport using the rapid filtration technique with nitrocellulose filters (0.45-µm pore size; Millipore). The transport experiment was carried out in presence of isolated vesicles, transport buffer (0.4 M glycerol, 0.1 M KCl, 20 mM Tris-MES, pH 7.4, and 1 mM DTT) and 5 µM of labelled genistein (^{3}H-genistein, 1850 Bq $filter^{-1}$). The mixture was loaded on a pre-wet filter at time points indicated in Figure XX and removed by suction. The membrane was rapidly washed twice with 2 mL of ice-cold of transport buffer. To verify if genistein was co-transported with protons, NH_4Cl 25 mM was included into the transport buffer assay. Moreover, to test the substrate affinity of the transporter, the assay was performed under same experimental conditions reported above in presence of different flavonoids (5 µM): diadzedin, genistin, kampferol, or quercetin. The radioactive measurements were determine with beta-counter (Tri-Carb 1900CA, Packard, Downers Grove, USA). As standards, solutions with known ^{3}H-genistein concentrations were used. The data are referred to the protein amount present inside the vesicles, quantified with the Bio-Rad Protein Assay Dye Reagent (Bio-Rad).

5.2.12 Protein subcellular localization in Arabidopsis thaliana protoplasts

To investigate *LaMATE2* localization, the transient expression of *LaMATE2*$_{ORF}$-GFP was performed in Arabidopsis mesophyll protoplasts. The plasmid harbouring the sequence for the Green Fluorescent Protein (GFP) was fused at the C-terminus of *LaMATE2* inside the pUC18-Sp-GFP6 vector (Komarova et al., 2002) using *NheI* and *SphI* restriction sites via PCR amplification. *AtPIP2a*-mCherry fluorescence was used as plasma membrane marker (Nelson *et al.*, 2007). Arabidopsis protoplasts were co-transformed with both constructs using the polyethylene glycol method (Jin et al., 2001). Expression of constructs was monitored using a Leica TCS SP5 microscope (Leica Microsystems, Wetzlar, Germany). The filter sets used were Filter set xx (excitation, BP458; beamsplitter, FT500; emission, BP 492-511 nm) for GFP and Filter set 20 (excitation, BP 540–552; beamsplitter, FT560; emission, BP 575–640) for mCherry.

5.3 Results

5.3.1 Genistein release

Figure 5.1 shows the release of genistein measured in root exudates of white lupine collected for 1 h. The measurements were performed on root apices for control plants and on apices and cluster roots at different developmental stages (juvenile, immature, mature and senescent) for the P-deficient ones. The release was significantly affected by the growth condition and the type of root tissues. The amount of genistein released by root apices of control plants was under the detection limit. On the contrary, the flavonoid release by apices in P-deficient plants was around 200 µmol g^{-1} FW h^{-1}. Concerning the cluster roots, the amount of genistein released depended on the developmental stage of the tissue. The highest amount of genistein was released from the juvenile stage of cluster roots and a progressive decrease was observed in the immature and mature cluster roots. In the senescent stage, the amount was below the detection limit.

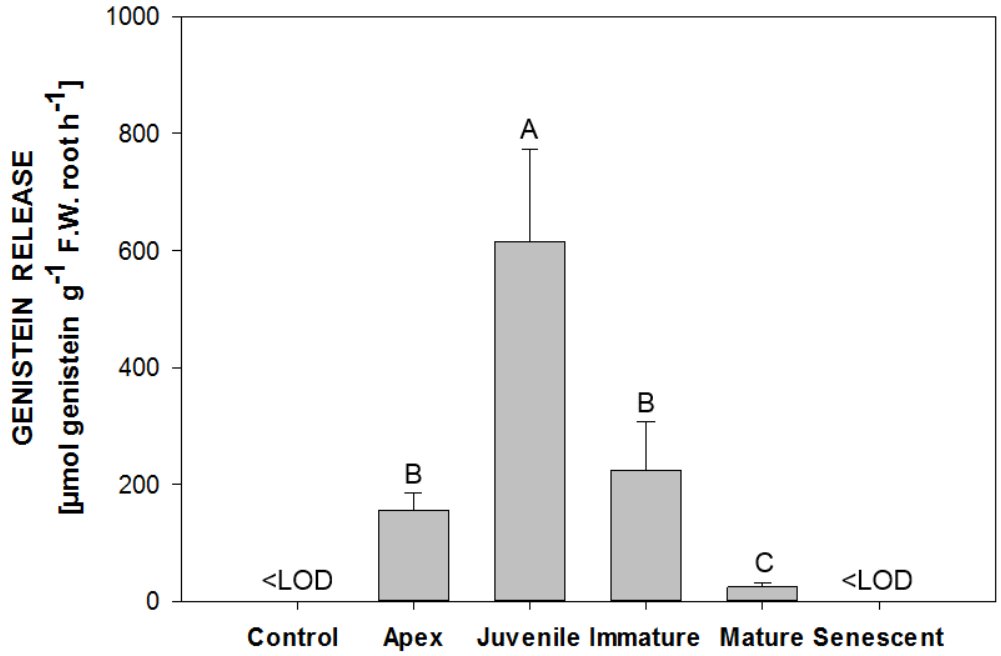

Figure 5.1 - Genistein release in control lupine root apices or in P-deficient root tissues. Data are means+SD of three independent experiments (capital letters refer to statistically significant differences among the mean, ANOVA Holm–Sidak, N=3, P <0.05). FW, fresh weight. <LOD, below the limit of detection.

5.3.2 Gene expression analysis

LaMATE2 expression patterns in different regions of P-deficient cluster roots as compared to apices of controls plants are shown in Figure 5.2. The profile of gene expression followed the same trend of genistein release. The highest expression level of *LaMATE2* was observed in juvenile cluster roots. An upregulation of this gene was also observed in the apices and mature cluster roots of P-deficient plants in comparison with control plants. On the other hand, the level of transcripts in immature and senescent cluster roots was comparable and not significantly different from the control (root apices of P-sufficient plants).

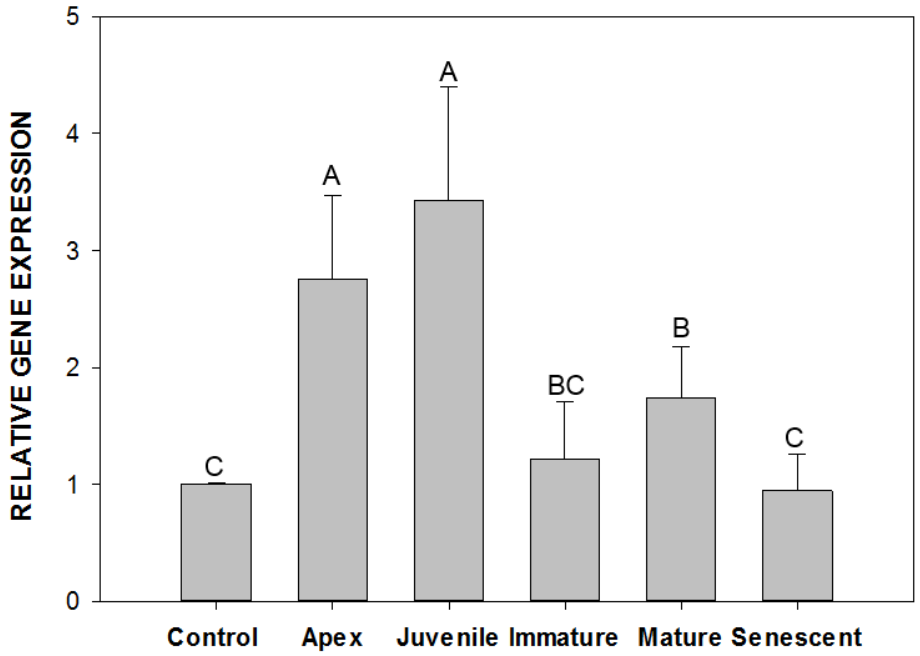

Figure 5.2 - *LaMATE2* expression analyses in root tissues of control and P-deficient plants. Data are means+SD of three independent experiments (capital letters refer to statistically significant differences among the means, ANOVA Holm–Sidak, N=3, P <0.05).

5.3.3 Transient expression of LaMATE2/GFP fusion protein in Arabidopsis protoplasts

To examine the subcellular localization of the transporter, C-terminal fusion protein of LaMATE2 and GFP (Green Fluorescent Protein) was transiently expressed in mesophyll *Arabidopsis thaliana* protoplasts (Fig. 5.3). *Arabidopsis* protoplasts were also co-transformed with AtPIP2a-mCherry fluorescence, a plasma membrane marker. In the figure 5.3, the signal of LaMATE2/GFP protein co-localized with the plasma membrane marker (Fig. 5.3C). In the panel A and B, the localization of LaMATE2/GFP and AtPIP2a-mCherry, respectively, are shown independently.

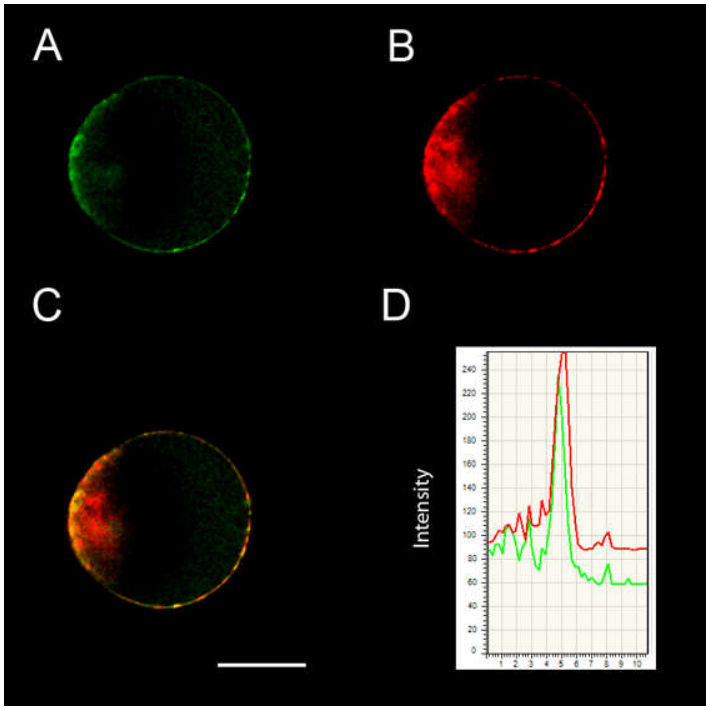

Figure 5.3 - Localization of LaMATE2. Transient expression in Arabidopsis mesophyll protoplasts of GFP fused in frame to the C-terminus of LaMATE2orf. A) GFP signal of LaMATE2orf-GFP, B) Plasma membrane marker AtPIP2a-mCherry signal, C) Overlay image of LaMATE2orf-GFP and AtPIP2a-mCherry fluorescence. Bars = 20 µm and D) Fluorescence intensity over distance plot of LaMATE2orf-GFP (green) and AtPIP2a-mCherry (red).

5.3.4 Agrobacterium-rhizogenes-mediated root transformation in white lupine using the pRedRoot binary vector

To investigate if LaMATE2 was putatively involved in genistein release an RNA-interference approach was used. The infection with *Agrobacterium rhizogenes* (Supplementary Figure 1) induced strong modifications of the root morphology; these changes were occurring with all the constructs, including the empty vector, indicating that they are not related to the gene of interest. Realtime RT-PCRs were performed on the root tissues corresponding to the juvenile and immature (Supplementary Figure 1) stages of cluster roots. Figure 5.4 shows that the *LaMATE2* expression was decreased in plants transformed with pRedRoot(pRR)::*LaMATE2* in comparison with the control plants transformed with the pRR empty vector. For control plants, data are referred to the average of *LaMATE2* expression in juvenile cluster roots of three independently transformed plants with the empty pRR vector. On the contrary, for the pRR::*LaMATE2*

transformations the three independently transformed plants are shown separately. Results show that the silencing reduced the expression of *LaMATE2* gene by 60-80% in juvenile cluster roots.

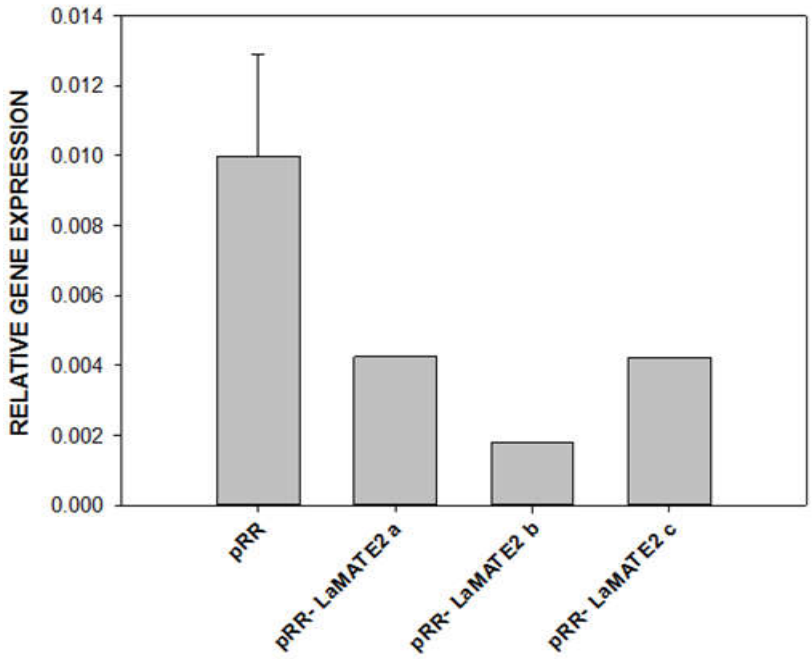

Figure 5.4 - *LaMATE2* expression analyses in roots of A. rhizogenes-transformed white lupinee plants. Control roots were transformed with the empty pRedRoot vector and the data are referred to the average of three independent plant transformation. LaMATE2 transcript levels of four 6-week-old White Lupine root cultures independently transformed with pRR-LaMATE2.

In parallel, the release of genistein was evaluated from the same tissues. In the three independent silenced plants, the release of this flavonoid dropped down to approximately 40-50% of the control (Fig. 5.5).

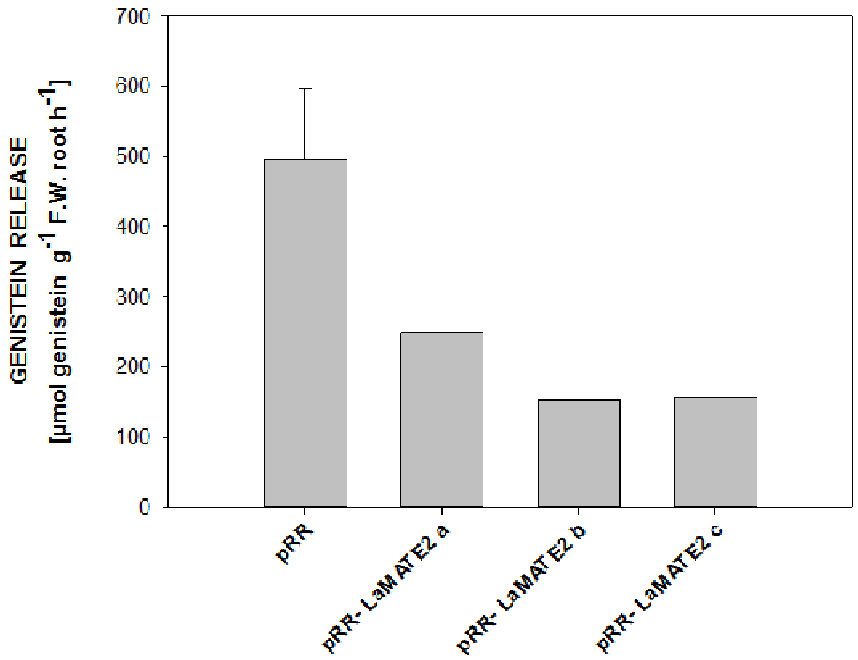

Figure 5.5 - Genistein release from roots of A. rhizogenes-transformed white lupine plants. Control roots were transformed with the empty pRedRoot vector meanwhile the other data are referred to three independently transformed plants with pRR-LaMATE2.

5.3.5 LaMATE2 mediates flavonoid transport in yeast vesicles

In order to biochemically characterize the transport activity of LaMATE2, the full length cDNA of *LaMATE2* was cloned in an yeast expression vector. *Saccharomyces cerevisiae* was transformed either with the pNEV empty vector or with the pNEV::*LaMATE2*$_{ORF}$ constructs and the microsomal fraction of yeast vesicles was isolated. The experiment was performed in presence of ^{3}H-genistein, and the flavonoid accumulation in the transformed yeast vesicles was detected at four different time points. Figure 5.6 shows that the accumulation of ^{3}H-genistein was 35% higher in microsomes transformed with pNEV::*LaMATE2*$_{ORF}$ compared to the pNEV empty vector. The ^{3}H-genistein accumulation in pNEV::*LaMATE2*$_{ORF}$ vesicles in presence of the transmembrane proton gradient uncoupler (NH_4Cl) was further decreased than in the control.

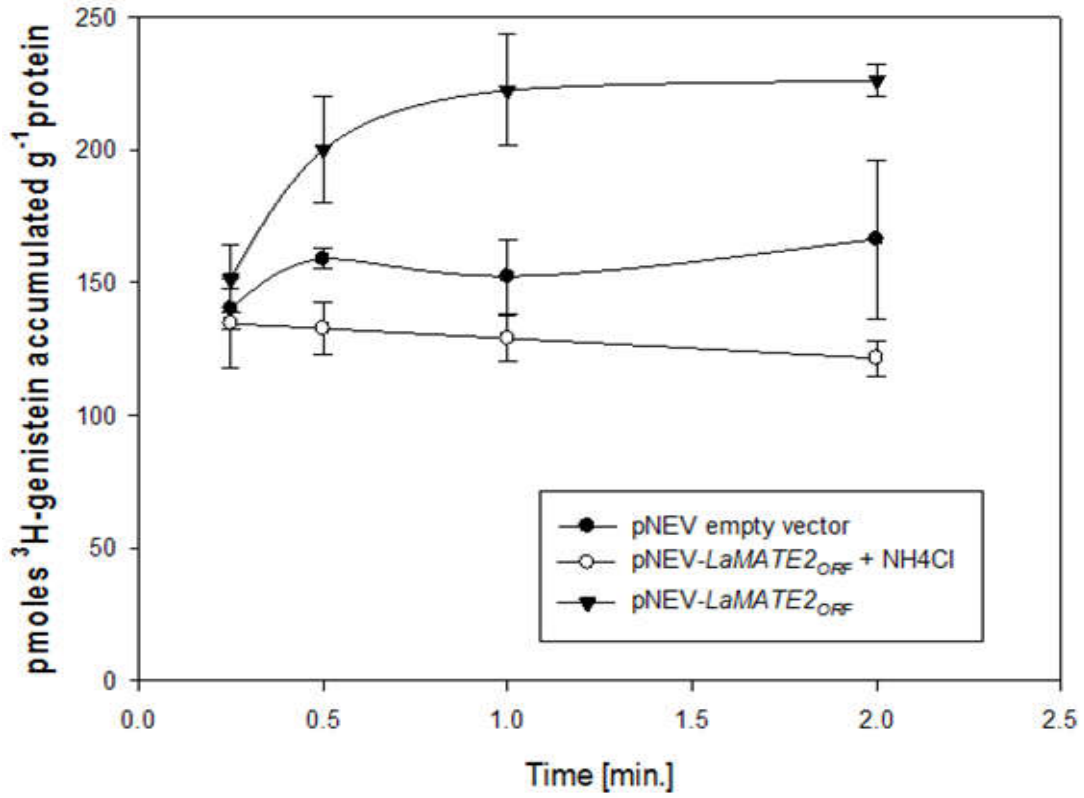

Figure 5.6 - Time-dependent uptake of 3H-genistein into vesicles isolated from yeasts transformed either with pNEV-LaMATE2 or the empty vector (pNEV) in presence or absence of NH4Cl.

In order to investigate the substrate specificity of the LaMATE2 transporter, the genistein accumulation assay was also performed in presence of different flavonoids or glycosylated flavonoids added at the same concentration of ^{3}H-genistein to pNEV::*LaMATE2*$_{ORF}$ transformed yeast vesicles (Fig. 5.7). Results showed that ^{3}H-genistein uptake was considerably reduced in presence of diadzedin and kampferol (60% and 80% respectively). In presence of the glycosylated flavonoids genistin and quercitin the accumulation was decreased by 35% and 20%, respectively.

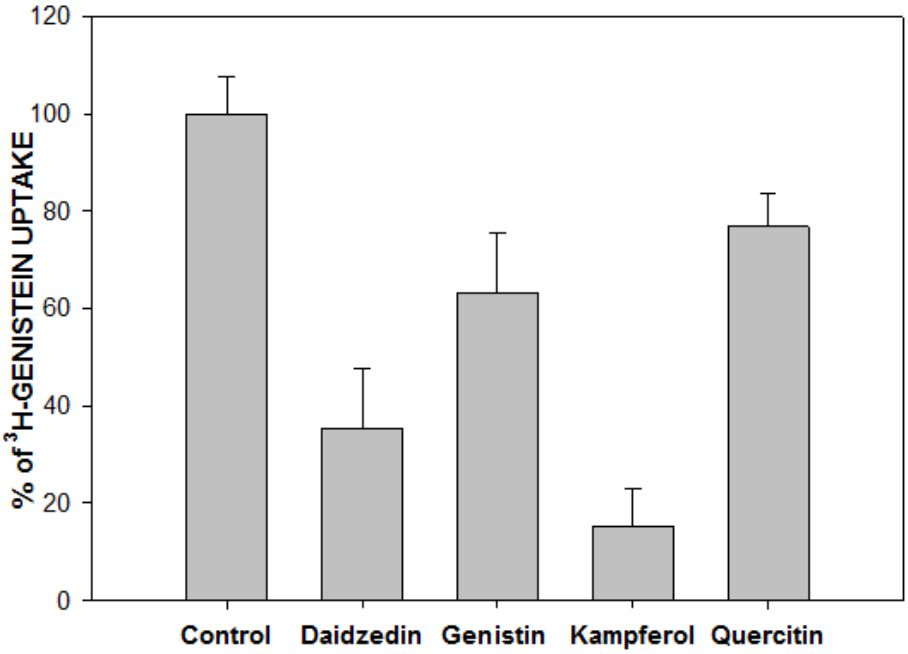

Figure 5.7 - Competition assay. ^{3}H-genitein uptake was measured in LaMATE2 vesicles in the presence of equimolar concentration of ^{3}H-genitein with or without another flavonoid (5 µM; daidzedin, glycosylated-genistein (genistin), kampferol, quercetin). The amount of accumulated ^{3}H-genitein was relativized to the control (absence of any other flavonoid.

5.4 Discussion

Phosphorus deficient white lupine plants induce the release of isoflavonoids from their roots, in particular from the structure called cluster roots (Weisskopf et al., 2006b). The main exudate released is genistein and, in much lower amount, some malonated glycoside genistein. These exudates have been shown to parallel the abundant release of citrate, possibly providing a mean to reduce the soil microbial degradation of the carboxylates thus favoring mobilization of both iron and phosphate (Weisskopf et al., 2006a; Tomasi et al., 2008; Cesco et al., 2010).

The root content of genistein within roots of P-deficient and P-sufficient plants or within different root tissues was essentially similar, even if the amount released by the different tissues was very different (Weisskopf et al., 2006b). This uncoupling between the root content and the amount released has been also observed for carboxylates (Neumann et al., 2000). These observations highlight the central role of mechanisms involved in the release of root exudates and/or the regulation of this process in determining the root exudate composition and amount.

In order to uncover this mechanism, candidate genes encoding for transporters were searched. In particular white lupine proteins that exhibited a high homology with fully characterized flavonoids transporters, AtTT12 and MtMATE2 (Marinova et al., 2007; Zhao et al., 2011) were considered. A match was found in the sequence of a partial cDNA isolated from juvenile cluster roots when compared to mature and senescent ones via an AFLP approach (Massonneau et al., 2001). The full-length sequence was recovered, named LaMATE2 and deposited in a database (XXX). The expression level of this gene exhibited a pattern of modulation, which followed the genistein release from the root tissues of P-sufficient and P-deficient white lupine plants (Figure 5.1 and 5.2). This associated higher release of genistein and higher amounts of LaMATE2 transcripts in root tissues, particularly apices and juvenile cluster roots, of P-deficient plants in comparison to older tissues or roots from P-sufficient plants and its similarity to characterized flavonoid transporters made LaMATE2 a strong candidate for the transport of this kind of compounds in white lupine roots.

Therefore to check its involvement in the root release of genistein a transient silencing approach was used to knockdown the *LaMATE2* expression. This approach has been chosen for the impossibility to obtain a white lupine knockout mutant and the availability of a method suitable for this kind of study (Uhde-Stone et al., 2005). The transformation with the *Agrobacterium rhizogenes*, independently of the construct, induced a strong morphological change of the whole

root structure (Supplementary Figure 1). The whole root of the transformed plants looked like to be completely covered by a cluster root-like structure. Comparing with the corresponding tissues of a plant transformed with an empty vector, the silencing reduced the expression level of *LaMATE2* transcript by 60-80 % in juvenile-like cluster root tissues (Fig. 5.4). From the same tissues, the release of genistein dropped down by 50-60 % compared to the control level. These results demonstrated that LaMATE2 is involved in the release of genistein from roots of white lupine plants. However to clarify the role of this protein, its localization has been determined, since some of its previously described homologues are tonoplastic transporters (Marinova *et al.*, 2007; Zhao et al., 2011). Figure 5.3 shows that LaMATE2 fused with GFP co-localized with the plasmalemma marker (AtPIP2a-mCherry) when expressed in *Arabidopsis* mesophyll cells. Hence LaMATE2 is not involved in the vacuolar storage or in the internal trafficking but in the transport in or out of the cells.

Finally to evaluate the transport activity of LaMATE2 transporter, this protein was expressed in yeast. Using isolated inside-out vesicles, the accumulation of radiolabeled genistein was tested in different conditions. Compared to the vesicles of empty-vector transformed yeast, those expressing LaMATE2 exhibited a higher capability to accumulate genistein inside the vesicles (Fig. 5.4). As MATE proteins in plants are described to co-transport their substrate using the energy supplied by the transmembrane proton or sodium gradient (Tanaka et al., 2013), the transport activity of LaMATE2 was also evaluated after the disruption of the transmembrane proton gradient. Results showed that without the pH gradient the genistein transport activity was greatly inhibited, demonstrating proton gradient dependence of the genistein transport activity (Fig. 5.5). Finally many characterized MATE transporters can exhibit a broad range of substrate affinity (Takanashi et al., 2014). In this work, some other flavonoids and a glycosidated genistein (genistin) have been tested. All these molecules competed with the genistein transport activity dependent on LaMATE2 protein, demonstrating the broad range affinity of this transporter. However considering the root content and root exudate composition of white lupine plants (Weisskopf et al., 2006b; Cesco et al., 2010), LaMATE2, at least in roots of P-deficient white lupine, should enter mostly in contact with genistein and diverse derivated forms (hydroxides, glycosides and/or malonated) (Weisskopf et al., 2006b).

In conclusion, this work functionally characterized the first known transporter involved in the release of flavonoids from roots. LaMATE2 protein is able to transport some free- and glycosilated- flavonoids through the plasma membrane, via a secondary active co-transport of H^+. The results of the RNA interfering approach and the present knowledge on the composition of root content and exudates of white lupine plants, strongly suggest that LaMATE2 is mainly responsible of the root release of genistein and its derivates into the rhizosphere.

5.5 Supplementary Material

Supplementary Figure 1 – Comparison between the root systems of white lupine plants grown under P-deficiency (A) and white lupine plants transformed with pRedRoot(pRR)::*LaMATE2* (B).

5.6 References

Baetz U, Martinoia E. (2014). Root exudates: the hidden part of plant defense. Trends in Plant Science 19: 90-98.

Bieleski RL. (1973). Phosphate Pools, Phosphate Transport, and Phosphate Availability. Annual Review of Plant Physiology 24: 225-252.

Cesco S, Neumann G, Tomasi N, Pinton R, Weisskopf L. (2010). Release of plant-borne flavonoids into the rhizosphere and their role in plant nutrition. Plant and Soil 329: 1-25.

Dinkelaker B, Römheld V, Marschner H. (1989). Citric acid excretion and precipitation of calcium citrate in the rhizosphere of white lupine (Lupinus albus L.). Plant Cell and Environment 12: 285-292.

Fourcroy P, Siso-Terraza P, Sudre D, Saviron M, Reyt G, Gaymard F, Abadia A, Abadia J, Alvarez-Fernandez A, Briat JF. (2013). Involvement of the ABCG37 transporter in secretion of scopoletin and derivatives by Arabidopsis roots in response to iron deficiency. New Phytologist: 201: 155-67.

Gietz RD, Woods RA. (2002). Transformation of yeast by lithium acetate/single-stranded carrier DNA/polyethylene glycol method. Methods in enzymology 350: 87-96.

Jin JB, Kim YA, Kim SJ, Lee SH, Kim DH, Cheong G-W, Hwang I. (2001). A new dynamin-like protein, ADL6, is involved in trafficking from the trans-Golgi network to the central vacuole in Arabidopsis. Plant Cell 13: 1511–1526

Klein M, Mamnun YM, Eggmann T, Schüller C, Wolfger H, Martinoia E, Kuchler K. (2002). The ATP-binding cassette (ABC) transporter Bpt1p mediates vacuolar sequestration of glutathione conjugates in yeast. Febs Letters 520: 63-67.

Kochian LV, Piñeros MA, Liu J, Magalhaes JV. (2015). Plant Adaptation to Acid Soils: The Molecular Basis for Crop Aluminum Resistance. Annual Review of Plant Biology 66: 571-598.

Komarova, Y.A., I.A. Vorobjev, and G.G. Borisy. (2002). Life cycle of MTs: persistent growth in the cell interior, asymmetric transition frequencies and effects of the cell boundary. J. Cell Sci. 115: 3527–3539.

Koressaar T, Remm M. (2007). Enhancements and modifications of primer design program Primer3. Bioinformatics 23: 1289-1291.

Lambers H, Martinoia E, Renton M. (2015). Plant adaptations to severely phosphorus-impoverished soils. Current Opinion in Plant Biology 25: 23-31.

Livak KJ, Schmittgen TD. (2001). Analysis of Relative Gene Expression Data Using Real-Time Quantitative PCR and the 2−ΔΔCT Method. Methods 25: 402-408.

Marinova K, Kleinschmidt K, Weissenbock G, Klein M. (2007). Flavonoid Biosynthesis in Barley Primary Leaves Requires the Presence of the Vacuole and Controls the Activity of Vacuolar Flavonoid Transport. Plant Physiology 144: 432-444.

Marschner P.(2012). Marschner's Mineral Nutrition of Higher Plants. Waltham.

Massonneau A, Langlade N, Leon S, Smutny J, Vogt E, Neumann G, Martinoia E. (2001). Metabolic changes associated with cluster root development in white lupine (*Lupinus albus* L.): relationship between organic acid excretion, sucrose metabolism and energy status. Planta 213: 534-542.

Nelson BK, Cai X, Nebenführ A. (2007). A multicolored set of in vivo organelle markers for co-localization studies in Arabidopsis and other plants. The Plant Journal 51: 1126-1136.

Neumann G, Massonneau A, Langlade N, Dinkelaker B, Hengeler C, Römheld V, Martinoia E. (2000). Physiological aspect of cluster root function and development in phosphorus-deficient White Lupine (*Lupinus albus* L.). Annals of Botany 85:909-919.

Neumann G, Massonneau A, Martinoia E, Römheld V. (1999). Physiological adaptations to phosphorus deficiency during proteoid root development in white lupine. Planta 208:373-382.

Pii Y, Mimmo T, Tomasi N, Terzano R, Cesco S, Crecchio C. (2015). Microbial interactions in the rhizosphere: beneficial influences of plant growth-promoting rhizobacteria on nutrient acquisition process. A review. Biology and Fertility of Soils 51:403-415.

Purnell HM. (1960). Studies of the family Proteaceae. Anatomy and morphology of the roots of some Victorian species. Australian Journal of Botany 8:38-50.

Quandt HJ, Pühler A, Broer I. Transgenic root-nodules of Vicia hirsuta - a fast and efficient system for the study of gene-expression in indeterminate-type nodules. MPMI-Molecular Plant Microbe Interactions 6:17.

Raghothama K, Karthikeyan A. (2005). Phosphate Acquisition. Plant and Soil 274:37-49.

Rodriguez-Celma J, Lin WD, Fu GM, Abadia J, Lopez-Millan AF, Schmidt W. (2013). Mutually Exclusive Alterations in Secondary Metabolism Are Critical for the Uptake of Insoluble Iron Compounds by Arabidopsis and Medicago truncatula. Plant Physiology 162:1473-1485.

Sauer N, Stolz J. (1994). SUC1 and SUC2: two sucrose transporters from Arabidopsis thaliana; expression and characterization in baker's yeast and identification of the histidine-tagged protein. The Plant Journal 6:67-77.

Schachtman DP, Reid RJ, Ayling SM. (1998). Phosphorus uptake by plants: from soil to cell. Plant Physiology 116:447-453.

Takanashi K, Shitan N, Yazaki K. (2014). The multidrug and toxic compound extrusion (MATE) family in plants. Plant Biotechnology 31:417-430.

Tanaka Y, Hipolito CJ, Maturana AD, Ito K, Kuroda T, Higuchi T, Katoh T, Kato HE, Hattori M, Kumazaki K, Tsukazaki T, Ishitani R, Suga H, Nureki O. (2013). Structural basis for the drug extrusion mechanism by a MATE multidrug transporter. Nature 496:247-251.

Tomasi N, Weisskopf L, Renella G, Landi L, Pinton R, Varanini Z, Nannipieri P, Torrent J, Martinoia E, Cesco S. (2008). Flavonoids of white lupine roots participate in phosphorus mobilization from soil. Soil Biology and Biochemistry 40:1971-1974.

Tommasini R, Evers R, Vogt E, Mornet C, Zaman G, Schinkel AH, Borst P, Martinoia E. (1996). The human multidrug resistance-associated protein functionally complements the yeast cadmium resistance factor 1. Proceedings of the National Academy of Sciences 93:6743-6748.

Uhde-Stone C, Liu J, Zinn KE, Allan DL, Vance CP. (2005). Transgenic proteoid roots of white lupine: a vehicle for characterizing and silencing root genes involved in adaptation to P stress. Plant Journal 44:840-853.

Untergasser A, Cutcutache I, Koressaar T, Ye J, Faircloth BC, Remm M, Rozen SG. (2012). Primer3—new capabilities and interfaces. Nucleic Acids Research 40:e115.

Weisskopf L, Abou-Mansour E, Fromin N, Tomasi N, Santelia D, Edelkott I, Neumann G, Aragno M, Tabacchi R, Martinoia E. (2006a). White lupine has developed a complex strategy to limit microbial degradation of secreted citrate required for phosphate acquisition. Plant Cell and Environment 29:919-927.

Weisskopf L, Tomasi N, Santelia D, Martinoia E, Langlade NB, Tabacchi R, Abou-Mansour E. (2006b). Isoflavonoid exudation from white lupine roots is influenced by phosphate supply, root type and cluster-root stage. New Phytologist 171:657-668.

Weston LA, Ryan PR, Watt M. (2012). Mechanisms for cellular transport and release of allelochemicals from plant roots into the rhizosphere. Journal of Experimental Botany.

Zhao J, Huhman D, Shadle G, He X-Z, Sumner LW, Tang Y, Dixon RA. (2011). MATE2 Mediates Vacuolar Sequestration of Flavonoid Glycosides and Glycoside Malonates in Medicago truncatula. The Plant Cell 23:1536-1555.

6. EXUDATION PATTERN AND TRANSCRIPTOME PROFILING OF PHOSPHORUS AND IRON DEFICIENT APPLE TREE ROOTS

Exudation pattern and transcriptome profiling of phosphorus and iron deficient apple tree roots

Fabio Valentinuzzi[1], Silvia Venuti[2] Youry Pii[1], Laura Zanin[2], Roberto Pinton[2], Fabio Marroni[2], Michele Morgante[2], Stefano Cesco[1], Nicola Tomasi[2], Tanja Mimmo[1]

[1]Faculty of Science and Technology, Free University of Bozen-Bolzano, Piazza Università 5, 39100 Bolzano, Italy

[2]Dipartimento di Scienze Agrarie e Ambientali, University of Udine, Via delle Scienze 208, 33100 Udine, Italy

Abstract

Iron (Fe) and phosphorus (P) are two of the essential nutrients, which are fundamental to ensure the optimal growth and high quality yields of plants. Even though the total content of these elements is high usually in many soils, the plant available fraction is very often below plants requirements. In addition, in alkaline soils with high carbonate levels, P and Fe deficiency very often coexist. The low availability of these two nutrients represents a major constraint for fruit tree cultivation such as apple (*Malus x domestica* Borkh.) leading very often to a decrease of fruit productivity and quality worsening. The release of inorganic and organic substances by plant roots is one of the strategies adopted by plants to overcome nutrient deficiencies. The aim of this study was thus to characterize the exudation pattern of *Malus x domestica* Borkh. grown either in a full nutrient, phosphorus (P) and iron (Fe) deficient solution. In addition, a transcriptomic approach, using RNA-seq technique was undertaken to evaluate the differential gene expression in the three growing conditions and to unravel the molecular entities involved in physiological responses of apple tree plants toward nutrients starvation. The analysis of root exudates showed that Fe and P shortage affected the release of C and N. However, the qualitative analysis determined a high release of phenols and flavonoids in particular in control and P deficient plants and highlighted the presence of oxalic acid in all the treatments that has never been observed before in apple exudates. RNA-seq results revealed the differential expression of 397 genes in Fe and P deficiency. Comparing Fe deficient and control plants 254 genes were differentially expressed, being 44 upregulated and 210 downregulated, while in P-deficient plants, compared to control samples, 143 genes resulted differentially expressed, being 105 of them upregulated and 38 downregulated. Besides this, it was also highlighted that the lack of the

two essential nutrients affected different metabolic pathways, thus suggesting that apple tree plants might adopt different strategies to cope with the two nutritional disorders. These results, which for the first time determined the root exudates released by apple trees and the metabolic pathways involved in the response to Fe and P shortage, will be of help for a deep understanding of the mechanisms carried out by woody plants to overcome low nutrient availability conditions.

6.1 Introduction

Iron (Fe) and phosphorus (P) are essential nutrients for plant growth, crop productivity and crop quality. In most soils, even though their total content is high, the plant available fraction is very often below the one required by plants for optimal growth. In alkaline soils with high carbonate levels P and Fe deficiency very often coexist. Considering that calcareous soils account for one-third of the earth's surface (Hansen et al. 2006) the main constraints for successful cultivation of fruit tree crops as apples are represented by the low availability of these two nutrients. Yield and quality loss are very often prevented by the application of organic or mineral fertilizers or in the case of Fe of synthetic chelates. In the short term this might represent a valuable option. However, both P and Fe deficiencies are difficult to correct since, especially in calcareous soils, the nutrients applied as fertilizers are quickly transformed into unavailable forms promoting retrogradation instead of solubilization processes. These agronomic practices should therefore be avoided considering both environmental and economic aspects.

Plant nutrient availability and thus the nutrient uptake is yet controlled by many plant factors. The nutrient use efficiency depends in fact strictly on the plant species and genotypes even if plants are grown in the same conditions. Plants have evolved different strategies to cope with nutrient shortage that include the release of inorganic (protons) and organic (organic acids, phenolic compounds, phytosiderophores) substances able, by acidifying the rhizosphere and reduction-complexation processes, to increase the availability of barely available P and Fe pools in soil (Mimmo et al. 2014). In addition, plants can also increase the spatial availability of nutrients increasing their root surface by either stimulating the growth of fine roots and root hairs or by enhancing mycorrhizal colonization (Neumann & Römheld 2011). In particular, concerning Fe, plants have evolved two strategies (*Strategy I* in nongraminaceous plants and *Strategy II* in graminaceous plants) to efficiently mobilize and take up Fe from soil. *Malus spp.* adopts the *Strategy I* response which relies on the increase in Fe solubility by rhizosphere

acidification and release of complexing and reducing compounds. Iron (III) is consequently reduced at the root surface and taken up by specific transporters (Marschner & Römheld 1994). Therefore, to cope with Fe and P-limiting stress it is crucial to understand the mechanisms underlying their use efficiency and the mechanisms operating that plants exploit to overcome the problem. The molecular characterization of the genes involved in nutrient mobilization and uptake has become an ever more urgent task, because of the availability of both the complete genome sequences of model and agronomic plants, and the so-called "OMICS" tools (e.g. transcriptomics, proteomics, metabolomics and ionomics). At molecular level, plant responses to nutrients deficiencies have been recently analyzed on the basis of large-scale changes in the transcriptome (Thimm et al. 2001; O'Rourke et al. 2009), proteome (Brumbarova et al. 2008; Li et al. 2008; Rellán-Álvarez et al. 2010; Donnini et al. 2010; Lan et al. 2011; Rodríguez-Celma et al. 2011) and metabolome (Rellán-Álvarez et al. 2010); however, the molecular mechanisms involved in Fe and P deficiency have been widely studied mainly in model plant species (i.e. herbaceous plants). Little research has been done on fruit tree crops as apple plants. Therefore, in this study we aimed at characterizing the exudation pattern of *Malus x domestica* Borkh. grown under control conditions and phosphorus (P) and iron (Fe) deficiency. In addition, in this work a differential gene expression analysis based on the RNA-seq technique has been undertaken. The M9 apple rootstock, grown in either Fe or P deficiency, was chosen as model to better understand the strategies exploited by this nutrients-efficient genotype to cope with nutrients shortage at the molecular level. The analysis revealed the existence of a core set of genes that are commonly regulated to counteract both Fe and P deficiency. Besides this, it was also highlighted that the lack of the two essential nutrients affected different metabolic pathways, thus suggesting peculiarity in the metabolic reprogramming of cells.

6.2 Materials and methods

6.2.1 Plant growth

Apple rootstocks *(Malus x domestica,* Borkh.*,* M9) were pre-grown in sand, then transferred and grown in hydroponic conditions in an aerated nutrient solution with the following composition: KH_2PO_4 0.25 mM, $Ca(NO_3)_2$ 5 mM, $MgSO_4$, 1.25 mM, K_2SO_4 1.75 mM, KCl 0.25 mM, Fe(III)NaEDTA 20 µM, H_3BO_4 25 µM, $MnSO_4$ 1.25 µM, $ZnSO_4$ 1.5 µM, $CuSO_4$ 0.5 µM, $(NH_4)_6Mo_7O_{24}$ 0.025 µM. Plants were grown in individual black pots and nutrient solutions were

prepared using distilled water at 5.5 μS/m (all nutrients <limit of quantification (LOQ)). Apple trees were either grown in a full nutrient solution (control), either in a zero Fe solution (-Fe), either in a zero P (-P) nutrient solution. Four apple trees were used for each treatment. The nutrient solution in the pots was renewed twice a week. Plants were grown in a growth chamber under controlled conditions (day 14h 24°C 70% RH, night 10h 19°C 70% RH).

6.2.2 Characterization of plant growth

Plants were harvested separating roots and shoots and Fresh weight (FW) of roots and shoots together with the root to shoot ratio were assessed. Light transmittance of fully expanded leaves was determined using a portable chlorophyll meter SPAD-502 (Minolta, Osaka, Japan) and presented as SPAD index values. Measurements were carried out weekly on young leaves (at least 2 per plant) and five SPAD measurements were taken per leaf and averaged.

6.2.3 Collection of root exudates

Apple root exudates were collected weekly for three weeks (at day 35, 42 and 49 after transferring the plants to the hydroponic solution – DAT) after the first appearance of nutrient deficiency symptoms at the leaf level. Plants were removed from the nutrient solutions and roots where washed several times with distilled water in order to remove any traces of nutrient solution. Plants were then transferred in smaller pots containing 250 mL of water. Root exudates were collected for 24 hours continuously aerating the solution and covering the pots with aluminium foil to maintain the roots in the dark. After 24h plants were removed and transferred to pots with fresh nutrient solution. Root exudate solutions were filtered at 0.45 μm (Spartan RC, Whatman), frozen at -20°C, lyophilized and resuspended in ultrapure distilled water.

6.2.4 Organic acid analysis

Organic acids were separated by high performance liquid chromatography (HPLC) using a cation exchange column (Phenomenex - Rezex ROA), with an isocratic elution with 10 mM H_2SO_4 as carrier solution at a flow rate of 0.6 mL min^{-1}. Organic acids were detected at 210 nm using a Waters Photodiode array detector (PDA 2998 Waters Spa, Italy).

6.2.5 Total phenols and flavonoids analysis

Total phenols concentration in root exudates was determined colorimetrically using the Folin Ciocalteau assay as described by (LOWRY et al. 1951). Total flavonoid concentration was determined colorimetrically as described by Atanassova et al. 2011.

6.2.6 Elemental analysis

Oven-dried samples (60°C) of shoots and roots were acid digested with concentrated ultrapure HNO_3 (650 mL L^{-1}; Carlo Erba, Milano, Italy) using a single reaction chamber (SRC) microwave digestion system (UltraWAVE, Milestone, Shelton, CT, USA). Iron, P, Cu, Zn and Ca concentrations were then determined by ICP-OES (Spectro CirosCCD, Spectro, Germany).
Total organic carbon (TOC) and total nitrogen (TN) was determined using a Flash EA 1112 elemental analyzer (Thermo Scientific, Germany).

6.2.7 RNA extraction, cDNA library preparation and sequencing

Total RNA was extracted from three biological replicates of 12 root samples (Control, Pi and Fe deficient plants) using the Spectrum™ Plant Total RNA Kit (Sigma Aldrich). RNA samples were quantified using *Qubit*™ 2.0 Fluorometer (Life Technology), and RNA integrity was checked with the RNA6000 Nano Assay using the Agilent 2100 Bioanalyzer (Agilent Technologies). cDNA library preparation and sequencing reactions were performed by IGA Technology Services s.r.l. (Udine, Italy). An amount of 2 µg of total RNA was used for library preparation following the Illumina protocol TrueSeq 2.0. Briefly, RNA was fragmented into fragment with an average of 500 pb. mRNA was purified using poly T beads. The first- and second-strand cDNAs were synthesized and end repaired. Adaptors were ligated after adenylation at the 3' ends and cDNA templates were enriched by PCR. The 50 bp single end reads were obtained using an Illumina Hiseq2000 platform.

6.2.8 Sequence processing

Adapters were removed using cutadapt (http://code.google.com/p/cutadapt/) (Martin., 2011)and the reads were trimmed for quality with ERNE-FILTER (http://erne.sourceforge.net). Alignment against the genome of *M. x domestica* (http://genomics.research.iasma.it/) using the transcriptome of *M. x domestica* (reference v.1.0, including 63541 annotated genes) as a guide for transcript assembly was performed with TopHat version 2.0.5 (Kim et al.,2013) with default parameters. Transcript expression was estimated using cufflinks (Trapnell et al, 2010), and

differential expression evaluated using cuffdiff and differential expression evaluated using cuffdiff software (P-value ≤ 0.05, n=3 Trapnell et al 2012).Differentially expressed genes were then loaded on Blast2Go v. 2.5.1 (http://www.blast2go.com/b2glaunch) for Blastx and gene ontology analysis. Ontology annotations were then refined using InterPro Scan, ANNEX, GoSlim and KEGG (Kyoto Encyclopaedia of Genes and Genomes; http://www.genome.jp/kegg) functions of the Blast2Go platform.

6.2.9 Statistical analysis

The results are presented as means of at least three replicates ± standard error (SE). Statistical analysis was performed using Statgraphics (Statpoint technologies, INC., Warrenton, VA, USA). Data were analysed by analysis of variance (ANOVA), and means were compared using SNK's test at $p < 0.01$ to determine the significance of differences found.

6.3 Results and discussion

Worldwide fruits trees as apple are affected by nutritional disorders when cultivated on high pH and calcareous soils. Despite the natural high abundance of Fe and P in soil, their bioavailable concentration is very often below the plant requirement for optimal growth and productivity. The response to this abiotic stress depends however on the environmental conditions, the plant species and the plant genotype. In case of apple plants, the rootstock plays thereby a pivotal role. In Europe, M9, M26 and M26 are the most common rootstocks used for high density plantations. These "dwarfing" rootstock clones are used since they are known to be nutrient-efficient genotypes. For instance, in Fe deficiency they induce a series of physiological and morphological changes in the roots such as the formation of root hairs, transfer cells, acidification of the rhizosphere and an increased root ferric chelate reductase (FRO) activity (Wang et al., 2010).

In fact, the results of the present study showed that, at the physiological level, Fe and P shortage did not affect significantly the shoot and root biomass (Table 6.1). As expected, Fe deficiency caused a decrease in the leaf chlorophyll content expressed as SPAD index of approximately 20 units (Table 6.1).

Table 6.1 - Fresh weight and Shoot/root ratio of apple plants grown in a full nutrient (control), zero Fe (-Fe) and zero P (-P) solution; the SPAD values (ΔSPAD) calculated as difference between the values determined at harvest and day 7 are also shown; Legend; FW = fresh weight; mean ± SE.

	Control	-P	-Fe
FW root (g/plant)	7.41 ± 0.94	6.02 ± 0.62	7.81 ± 1.95
FW shoot (g/plant)	16.90 ± 2.72	12.71 ± 1.84	14.56 ± 1.63
Shoot/Root	2.28 ± 0.17	2.10 ± 0.13	1.91 ± 0.32
Δ SPAD	-3.90 ± 0.64	-0.38 ± 0.07	-22.12 ± 0.89

Table 6.2 shows the content of macro-and micronutrients determined in the shoots and roots of apple plants at harvest after 7 weeks. Results showed that roots of Fe deficient plants have a 4-fold lower content of the micronutrient compared to the other treatments. Even though these plants display the same Fe content in the leaves as the control, the translocation factor (defined as the ratio between the Fe concentration in roots and shoots) was severely reduced (2 vs. 11). The high Fe concentration determined in the roots of control plants could be ascribable to both symplastic and apoplastic pools. On the other hand, the roots of Fe starved plants were grown in a Fe-free nutrient solution and it can be hypothesized that the micronutrient belongs entirely to the symplastic fraction whereas the apoplastic fraction has already been mobilized to cope with Fe shortage. Several studies highlight that plants are able to synthesize phenols that act as Fe-ligands facilitating the reutilization of apoplastic Fe in roots (Jin et al., 2007). Moreover, these compounds can be increased or synthesized de novo, not only under Fe deficient conditions, but also as a response to other nutrient deficiencies.

Table 6.2 - Macro-and micronutrients of shoots and roots of apple trees at harvest grown in a full nutrient (control), zero Fe (-Fe) and zero P (-P) solution; DW = dry weight; mean ± SE (n=3).

	Control		-P		-Fe	
	Roots	Shoots	Roots	Shoots	Roots	Shoots
Fe (μg g^{-1} DW)	1871.73 ± 215.97	168.47 ± 4.65	2113.53 ± 289.67	186.28 ± 12.64	557.73 ± 21.17	191.25 ± 18.62
Cu (μg g^{-1} DW)	0.20± 0.031	0.026± 0.01	0.20 ± 0.01	0.026 ± 0.01	0.57 ± 0.08	0.029 ± 0.01
Zn (μg g^{-1} DW)	405.20 ± 17.67	61.27 ± 5.12	374.40 ± 23.601	73.49 ± 6.31	1345.47 ± 105.83	99.95 ± 2.04
Mn (μg g^{-1} DW)	788.26 ± 179.21	92.13 ± 4.28	539.73 ± 44.35	111.18 ± 9.29	1100.20 ± 191.04	127.35 ± 10.42
P (mg g^{-1} DW)	3.54 ± 0.18	6.18 ± 0.11	2.24 ± 0.12	3.81 ± 0.20	4.53 ± 0.49	10.73 ± 1.44
Ca (mg g^{-1} DW)	16.46 ± 0.91	30.73 ± 1.52	14.89 ± 0.58	27.21 ± 1.91	13.56 ± 0.30	61.27 ± 1.91
Mg (mg g^{-1} DW)	4.13 ± 0.06	7.12 ± 0.16	4.01 ± 0.16	7.65 ± 0.51	4.71 ± 0.42	9.37 ± 0.47
S (mg g^{-1} DW)	4.07 ± 0.21	3.16 ± 0.14	4.30 ± 0.27	3.74 ± 0.03	5.36 ± 0.73	4.78 ± 0.45
K (mg g^{-1} DW)	14.21 ± 0.09	4.48 ± 0.28	14.26 ± 0.07	14.98 ± 5.66	12.74 ± 1.11	10.26 ± 5.50

Two-way ANOVA results:

Fe, Cu, Zn, Ca, Mg, P: treatment (P<0.001), plant organ (P<0.001), treatment x plant organ (P=0.001);Mn: treatment (ns), plant organ (P<0.001), treatment x plant organ (P<0.001); S: treatment (P<0.01), plant organ (P<0.05), treatment x plant organ (P<0.05);K treatment (ns), plant organ (ns), treatment x plant organ (ns);ns = not significant.

Under these stressed conditions carbohydrates can be diverted into secondary metabolism to produce phenols (Donnini et al. 2012; Vigani et al. 2012; Tato et al. 2013).

In addition, as reported in literature (Pestana et al. 2012; Welch et al. 1993), Fe shortage increases the uptake of micronutrients as Cu, Zn and Mn (Table 6.2). Interestingly, also the root to shoot transfer of all the macronutrients analysed increased significantly.

Regarding P, as expected, its shortage caused a decrease in P content of roots and shoots and, concerning the micronutrient concentration in the shoots, showed a similar behaviour with respect to Fe shortage. Conversely, their concentrations decreased significantly in the roots compared to the control. Beside P as previously described, the concentrations of the macronutrients did not show any significant changes compared to the control both in shoots and roots. The only exception is represented by K that strongly increased in the shoots of P deficient plants. These interferences within the nutrient uptake and translocation might be explained by considering the different mechanisms that plants exploit to absorb ions. For instance, one of the mechanisms adopted by plants subjected to Fe and P stress is to acidify the rhizosphere soil. Thus, the increased positive charge at the root surface could allow cations to enter the cytoplasm via electrochemical gradient through channels and carriers (White, 2003).

The release of protons and low molecular weight organic compounds known as root exudates are one of the strategies adopted by plants to modulate nutrient availability (Fe, P, Zn; Dakora and Phillips 2002). Figure 6.1 shows the total concentration of carbon (C) and nitrogen (N) detected in the root exudates of apple roots at 35, 42 and 49 days after transferring the plants to the hydroponic solution (DAT). Carbon containing compounds might comprise organic acids, amino acids, phenolic compounds, sugars, vitamins, hormones, fatty acids and sterols, whereas nitrogen bearing compounds could encompass amino acids, amino sugars, enzymes and peptides (Mimmo et al. 2014). Iron and P shortage caused a reduction of C and N release most likely due to an impaired photosynthetic activity and/or interfered metabolism. However, the qualitative analysis highlighted the presence of oxalic acid (Figure 6.2) in all the treatments that has never been observed elsewhere. It is interesting to note that oxalic acid is part of the response mechanism of P deficient plants (Gerke et al. 2000) but could also be released from mycorrhizal fungi which are well known for their role in enhancing P uptake in host plants (Gnekow & Marschner 1989).

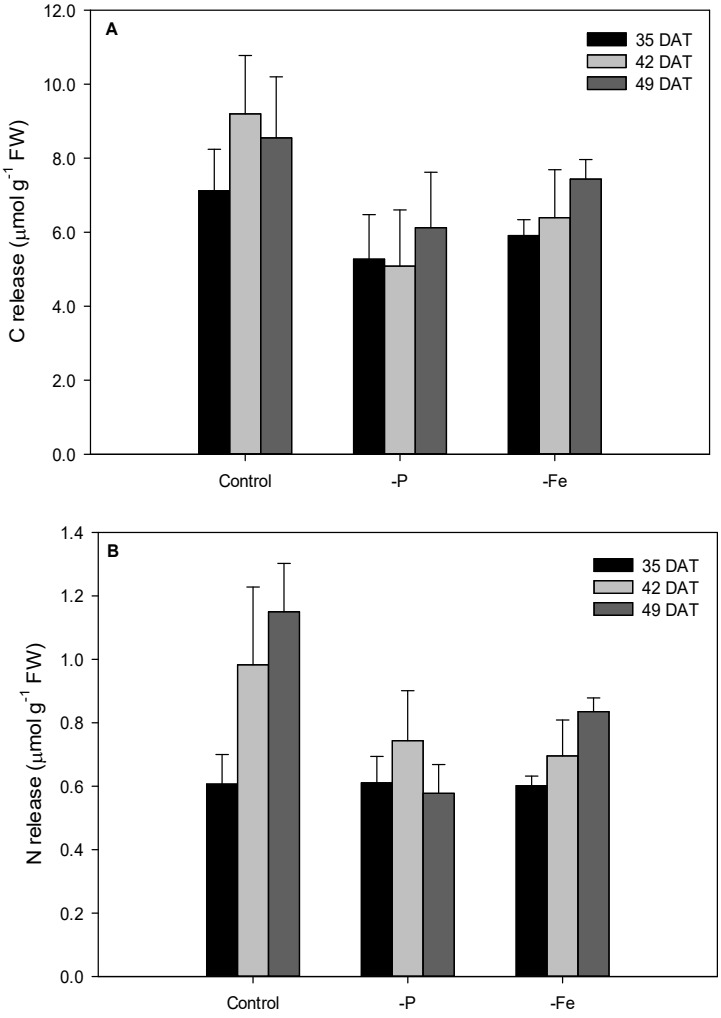

Figure 6.1 - Total carbon (A) and total nitrogen (B) released by apple roots grown in a full nutrient solution (control), phosphorus (-P) and iron-deficient (-Fe) solution at 35, 42 and 49 days after transferring the plants to the nutrient solution (DAT). Data are presented as means ± standard error (SE), n= x; Two-way ANOVA results: Carbon release: treatment ($P<0.05$), sampling time ($P<0.05$), treatment x sampling time (ns); Nitrogen release: treatment ($P<0.05$), sampling time ($P<0.05$), treatment x sampling time (ns); ns= not significant.

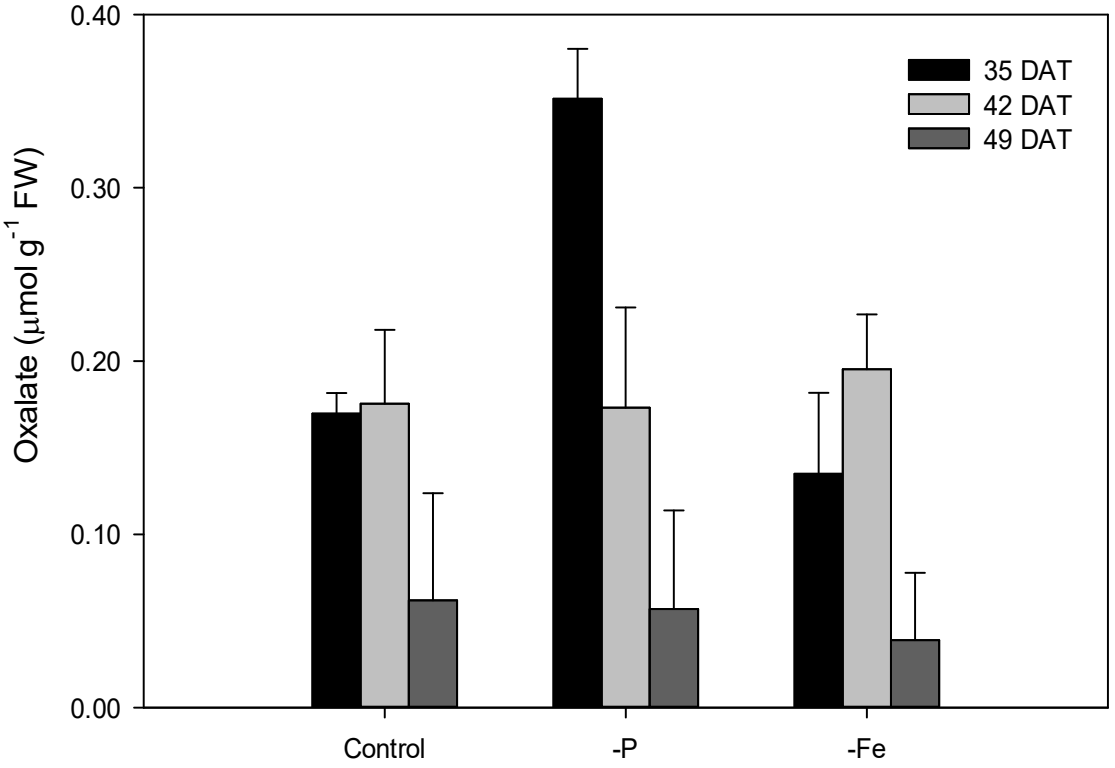

Figure 6.2 - Oxalate released by apple roots grown in a full nutrient solution (control), phosphorus (-P) and iron-deficient (-Fe) solution at 35, 42 and 49 days after transferring the plants to the nutrient solution (DAT). Data are presented as means ± standard error (SE), n= x; Two-way ANOVA results: treatment (P<0.001), sampling time (ns), treatment x sampling time (ns); ns= not significant.

Almost 50 % of the total carbon released is represented by phenolic compounds (Fig. 6.3A), which are commonly found in the exudates of *Malus* spp (Zhang et al. 2007). Flavonoids belong to the same compound class and were mainly released by control and P deficient plants, especially at 35 DAT (Fig. 6.3 B). In fact, it has been recently reviewed that flavonoids play a fundamental role in the nutrient cycling and availability for plants (Cesco et al. 2012).

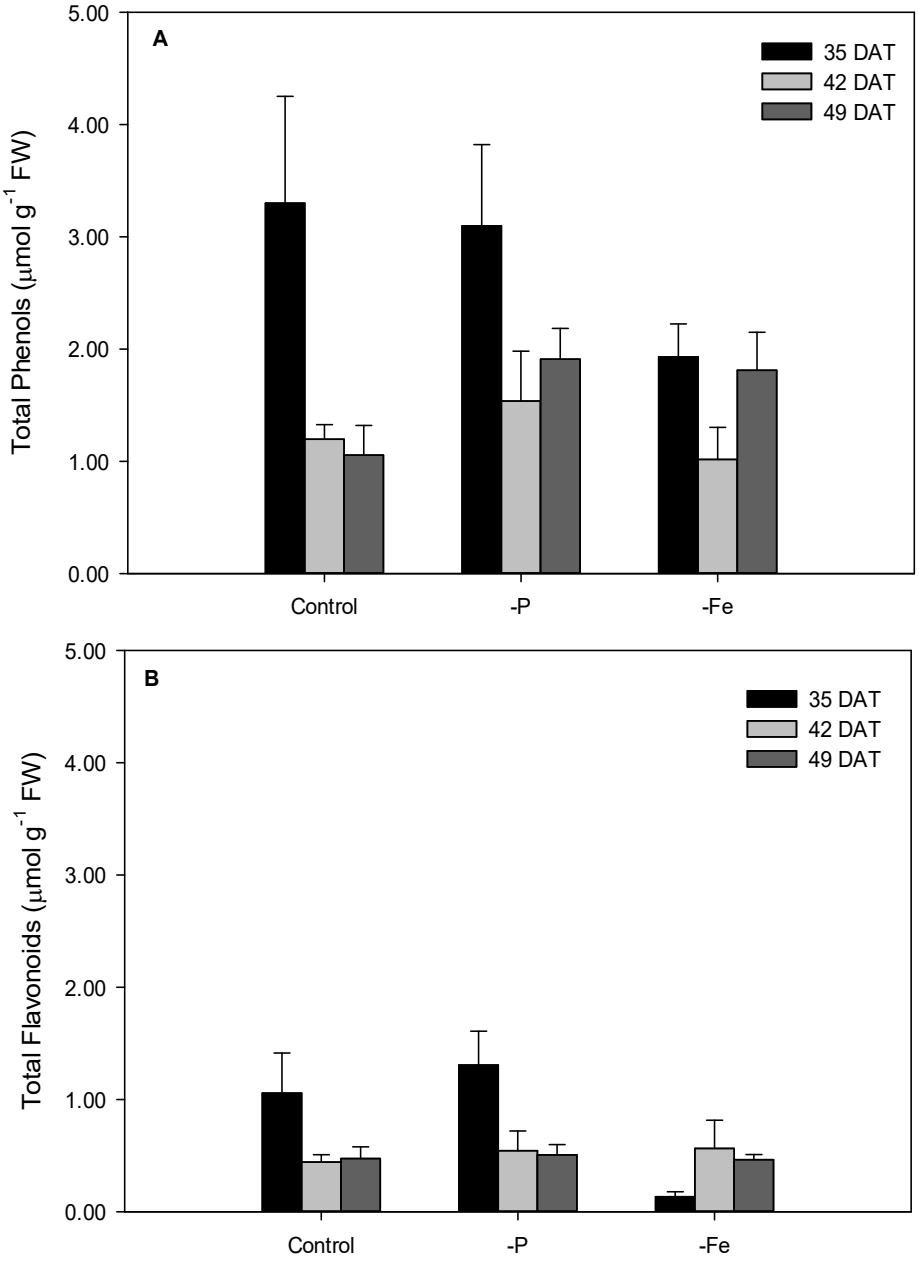

Figure 6.3 - Total phenols expressed as gallic acid equivalents (A) and total flavonoids expressed as catechin equivalent (B) released by apple roots grown in a full nutrient solution (control), phosphorus (-P) and iron-deficient (-Fe) solution at 35, 42 and 49 days after transferring the plants to the nutrient solution (DAT). Data are presented as means ± standard error (SE), n= x; Two-way ANOVA results: Total phenols: treatment (ns), sampling time (P<0.001), treatment x sampling time (ns); Total phenols: treatment (P<0.05), sampling time (ns), treatment x sampling time (P<0.05) ns= not significant.

To further characterize plant responses to nutritional stresses a transcriptomic approach was adopted. A RNA-seq analysis was carried out on apple trees roots grown in hydroponic nutrient solution, either Fe- free, P-free or complete (control sample). The analysis on the whole identified 397 differentially expressed genes in the two treatments (-Fe and –P) as compared to the control samples. In particular, comparing Fe deficient and control plants 254 genes were differentially expressed, being 44 upregulated and 210 downregulated. In the case of P-deficient plants vs. control samples, 143 genes resulted differentially expressed, being 105 of them upregulated and 38 downregulated (Tab. 6.3).

Table 6.3 - Differentially expressed transcripts resulting from transcriptional profile comparisons obtained by RNA-seq analysis of apple trees roots, either Fe or P starved.

	Total transcript	Upregulated	Downregulated	Contra-regulated
-Fe vs. CTR	254	44	210	-
-P vs. CTR	143	105	38	-
(-Fe vs. CTR) vs. (-P vs. CTR)	21	4	15	2

The differentially expressed genes were annotated according to the Gene Ontology (GO) terms that are a dynamically structured control vocabulary that can be used to describe the functions of genes. Following the GO protocols, genes can be classified into three major categories based on sequence homology, namely, biological process, molecular function, and cellular components, and their sub-categories (Ashburner et al. 2000). The two sets of differentially expressed genes representing both samples, namely –Fe vs. CTR and –P vs. CTR (Tab. 6.3), were classified as belonging to the biological process category of the GO. As shown in Figure 6.4, the majority of the differentially expressed transcripts in the Fe starved plants belong to the metabolic process, cellular process, response to stimuli, biological regulation and developmental process subcategories. Also in the case of P deficient plants, the most abundant GO subcategories are represented by metabolic process, cellular process, response to stimuli and biological regulation. However, except for the biological regulation subcategory, the percentage of transcript of –P sample is, in the above-mentioned groups, always lower as compared to –Fe sample (Fig. 6.4).

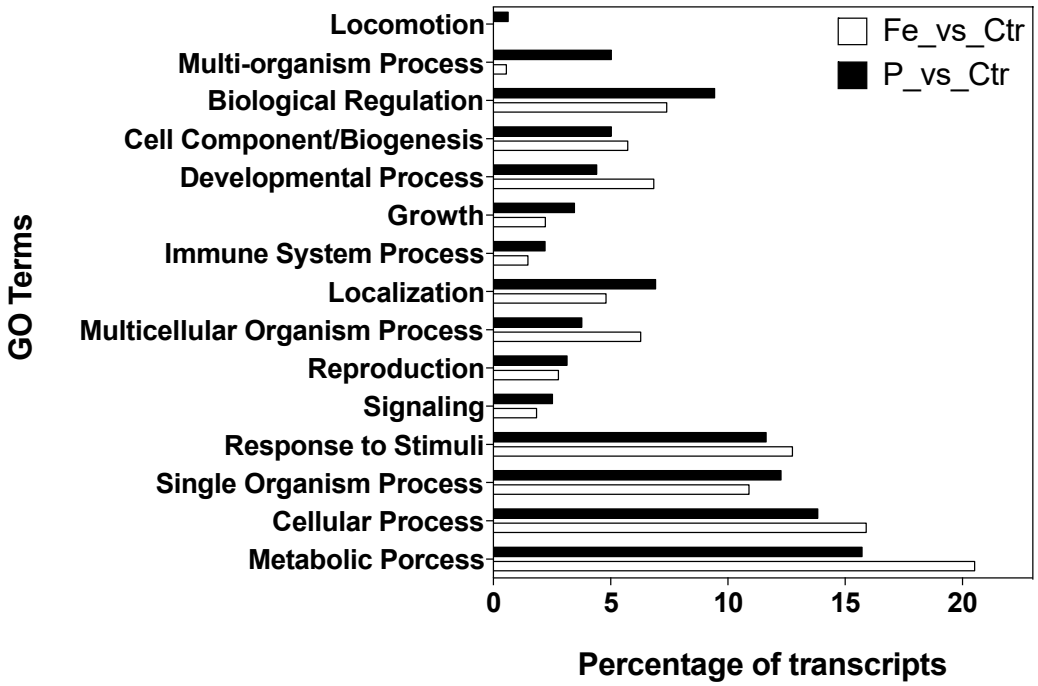

Figure 6.4 - Functional categories distribution of differentially expressed transcripts. Distribution in main functional categories according to the GO "biological process" terms.

This might suggest that apple tree plants adopt different strategies to cope with the two nutritional disorders. This hypothesis could be also strengthened by the fact that –Fe plants predominantly repress genes whilst –P plants mostly up-regulate transcripts (Tab. 6.3). In addition, -Fe and –P plants share only 21 differentially expressed genes, 4 of which are upregulated, 15 downregulated and 2 contra-regulated in both samples (Tab. 6.3). Thus, the 19 common genes that are differentially expressed in the same manner in the two treatments might constitute a core gene system that plants adopt to respond to these two nutritional stresses.

Despite the genome of *Malus x domestica* has been recently sequenced (Velasco et al. 2010), the annotated genes cover approximately 14% of whole genome. For this reason, the majority of the differentially regulated genes obtained by RNA-seq analysis resulted to have an unknown function, therefore further investigations will be required to understand in depth the meaning of the transcriptional modulations induced by the nutrients starvation.

Nevertheless, in the case of Fe starved plants we observed a downregulation of genes encoding enzymes involved in Carbon metabolic pathways (Tab. 6.4). This result is in good agreement with the reduction of the total C released by Fe-starved plants (Fig. 6.1A) and most probably

represents a consequence of the impaired photosynthetic activity induced by the lack of Fe (Tab. 6.1). On the other hand, Fe deficient plants showed a strong upregulation of genes encoding enzymes (i.e. synthase and oxygenase) involved in the biosynthesis of flavonoids (Table 6.4 and Fig. 6.5). Interestingly, the same metabolic pathway resulted also upregulated in the P-starved plants, being these two enzymes part of the common core gene set modulated as a consequence of the nutrients starvation (Tab. 6.4 and Tab. 6.5). The upregulation of the flavonoid biosynthetic pathway is in good accordance with the presence of flavonoids in the root exudates of both Fe-deficient and P-deficient plants (Fig. 6.3B). Beside that of flavonoids, also the biosynthetic pathways of flavons and flavonols were upregulated. As already mentioned, these classes of compounds are exuded by plants to enhance the bioavailability of sparingly soluble nutrients, as for example P and Fe (Cesco et al. 2012). In addition, P deficient plants displayed also the upregulation of metabolic pathways involved in the energy extraction from the substrate (i.e. oxidative phosphorylation) and in the management of the amino acid pool (e.g. phenylalanine, cysteine and methionine metabolism) and on the biosynthesis of "effector" molecules, as for example monoterpenoids that are involved in the defence response, steroids that are precursors of the hormones class of brassinosteroids and zeatine that belongs to the hormone group of cytokinins. Both brassinosteroids and citokinins are plant hormones involved in the regulation of plants growth and development, suggesting that P-deficient apple trees might respond to P-starvation by activating morphogenetic responses.

Table 6.4 - Log_2(Fold Change) values and annotation of transcripts differentially expressed in the root tissue of apple tree plants deprived of Fe.

Gene_ID	Log_2 (Fold Change)	Metabolic Pahway	Enzymatic Activity	Enzyme_ID
XLOC_000498	-2.60	Glycerolipid metabolism	lipase	ec:3.1.1.3
XLOC_006154	-2.66	Porphyrin and chlorophyll metabolism	ceruloplasmin	ec:1.16.3.1
XLOC_010667	-1.40	Thiamine metabolism	phosphatase	ec:3.6.1.15
XLOC_012105	-1.24	Ubiquinone and other terpenoid-quinone biosynthesis	ligase	ec:6.2.1.26
XLOC_017285	-1.32	Starch and sucrose metabolism	gentiobiase	ec:3.2.1.21
XLOC_018408	-2.19	Drug metabolism - cytochrome P450	transferase	ec:2.5.1.18
XLOC_019910	-2.22	Biosynthesis of unsaturated fatty acids	reductase	ec:1.1.1.100
XLOC_021220	-1.35	Galactose metabolism	galactosyltransferase	ec:2.4.1.67
XLOC_021424	-2.32	Alanine. aspartate and glutamate metabolism	asparaginase II	ec:3.5.1.1
XLOC_023149	-1.90	Drug metabolism - other enzymes	ali-esterase	ec:3.1.1.1
XLOC_026455	-1.92	Cysteine and methionine metabolism	oxidase	ec:1.14.17.4
XLOC_027646	-1.36	Fructose and mannose metabolism	2-dehydrogenase	ec:1.1.1.14
XLOC_030955	-1.79	Galactose metabolism	invertase	ec:3.2.1.26
XLOC_033237	-2.12	Ascorbate and aldarate metabolism	oxygenase	ec:1.13.99.1
XLOC_039996	-1.62	Amino sugar and nucleotide sugar metabolism	chitodextrinase	ec:3.2.1.14
XLOC_040729	-1.79	Carotenoid biosynthesis	epoxidase	ec:1.14.13.90
XLOC_043260	-1.68	Stilbenoid. diarylheptanoid and gingerol biosynthesis	O-hydroxycinnamoyltransferase	ec:2.3.1.133
XLOC_049520	-1.73	Pyruvate metabolism	lyase	ec:4.4.1.5
XLOC_049938	-1.57	Starch and sucrose metabolism	endo-1.3-beta-D-glucosidase	ec:3.2.1.39
XLOC_052608	-2.24	Starch and sucrose metabolism	trehalose 6-phosphatase	ec:3.1.3.12
XLOC_058674	-2.10	Pentose and glucuronate interconversions	lyase	ec:4.2.2.2
XLOC_060696	-2.02	Zeatin biosynthesis	O-beta-D-glucosyltransferase	ec:2.4.1.215
XLOC_062804	-1.82	Galactose metabolism	oxidase	ec:1.1.3.9
XLOC_070868	-1.59	Ascorbate and aldarate metabolism	oxidase	ec:1.10.3.3
XLOC_072867	-1.79	Phenylalanine metabolism	lactoperoxidase	ec:1.11.1.7
XLOC_073341	-1.74	Starch and sucrose metabolism	pectin demethoxylase	ec:3.1.1.11
XLOC_018401	1.93	Flavonoid biosynthesis	synthase	ec:1.14.11.23

Table 6.5 - Log_2(Fold Change) values and annotation of transcripts differentially expressed in the root tissue of apple tree plants deprived of P.

Gene_ID	Log2 (Fold Change)	Metabolic Pahway	Enzymatic Activity	Enzyme_ID
XLOC_069235	-2.25	Glycerophospholipid metabolism	N-methyltransferase	ec:2.1.1.103
XLOC_032343	-1.58	Amino sugar and nucleotide sugar metabolism	chitodextrinase	ec:3.2.1.14
XLOC_049824	1.85	Pentose and glucuronate interconversions	lyase	ec:4.2.2.2
XLOC_052133	1.95	Glycerophospholipid metabolism	phosphodiesterase	ec:3.1.4.46
XLOC_034100	2.00	Phenylalanine metabolism	lactoperoxidase	ec:1.11.1.7
XLOC_066132	2.34	Oxidative phosphorylation	diphosphatase	ec:3.6.1.1
XLOC_004567	2.68	Oxidative phosphorylation	reductase (H+-translocating)	ec:1.6.5.3
XLOC_054406	2.82	Zeatin biosynthesis	O-beta-D-glucosyltransferase	ec:2.4.1.215
XLOC_057031	3.02	Cysteine and methionine metabolism	dehydrogenase	ec:1.1.1.27
XLOC_030329	3.19	Monoterpenoid biosynthesis	synthase	ec:1.3.3.9
XLOC_011476	3.45	Steroid biosynthesis	monooxygenase	ec:1.14.13.132
XLOC_061663	3.70	Flavone and flavonol biosynthesis	3'.5'-hydroxylase	ec:1.14.13.88
XLOC_064676	3.72	Phenylalanine metabolism	dehydrogenase	ec:1.1.1.90
XLOC_018401	4.16	Flavonoid biosynthesis	synthase	ec:1.14.11.23
XLOC_075354	5.11	Flavonoid biosynthesis	oxygenase	ec:1.14.11.19

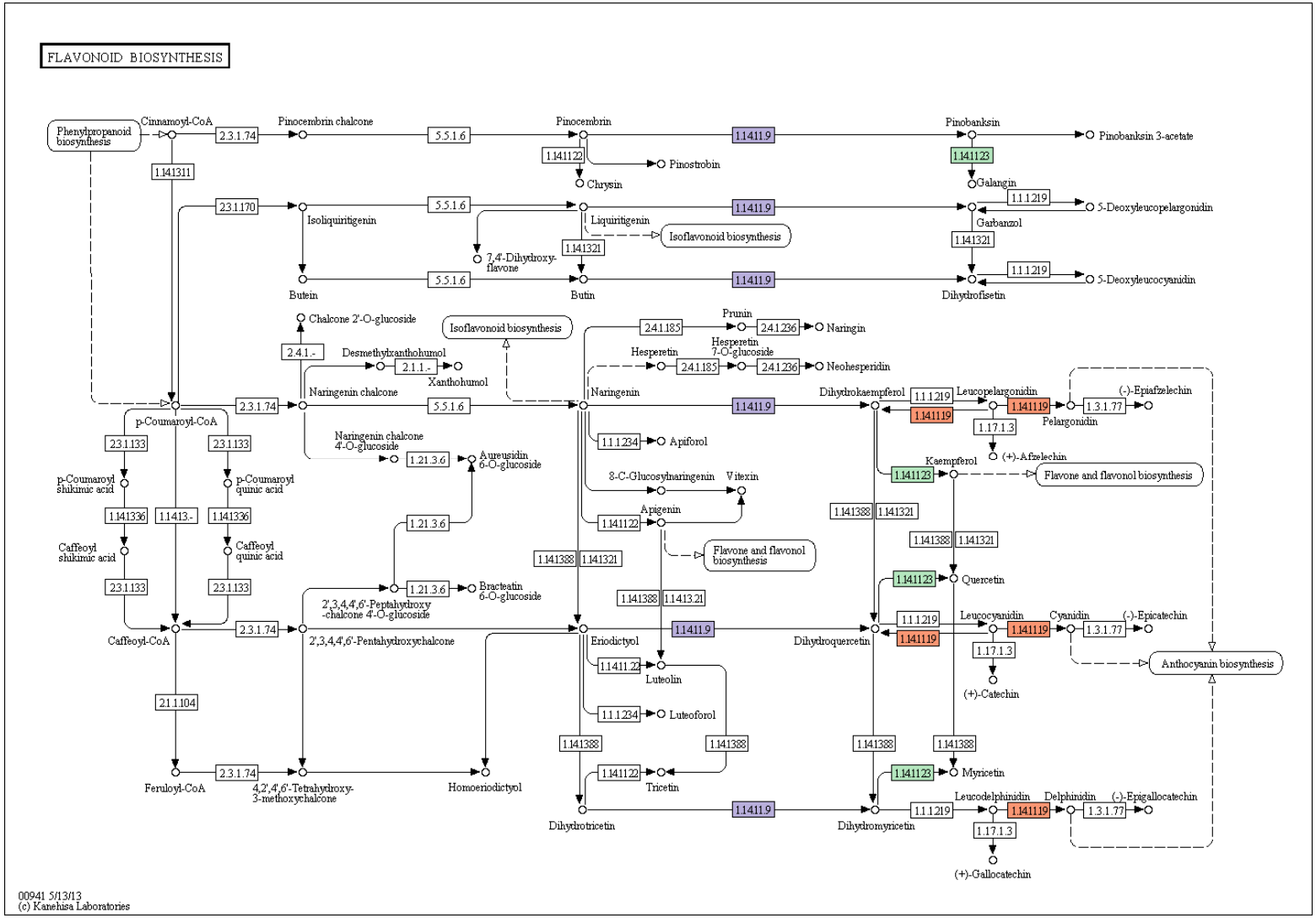

Figure 6.5 - KEGG map depicting the flavonoid metabolic pathway.

6.4 Conclusions

In conclusion, results obtained in this study shed light to exudation processes occurring in apple roots, grown in nutrient deficiency condition. The analysis of root exudates showed that the release of C and N were affected by root Fe and P shortage. However, the qualitative analysis determined a high release of phenols and flavonoids in particular in control and P deficient plants and revealed the presence of oxalic acid in all the treatments that has never been observed before in apple exudates.

The analysis on the whole transcriptome identified 397 differentially expressed genes in the two treatments (-Fe and –P) as compared to the control samples. Comparing Fe deficient and control plants 254 genes were differentially expressed, being 44 upregulated and 210 downregulated, while in P-deficient plants vs. control samples, 143 genes resulted differentially expressed, being 105 of them upregulated and 38 downregulated. Besides this, it was also highlighted that the lack of the two essential nutrients affected different metabolic pathways, thus suggesting that apple tree plants adopt different strategies to cope with the two nutritional disorders.

These results, which revealed different strategies in function of the specific nutrient shortage will contribute to a deep understanding of the mechanisms carried out by woody plants to overcome low nutrient availability conditions.

6.5 Acknowledgements

This work has been financially supported by: Italian MIUR (FIRB-Programma “Futuro in Ricerca”), Free University of Bolzano (TN5056).

6.6 References

Ashburner, M. et al. (2000). Gene ontology: Tool for the unification of biology. *Nature Genetics*, 25(1): 25–29.

Atanassova, M., Georgieva, S. & Ivancheva, K. (2011). Total Phenolic and Total Flavonoid Contents , Antioxidant Capacity and Biological Contaminants in Medicinal Herbs. Journal of the University of Chemical Technology and Metallurgy, 46(1): 81–88.

Brumbarova, T. et al. (2008). A proteomic study showing differential regulation of stress, redox regulation and peroxidase proteins by iron supply and the transcription factor FER. Plant Journal 54(2): 321–334.

Cesco, S. et al. (2012). Plant-borne flavonoids released into the rhizosphere: impact on soil bio-activities related to plant nutrition. A review. Biology and Fertility of Soils 48(2): 123–149.

Dakora, F.D. & Phillips, D.A. (2002). Root exudates as mediators of mineral acquisition in low-nutrient environments. Plant and Soil 245(1): 35–47.

Donnini, S. et al. (2012). Adaptive strategies of Parietaria diffusa (M.&K.) to calcareous habitat with limited iron availability. Plant, Cell and Environment 35(6): 1171–1184.

Donnini, S. et al. (2010). Proteomic characterization of iron deficiency responses in Cucumis sativus L. roots. BMC Plant Biology 10.

Gerke, J., Römer, W. & Beißner, L. (2000). The quantitative effect of chemical phosphate mobilization by carboxylate anions on P uptake by a single root. II. The importance of soil and plant parameters for uptake of mobilized P. Journal of Plant Nutrition and Soil Science 163(2): 213–219.

Gnekow, M.A. & Marschner, H. (1989). Influence of the fungicide pentachloronitrobenzene on VA-mycorrhizal and total root length and phosphorus uptake of oats (Avena sativa). Plant and Soil 114(1): 91–98.

Hansen, N. et al. (2006). Iron Nutrition in Field Crops. In L. L. Barton & J. Abadia, eds. Iron Nutrition in Plants and Rhizospheric Microorganisms. Springer Netherlands: 61–83.

Jin, C.W. et al. (2007). Iron Deficiency-Induced Secretion of Phenolics Facilitates the Reutilization of Root Apoplastic Iron in Red Clover. Plant Physiology 144(1): 278–285.

Lan, P. et al. (2011). ITRAQ protein profile analysis of Arabidopsis roots reveals new aspects critical for iron homeostasis. Plant Physiology 155(2): 821–834.

Li, J. et al. (2008). Proteomic response to iron deficiency in tomato root. Proteomics 8(11): 2299–2311.

Lowry, O.H. et al. (1951). Protein measurement with the Folin phenol reagent. The Journal of biological chemistry 193(1): 265–275.

Marschner, H. & Römheld, V. (1994). Strategies of plants for acquisition of iron. Plant and Soil 165(2): 261–274.

Martin, M., (2011). Cutadapt removes adapter sequences from high-throughput sequencing reads. EMBnet.journal 17: 10–12.

Mimmo, T. et al. (2014). Rhizospheric organic compounds in the soil-microorganism-plant system: their role in iron availability. European Journal of Soil Science 65(5): 629–642.

Neumann, G. & Römheld, V. (2011). Rhizosphere Chemistry in Relation to Plant Nutrition. In Marschner's Mineral Nutrition of Higher Plants: Third Edition. pp. 347–368.

O'Rourke, J.A. et al. (2009). Integrating microarray analysis and the soybean genome to understand the soybeans iron deficiency response. BMC Genomics 10.

Pestana, M. et al. (2012). Development and recovery of iron deficiency by iron resupply to roots or leaves of strawberry plants. Plant physiology and biochemistry : PPB / Société française de physiologie végétale, 53: 1–5.

Rellán-Álvarez, R. et al. (2010). Changes in the proteomic and metabolic profiles of Beta vulgaris root tips in response to iron deficiency and resupply. BMC Plant Biology 10.

Rodríguez-Celma, J. et al. (2011). Root responses of Medicago truncatula plants grown in two different iron deficiency conditions: Changes in root protein profile and riboflavin Biosynthesis. Journal of Proteome Research 10(5): 2590–2601.

Tato, L. et al. (2013). Low iron availability and phenolic metabolism in a wild plant species (Parietaria judaica L.). Plant Physiology and Biochemistry 72: 145–153.

Thimm, O. et al. (2001). Response of *Arabidopsis* to iron deficiency stress as revealed by microarray analysis. Plant Physiology, 127(3): 1030–1043.

Trapnell, C. et al. (2012). Differential gene and transcript expression analysis of RNA-seq experiments with TopHat and Cufflinks. Nature Protocols 7(3): 562–578.

Trapnell, C., Pachter, L. & Salzberg, S.L. (2009). TopHat: Discovering splice junctions with RNA-Seq. Bioinformatics 25(9): 1105–1111.

Velasco, R. et al. (2010). The genome of the domesticated apple (Malus × domestica Borkh.). Nature genetics 42(10): 833–9.

Vigani, G., Donnini, S. & Zocchi, G. (2012). Metabolic adjustment under fe deficiency in roots of dicotyledonous plants. In Iron Deficiency and its Complications. pp. 1–27.

Wang, J.-Y. et al. (2010). Proteomics approach to identify differentially expressed proteins induced by iron deficiency in root of Malus. Pakistan Journal of Botany 42(5): 3055–3064.

Welch, R. et al. (1993). Induction of iron(III) and copper(II) reduction in pea (Pisum sativum L.) roots by Fe and Cu status: Does the root-cell plasmalemma Fe(III)-chelate reductase perform a general role in regulating cation uptake? Planta 190(4).

White, P.J. (2003). Ion Transport. In B. Thomas, D. J. Murphy, & B. G. Murray, eds. Encyclopaedia of Applied Plant Sciences. Academic Press, London pp. 625–634.

Zhang, J.-H. et al. (2007). Bioassay and identification of root exudates of three fruit tree species. Journal of Integrative Plant Biology 49(3): 257–261.

7. FINAL CONCLUSIONS

The aim of this work was to deepen the knowledge about plant mechanisms involved in the acquisition of poorly available nutrients such as phosphorus (P) and iron (Fe) and to unravel possible links between the two responses. In particular, the physiological, metabolic and molecular aspects related to the acquisition and allocation of these nutrients were investigated, in order to define tools that might lead to the improvement of their use efficiency by crops.

The first part of the PhD project concerned *Zea mays* plant, one of the most widespread cultivated cereal species in the world, and was focused on the response mechanisms of this plant to Fe deficiency. Furthermore, this work would provide information about the capability of maize to use different natural Fe-sources. Transcriptional analyses showed that Fe deficiency induced the expression of genes involved in *Strategy II*, which increase extra-radical availability of Fe and its acquisition. Moreover, genes involved in the methionine cycle and in the synthesis and release of PS were upregulated. The treatments of Fe-deficient plants with three natural sources (Fe-citrate, Fe-PS and Ferrihydrite), determined a downregulation of *Strategy II* mechanisms, indicating that the sources were used by plants with different efficiency. Moreover, at physiological level, the nutritional status influenced the acquisition and allocation of this micronutrient. Indeed, roots of Fe-deficient maize plants accumulated more Fe than the sufficient ones, while an opposite behavior was detected in shoots. This suggests that the translocation system might be readily active in Fe-sufficient plants.

The capability of Fe-deficient plants to acquire P from readily- or scarcely-available forms was also evaluated. In –Fe plants, a higher P content in roots and shoots was detected in comparison with the Fe-sufficient plants. Moreover, it emerged from transcriptional data that genes encoding P transporters were upregulated in -Fe plants. In particular, ZmPHT1;7, which is putatively involved in the high affinity transport and translocation of P, seems to take part in the Fe-starvation response. Indeed, when Fe-deficient plants were treated (re-supplied) with natural Fe-sources, its transcription level was downregulated to the level of Fe-sufficient plants.

Furthermore the response of plants to Fe and P deficiency was also investigated in a tree plant species. RNA sequencing was carried out on apple tree roots and highlighted that the lack of Fe and P affected different metabolic pathways, thus suggesting that apple tree plants adopt different strategies to cope with these two nutritional disorders.

Another key point of the plant response to P and Fe deficiency is the release of root exudates which are able to mobilize both these poorly available nutrients in soils. White lupine was the model plant chosen for studying root exudation, especially when related to P deficiency. By using molecular, physiological and metabolic approaches the response of white lupine to Fe deficiency was characterized and some links between the plant responses to the two nutritional disorders (-Fe, -P) were identified. Assessing the transcriptional data in either growth conditions (-Fe and -P), a reciprocal interaction was observed between the plant adaptation to the two nutritional stresses. Indeed the low Fe availability triggers the positive modulation of P-deficiency-responsive genes and vice versa. Furthermore, the study of the root exudation patterns showed that compounds such as isoflavonoids (genistein and its derivatives) and coumarins (scopoletin and its derivatives) were released in response to either Fe or P deficiency. The chemical characterization of the root content showed that the same compounds are present but in glycosylated or malonate-glycoside forms.

Based on this work a gene, called *LaMATE2*, involved in the genistein release was identified and functionally characterized. This gene orter was overexpressed under P deficiency and, particularly, in cluster roots. Its silencing resulted in a strong alteration of genistein release from transformed roots. The protein was localized in the plasmalemma, as shown by the expression of a GFP-LaMATE2 construct in *Arabidopsis* protoplast. Finally, solute transport studies with *LaMATE2*-transformed yeast microsomes demonstrated that LaMATE2 protein catalyzed the transmembrane transport of genistein, and potentially also other flavonoids, via a co-transport with H^+

8. REFERENCES

Ai P, Sun S, Zhao J, Fan X, Xin W, Guo Q, Yu L, Shen Q, Wu P, Miller AJ, et al. (2009). Two rice phosphate transporters, OsPht1;2 and OsPht1;6, have different functions and kinetic properties in uptake and translocation. Plant J 57: 798–80.

Awad F and Römheld V. (2000). Mobilization of heavy metals from contaminated calcareous soils by plant born, microbial and synthetic chelators and their uptake by wheat plants. Journal of Plant Nutrition. 23: 1847 – 1855.

Badri, D. V. & Vivanco, J.M., (2009). Regulation and function of root exudates. Plant, Cell & Environment, 32(6): 666–681.

Bais HP, Park SW, Weir TL, Callaway RM and Vivanco JM. (2004). How plants communicate using the underground information superhighway. Trends in Plant Science 9: 26–32.

Bais HP, Weir TL, Perry LG, Gilroy S and Vivanco JM. (2006). The role of root exudates in rhizosphere interactions with plants and other organisms. Annual Review on Plant Biology. 57: 233 – 266.

Bayoumi S. A., Rowan M. G., Blagbrough I. S., Beeching J. R. (2008b). Biosynthesis of scopoletin and scopolin in cassava roots during post-harvest physiological deterioration: the E-Z-isomerisation stage. Phytochemistry 69: 2928–2936.

Battey, N.H. & Blackbourn, H.D. (1993). The control of exocytosis in plant cells. New Phytologist, 125(2): 307–338.

Badri, D. V. & Vivanco, J.M. (2009). Regulation and function of root exudates. Plant, Cell & Environment, 32(6): 666–681.

Bertin, C., Yang, X. & Weston, L.A. (2003). The role of root exudates and allelochemicals in the rhizosphere. Plant and Soil. 256(1): 67–83.

Bieleski, R.L. (1973). Phosphate Pools, Phosphate Transport, and Phosphate Availability. Annual Review of Plant Physiology 24(1): 225–252.

Broeckling CD, Broz AK, Bergelson J, Manter DK and Vivanco JM. (2008). Root exudates regulate soil fungal community composition and diversty. Applied and environmental microbiology. 743: 738–744.

Brüggemann, W. et al. (1990). Plasma membrane-bound NADH: Fe3+-EDTA reductase and iron deficiency in tomato (*Lycopersicon esculentum*). Is there a Turbo reductase? Physiologia Plantarum, 79(2): 339–346.

Brumbarova T, Bauer P, Ivanov R. (2015). Molecular mechanisms governing Arabidopsis iron uptake. Trend Plant Sci 2: 124-33

Chen YF, Wang Y and Wu WH. (2008). Membrane transporters for nitrogen, phosphate and potassium uptake in plants. Journal of Integrative Plant Biology. 50: 835 – 848.

Cheynier V, Comte G, Davies KM, Lattanzio V and Martens S, 2013. Plant phenolics: recent advances on their biosynthesis, genetics and ecophysiology. Plant Physiol Biochem, 72, pp. 1–20

Chong J, Baltz R, Schmitt C, Beffa R, Fritig B, Saindrenan P. (2002). Downregulation of a pathogen-responsive tobacco UDP-Glc:phenylpropanoid glucosyltransferase reduces scopoletin glucoside accumulation, enhances oxidative stress, and weakens virus resistance. The Plant Cell 14: 1093–1107.

Colangelo EP and Guerinot ML. (2004). The essential basic Helix-Loop-Helix protein FIT1 is required for the iron deficiency response. The Plant Cell. 16: 3400 – 3412.

Connolly, E.L., Campbell, N.H., Grotz, N., Prichard, C.L., and Guerinot, M.L. (2003). Overexpression of the FRO2 ferric chelate reductase confers tolerance to growth on low iron and uncovers posttranscriptional control. Plant Physiol. 133, 1102–1110.

Colombo, C. et al., 2014. Review on iron availability in soil: Interaction of Fe minerals, plants, and microbes. Journal of Soils and Sediments, 14, pp.538–548

Condron, L., Turner, B. & Cade-Menun, B. (2005). Chemistry and dynamics of soil organic phosphorus. In J. Sims & A. Sharpley, eds. Phosphorus: Agriculture and the Environment. American Society of Agronomy, Crop Science Society of America, Soil Science Society of America, Inc., Madison, WI, pp. 87–121.

Cornell R. M., and Schwertmann, U. (1996). The Iron Oxides: Structure, Properties, Reactions, Occurrence and Uses.VCH, Weinheim, Germany.

Curie C, Cassin G, Couch D, Divol F, Higuchi K, et al. (2009). Metal movement within the plant: contribution of nicotianamine and yellow stripe 1-like transporters. Ann. Bot. 103:1–11.

Curie C, Panaviene Z, Loulergue C, Dellaporta SL, Briat JF and Walker EL. (2001). Maize yellow stripe1 encodes a membrane protein directly involved in Fe(III) uptake. Nature. 409: 346–349.

Dakora, F.D. & Phillips, D.A. (2002). Root exudates as mediators of mineral acquisition in low-nutrient environments. Plant and Soil. 245(1): 35–47.

Dean, M., Rzhetsky, A. & Allikmets, R. (2001). The Human ATP-Binding Cassette (ABC) Transporter Superfamily. *Genome Research* , 11 (7): 1156–1166.

Decottignies, A. & Goffeau, A. (1997). Complete inventory of the yeast ABC proteins. Nature Genetics. 15(2): 137–145.

Delhaize E, Ryan PR, Hebb D,. Yamamoto Y, Sasaki T and Matsumoto H. (2004). Engineering high-level aluminum tolerance in barley with the *ALMT1* gene. Proceedings of the National Academy of Sciences of the United States of America. 101, 42: 15249 – 15254.

Dixon RA, Xie DY and Sharma SB. (2005). Proanthocyanidins: a final frontier in flavonoid research? New Phytologist. 165: 9–28.

Durrett, T.P., Gassmann, W. & Rogers, E.E. (2007). The FRD3-Mediated Efflux of citrate into the root vasculature is necessary for efficient iron translocation. Plant Physiology. 144: 197–205.

Eide, D. et al. (1996). A novel iron-regulated metal transporter from plants identified by functional expression in yeast. Proceedings of the National Academy of Sciences of the United States of America, 93(11): 5624–5628.

Field, B., Jordán, F. & Osbourn, A. (2006). First encounters – deployment of defence related natural products by plants. New Phytologist, 172(2): 193–207.

Fourcroy P, Sisó-Terraza P, Sudre D, Savirón M, Reyt G, Gaymard F, Abadía A, Abadia J, Alvarez-Fernández A, Briat JF (2014). Involvement of the ABCG37 transporter in secretion of scopoletin and derivatives by Arabidopsis roots in response to iron deficiency. New Phytol 201: 155-167.

Furihata T, Suzuki M, and Sakurai H. (1992). Kinetic characterization of two phosphate uptake gsystems with different affinities in suspension-cultured Catharanthus roseus protoplasts. Plant and Cell Physiology. 33: 1151–1157.

Furukawa, J. et al. (2007). An Aluminum-Activated Citrate Transporter in Barley. Plant and Cell Physiology. 48 (8): 1081–1091.

Gachon C, Baltz R, Saindrenan P. 2004. Over-expression of a scopoletin glucosyltransferase in Nicotiana tabacum leads to precocious lesion formation during the hypersensitive response to tobacco mosaic virus but does not affect virus resistance. Plant Molecular Biology 54: 137–146.

Gerke, J., Römer, W. & Jungk, A. (1994). The excretion of citric and malic acid by proteoid roots of *Lupinus albus* L.; effects on soil solution concentrations of phosphate, iron, and aluminum in the proteoid rhizosphere in samples of an oxisol and a luvisol. *Zeitschrift für Pflanzenernährung und Bodenkunde*, 157(4): 289–294.

Grabau, L.J., Blevins, D.G. & Minor, H.C. (1986). Plant nutrition during seed development, leaf Senescence, pod Retention, and seed weight of Soybean. Plant Physiology. 82(4): 1008–1012.

Green, L.S. & Rogers, E.E. (2004). FRD3 Controls Iron Localization in *Arabidopsis*. Plant physiology , 136 (1): 2523–2531.

Grotewold, E., (2004). The challenges of moving chemicals within and out of cells: insights into the transport of plant natural products. Planta. 219(5): 906–909.

Guern, J., Renaudin, J.P. & Brown, S.C. (1987). The compartimentation of secondary metabolites in plant cell cultures. In F. Constabel & I. K. Vasil, eds. Cell Culture and Somatic Cell Genetics of Plants. Academic Press, San Diego, CA, USA, pp. 43–76

Guerinot, M.L. (2010). Iron in Cell Biology of Metals and Nutrients. In Hell, R. and Mendel, R. (Eds) Plant Cell Monographs 17: 75-94.

Hamburger D, Rezzonico E, MacDonald-Comber PJ, Somerville C, Poirier Y. (2002). Identification and characterization of the Arabidopsis PHO1 gene involved in phosphate loading to the xylem. The Plant Cell 14: 889–902.

Hansen, J.C., Cade-menun, B.J. & Strawn, D.G. (2004). Phosphorus Speciation in Manure-Amended Alkaline Soils. 1527: 1521–1527.

Harrison, A. (1987). Soil Organic Phosphorus—A Review of World Literature, CAB International, Wallingford, Oxon, UK.

Hindt MN, Guerinot ML (2012) Getting a sense for signals: regulation of the plant iron deficiency response. Biochim Biophys Acta, Mol Cell Res 1823:1521–1530

Higgins, C.F. (1992). ABC Transporters: From Microorganisms to Man. Annual Review of Cell Biology, 8(1): 67–113.

Hinsinger, P. (2001). Bioavailability of soil inorganic P in the rhizosphere as affected by root-induced chemical changes: A review. Plant and Soil. 237(2): 173–195.

Hiradate S, Ma JF and Matsumoto H. (2007). Strategies of Plants to Adapt to Mineral Stresses in Problem Soils. Advances in Agronomy 96: 65-132.

Hoekenga OA, Maron LG, Piñeros MA, Cançado GM, Shaff J, Kobayashi Y, Ryan PR, Dong B, Delhaize E, Sasaki T, Matsumoto H, Yamamoto Y, Koyama H and Kochian LV. (2006). AtALMT1, which encodes a malate transporter, is identified as one of several genes critical for aluminum tolerance in Arabidopsis. Proceedings of the National Academy of Sciences of the United States of America. 103: 9738–9743.

Holden, M.J. et al. (1991). Fe^{3+}-chelate reductase activity of plasma membranes isolated from tomato (*Lycopersicon esculentum* Mill.) roots: Comparison of enzymes from Fe-deficient and Fe-sufficient roots. Plant Physiology, 97(2): 537–544.

Jones, D., Darrah, P. & Kochian, L. (1996). Critical evaluation of organic acid mediated iron dissolution in the rhizosphere and its potential role in root iron uptake. Plant and Soil. 180(1): 57–66.

Jones DL and Brassington DS. (1998). Sorption of organic acids in acid soils and its implications in the rhizosphere. European Journal of Soil Science. 49: 447–455.

Ishimaru Y, Kakei Y, Shimo H, Bashir K, Sato Y et al. (2011). A rice phenolic efflux transporter is essential for solubilizing precipitated apoplasmic iron in the plant stele. J. Biol. Chem. 286: 24648-55.

Keating G. J., O'kennedy R. (1997). The chemistry and occurrence of coumarins, in Coumarins: Biology, Applications and Mode of Action, eds O'kennedy R., Thornes R. D., editors. (Chichester: John Wiley & Sons;), 23–66 ISBN: 978-0-471-96997-6

Kobayashi T and Nishizawa NK, (2012). Iron uptake, translocation, and regulation in higher plants. Annual Review of Plant Biology 63: 131–152.

Kovermann P, Meyer S, Hortensteiner S, Picco C, Scholz-Starke J, Ravera S, Lee Y and Martionia E. (2007). The Arabidopsis vacuolar malate channel is a member of the ALMT family. The Plant Journal. 52: 1169–1180.

Koike S, Inoue H, Mizuno D, Takahashi M, Nakanishi H, et al. (2004). OsYSL2 is a rice metalnicotianamine transporter that is regulated by iron and expressed in the phloem. Plant J. 39: 415–24.

Kuroda, T. & Tsuchiya, T. (2009). Multidrug efflux transporters in the MATE family. Biochimica et Biophysica Acta (BBA) - Proteins and Proteomics, 1794(5): 763–768.

Lambers, H. et al. (2006). Root structure and functioning for efficient acquisition of phosphorus: Matching morphological and physiological traits. *Annals of botany*, 98(4): 693–713.

Landsberg, E. Ch. (1982). Transfer cell formation in the root epidermis: A prerequisite for fe-efficiency? Journal of Plant Nutrition, 5(4-7): 415–432.

Li, D., Zhu, H., Liu, K., Liu, X., Leggewie, G., Udvardi, M. and Wang, D. (2002).Purple acid phosphatases of Arabidopsis thaliana. Comparative analysis and differential regulation by phosphate deprivation. J. Biol. Chem. 277: 27772–27781.

Li, L. et al. (2002). Functional cloning and characterization of a plant efflux carrier for multidrug and heavy metal detoxification. Journal of Biological Chemistry. 277 (7): 5360–5368.

Ligaba A, Katsuhara M, Ryan PR, and Shibasaka Mineo. (2006). The BnALMT1 and BnALMT2 Genes from Rape Encode Aluminum-Activated Malate Transporters That Enhance the Aluminum Resistance of Plant Cells. Plant Physiology. 142: 1294-1303.

Lin, Y., Irani, N. & Grotewold, E. (2003). Sub-cellular trafficking of phytochemicals explored using auto-fluorescent compounds in maize cells. BMC Plant Biology, 3(1): 10.

Lindsay WL. (1979). Chemical equilibria in soils. John Wiley and Sons, NY. p. 449.

Lindsay WL and Schwab AB. (1982). The chemistry of iron in soils and its availability to plants. Journal of Plant Nutrition. 5: 821-840.

Linkohr BI, Williamson LC, Fitter AH and Leyser HMO. (2002). Nitrate and phosphate availability and distribution have different effects on root system architecture of Arabidopsis. The Plant Journal. 29: 751-760.

Liu, J. et al. (2009). Aluminum-activated citrate and malate transporters from the MATE and ALMT families function independently to confer *Arabidopsis* aluminum tolerance. The Plant Journal, 57(3): 389–399.

Loyola-Vargas, V. et al. (2007). Effect of transporters on the secretion of phytochemicals by the roots of Arabidopsis thaliana. Planta, 225(2): 301–310.

Lucena JJ. (2000). Effect of bicarbonate, nitrate and other environmental factors on iron deficiency chlorosis. A rewiew. Journal of Plant Nutrition. 23: 1591 – 1606.

Ma Z, Bielenberg DG Brown KM and Lynch JP. (2001). Regulation of root hair density by phosphorus availability in Arabidopsis thaliana. Plant Cell & Environment. 24: 459–467.

Ma, J. F., Ueno, H., Ueno, D., Rombola, A. D, and Iwashita, T. (2003) Characterization of phytosiderophores secretion in Festuca rubra. Plant Soil 256: 131-137.

Ma JF, Nomoto K (1996) Effective regulation of iron acquisition in graminaceousplants. The role of mugineic acids as phytosiderophores. PhysiologiaPlantarum 97: 609-617.

Maathuis FJM. (2009). Physiological functions of mineral macronutrients. Current Opinion in Plant Biology. 12: 250 – 258.

Magalhaes, J. V et al. (2007). A gene in the multidrug and toxic compound extrusion (MATE) family confers aluminum tolerance in sorghum. Nature genetics, 39(9): 1156–61.

Marschner, H., Römheld, V. & Kissel, M. (1986). Different strategies in higher plants in mobilization and uptake of iron. *Journal of Plant Nutrition*, 9(3-7): 695–713.

Marschner, H., Römheld, V. & Kissel, M. (1987). Localization of phytosiderophore release and of iron uptake along intact barley roots. *Physiologia Plantarum*, 71(2): 157–162.

Marschner, P. (2011). Marschner´s Mineral Nutrition of Higher Plants 3rd ed., Academic Press, London.

Mathesius, U. & Watt, M. (2011). Rhizosphere Signals for Plant–Microbe Interactions: Implications for Field-Grown Plants U. E. Lüttge et al., eds., Berlin, Heidelberg: Springer Berlin Heidelberg.

Meyer, S. et al. (2010). Intra- and extra-cellular excretion of carboxylates. Trends in plant science. 15(1): 40–7.

Miller SS, Liu J, Allan DL, Menzhuber CJ, Fedorova M and Vance CP. (2001). Molecular control of acid phosphatase secretion into the rhizosphere of proteoid roots from phosphorus-stressed white lupine. Plant Physiology. 127: 594 – 606.

Mimura T. Regulation of phosphate transport and homeostasis in plant cells. Int Rev Cytol. (1999). 191:149–200.

Morrissey J, Baxter IR, Lee J, Li L, Lahner B, Grotz N, Kaplan J, Salt DE, Guerinot ML. (2009). The ferroportin metal efflux proteins function in iron and cobalt homeostasis in Arabidopsis. Plant Cell 21: 3326–3338.

Mortvedt JJ. (1991). Correcting iron deficiencies in annual and perennial plants: present technologies and future prospects. Plant and Soil. 130: 273-279.

Motoda H, Sasaki T, Kano Y, Ryan PR, Delhaize E, Matsumoto H and Yamamoto Y. (2007). The membrane topology of ALMT1, an aluminum-activated malate transport protein in wheat (*Triticum aestivum*). Plant Signal & Behaviour. 2: 467–472.

Neumann G and Romheld, V. (1999). Root excretion of carboxylic acids and protons in phosphorus-deficient plants. Plant and Soil. 211: 121–130.

Neumann G, Massonneau A, Martinoia E and Romheld V. (1999). Physiological adaptations to phosphorus deficiency during proteoid root development in white lupine. Planta. 208: 373–382.

Neumann G and Römheld V. (2007). The release of root exudates as affected by the plant's physiological status. In: Pinton R, Varanini Z, Nannipieri P (eds). The rhizosphere: biochemistry and organic substances at the soil–plant interface. CRC, Boca Raton, pp 23–72

Nozoye T, Nagasaka S, Kobayashi T, Takahashi M, Sato Y, Sato Y, Uozumi N, Nakanishi H, Nishizawa N. (2011). Phytosiderophore efflux transporters are crucial for iron acquisition in graminaceous plants. Journal of Biological Chemistry. 286: 5446-5454.

Ogo Y, Itai R, Nakanishi H, Inoue H, Kobayashi T, Suzuki M, Takahashi M, Mori S, Nishizawa N. (2006). Isolation and characterization of IRO2, a noveliron-regulated bHLH transcription factor in graminaceous plants. Journal ofExperimental Botany 57: 2867 - 2878.

Olsson PA, van Aarle IM, Allaway WG, Ashford AE and Rouhier H. (2002). Phosphorus Effects on Metabolic Processes in Monoxenic Arbuscular Mycorrhiza Cultures. Plant Physiology. 130: 1162–1171.

Omote, H. et al. (2006). The MATE proteins as fundamental transporters of metabolic and xenobiotic organic cations. Trends in Pharmacological Sciences, 27(11): 587–593.

Rogers, E.E. & Guerinot, M. Lou. (2002). FRD3, a Member of the Multidrug and Toxin Efflux Family, Controls Iron Deficiency Responses in *Arabidopsis*. *The Plant Cell Online*, 14 (8): 1787–1799.

Plaxton, W. C., and Tran, H. T. (2011). Metabolic adaptations of phosphate-starved plants. Plant Physiol. 156: 1006–1015. doi: 10.1104/pp.111.175281

Pierzynski, G., McDowell, R. & Sims, J. (2005). Chemistry, cycling, and potential moment of inorganic phosphorus in soils. In J. Sims & A. Sharpley, eds. Phosphorus: Agriculture and the Environment. American Society of Agronomy, Crop Science Society of America, Soil Science Society of America, Inc., Madison, WI, pp. 53–86.

Piñeros MA, Cançado GM, Maron LG, Lyi SM, Menossi M, Kochian LV. (2008). Not all ALMT1-type transporters mediate aluminum-activated organic acid responses: the case of ZmALMT1 - an anion-selective transporter. The Plant Journal. 53: 352–367.

Pinton R, Varanini Z and Nannipieri P. (2001). The rhizosphere as a site of biochemical interactions among soil components, plants and microorganisms. In: Pinton R, Varanini Z, Nannipieri P. In: The rhizosphere: biochemistry and organic substances at the soil-plant interface. p. 1-17, NEW YORK: Dekker.

Raes, J., Rohde, A., Christensen, J.H., Van de Peer, Y., and Boerjan, W. (2003). Genome-wide characterization of the lignification toolbox in Arabidopsis. Plant Physiol. 133: 1051–1071.

Raghothama, K.G. (1999). Phosphate acquisition. Annual Review of Plant Biology 50: 665–693.

Ramakrishna A and Ravishankar GA, 2011. Influence of abiotic stress signals on secondary metabolites in plants. Plant Signal. Behav. 6: 1720–1731.

Rellan Alvarez R, Giner-Martínez-Sierra J, Orduna J, Orera I, Rodríguez-Castrillon JA, García-Alonso JI, Abadía J and Alvarez-Fernandez A. (2010). Identification of a tri-iron(III), tri-citrate complex in the xylem sap of iron-deficient tomato resupplied with iron: new insights into plant iron long-distance transport. Plant and Cell Physiology. 51: 91–102.

Richardson, A., Barea, J.-M., McNeill, A., Prigent-Combaret, C. (2009). Acquisition of phosphorus and nitrogen in the rhizosphere and plant growth promotion by microorganisms. Plant and Soil 321: 305-339

Richardson AE. (1994). Soil microorganisms and phosphorus availability. Soil Biota 50–62.

Rogers EE and Guerinot ML. (2002). FRD3, a member of the multidrug and toxin efflux family, controls iron deficiency responses in Arabidopsis. Plant Cell. 14: 1787–1799.

Römheld, V. & Kramer, D. (1983). Relationship between proton efflux and rhizodermal transfer cells induced by iron deficiency. Zeitschrift für Pflanzenphysiologie.113(1): 73–83.

Romheld V and Marschner H. (1986). Evidence for a specific uptake system for iron phytosiderophores in roots of grasses. Plant Physiology. 80: 175–180.

Römheld, V. (1987). Different strategies for iron acquisition in higher plants. Physiologia Plantarum. 70(2): 231–234.

Sánchez-Fernández, R. et al. (2001). The *Arabidopsis thaliana* ABC Protein superfamily, a somplete inventory. Journal of Biological Chemistry. 276 (32): 30231–30244.

Santi S, Cesco S, Varanini Z and Pinton R. (2005). Two plasma membrane H+-ATPase genes are differentially expressed in iron-deficient cucumber plants. Plant Physiology and Biochemistry. 43: 287–292.

Santi, S. & Schmidt, W. (2009). Dissecting iron deficiency-induced proton extrusion in *Arabidopsis* roots. New Phytologist, 183(4): 1072–1084.

Sasaki T, Yamamoto Y, Ezaki B, Katsuhara M, Ahn SJ, Ryan PR, Delhaize E and Matsumoto H. (2004). A weat gene encoding an aluminium-activated malate transporter. The Plant Journal. 37: 645–653.

Sbabou, L. et al. (2010). Molecular analysis of SCARECROW genes expressed in white lupine cluster roots. Journal of experimental botany. 61(5): 1351–1363.

Schachtman, D., Reid, R. & Ayling, S. (1998). Phosphorus uptake by plants: from soil to cell. Plant physiology, 116(2): 447–453.

Schmidt W. (1999). Mechanisms and regulation of reduction-based iron uptake in plants. New Phytol 141:1–26.

Shimizu BI, 2014. 2-Oxoglutarate-dependent dioxygenases in the biosynthesis of simple coumarins. Frontiers in Plant Science 5: 549

Sims, J.T., Pierzynski, G.M. (2005). Chemistry of phosphorus in soil. In: Tabatabai, A.M., Sparks, D.L. (Eds.), Chemical Processes in Soil. SSSA Book Series 8. SSSA, Madison.

Stefanovic A, Ribot C, Rouached H, Wang Y, Chong J, Belbahri L, Delessert S, Poirier Y. (2007). Members of the PHO1 gene family show limited functional redundancy in phosphate transfer to the shoot, and are regulated by phosphate deficiency via distinct pathways. The Plant Journal 50: 982–994.

Taiz L and Zeiger E. (1998). ‘‘Plant Physiology,’’ 2nd ed. Sinauer Associates, Sunderland, Massachusetts.

Thomine S, Wang R, Ward JM, Crawford NM, Schroeder JI.2000. Cadmium and iron transport by members of a plant metal transporter family in Arabidopsis with homology to Nramp genes. Proceedings of the National Academy of Sciences, USA 97, 4991–4996.

Tohge T, Watanabe M, Hoefgen R and Fernie AR, 2013. Shikimate and phenylalanine biosynthesis in the green lineage. Frontiers in Plant Science 4: 62

Treeby M, Marschner H and Römheld V. (1989). Mobilization of iron and other micronutrient cations from a calcareous soil by plant-borne, microbial, and synthetic metal chelators. Plant and Soil. 114: 217–226.

Uren NC. (2007). Types, amounts and possible functions of compounds released into the rhizosphere by soil-grown plants. In: The rhizosphere: biochemistry and organic substances at the soil-plant interface. CRC, Boca Raton, pp. 19–40.

Valentinuzzi F, Pii Y, Vigani G, Lehmann M, Cesco S and Mimmo T, 2015. Phosphorus and iron deficiencies induce a metabolic reprogramming and affect the exudation traits of the woody plant *Fragaria×ananassa*”. Journal of Experimental Botany. 66, 20, pp. 6483–6495

Vance, C.P., Uhde-Stone, C. & Allan, D.L. (2003). Phosphorus acquisition and use: critical adaptations by plants for securing a nonrenewable resource. New Phytologist, 157: 423–447.

Varotto, C., Maiwald, D., Pesaresi, P., Jahns, P., Salamini, F., and Leister, D. (2002). The metal ion transporter IRT1 is necessary for iron homeostasis and efficient photosynthesis in Arabidopsis thaliana. Plant J. 31, 589–599

Vert G, Grotz N, Dédaldéchamp F, Gaymard F, Guerinot ML, Briat J-F, Curie C. 2002. IRT1, an Arabidopsis transporter essential for iron uptake from the soil and for plant growth. *Plant Cell*

14: 1223–1233.

Vigani, G. et al. (2013). Cellular iron homeostasis and metabolism in plant. Frontiers in Plant Science, 4(DEC).

Walker, TS, Bais HP, Grotewold E and Vivanco JM, 2003. Root exudation and rhizosphere biology. Plant Physiology 132: 44 – 51.

Wasaki J, Yamamura T, Shinano T and Osaki M. (2003). Secreted acid phosphatase is expressed in cluster roots of lupine in response to phosphorus deficiency. Plant and Soil 248: 129–136.

Watt, M. & Evans, J.R. (1999). Proteoid roots. Physiology and development. Plant Physiology, 121(2): 317–323.

Weir TL, Bais HP, Stull VJ, Callaway RM, Thelen GC, Bhamidi S, Stermitz FR and Vivanco JM. (2006). Oxalate contributes to the resistance of Gaillardia grandiflora and Lupinus sericeus to a phytotoxin produced by Centaurea maculosa. Planta. 223: 785–795.

White PJ, Broadley MR. (2009) Biofortification of crops with seven mineral elements often lacking in human diets – iron, zinc, copper, calcium, magnesium, selenium and iodine. New Phyt 182: 49-84.

Williamson LC, Ribrioux SP, Fitter AH, Leyser HM. (2001). Phosphate Availability Regulates Root System Architecture in Arabidopsis. Plant Physiology. 126: 875 – 882.

Wu Q., Zou L., Yang X. W., Fu D. X. (2009). Novel sesquiterpene and coumarin constituents from the whole herbs of Crossostephium chinense. J. Asian. Nat. Prod. Res. 11: 85–90.

Yazaki, K. (2005). Transporters of secondary metabolites. Current Opinion in Plant Biology. 8(3 SPEC. ISS.): 301–307.

Yi Y and Guerinot ML. (1996). Genetic evidence that induction of root Fe(III)-chelate reductase activity is necessary for iron uptake under iron deficiency. The Plant Journal. 10: 835 – 844.

Yuan Y, Wu H, Wang N, Li J, Zhao W, Du J, Wang D, Ling HQ (2008) FITinteracts with AtbHLH38 and AtbHLH39 in regulating iron uptake geneexpression for iron homeostasis in Arabidopsis. Cell Res 18: 385-397

Zhang, F. et al. (2010). Rhizosphere Processes and Management for Improving Nutrient Use Efficiency and Crop Productivity: Implications for China. Advances in Agronomy. 107: 1–32.

9. ACKNOWLEDGEMENTS

I would like to thank to my supervisor Prof. Roberto Pinton for giving me the great opportunity to work in his group and for his guidance during these years. Moreover, I would like to express my deepest thanks to Dr. Nicola Tomasi. You always encouraged and supported me, giving to me the opportunity and the freedom to develop as researcher.

A special thanks goes to Dr Laura Zanin. Your professionality and your passion for research is for me an inspiration. You have been a guide and a great friend for me during these years.

I would also like to thank my collegues: Dr Serena Foria, Dr Monica Massaro, Dr. Laura Zanon, Dr Gabriele di Gaspero and Dr Rossella Monte. There are no words to express how much your support and your friendship have been fundamental. We shared many special moments together.

A sincere thanks goes to Dr. Fabio Valentinuzzi. Your presence has always been a constant in my life.

Many thanks to Dr Ana Maria Àlvarez-Fernandez and Prof Javier Abadia whose made possible my great experience at the Aula Dei Experimental Station in Zaragoza. Thanks to Adrian for his help during the experiments.

My deepest thanks to Prof. Enrico Martinoia for giving me the opportunity to work in his lab and to Dr. Rita De Brito Francisco for her precious help during my stay.

I would also like to thank Dr. Fabio Marroni and Prof. Michele Morgante for their collaboration in the sequencing experiments.

Many thanks to all the people that in one way or another accompanied me during my PhD, my colleagues and Friends.

Last but not least, a special thanks to Matteo and my family. I cannot be grateful enough for your continuous help, love and support.